Temperature Effects on Pre-cure and Post-cure Properties of Dental Resin Composites

A thesis submitted to The University of Manchester for the degree of

Doctor of Philosophy

in the Faculty of Biology Medicine and Health

2020

Jiawei Yang

School of Medical Sciences

Division of Dentistry

Table of Contents

Word count: 34,330

List of Figures

List of Tables

List of Abbreviations

AAT	Avery Adhesive Test
AF	*Admira Fusion*
AFM	Atomic Force Microscopy
ATR	Attenuated total reflectance
BBR	*Beautifil-Bulk Restorative*
bis-EMA	Bisphenol-A epoxylated dimethacrylate
bis-GMA	Bisphenol-A glycidyl dimethacrylate
°C	Degree Celsius
C=C	Carbon double bond
C-C	Carbon single bond
cm^{-1}	Wavenumber unit
CQ	Camphorquinone
DC	Degree of conversion
DMAEMA	Dimethylaminoethyl methacrylate
DVC	Digital volume correlation
EDMA	Ethylene glycol dimethacrylate
FBO	*Filtek One Bulk Fill*
F$_{max}$	Maximum separation force
F$_p$	Maximum packing force
FSU	*Filtek Supreme Ultra*
FTIR	Fourier Transform Infrared
g/mol	Gram per mole
h	Hour
HZ	*Harmonize*
K$_C$	Critical stress intensity
K$_{IC}$	Fracture toughness
LCU	Light-curing unit
LED	Light-emitting diode
LVDT	Linear variable displacement transducer
min	Minute
mm	Millimetre
mm/s	Millimetre per second
MPa	Megapascal
mW/cm^2	Milliwatts per square centimetre
N	Newton
nm	Nanometre
OCT	Optical Coherence Tomography
-OH	Hydroxyl group
ORMOCERs	Organically modified ceramics
Pa s	Pascal-second (unit of dynamic viscosity)

PI	Photo-initiator
PPF	Prepolymer fillers
PS	Polymerization shrinkage strain
PSA	Pressure Sensitive Adhesives
QTH	Quartz tungsten halogen
RAFT	Reversible Addition-Fragmentation Transfer agent
RBCs	Resin-based composites
ROM	Rule of mixtures
s	Second
SEM	Scanning Electron Microscopy
SENB	Single-edge notch three-point bending
SF3	*SonicFill* 3
TEC	*Tetric EvoCeram*
TEGDMA	Triethylene glycol dimethacrylate
$\mathbf{T_g}$	Temperature of glass transition
TPH	*TPH LV*
TPO	2, 4, 6-trimethyl-benzoyl diphenylphosphine oxide
UDMA	Urethane dimethacrylate
UE	Ultrasonic energy
UV	Ultraviolet
VC	*Viscalor*
VHN	Vickers micro-hardness number
vol.%	Volume content percentage
$\mathbf{W_p}$	Work of packing
$\mathbf{W_s}$	Work of probe-separation
wt.%	Weight content percentage
γ-MPS	γ-methacryloxypropyltrimethoxysilane
μCT	Micro-Computed Tomography
μm	Micrometre
φ	Diameter

Abstract

Resin-based composites (RBCs) with good aesthetic and mechanical properties have been extensively studied. The successful placement of RBCs mainly depends on their pre-cure properties, which are related to material composition and viscosity. Various strategies, including modifications of the material composition and application of ultrasound energy, have been introduced to reduce viscosity. In accordance with the Arrhenius Equation, pre-heating will reduce viscosity to improve flowability and ease extrusion during handling. Increased monomer mobility also improves the degree of conversion and post-cure mechanical properties [1-3]. However, pre-heating also has potential risks of damaging the dental pulp tissues.

This study aimed to investigate temperature effects on the pre-cure and post-cure properties of *Viscalor*, a thermo-viscous bulk-fill composite and compare it with a wide range of commercial photo-cured RBCs. *Viscalor* was pre-heated using a Caps Warmer device in T3 mode (at 68 °C) for 30 s and 3 min, respectively. Stickiness and packability were measured via a Texture Analyzer using different experimental settings and temperatures. The extrusion force was determined using a universal testing machine.

Regarding post-irradiation properties, FTIR was used to measure the degree of conversion and polymerization kinetics at 5 min and 24 h post-cure. Polymerization shrinkage strain kinetics were measured using the bonded-disk technique. Surface micro-hardness, surface properties after three-body abrasion and static creep behaviour of RBCs were also investigated. Fracture toughness of several bulk-fill composites was measured using a single-edge notch three-point bending method.

The measured properties varied with material composition. A 3 min pre-heating period improved pre-cure properties of *Viscalor* but did not adversely influence its post-cure properties. Interim conclusions recognise the benefits of pre-heating

Viscalor for 3 min. However, more research is necessary to investigate the clinical relevance of pre-heated *Viscalor*.

Declaration

No portion of the work referred to in the thesis has been submitted in support of an application for another degree or qualification of this or any other university or other institute of learning.

Jiawei Yang

2020

Copyright Statement

i. The author of this thesis (including any appendices and/or schedules to this thesis) owns certain copyright or related rights in it (the "Copyright") and she has given The University of Manchester certain rights to use such Copyright, including for administrative purposes.

ii. Copies of this thesis, either in full or in extracts and whether in hard or electronic copy, may be made **only** in accordance with the Copyright, Designs and Patents Act 1988 (as amended) and regulations issued under it or, where appropriate, in accordance with licensing agreements which the University has from time to time. This page must form part of any such copies made.

iii. The ownership of certain Copyright, patents, designs, trademarks and other intellectual property (the "Intellectual Property") and any reproductions of copyright works in the thesis, for example graphs and tables ("Reproductions"), which may be described in this thesis, may not be owned by the author and may be owned by third parties. Such Intellectual Property and Reproductions cannot and must not be made available for use without the prior written permission of the owner(s) of the relevant Intellectual Property and/or Reproductions.

iv. Further information on the conditions under which disclosure, publication and commercialisation of this thesis, the Copyright and any Intellectual Property University IP Policy (see http://documents.manchester.ac.uk/display.aspx?DocID=24420, in any relevant Thesis restriction declarations deposited in the University Library, The University Library's regulations (see http://www.library.manchester.ac.uk/about/regulations/) and in The University's policy on Presentation of Theses.

Acknowledgement

Firstly, I would like to thank my parents for being patient and supportive for me during my MSc and PhD studies in Manchester.

I would like to express my sincere gratitude to my supervisors, Professor David C. Watts and Professor Nikolaos Silikas, for their guidance, support, encouragement and advice throughout my project. I appreciate the time and energy that you have given to this work.

My sincere thanks to Brian Daber for his help and support with the lab work.

I also would like to thank Julie Spellman, Kimberley Britt, Lucy O'Malley and Joy Stewart for all the assistance and help they offered to me.

Many thanks for all my friends and colleagues in the Division of Dentistry, School of Medical Science, University of Manchester for their support and love.

Last but not least, I would like to thank Abdulrahman, Ahmed, Fatima, Hamad, Khaled, Maryem and Mutaz for their endless love and support through my project.

To the memory of my grandfather.

Chapter One

Introduction and Literature Review

1.1 Introduction

Dental caries is the main cause of almost 85 % of dental diseases [4, 5]. Dental plaque forms via the residual bacteria from saliva and results in dental caries at any site of the tooth in the oral environment [5, 6]. To avoid the sequelae of dental caries, scientists and dentists keep striving to control the progression of dental caries through prevention and restoration [6].

Indirect and direct restorative materials are used to repair or replace the tooth damage caused by dental disease or trauma [4, 6]. The former are fabricated extraorally and used for repairing large cavities. The latter are directly placed on the tooth structure to fill cavities [6, 7]. Silicate cement was introduced as a direct restorative material in the 1800s to prevent dental caries via releasing fluoride [6, 7]. Acrylic resins soon replaced the silicate cement with improved mechanical properties and color appearance [7]. In 1956, Bowen used epoxy resins in restorative materials [8]. Later, bisphenol-A glycidyl dimethacrylate (bis-GMA) replaced epoxy groups in Bowen's resins. The inorganic filler particles were also added into the resin matrix to reduce polymerization shrinkage [9, 10].

Recently, the demands for restorative materials having a similar appearance to the natural tooth, time-saving fabrication processes and superior properties are increasing [4, 6]. Thus, the resin-based composites (RBCs), known as a reinforced polymer system, have become the dominant direct restorative materials used in dentistry [4, 6, 7, 11, 12].

Many commercial RBCs are available for various clinical applications. The average longevity of restorations is about 10 years. The main reasons for replacement are secondary caries, marginal irregularities and bulk fractures [13-15]. Developments in composite technology lead to reduced polymerization shrinkage, sufficient fracture resistance and enhanced mechanical properties [11]. Various manipulation techniques have also been introduced to ease handling and improve degree of polymerization.

The following briefly reviews the RBC systems, including resin matrix, filler technology and coupling agents. The properties and characterizations related to the current study are also addressed.

1.2 Resin matrix

Generally, dental RBCs consist of three major components: cross-linked resin matrix, inorganic fillers and coupling agents. After free-radical polymerization of monomers, the resin matrix transfers from a fluid phase to a rigid solid and provides a continuous phase within which filler particles are dispersed [4, 6]. The resin matrix usually contains 1) monomer system, 2) initiating system and 3) additives (such as inhibitor) that to ensure a stable and optimum matrix [7, 16]. Many properties of RBCs are related to the resin matrix, for example, rheology, degree of polymerization, polymerization shrinkage, storage stability and wear resistance [11]. Material rheology and handling properties are related to monomer composition. The polarity and hydrophilicity of the resin monomer may also affect the attachment between the unset composite and the instrument surface, which will further influence the perceived and measured stickiness/packability behaviour.

1.2.1 Monomer system

The monomer system consists of one or more types of monomer molecules that react with each other via polymerization - the process of monomer connection and conversion to a three-dimension network [17, 18]. Monomer, the relatively small repeating unit, is the starting point for polymerization. The commonly used monomers for dental resin-based composites are dimethacrylate monomers, such as bis-GMA, urethane dimethacrylate (UDMA) and triethylene glycol dimethacrylate (TEGDMA) [19]. They have two reactive (polymerizable) carbon double bonds (C=C). As the basis of the resin matrix, the monomer system should fulfill various physio-chemical requirements, including low volume shrinkage, storage stability and optimal mechanical properties, regarding the composites formed [17, 20].

Bis-GMA is the predominantly used monomer. As shown in Figure 1.1, the stiff aromatic backbone and the presence of hydrogen bonds between the hydroxyl groups (-OH) in neighbouring molecules result in high viscosity (1100 Pa s at ambient temperature) [21, 22]. The limited mobility of polymer chains reduces the chance to react with proximity and the final degree of conversion (DC) [23, 24]. However, its rigid structure provides different desirable properties, for example, low polymerization shrinkage and high modulus [21, 24, 25].
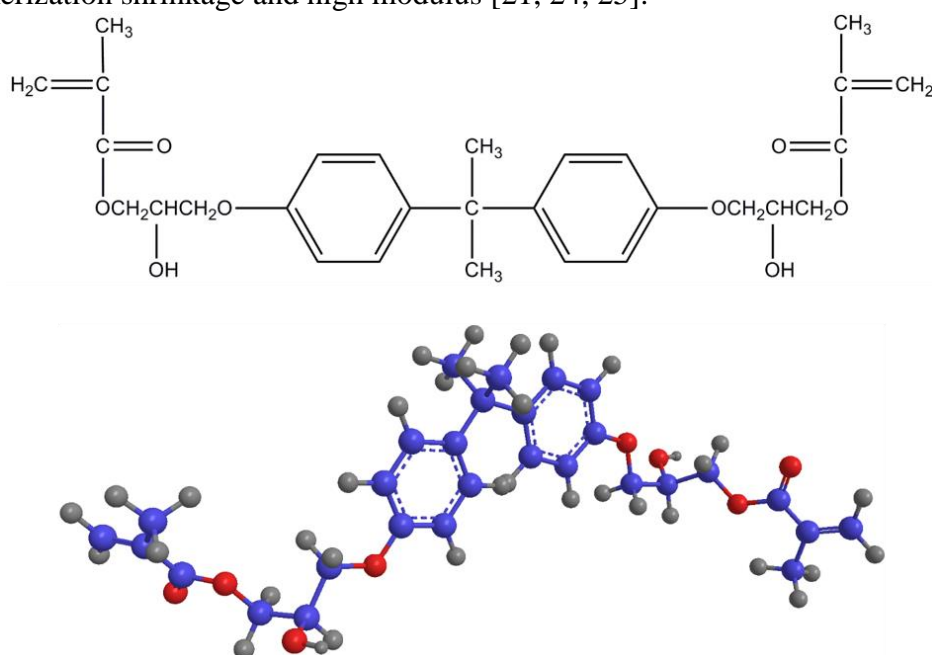
Figure 1.1 Chemical structure of bis-GMA.

As the ethoxylated version of bis-GMA, bisphenol-A ethoxylated dimethacrylate (bis-EMA) was introduced (Figure 1.2) [26]. The lack of two -OH groups on its chemical structure results in a flexible polymer chain, increased DC and reduced water sorption

[24, 27, 28]. However, the lack of hydrogen bonding has deleterious effects on wear resistance and mechanical properties [29, 30].
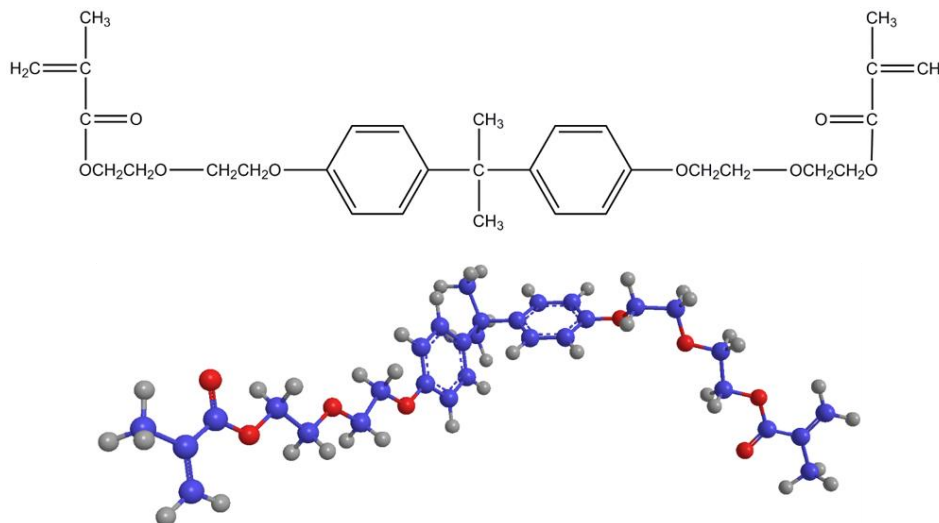
Figure 1.2 Chemical structure of bis-EMA.

To balance the reactivity and mobility of the monomer system, low-viscous monomers are added. As shown in Figure 1.3, the presence of ester groups makes UDMA chains flexible and easy to react with neighbouring molecules, which increases the final DC [31]. However, the low-viscous UDMA systems (11 Pa s at ambient temperature) show more polymerization shrinkage than that of bis-GMA systems [22, 24]. UDMA has a lower molecular weight (470 g/mol) than bis-GMA (512 g/mol) [17]. During polymerization, the intermolecular van der Waals distances (0.3-0.4 nm) converts into covalent bonds (C-C) (0.15 nm) and shrinkage occurs [28, 32]. Comparing same-length polymer chains, the shrinkage amount of long-chain monomer (with large molecular weight) is less than that with the short-chain monomer [11, 28, 33].
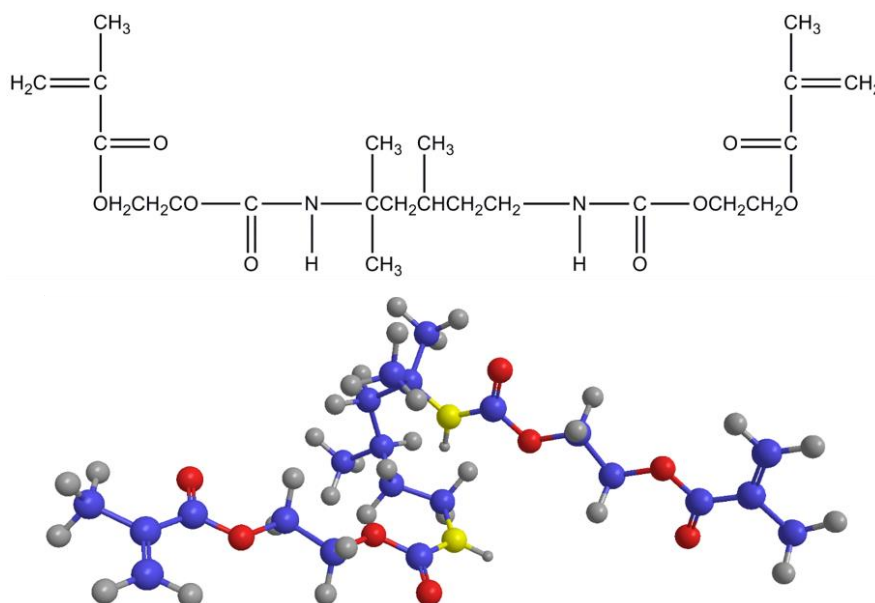
Figure 1.3 Chemical structure of UDMA.

The addition of reactive diluents is another method to control the initial viscosity of the monomer system. The commonly used diluents are ethylene glycol dimethacrylate (EDMA) and TEGDMA [7, 11]. TEGDMA (Figure 1.4) has a much lower molecular weight (286 g/mol) and viscosity than that of bis-GMA and UDMA [17]. By increasing the amount of TEGDMA in UDMA/TEGDMA mixtures (from 19.6 % to 79.1 %), the overall viscosity decreased from 0.655 to 0.048 Pa s [34]. The high double bond content within TEGDMA enhances the degree of polymerization but also increases polymerization shrinkage [7, 32]. The high flexibility of the TEGDMA polymer chain facilitates the water sorption and increases hydrophilicity [22, 35, 36].
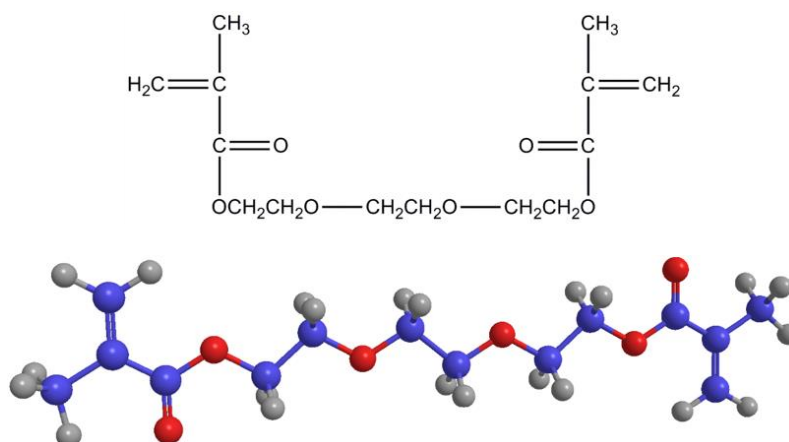
Figure 1.4 Chemical structure of TEGDMA.

Internal stress occurs during polymerization and within the context of a bonded restoration within a cavity, some of the shrinkage (strain) tendency is manifested as shrinkage stress [37]. The increased shrinkage stress may lead to micro-leakage, recurrent caries and restoration failure [7]. The concept of modifying monomer formulation is a new strategy. The use of liquid crystalline monomers [38, 39], silorane-based monomers [37, 40-42] and monomers with high molecular weight [43] showed low shrinkage stress. Ring-opening polymerization also results in a reduced amount of shrinkage due to its polymerization mechanism, in which the dimensional change from intermolecular distance to covalent bond is nearly eliminated [44].

Organically modified ceramics (ORMOCERs) monomers are grafted via covalent or iono-covalent chemical bonds through sol-gel reactions [17, 45]. Admixed ORMOCERs matrix (a mixture of conventional dimethacrylate matrix and ORMOCERs matrix) has been commercially realized [45, 46]. However, high polymerization shrinkage remains a concern due to the presence of the dimethacrylate component [45]. The pure ORMOCERs-matrix composites showed improved mechanical properties and solvent resistance, compare to admixed ORMOCERs-matrix composites and microhybrid composites [46, 47]. Further development is focus on reducing the viscosity of the ORMOCERs matrix to ensure high filler loading and good clinical performance [45].

1.2.2 Polymerization reaction

There are three main phases of polymerization reaction: initiation, chain propagation and termination. The external energy activates the double carbon bonds within the free radical generators and forms free radicals. During the initiation, the free radical reaches the highly electron-rich area of monomers and initiates the polymerization [48]. This process continues with more monomers activated. During chain propagation, polymer chain length increases and develops a polymer network. Since the localized viscosity increases (gel effect), free radicals are hard to collide with each other to terminate the polymerization [49]. The rate of monomer consumption

suddenly increases and leads to auto-acceleration [50]. Upon further polymerization, the limited mobility of available monomers reduces the rate of reaction [48]. Termination could occur via free radical combination/disproportionation termination and chain transfer [49].

The initial free radicals can be activated via various methods, such as chemical activation [51], external energy activation (heat [7, 52], microwave [53] and light) and combined activation systems. Light-curing activation uses light as the energy source to activate one paste system, not like chemical-activation mixing two pastes. Ultraviolet (UV) cured material first become available in the early 1970s for fissure sealants [54, 55]. Due to the limited depth of cure, potential damage to soft tissues and ophthalmologic damage to the clinicians, UV light-curing was replaced by visible light-curing in the late 1970s [48]. Visible light, more accurately blue light, became the most popular energy source for dental photo-cured RBCs [54].

1.2.3 Photo-initiating system

1.2.3.1 Photo-initiators (PIs)

The PIs absorb light irradiation at the appropriate wavelength, delivered by the light-curing unit (LCU) and transform into an excited state to initiate polymerization [48, 56]. Depending on the photo-initiating system used, the excited compound either directly break down via triplet-state homolytic bond cleavage into radicals (Type I PIs), or react with the activator to form free radicals (Type II PIs) [48, 57]. The Type I PIs have high absorbency and efficient quantum yields and the typical product is 2, 4, 6-trimethyl-benzoyl diphenylphosphine oxide (TPO) [48, 57]. The Type II PIs are more suitable for visible light-curing and camphorquinone (CQ)/tertiary amine system is commonly used [57, 58]. CQ absorbs light in the range of 400-500 nm and the peak absorption is at 470 nm [54]. The CQ/dimethylaminoethyl methacrylate (DMAEMA) system results in a high DC and good optical properties of the RBCs, so it is widely used [7, 58, 59]. However, the yellow color of CQ may affect the final restoration

color [48, 55]. The germanium-based PIs with a short wave spectrum are designed and show high reactivity and good color-stability [48, 57].

The efficiency of the PI system mainly depends on the match between the emission spectrum of the light source and the absorption spectrum of the PI system [55, 56]. Sufficient quantum efficiency and high reactivity at low concentrations are also key factors [57]. These are closely related to the LCU used and the light-curing technique.

1.2.3.2 Light-curing unit (LCU)

There are different types of visible LCU available on the market, including quartz tungsten halogen (QTH) lamps, plasma (xenon) arc lamps, argon laser lamps and light-emitting diode (LED) lamps [11]. QTH lamps radiate a wide range of wavelengths - some of which require filtering to keep light in the violet-blue range (400-500 nm) [48, 60]. The high electric current leads to high operating temperatures of QTH, which needs cooling system [48, 59]. Plasma lamps have intensive light sources allowing short curing time [60]. Similar to QTH, plasma lamps need filtering unnecessary wavelengths to limit radiant emitting [48]. Argon laser lamps have the highest intensity with single wavelength emitting at 490 nm and low generated heat [60]. However, the cost of laser lamps is higher than that of QTH. LED lamps emit light via quantum-mechanical effect instead of heating filaments, thus less heat is generated [59]. The wavelength of blue LEDs matches the peak absorption of CQ, but the narrow bandwidth limits their use to activate the PI system that has a low absorption spectrum [55].

To save treatment time and according to reciprocity law - short exposure duration can be used with high radiant intensity - LCUs with high radiant emittance are developed [61-63]. However, due to the insufficient flow of polymer chains, the high light intensity may lead to high polymerization shrinkage [61, 64]. Temperature rise induced by LCU also has potential damage to surrounding soft tissue and pulp [48, 61]. The extent of temperature rise depends upon the anatomy of the tooth, thickness

of the remaining pulpal wall and light-curing technique [48, 65-68]. Soft-start curing, start curing with low intensity and complete with high intensity, has been used to reduce polymerization shrinkage during light-curing [54, 69].

1.2.3.3 Depth of cure

In addition to damaging the soft tissues, limited depth of cure is another reason that the UV light-curing was substituted by visible light-curing. The maximum effective cure depth for UV light-cured composites is about 1 mm, whereas 2 mm or more is achievable for visible light-cured composites [11]. Light penetration and photo-initiator concentration would reduce with curing depth increasing [18, 70-72]. When light is applied to the composites, both upper and lower surfaces reflect light [11]. Resin components, filler particles and additives absorb and scatter the light [48, 70]. These affect light penetration and results in a poor depth of cure. Long exposure duration could compensate for the limited light penetration but may raise the risk of high temperature [11, 70, 73]. Since about 2010, the so-called bulk-fill composites have been introduced with a cure depth of 4-5 mm [70, 74].

Besides, the quality of the LCU and curing technique may influence the depth of the cure and mechanical properties of composites [48, 75]. The incremental technique is recommended to ensure adequate curing and reduce polymerization shrinkage [11, 76]. The curing efficiency decreases with the increasing distance between the LCU tip and the surface of the composites [54, 69, 77]. The LCU tip should be parallel to the composite surface as close as possible and avoid contamination by the composite [69]. Other factors, including LCU beam uniformity, LCU tip size and clinical manipulation skill, all influence the depth of cure [48, 78-80].

1.3 Fillers

As reinforcement fillers, in the 1950s, quartz particles were added to the composites [54]. Quartz particles are hard and chemically inert, whereas it can be easily pulled

out during polishing and leave a rough surface [7]. Later, softer fillers have replaced quartz fillers to enhance abrasion resistance [7]. Since quartz-reinforced composites are not radiopaque, the addition of fillers that contain heavy metal atoms can assist optimal diagnostic contrast [6]. The use of inorganic fillers can also reduce polymerization shrinkage, impart radiopacity and improve aesthetic [54]. Generally, fillers are fabricated through a grinding process or sol-gel precipitation [7]. A further method is burning certain compounds of elements in oxygen to form the oxide of the element in the fine-particle form [81, 82].

Filler characteristics, including filler composition, content, size and shape, have significant influences on material viscosity and pre-cure properties [83-87]. Small and irregular filler particles with high filler loading may increase material viscosity and lead to poor cavity adaptation [85-87]. However, Lee et al. concluded that viscous materials show low stickiness [84].

Filler morphology is mainly determined by the mode of particle synthesis, particularly the grinding process [54]. Kim et al. compared four types of filler morphology and concluded that round filler particles produce the highest filler volume fraction [88]. RBCs reinforced with irregular-fillers show good mechanical properties due to the interlock between fillers [89]. Flake-shaped glasses are flat platelets with a thickness of 5 μm and can mix well with the resin matrix. However, due to the stacking of the flakes, the depth of cure may reduce with increasing filler content and results in low mechanical properties [90-92]. Short glass fibers have a high aspect ratio (length to diameter) and according to the pull-out mechanism that strong fibers bridge cracks to prevent brittle rupture, they can improve the fracture toughness of composites [54, 93]. The fiber-reinforced increment works as a shrinkage breaker and protects the interfacial integrity of the deep cavity floor [94]. The efficiency of short glass fibers reinforcement depends on fiber composition, length, orientation and the adhesion between fibers and the matrix [93-95]. As Mansoura et al. suggested, filler shape should be considered as a secondary fine-tuning factor for adjusting composite properties [89, 96].

New filler technology has been developed by modifying filler composition and structure [7, 54]. A similar/matched refractive index between filler and resin matrix increases the depth of cure and DC [54, 97]. Small-sized filler particles could increase light transmission, whereas the increased filler content has the opposite effect [54]. Adequate opacity is vital to mimic the natural appearance of natural teeth [54]. Thus, the balance between light transmission and opacity needs to be considered. Smart composites, which contain therapeutic fillers, can be used to prevent or treat oral disease and facilitate remineralization of tooth lesions via releasing ions [7, 98]. Fluoride-containing fillers were firstly used in the 1970s to improve the cariostatic demineralization effect [7].

1.4 Coupling agents

Insufficient stress transfer between phases may make the resin matrix carry most of the stress and leads to creep and fracture of composites [11]. Coupling agents ensure the strong bonding between fillers and resin matrix and help filler particles to disperse in the resin matrix [99]. The major problem is that the hydrophobic resin matrix cannot wet the surface of hydrophilic fillers [7, 11]. The use of bifunctional coupling agents, for example, organosilanes, solves the problem [7, 11, 100]. Two ends of bifunctional silane coupling agents can react with the filler surface and the resin matrix, forming Si-O-Si bonds and covalent bonds, respectively [7, 54]. The chemical bonding between phases are enhanced and prevent initial cracks formation. The commonly used silane coupling agent is γ-methacryloxypropyltrimethoxysilane (γ-MPS) [100, 101].

Since the coupling agents contain hydrophilic groups, water could hydrolyze the filler/matrix interlayer and weaken the interlayer bonding [100, 102]. Besides, hydrophilic monomers may increase the risk of hydrolysis [100]. Thus, a hydrophobic silane coupling agent, poly-fluoroalkyl silane, is used to enhance water resistance [100]. Silanes with long functional structures show better mechanical properties and hydrolytic stability, compared to silanes with shorter functional structures [103, 104].

1.5 Classifications of RBCs

1.5.1 Classification by filler size

The first used quartz filler has an average particle size of 70 μm [11]. The use of smaller particles fills the space between the bigger particles and also improves the polishability and aesthetic of RBCs [6, 105]. However, high surface-to-volume ratio limits the mixing between filler and matrix [6]. Thus, the balance between filler particle size and workability should be considered.

An old classification based on filler size was set up by Lutz and Phillips in 1973 [106]. The general classification by filler size is shown in Table 1.1. Macrofillers with an average size of 10-100 μm reinforced the resin matrix [6]. However, the resultant high wear resistance may damage the enamel of the opposing teeth and reduce the polishability and aesthetic [7]. Microfillers, with an average size of 0.03-0.5 μm, were introduced in the late 1970s to overcome the mentioned disadvantages of macrofillers [11]. But the small particle size limits the mixing between the matrix and fillers, which affects the strength and stiffness of the composites [11]. Further development in filler particle size yielded midfillers, minifillers and finally the hybrid fillers [7]. Microhybrid fillers are a combination of macrofillers and microfillers [106]. With the contribution of both large and small particles, microhybrid composites show good mechanical properties and wear resistance.

Table 1.1 Classification of RBCs by filler size [6].

Class of filler	Particle size
Macrofillers	10-100 μm
Small/fine fillers	0.1-10 μm
Midfillers	1-10 μm
Minifillers	0.1-1 μm
Microfillers	0.01-0.1 μm (agglomerated)
Nanofillers	5-100 nm

Additionally, with the development of nanotechnology, composites reinforced by nanofillers have long-term gloss [107]. Since nanoclusters (agglomeration of nanofillers) may scatter the light and affect the depth of cure, discrete nanofillers, smaller than visible light wavelength, have been introduced [108, 109].

1.5.2 Classification by filler content

A classification based on filler size is not exact since it cannot reflect filler composition, morphology or content [108]. The filler content is related to composite mechanical properties, such as compressive strength, flexural strength and hardness [88, 110]. According to the rule of mixtures (ROM), filler content correlates to elastic moduli, which describes the deformation performance of the material [96, 108, 110]. Also, the increased filler content reduces the matrix part, which leads to reduced polymerization shrinkage and water sorption decrease [111]. Thus, the classification by filler content is important for predicting the performance of the composites.

The filler content or filler loading can be expressed into weight % (filler mass) or volume % (volume content) [108]. The volume % is frequently used and typically 10-15 % less than weight % [7]. 50 vol.% is the balance level of matrix/filler and 74 vol.% is the upper limit for remaining good wettability between matrix and fillers [108]. Thus, the RBCs can be classified into three categories: ultra-low fill (<50 vol.%), low-fill (50-74 vol.%) and compact-fill (>74 vol.%) [108]. By incorporating different filler sizes, hybrid composites are formulated with high filler content.

1.5.3 Classification by viscosity

Apart from the old classification based on filler size, RBCs can be classified based on viscosity/fluidity [83, 112, 113]. Highly filled packable RBCs, the paste-like composites with good reproduction of occlusal anatomy, are commonly used [16]. The conventional universal RBCs have a high filler content of 50-70 vol.%, which enhances their physical and mechanical properties [114]. But the increased viscosity

makes it difficult to manipulate and leads to poor cavity adaptation and final microleakage [1, 34].

Lightly filled flowable RBCs with a low filler content of 37-53 vol.% were introduced in late 1996 [83, 114, 115]. The reduced viscosity enables easy manipulation via small gauge needles and good marginal adaptation [83, 116]. Flowable RBCs are ideal for filling the deep irregular cavity [114]. The use of a flowable liner with regular composites showed low marginal fractures and leakage [2, 116, 117]. However, the low filler loading may affect wear resistance, overall strength and radiopacity of flowable RBCs [114, 118]. The high resin matrix content may cause great polymerization shrinkage, low elastic modulus and high dimensional change [83, 111, 119].

1.5.4 Classification by placement technique

To reduce polymerization shrinkage stress occurs during light-curing, the incremental filling technique is used [12, 76, 120]. Due to the limited depth of cure, the increment thickness is usually 2 mm [121]. There are different filling options, for example, lateral and oblique filling (Figure 1.5) [76]. The multiple small increments achieve the complete cure in the cavities deeper than 2 mm. However, the long chairside time increases the technique sensitivity and risk of contamination [120]. The entrapment of air and the gaps between increments may also cause leakage and staining [120].

(a) **(b)**
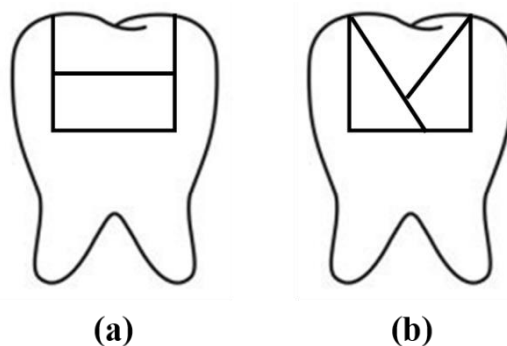
Figure 1.5 Different filling options: (a) lateral and (b) oblique filling.

To simplify the clinical procedure, bulk-fill RBCs, with a depth of cure of 4-5 mm, have been developed [120]. The use of bulk-fill RBCs is convenient and reduces volumetric polymerization shrinkage [120, 122]. With developed monomer and filler technology, bulk-fill RBCs show high translucency and optimized physical/mechanical properties [120]. There are two types of bulk-fill RBCs, low-viscous (flowable) and high-viscous (sculptable) bulk-fill RBCs [122-124]. The former exhibits better cavity adaptation but needs a layer of capping to enhance its mechanical properties and restore the tooth's outer anatomy [120, 124]. The latter is widely used for restoring deep cavities and showing low shrinkage stress. However, some bulk-fill RBCs have inferior mechanical properties, which questioning their use under high occlusal load [120, 122, 125]. The reduced hardness of bulk-fill RBCs after ethanol storage also raises concerns about their long-term stability [122].

1.6 Viscosity

The rheological nature of unset RBCs affects their handling properties and clinical success [112, 113, 126]. Viscosity, material's ability to resist the force that tends to make it flow, directly relates to material handling properties, operating time and quality of restoration [34, 84, 127, 128]. The benefits of low viscosity include easy extrusion during manipulation, good marginal adaptation and penetration to irregularities. However, extremely low-viscous composites with high flowability are difficult to control [34]. The material composition mainly affects the viscosity, for example, high-viscous monomers, increased filler content, irregular filler particles and incorporation of glass fibers, may all lead to high viscosity [83-87]. As mentioned in 1.5.3, flowable RBCs were introduced with moderate viscosity and acceptable clinical performance. New monomer formulations with low viscosity have been developed and show enhanced properties [22, 87].

Other external factors are influencing the viscosity of RBCs. As pseudoplastic materials, RBCs exhibit shear-thinning behaviour, that when the external stress is rapidly applied, composites flow readily [84, 113, 129]. During clinical manipulation,

constant and dynamic stress applied to the materials, which may influence their viscosity [113].

According to the Arrhenius Equation (Equation 1.1), viscosity decreases with temperature:

$$\eta = Ae^{E_a/RT} \qquad \text{(Equation 1.1)}$$

where η, A, E_a, R and T represent viscosity, pre-exponential factor, the activation energy for the reaction, universal gas constant and temperature, respectively [34]. Due to the thermal vibrational forces, polymer chain mobility increases with temperature, which enhances the rate of polymerization, depth of cure and monomer conversion [113, 130-133]. Thus, pre-heating is recommended before clinical restoration to obtain ideal material flowability and marginal adaptation. The commonly used heating devices are Calset heater (AdDent Inc., Danbury, CT, USA) [2, 134] and ENA heat (Micerium, Avegno, Italy) [135, 136].

The risk of elevated temperature to the oral cavity requires consideration. With a temperature increase (above normal oral temperature) of 5.5 to 16 °C, the possibility of pulp necrosis increases from 15 % to 100 % [137]. However, some studies found that the actual composite temperature is lower than the pre-set temperature of the heating device and will drop rapidly after removal from the heater [138-141]. Some *in vivo* measurements have also demonstrated slower temperature changes within the pulp compared to the previous *in vitro* measurements, due to dynamic temperature regulation by the surrounding soft tissue and constant blood flow [48, 142]. The extent of composite temperature change depends upon material thermal properties and the manipulation skills [140, 143].

The *SonicFill* system (Kerr, USA), including a specially designed handpiece and a new nanohybrid composite, was introduced in 2011 and become a time-saving system for dental restoration [144]. *SonicFill* has a highly filled resin matrix that incorporates special viscosity modifiers, which are sensitive to ultrasonic energy (UE) [144]. When

UE is applied, viscosity modifiers respond to it and reduce the viscosity by 87 %. Once UE is stopped, composites return to the initial state, which is perfect for carving and contouring [144]. The high-speed manipulation achieves high-quality restorations with sufficient strength and adequate depth of cure [144-147]. However, the high-viscous *SonicFill* showed higher polymerization shrinkage stress than that of low-viscous bulk-fill RBCs [148]. *SonicFill* using sonication also showed inferior mechanical properties compared to that using incremental placement techniques [149]. In Hirata et al.'s study, sonication improved handling properties of other types of bulk-fill RBCs but increased void volume [150].

1.7 Handling properties

With the development of RBCs, studies are mainly concerned with their post-irradiation physical and mechanical properties. The pre-cure handling properties, including ease of placement, stickiness and packability, are less investigated [151]. To avoid technique sensitivity and the formation of voids/gaps, careful placement technique and good cavity adaptation are needed [75, 152]. Handling properties are related to material composition and rheology and affect the selection of the appropriate material for successful clinical restoration [138].

1.7.1 Stickiness

Stickiness describes the adhesion force between two contacted surfaces [153]. The clinical relevance of sufficient material stickiness is to make sure good adhesion and adaptability to the tooth cavity. However, extremely high material stickiness requires careful manipulation and may result in porosities/voids in the restoration [126, 127].

In 1997, Chuang et al. used the *Avery Adhesive Test* (AAT) to measure the adhesive properties of Pressure Sensitive Adhesives (PSA) [154]. The usage of a spherical probe ensured contact consistency and reproducible data [154]. In 2003, a new method was introduced using a flat-ended steel probe [127]. The mechanisms of the mentioned stickiness measurements are similar [75]. Composites are packed into the mould and a flat-ended steel probe descends into the material at a constant speed until reaching the pre-set force or depth. Then the probe ascends and material separates from the probe.
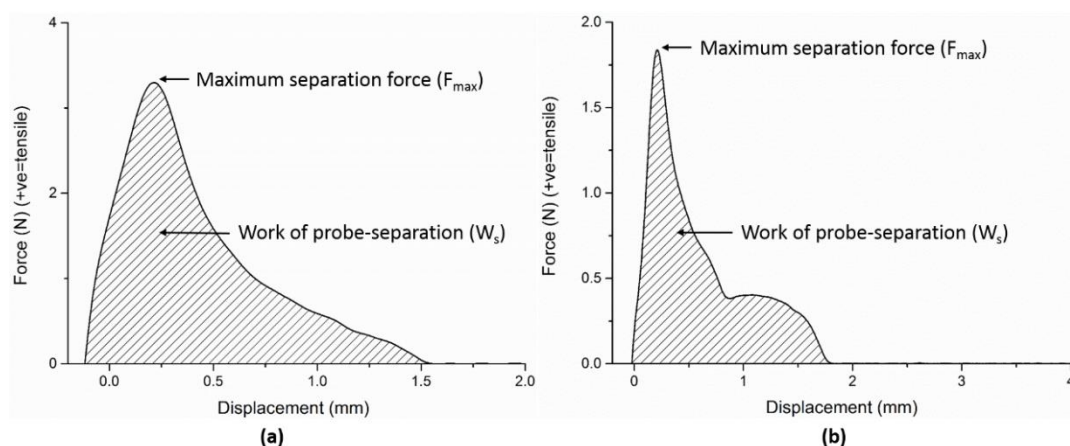
Figure 1.6 (a) Type I and (b) Type II force/displacement curves during stickiness measurement.

The force data are usually plotted against time or probe displacement. Two types of force/displacement plots (Type I and Type II), with one or two peaks in the graph, are commonly observed (Figure 1.6). When the probe is moving upward, the attached material starts stretching and generates tensile stress on the probe. With further elongating, tensile stress increases until reaching the interfacial strength, then stress dramatically reduces back to zero with material separation [154]. However, when material elongates at the molecular level, polymer chains slip past each other and continue straightening until there is no more slack [154]. If the tensile stress exceeds the force needed to straighten the polymer chains, the second peak appears in the plot [154]. The peak height represents F_{max}, the maximum separation force. And the integrated area under the curves describes W_s, the work of probe-separation. The peak height in Type I plots, also called initial peak height, is related to material wettability

and resistance to separation force [126, 128]. The second peak height in Type II plots is determined by the material's degree of crosslinking [154]. The W_s illustrates the energy needs to separate material, which may relate to molecular cohesion and the degree of crosslinking [126, 154, 155].

Ideally, RBCs should be less sticky to the instrument while extruding, but stickier to the cavity wall after placement [126-128]. As mentioned in 1.6, rheological properties affect handling properties. Lee et al. concluded that viscous materials show low stickiness and viscosity relates to temperature and filler volume [84]. High filler loading with small filler size and irregular filler shape results in high viscosity and may lead to low material stickiness [83, 84, 112, 127, 128, 156, 157]. During the insertion of RBCs, extrusion speed, temperature and wet conditions may affect stickiness behaviour [127]. Some studies demonstrated that stickiness increases with temperature due to the reduced viscosity and better interaction between material and probe [126, 156]. However, other studies reported low stickiness results since the temperature rise decreases viscoelasticity and makes the material more extensible [128, 155]. Rosentritt et al. found that both storage and application temperature affect material stickiness and the latter has a significant influence on the wettability of material [155]. Thus, it is important to guarantee a warm storage condition and constant application temperature.

Unplugging speed during measurement also influences stickiness. Due to less relaxation time for monomer chains to adjust to the applied force, stickiness may increase with high probe separation speed [126, 128]. But another study reported low material stickiness at high unplugging speed and this may be attributed to material inherent characteristics [156].

1.7.2 Packability

The adaptability of materials relates to their stickiness, firmness and hardness [155]. Adequate consistency and packability are important for material adapting to the tooth cavity with different dimensions [127, 158]. Since there was no acceptable measurement or criteria to compare consistency, in 1998, Tyas et al. designed a method by packing material into an 8 mm x 8 mm cylindrical mould and pressing with a flat-ended glass rod (φ= 4.37 mm) [151, 158]. The reproducible results showed that consistency increased with filler content [158].
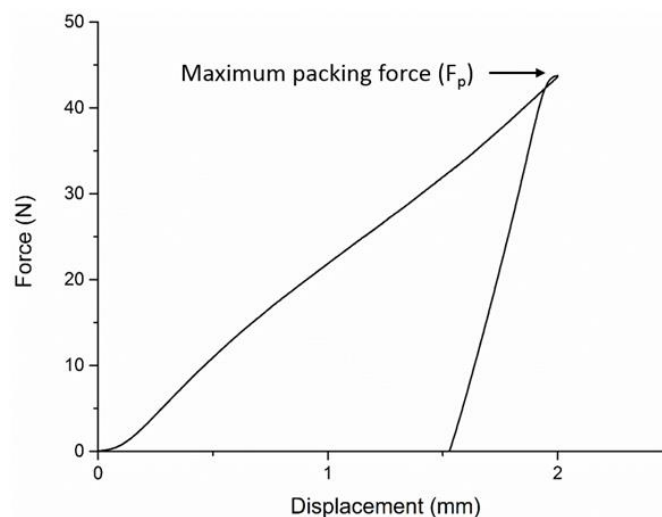
Figure 1.7 Typical force/displacement curve during packability measurement.

Similar to stickiness measurement, within the force/displacement plots, peak height represents F_p, the maximum packing force and W_p, the integrated area under the curves, represents the work of packing (Figure 1.7). With deeper probe penetration into the material, more material wets the probe and results in more adhesion [155]. Kaleem et al. found that the high probe-to-cavity ratio requires more packing force [151]. Manipulation counts, paste aging and pre-polymerization of material also have influences on material adhesion behaviour [155, 159]. Packing force decreases with temperature, due to the reduced viscosity and improved movability of material [151, 155]. The effects of material composition, such as monomer and filler content, need further study to define the ideal range of packability concerning clinical behaviour.

1.8 Degree of conversion (DC)

The degree of conversion (DC) indicates the conversion percentage of C=C bonds to C-C bonds during the polymerization. Due to the limited mobility of double bonds and radicals, polymerization cannot reach 100 % completion [160, 161]. Thus, DC is commonly in the range of 50-70 % at room temperature [54, 162, 163]. Once irradiation stops, no more primary radical forms, but the unreacted macro-radicals continue reacting with C=C bonds at a retarded rate, which is known as the dark reaction [164, 165]. The polymer network continues developing and DC at 24 h post-irradiation is in the range of 68-86 % [160, 163]. DC determines RBC properties, such as mechanical stability, marginal integrity and long-term performance [160]. Insufficient DC may result in poor mechanical properties and biocompatibility [54, 166]. However, excessive DC may cause high polymerization shrinkage [18, 54].

DC can be directly measured using Fourier Transform Infrared (FTIR) Spectroscopy with an attenuated total reflectance (ATR) attachment. The spectrum range of 1450-1700 cm^{-1} is selected to identify the peak heights of the aliphatic C=C absorbance peak at 1640 cm^{-1} and the aromatic C=C absorbance peak at 1610 cm^{-1} [54]. DC is calculated as:

$$DC \% = 1 - \frac{(H_{C=C}/H_{reference})_{cured}}{(H_{C=C}/H_{reference})_{uncured}} \times 100 \% \quad \text{(Equation 1.2)}$$

where $H_{C=C}$ and $H_{reference}$ represent peak height of C=C and the reference band. The reason for comparing peak height rather than peak area is to reduce the effect of baseline changes [54]. To estimate the cure efficiency, DC can be indirectly demonstrated by measuring micro-hardness and depth of cure of RBCs [75, 167]. However, the hardness and depth of cure depend not only on DC but also on other factors, such as composite composition and light-curing technique [54, 167]. Hence, the accuracy of indirect measuring DC merits further studies.

Both intrinsic and extrinsic factors affect DC and the former includes monomer viscosity, filler characteristics and photo-initiator concentration [54, 163, 167, 168]. High-viscous monomers limit free radical mobility and result in low DC. The extent of dark reaction or post-irradiation also affects the final DC [160]. A large quantity of filler within the resin matrix may attenuate light transmission. Inadequate light penetration causes incomplete polymerization and reduces DC. Filler size, which is similar to, or greater than the visible light wavelength, may affect the light transmission and the final DC [7]. Extremely high or low photo-initiator concentration may affect the polymerization extent and the final DC due to reaction inhibition or inadequate activation [7, 54]. Some newly developed photo-initiator systems, such as Ivocerin and Benzoyl Germaniumare, are more photo-reactive than CQ/DMAEMA system and show increased DC [167, 169].

The extrinsic factors include specimen thickness and variables within the light-curing process. The final DC is related to the light energy of LCU - the product of LCU irradiance and exposure duration. The adequate light output with long exposure duration enhances the final DC [73, 160]. The heat generated from the LCU and pre-heating prior to polymerization may favour the mobility of polymer chains and increase the DC [2, 3, 54]. To ensure enough light penetration, the optimum curing thickness of conventional RBCs is 0.5-2 mm [7]. With improved translucency, bulk-fill RBCs with greater curing thickness (4-5 mm) achieve comparable or higher DC than that of conventional RBCs [163, 167].

1.9 Polymerization shrinkage

During polymerization, polymer chains become more closely packed with the reduction of overall free volume, so that volumetric shrinkage occurs [170]. Depending on the magnitude of volumetric shrinkage, contraction stress develops and leads to residual stress within composites and at the bonded interface [119, 171, 172]. Not all shrinkage leads to shrinkage stress since, at the early stage of polymerization, resin flow could compensate for the developed stress [173]. However, with rapid

polymerization, unavoidable shrinkage stress may cause interfacial gap formation, microleakage, secondary caries and restoration failure [173-175].

Apart from shrinkage strain, shrinkage stress is determined by material composition and viscoelastic properties and light-curing protocol [119, 172, 175]. Moreover, factors such as cavity/tooth geometry, boundary condition and the configuration factor (C-factor) interact with each other and influence the resultant stress [172, 173]. C-factor is the ratio of bonded to unbounded surfaces (Figure 1.8) and the higher the C-factor, the greater the shrinkage stress develops at the interface [4, 176]. Some studies investigated the effect of C-factor on shrinkage stress, in which the increased specimen thickness causes high shrinkage stress [176, 177]. A low C-factor and increased free surfaces allow stress-relief and eliminate partial stress [177]. C-factor strongly affects the internal adaptation of materials [178]. However, the stress distribution in the tooth cavity does not only depend on C-factor but also how it is created and the remaining tooth structure [4, 176].
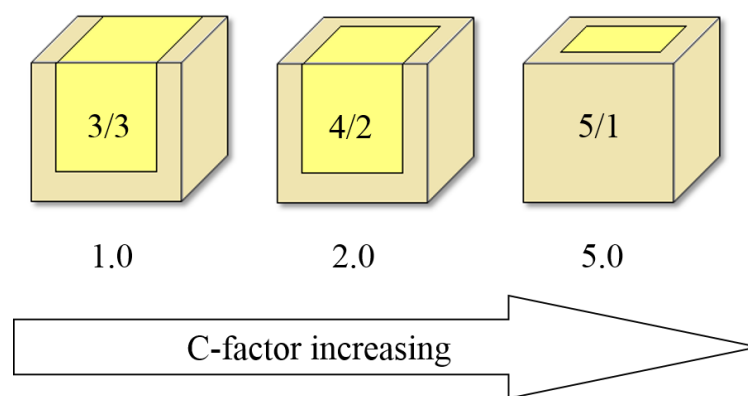
Figure 1.8 Cavity configuration factor (C-factor).

Different methods have been suggested to reduce polymerization shrinkage strain, for example, using low-shrinkage monomers [38, 172], increasing filler content [119], placing RBCs with incremental technique [179] and curing RBCs via the soft-start technique [60]. Monomer chain length, molecular weight and functionality mainly determine the polymerization shrinkage strain [7, 28, 180]. As mentioned in 1.2.1, the long-chain monomer with high molecular weight leads to low polymerization shrinkage strain [119, 180]. The amount of monomer undergoing polymerization per

volume unit depends on the monomer functionality, which also affects the polymerization shrinkage strain [32]. With updated monomer and filler technology, bulk-fill RBCs show lower polymerization shrinkage strain compared to conventional RBCs with similar consistency [171, 181]. However, due to its high C-factor, the bulk filling technique may cause a sudden shrinkage and more cuspal deflection at the early stage of polymerization [76].

The majority of polymerization shrinkage strain occurs in the initial seconds after irradiation and half amount of strain develops in the first second [170]. Thus, long enough exposure duration is recommended to avoid post-irradiation shrinkage strain [170]. The complete polymerization represents higher DC and more free volume reduction, which explains why polymerization shrinkage strain increases with DC [64, 138]. Pre-heating has a similar influence on polymerization shrinkage strain, but the improved flowability after pre-heating could compensate for the marginal issues [2, 182].
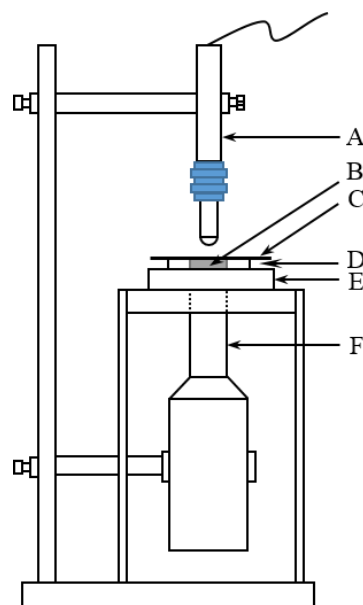
Figure 1.9 Instrument for bonded-disk shrinkage strain measurement. A, LVDT transducer; B, specimen; C, glass cover-slip; D, brass ring; E, rigid glass slide; F, light-curing unit.

There are various methods described to measure polymerization shrinkage strain, including mercury dilatometry, Archimedes' principles of buoyancy and the bonded-

disk technique [74, 75, 182, 183]. For the commonly used bonded-disk technique (Figure 1.9), composite pastes are placed into a brass ring, which is firmly bonded to a thick glass slide. The upper surface of composites is covered by a compliant glass cover-slip to ensure low C-factor (0.5-1.0), which could bear the developed shrinkage stress [176]. A calibrated linear variable displacement transducer (LVDT) probe contacts the centre of the cover-slip. Once light irradiates from the bottom, shrinkage occurs and the vertical displacement is monitored by the LVDT probe. Since there is no change in the specimen circumference, the vertical thickness change is approximately equivalent to the volumetric shrinkage strain of the specimen [183]. Recently, technologies like micro-Computed Tomography (μCT), Optical Coherence Tomography (OCT) and digital volume correlation (DVC) enable visualization of volumetric shrinkage changes and local strains and study of correlations between polymerization shrinkage and formed interfacial gaps [170, 171, 181].

1.10 Wear resistance

In the oral environment, there are many wear processes between the opposite teeth or restorative materials [184, 185]. Surface substrates are gradually removed after mechanical friction and may lead to pathological damage to teeth and restoration failure [184, 186]. Therefore, it is important to assess the wear behaviour and improve the wear resistance of natural teeth and restorative materials. Generally, there are four types of wear mechanisms, including 1) adhesive wear, 2) abrasive wear, 3) fatigue wear and 4) corrosive wear [185-187].

RBCs composition, such as monomer formulation, filler characteristics and the quality of the filler/matrix interface, influence their physical and mechanical properties [11, 185]. And in turn, these properties also affect wear resistance [185]. The wear of the soft resin matrix is higher than that of filler particles [188]. Thus, the addition of filler particles reinforce the matrix and improve the wear resistance. Filler size, shape and content all have effects on wear resistance [185, 189]. Small filler particles with high filler content may shorten the inter-particle distance and enhance

the wear resistance [187, 189, 190]. Nanofilled composites show higher wear resistance compared to microfilled composites, due to the superior filler/matrix interface [187, 191]. With an identical filler size, the increased specific surface area of the irregular shaped filler enables higher wear resistance than that of RBCs with round fillers [189].

The clinical assessment of wear behaviour includes direct and indirect methods. The former is based on the *United States Public Health Service* (USPHS) criteria [186, 192]. Three categories, alpha (no wear), bravo (detectable wear) and charlie (excessive wear), define the wear extent [192]. The latter includes comparing replica models of the restoration with a calibrated reference and using a 3D scanning system to compare sequential three-dimensional images [186, 192].

Assessment of wear resistance in the laboratory involves two aspects: wear simulation and wear analysis. Different wear machines are developed to simulate all wear conditions or the specific wear mechanism [193]. However, due to distinct operational concepts and measurement setup, results are hard to compare [185]. Wear analysis/measurement is about comparing related properties before and after wear simulations, such as gloss, surface roughness and volume loss [185, 194, 195]. A smooth surface is essential to reduce bacterial accumulation and prolong restoration longevity [196]. Gloss and surface roughness are commonly studied to illustrate wear resistance of RBCs. They are related to material inherent characteristics and measurement setup during wear simulations [105, 190, 196-199]. The smooth surface often has high gloss and low surface roughness [190].

1.11 Creep behaviour

The viscoelasticity of RBCs enables them to have both viscous and elastic properties against the applied force [4, 127]. The viscoelastic behaviour can be explained by a mechanical model containing spring and dashpot [4]. According to Hooke's law, the applied stretching force (F) on the spring is proportional to its displacement (x). Thus,

it can be deduced that the stress (σ) is proportional to the strain (ε), with the elastic modulus (E) as the constant:

$$\sigma = E\varepsilon \quad \text{(Equation 1.3)}$$

When pulling the dashpot, the fluid viscosity (η) is the constant of the proportionality between shear stress (τ) and the shear strain rate (dε/dt), in which the stress is time-dependent:

$$\tau = \eta\frac{d\varepsilon}{dt} \quad \text{(Equation 1.4)}$$
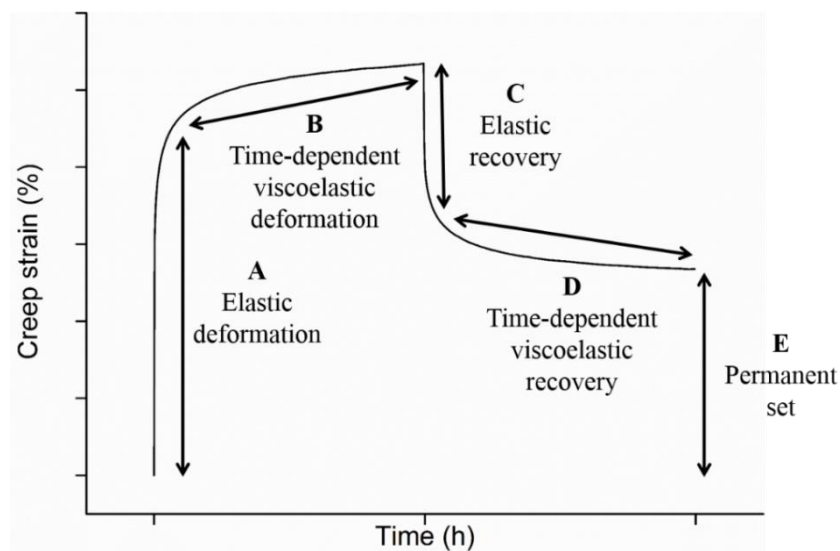
Figure 1.10 Creep strain curve.

The ideal paralleled spring/dashpot mechanical model demonstrates the viscoelastic behaviour and the static creep strain curve is shown in the Figure 1.10. The creep obtained is known as static creep. The maximum creep strain, maximum creep recovery, permanent set and creep recovery % are calculated as:

$$\text{Maximum creep strain} = A + B \quad \text{(Equation 1.5)}$$

$$\text{Maximum creep recovery} = C + D \quad \text{(Equation 1.6)}$$

$$\text{Permanent set} = E \quad \text{(Equation 1.7)}$$

$$\text{Creep recoveery \%} = \frac{C+D}{A+B} \times 100\% \quad \text{(Equation 1.8)}$$

In addition to static creep, dynamic creep usually happens under altered stress during fatigue tests [200, 201].

Creep behaviour and stress relaxation of RBCs are important to their dimensional stability and long-term performance. The rigid monomer structure presents good resistance against the applied load [202, 203]. With increased filler content, the reinforcement effect improves and creep strain decreases [202, 204]. DC is related to monomer composition and affects creep behaviour [203]. The more complete the polymerization, the higher the DC and the less creep deformation [200, 205]. Water absorption increases swelling stress within the resin matrix [201]. The resulted plasticization effect may lead to debonding between filler/matrix interfaces, which increases creep strain and reduces the percentage of creep recovery [202]. Temperature also influences creep behaviour. Elevated temperature may result in high creep deformation and a low percentage of creep recovery [206].

1.12 Surface hardness

The surface hardness of RBCs refers to their resistance to the indentation or local deformation [4, 185]. Hardness is calculated based on the measurement principle and is not an intrinsic material property [185]. Various surface hardness measurements have been widely used to determine the extent of polymerization and indirectly reflect the depth of cure [207]. During measurement, an indenter with a standardized load or weight is pressed into the specimen surface for a fixed period [185]. Once the indenter is removed, the width and area of the symmetrically shaped indentation are recorded under a microscope and calculated into hardness results [4].

To obtain reproducible results and avoid damaging specimens with over-range load/indentation, different ranges of measurement, macro-, micro- and nano-scaled, are used [185]. The classically used indentation or scratch tests include Vickers, Knoop, Rockwell, Brinell, Barcol and Shore A hardness [4, 75, 185]. Since the surface deformation happens with both elastic and viscous components, a dynamic

measurement is recommended to monitor the development of indentation depth with the applied load throughout the testing cycle [185]. Nano-indentation can apply milligram-ranged force and is useful to determine material hardness, elastic modulus and fracture toughness [4, 208].

Hardness is sensitive to filler characteristics so that high filler content with small filler size may increase composite hardness [75, 135, 209, 210]. The bottom/top surface hardness ratio describes the extent of polymerization and depth of cure [1, 75]. A ratio of more than 80 % is often taken to indicate adequate polymerization throughout the composite thickness [169]. Due to the decreased light transmission, bottom surface hardness reduces with the composite thickness [18, 209, 211]. Small filler size and the new photo-initiator systems may enhance translucency and depth of cure of composites and thus the overall DC and hardness [209]. Some studies found a positive correlation between hardness and DC [1, 212]. Because polymerization continues at post-irradiation, there are higher hardness results after 24 h or a longer storage period [162, 211, 213]. Pre-heated composites show a greater depth of cure and surface hardness than that of non-heated composite, due to the improved monomer mobility and DC [1, 135, 211, 213].

External factors, such as indentation optical reading, sampling sites and load/period applied, also affect hardness results [75, 185]. The smooth samples should be well prepared and perpendicularly placed under the indenter to obtain a regular indentation shape and accurate reading [185]. The applied load and period also need to be controlled precisely to avoid sample damage.

1.13 Fracture toughness

Bulk fracture and secondary caries are the common reasons for replacing restorations [214]. The ability to resist crack propagation under stress without fracture is known as fracture toughness [207, 215]. It is an intrinsic property of the material and should be independent of measurement methods and sample geometry [185]. In the early 20th

century, Griffith realized that due to the existence of inherent flaws, brittle materials have low fracture toughness [215-217]. Later, Irwin found that ductile materials have similar crack growth within their plastic parts [215, 218]. Then he termed the stress field around the sharp crack tip as stress intensity factor, K [215, 218]. The critical stress intensity value is called K_c, in which minimal plastic deformation happens [185]. There are different failure modes can be conducted: (I) plane strain, (II) plane stress and combined mode [185, 215, 219]. Fracture toughness of RBCs correlates to their clinical fractures, marginal breakdown and wear resistance [185, 219, 220]. Thus, it is vital to evaluate fracture toughness to predict and prevent clinical failure.

Numerous methods are available to characterize fracture toughness, including compact tension, double torsion, chevron notch, indentation fracture, indentation strength and single-edge notch three-point bending (SENB) [185, 216]. SENB is the most commonly used method, in which the load is applied upon the notched beam, causing crack propagation and beam fracture (Figure 1.11) [185, 219, 221]. The notch can be created in different ways, for example, packing material around the sharp blade within the mould and sawing the sample after preparation [219]. The former may result in a resin-rich area at the notch tip and lead to low resistance to the crack propagation. The latter is more accurate and easier to control.
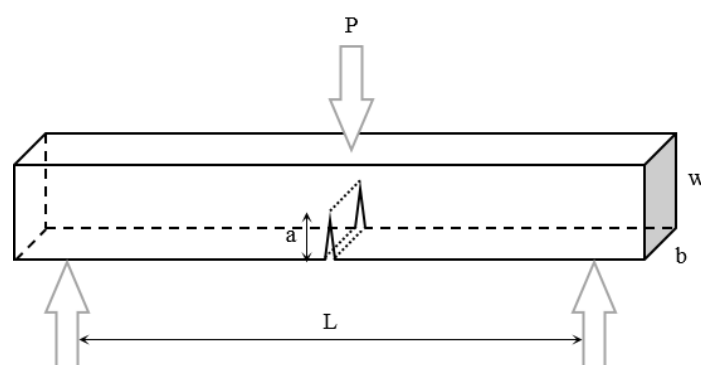
Figure 1.11 Specimen geometry for determination of fracture toughness by SENB. P, load at fracture; a, notch length; w, width of the specimen; b, thickness of the specimen; L, distance between the supports.

Some studies investigated the fracture toughness of various categories of commercial dental composites. They concluded that glass ionomer cement (GIC) has the lowest

fracture toughness, whereas ORMOCER-based, packable and micro-hybrid RBCs have the highest values [215, 219, 222]. Bulk-fill RBCs also exhibit high fracture toughness [222]. This may be attributed to their composition. Crack propagation needs more energy to grow between the randomly distributed particles [223]. Therefore, high filler volume, especially combined with small particles, may increase fracture toughness [215, 221, 223]. However, beyond the critical filler volume (55-65 vol.%), fracture toughness may remain constant or decrease [215, 223]. High composite viscosity causes more voids/porosities within specimen, which makes it more susceptible to fracture [215]. However, some studies reported weak correlations between fracture toughness and filler volume [215, 224]. Other filler properties, such as particle agglomeration and distribution, may also influence fracture resistance [215]. The addition of fibers could improve fracture toughness and this relates to fiber length and diameter [207, 221]. Resin matrices with high strength may lead to a more solid network and higher fracture toughness [221, 223].

In addition to composition, fracture toughness depends on storage condition, measurement setup and clinical manipulation [207, 221-223]. After water storage, hydrolysis occurs at the filler/matrix surface. The degradation and deterioration of the cross-linked matrix may reduce fracture toughness and other mechanical properties [221, 225]. Theoretically, fracture toughness results are independent of testing methods. However, Fujishima et al. compared four testing methods and found that fracture toughness results are method dependent [226]. Pre-heating material prior placement could ease the insertion and avoid voids and air entrapment. The tip of the notch is often sharpened cautiously using a razor blade or abrasive paste to create the true pre-crack [185]. Samples are sensitive to the notch size, which makes it difficult to compare fracture toughness values among studies [221, 223]. Hence, identical sample preparation and measurement settings are required to ensure valid results.

Chapter Two
Aims and Objectives

Viscalor, as used in this study, was a pre-market experimental version. The exact formulation is unknown. Therefore results obtained may differ from those measured using the final commercial version.

The overall aims of this study were:

To investigate temperature effects on the pre-cure and post-cure properties of *Viscalor* and compare it with a wide range of commercial RBCs.

The specific objectives of this study were:

Chapter 3:

Using a probe method to investigate the effects of probe withdrawal speed and temperature on stickiness behaviour of different RBCs and to investigate the effect of pre-heating time on stickiness of *Viscalor*.

Chapter 4:

Using a probe method to assess the effects of probe penetration distance, probe packing speed and temperature on packability of a wide range of RBCs and to investigate the effect of pre-heating time on packability of *Viscalor*.

Chapter 5:

To measure temperature effects on stickiness and packability of different RBCs and to investigate the effect of pre-heating time on pre-cure properties of *Viscalor*, including extrusion forces.

Chapter 6:

To evaluate effects of pre-heating time and exposure duration on the degree of conversion (DC), maximum rate of polymerization (RP_{max}), polymerization shrinkage strain (PS) and surface micro-hardness (VHN) of *Viscalor*.

Chapter 7:

To measure gloss and surface roughness of different RBCs before and after toothbrushing simulations and to investigate the effect of pre-heating time on surface profiles of *Viscalor*.

Chapter 8:

To determine the effect of variations in composition of RBCs on their creep behaviour under different storage conditions and to assess the effect of pre-heating time on the viscoelastic stability of *Viscalor*.

Chapter 9:

To determine polymerization shrinkage strain (PS), maximum rate of polymerization shrinkage strain (PS R_{max}) and fracture toughness (K_{IC}) of different types of bulk-fill composites and to investigate the effect of pre-heating time on PS, PS R_{max} and K_{IC} of *Viscalor*.

The general outline of the studies is shown in Figure 2.1.
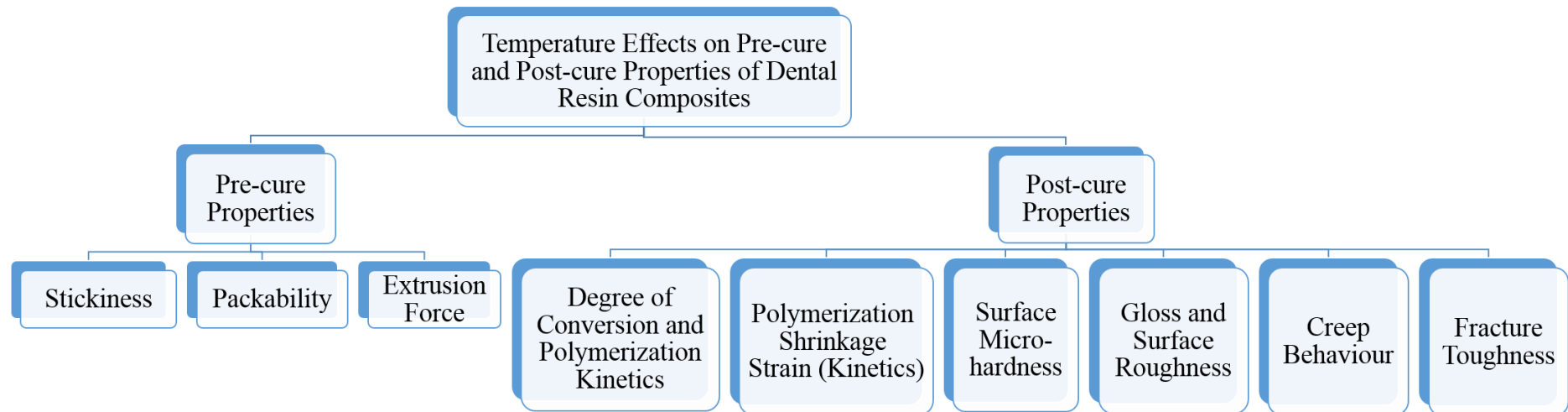
Figure 2.1 General outline of this study.

Chapter Three

Effects of Pre-heating and Experimental Setting on Stickiness of Resin-based Composites

Abstract

Objectives. To determine the effects of probe withdrawal speed (2, 4, 6, 8 and 10 mm/s) and temperature (22 and 37 °C) on stickiness parameters: maximum separation force (F_{max}) and work of probe-separation (W_s) of different unset resin-based composites (RBCs); and to investigate the effect of pre-heating time on *Viscalor* stickiness.

Methods. A Texture Analyzer was used to determine stickiness parameters (F_{max} and W_s) of RBCs. *Viscalor* was pre-heated using a Caps Warmer (VOCO, Germany) in T3 mode (at 68 °C) for 30 s (T3-30s) and 3 min (T3-3min), respectively. The composite paste was packed into a cylindrical cavity (7 mm $\times$ 5 mm) controlled at either 22 or 37 °C. A flat-ended probe was lowered into the composite paste at a constant speed until a pre-set force was reached, then the probe descended at different speeds. The peak height in the force/displacement plot was the maximum separation force (F_{max}, N) and the integrated area under the curve was the work of probe-separation (W_s, N mm). Data were analysed using one-way ANOVA, independent T-test and Tukey post-hoc tests ($p<0.05$).

Results. Stickiness parameters (F_{max} and W_s) varied with tested RBCs ($p<0.001$) and increased with probe withdrawal speed. However, F_{max} ($p=0.523$) and W_s ($p=0.765$) did not significantly change between 8 and 10 mm/s. Temperature rise increased W_s ($p<0.001$), but reduced F_{max} ($p<0.001$). Pre-heating *Viscalor* for either 30 s or 3 min increased W_s ($p<0.001$), whereas reduced F_{max} ($p=0.007$).

Significance. F_{max} and W_s were useful parameters to describe RBC stickiness and influenced by material composition, probe withdrawal speed and temperature. Pre-heated *Viscalor* showed higher W_s and lower F_{max} than room-temperature *Viscalor*. A long pre-heating period of 3 min increased W_s but did not significantly change F_{max}.

Key words: resin-based composite; handling properties; stickiness; pre-heating

3.1 Introduction

Resin-based composites (RBCs) have gradually replaced amalgams and been widely used in dentistry for decades. To save chairside operating time and achieve good clinical performance, 'technique sensitivity' should be minimized [75]. It depends not only upon clinician skills but also on material handling properties [152]. The pre-cure handling characteristics, including ease of placement, flowability and stickiness, mainly determine the success and longevity of the restoration [138].

Stickiness indicates how sticky a material is to the cavity wall and instrument during manipulation. The material stickiness to the cavity wall and instrument should be balanced [126, 128]. Adequate stickiness of material to the cavity wall helps to ensure marginal integrity. However, high material stickiness to the instrument may lead to air entrapment and void formation in the restoration [127]. With the development of the probe method, stickiness data of different types of RBCs have been studied and discussed [126-128]. Generally, there are two types of force/displacement plots (Type I and Type II) obtained during stickiness measurement [128]. The former has a single peak, and the latter has two peaks. The peak height represents the maximum force obtained during probe-separation (F_{max}, N). The area under the curve is calculated as the work of probe-separation (W_s, N mm).

Rheological behaviour mainly determines RBC pre-cure handling properties, such that high-viscous composites tend to have low stickiness [84, 156]. This is also related to the material composition. Due to its chemical structure, bis-GMA has a higher viscosity than other monomers, which may limit the monomer mobility and reduce the final degree of conversion [31, 111]. Diluent monomers or viscosity controllers are added to modify the viscosity of the monomer system and improve filler loading [34]. However, highly filled packable composites exhibit high viscosity, which may lead to poor marginal adaptation and restoration failure [1]. At a constant filler volume, large filler particles or round filler particles may reduce viscosity [84, 86, 128]. The former enables low filler loading, and the latter reduces friction between

particles. Lightly filled flowable RBCs are available with easy manipulation, however the resultant high polymerization shrinkage still limits their usage [83, 116].

According to the Arrhenius Equation (Equation 1.1), viscosity decreases with temperature in an exponential relationship [34].

$$\eta = Ae^{E_a/RT} \qquad \text{(Equation 1.1)}$$

Thus, 'pre-heating' or 'pre-warming' were proposed for use before clinical manipulation for easier extrusion and better adaptation to the cavity [1, 2, 113, 116, 132]. Higher temperatures may lead to relatively higher stickiness due to the enhanced wettability between composites and instruments [126, 156]. However, some studies found that temperature rise makes materials more extensible and reduces stickiness [128, 151]. Different results may be attributed to various tested composites and experimental setups.

Thus, the objectives of the present study were to investigate the effects of probe withdrawal speed and temperature on pre-cure stickiness parameters (F_{max} and W_s) of different unset RBCs and to determine the effect of pre-heating time on *Viscalor* stickiness. The Null Hypotheses of this study were:
(1) there were no differences between the stickiness parameters (F_{max} and W_s) of different tested composites,
(2) F_{max} and W_s did not vary with probe withdrawal speed,
(3) F_{max} and W_s did not vary with temperature and
(4) pre-heating time did not affect *Viscalor* stickiness.

3.2 Materials and methods

Five commercial RBCs and *Viscalor*, pre-heated using a Caps Warmer (VOCO, Germany), were investigated (Table 3.1).

Table 3.1 Manufacturer information of investigated composites.

Materials	Code	Manufacturer	Resin system	Filler vol.%	Filler wt.%
Admira Fusion	**AF**	VOCO, Germany	ORMOCER®	-	84
Filtek Supreme Ultra	**FSU**	3M ESPE, St. Paul, USA	bis-GMA, UDMA, TEGDMA, bis-EMA	63.3	78.5
TPH LV	**TPH**	Dentsply, Germany	Urethane modified bis-GMA, TEGDMA, polymerizable dimethacrylate	54.6	75.5
Tetric EvoCeram	**TEC**	Ivoclar Vivadent, USA	bis-GMA, urethane dimethacrylate, bis-EMA	54	75
Harmonize	**HZ**	Kerr, USA	bis-GMA, bis-EMA, TEGDMA	64.5	81
Viscalor	**VC**	VOCO, Germany	bis-GMA, aliphatic dimethacrylate	-	83

A Texture Analyzer (Figure 3.1) (TA.XT2i, Stable Micro Systems, Godalming, Surrey, UK) was used to measure stickiness parameters: maximum separation force (F_{max}, N) and work of probe-separation (W_s, N mm). The applied force was measured by a force transducer, which connected to the stainless-steel probe (ϕ =6 mm). The composite paste was carefully packed into a brass cavity (ϕ = 7 mm, depth = 5 mm) controlled at either 22 or 37 °C (Figure 3.2) (n=5). *Viscalor* was pre-heated using a Caps Warmer in T3 mode (at 68 °C) for 30 s (T3-30s) and 3 min (T3-3min), respectively (Figure 3.3).
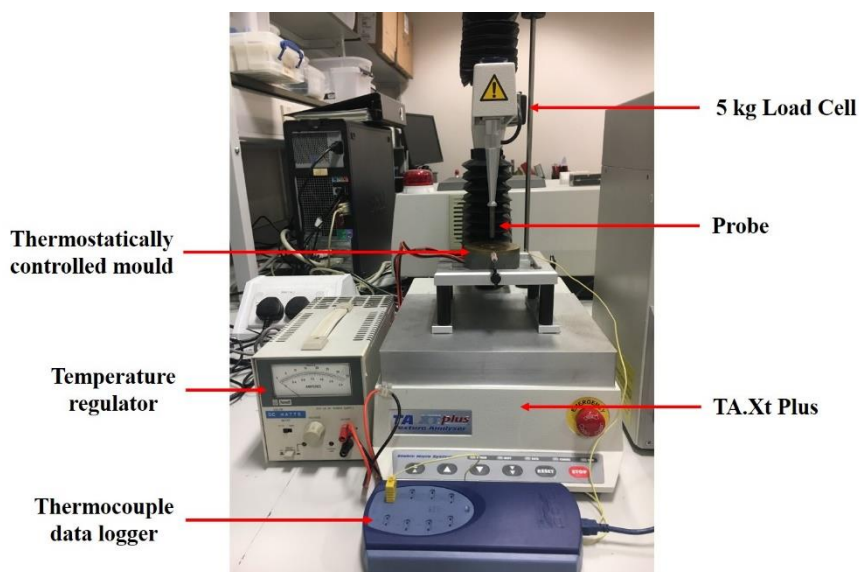
Figure 3.1 Experimental setup used for stickiness measurement.
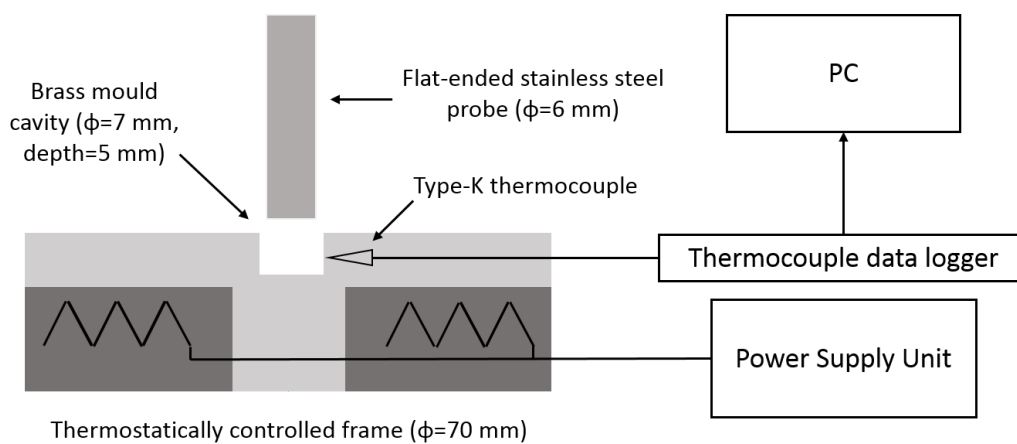
Figure 3.2 Mould setup with temperature regulation.

Figure 3.3 Caps Warmer (VOCO, Germany).

During the 'bonding' phase, the probe descended onto and into the surface of the unset composite paste at a pre-test speed of 0.50 mm/s. When a 'trigger' force of 0.05 N was registered, data acquisition commenced at a rate of 400 p/s. Composite paste started deforming and wetting the probe. The probe continued moving down at a test speed of 0.50 mm/s until a compressive force of 1 N was recorded. In the subsequent 'debonding' phase, the probe ascended at a pre-determined speed of 2, 4, 6, 8 and 10 mm/s. Since the composite paste adhered to the probe, it elongated and exerted tensile force on the probe. With further elongation, tensile stress increased until it reached the interfacial strength and the composite paste separated from the probe.

Data were entered into statistical software (SPSS, SPSS Inc., Illinois, USA) and analysed using one-way ANOVA, independent T-test and Tukey post-hoc tests ($p<0.05$). Homogeneity of variance was calculated using the Kruskal-Wallis Test ($p<0.05$).

3.3 Results

In the present study, the RBCs varied in F_{max} ($p<0.001$) and W_s ($p<0.001$). The subsets for F_{max} and W_s are shown in Table 3.2 and 3.3. Admira Fusion and TPH LV showed the highest and the lowest F_{max} and W_s, respectively.

F_{max} and W_s measured at different probe withdrawal speeds are summarised in Tables 3.4-3.5 and Figures 3.4-3.5. F_{max} and W_s ranged from 1.50 to 5.59 N and from 0.79 to 5.81 N mm, respectively. F_{max} and W_s increased with probe withdrawal speed and there were no significant differences between 8 and 10 mm/s for both F_{max} ($p=0.523$) and W_s ($p=0.765$).

Temperature rise significantly reduced F_{max} ($p<0.001$) but increased W_s ($p<0.001$) (Figure 3.6). However, the increased temperature had no significant effects on F_{max} of TPH LV ($p=0.866$), Harmonize ($p=0.289$), *Viscalor* (no heat) ($p=0.096$) and W_s of Filtek Supreme Ultra ($p=0.887$).

Pre-heating *Viscalor* for either 30 s or 3 min increased W_s (p<0.001), but reduced F_{max} (p=0.007) (Figure 3.7). A long pre-heating period of 3 min did not significantly reduce F_{max} at 22 (p=0.785) and 37 °C (p=0.163), but significantly increased W_s at 22 (p=0.004) and 37 °C (p<0.001).

Table 3.2 Materials subsets identified by post-hoc Tukey test for F_{max}.

F_{max}	1 (p=1.000)	2 (p=0.136)	3 (p=0.220)	4 (p=1.000)
	TPH	HZ	TEC	AF
		VC (T3-30s)	VC (T3-3min)	
		TEC	FSU	
		VC (T3-3min)	VC (no heat)	
		FSU		

Table 3.3 Materials subsets identified by post-hoc Tukey test for W_s.

W_s	1 (p=0.670)	2 (p=0.125)	3 (p=0.856)	4 (p=0.409)	5 (p=0.691)
	TEC	FSU	HZ	VC (no heat)	AF
	TPH	HZ	VC (no heat)	VC (T3-30s)	VC (T3-3min)
	FSU				

Table 3.4 Stickiness parameter: F_{max} (N) at different probe withdrawal speeds at 22 and 37 °C.

Materials	F_{max} (N) at 22 °C					F_{max} (N) at 37 °C				
	2 mm/s	4 mm/s	6 mm/s	8 mm/s	10 mm/s	2 mm/s	4 mm/s	6 mm/s	8 mm/s	10 mm/s
Admira Fusion	3.28[a A] (0.10)	4.06[a B,G] (0.20)	5.38[a C] (0.20)	5.59[a C,D] (0.12)	5.90[a D] (0.08)	3.12[a A] (0.08)	3.81[a B] (0.22)	4.35[a E,G] (0.29)	4.74[a E,F] (0.26)	4.93[a F] (0.30)
Filtek Supreme Ultra	2.94[b A] (0.04)	4.11[a B] (0.08)	4.41[b C] (0.08)	4.54[b C] (0.10)	4.53[b C] (0.06)	2.07[b D] (0.02)	2.82[b,c A] (0.05)	3.35[b,d,f E] (0.10)	3.85[b F] (0.07)	3.77[b,e F] (0.07)
TPH LV	1.91[c A] (0.06)	2.55[b B] (0.08)	2.91[c C,E] (0.09)	2.82[c C,E,F] (0.05)	2.79[c C,F] (0.06)	1.50[c D] (0.14)	2.69[b B,F] (0.06)	2.74[c B,C,F] (0.09)	2.92[c C,E] (0.13)	3.02[c E] (0.17)
Tetric EvoCeram	2.86[b,e A] (0.04)	3.65[c B,E,F] (0.06)	3.81[d B,C,F] (0.07)	3.92[d B,C] (0.05)	4.11[d C] (0.08)	2.21[b D] (0.11)	3.40[e E] (0.22)	3.44[b E] (0.28)	3.54[d,e E,F] (0.16)	3.57[b,d E,F] (0.27)
Harmonize	2.51[d,f A] (0.04)	3.35[d B] (0.05)	3.57[e C,G] (0.06)	3.64[e C,D] (0.08)	3.63[e C,D,G] (0.07)	1.70[d E] (0.06)	3.00[c,d F] (0.08)	3.41[b,d B,G] (0.07)	3.83[b,d D] (0.23)	3.77[b,e C,D] (0.15)
Viscalor **(no heat)**	3.03[b A] (0.21)	3.65[c B] (0.28)	3.82[d B] (0.07)	4.47[b C] (0.11)	5.06[f D] (0.03)	2.19[b E] (0.07)	3.20[d,e A] (0.14)	3.82[e B] (0.03)	4.48[a C] (0.02)	4.41[f C] (0.08)
Viscalor **(T3-30s)**	2.67[d,e A] (0.08)	3.40[c,d B] (0.07)	3.89[d C] (0.05)	4.26[f D] (0.14)	4.58[b E] (0.04)	2.17[b F] (0.08)	2.58[b A] (0.11)	3.03[c,f G] (0.12)	3.26[e B] (0.08)	3.33[c,d B] (0.10)
Viscalor **(T3-3min)**	2.39[f A] (0.09)	3.52[c,d B] (0.08)	3.91[d C] (0.16)	4.39[b,f D] (0.06)	4.91[f E] (0.24)	2.19[b A] (0.11)	2.69[b F] (0.05)	3.10[d,f G] (0.07)	3.50[e B] (0.04)	4.01[e C] (0.22)

For each speed, the same lower case superscript letters indicate homogeneous subsets among the materials. For each material, the same CAPITAL superscript letters indicate homogeneous subsets among different conditions.

Table 3.5 Stickiness parameter: W_s (N mm) at different probe withdrawal speeds at 22 and 37 °C.

Materials	W_s (N mm) at 22 °C					W_s (N mm) at 37 °C				
	2 mm/s	4 mm/s	6 mm/s	8 mm/s	10 mm/s	2 mm/s	4 mm/s	6 mm/s	8 mm/s	10 mm/s
Admira Fusion	2.12[a A] (0.22)	2.42[a A] (0.23)	3.33[a B] (0.24)	3.59[a B,C] (0.18)	4.19[a C,D] (0.25)	3.61[a B,C] (0.74)	3.67[a B,C] (0.30)	4.21[a C,D] (0.27)	4.85[a D] (0.17)	4.77[a D] (0.23)
Filtek Supreme Ultra	1.26[b,d A] (0.09)	1.56[c B,F] (0.14)	1.81[b,c B,C] (0.17)	2.02[b C,D] (0.10)	2.22[b D] (0.16)	0.97[b E] (0.09)	1.41[b A,F] (0.04)	1.80[b B,C] (0.14)	2.26[b D,G] (0.08)	2.52[b,c G] (0.19)
TPH LV	0.88[b,c A] (0.03)	1.09[b A,B] (0.10)	1.56[c,d C,D] (0.06)	1.81[b,c D,E] (0.05)	1.91[b E,F,G] (0.08)	1.30[b,c B,C] (0.17)	1.88[b E,F] (0.17)	2.05[b,c E,F,G] (0.20)	2.16[b F,G] (0.21)	2.19[c,d G] (0.16)
Tetric EvoCeram	0.79[c A] (0.06)	1.03[b A,B] (0.06)	1.24[d B,C] (0.11)	1.48[c C,D] (0.04)	1.84[b D,E] (0.07)	1.29[b,c B,C] (0.15)	1.58[b C,D] (0.30)	1.64[b C,D] (0.25)	2.14[b E] (0.17)	2.08[d E] (0.37)
Harmonize	1.04[b,c,d A] (0.04)	1.34[b,c A,B] (0.08)	1.67[b,c,d B,C] (0.15)	1.93[b,c C] (0.11)	2.00[b C] (0.11)	2.03[d C,D] (0.13)	2.46[c,d D] (0.50)	3.18[d E] (0.19)	3.08[c E] (0.28)	3.34[e E] (0.14)
Viscalor **(no heat)**	1.42[d A] (0.23)	1.33[b,c A] (0.12)	2.13[b B] (0.13)	2.29[b B] (0.08)	3.16[c C] (0.17)	2.35[d B,E] (0.13)	2.92[c C,D] (0.23)	2.93[d C,D] (0.28)	3.03[c C,D] (0.22)	2.72[b D,E] (0.15)
Viscalor **(T3-30s)**	2.62[e A,E] (0.21)	2.91[d A,B] (0.18)	3.19[a B] (0.19)	3.60[a C] (0.25)	3.74[d C] (0.14)	1.71[c,d D] (0.12)	1.92[b,d D] (0.26)	2.37[c E] (0.07)	2.74[c A] (0.13)	2.79[b A] (0.12)
Viscalor **(T3-3min)**	1.89[a A] (0.36)	2.07[a A,B] (0.39)	2.86[a B,C] (0.51)	3.08[d C] (0.59)	3.48[c,d C] (0.44)	4.69[e D] (0.60)	4.84[e D] (0.26)	5.22[e D,E] (0.23)	5.47[d D,E] (0.17)	5.81[f E] (0.15)

For each speed, the same lower case superscript letters indicate homogeneous subsets among the materials. For each material, the same CAPITAL superscript letters indicate homogeneous subsets among different conditions.
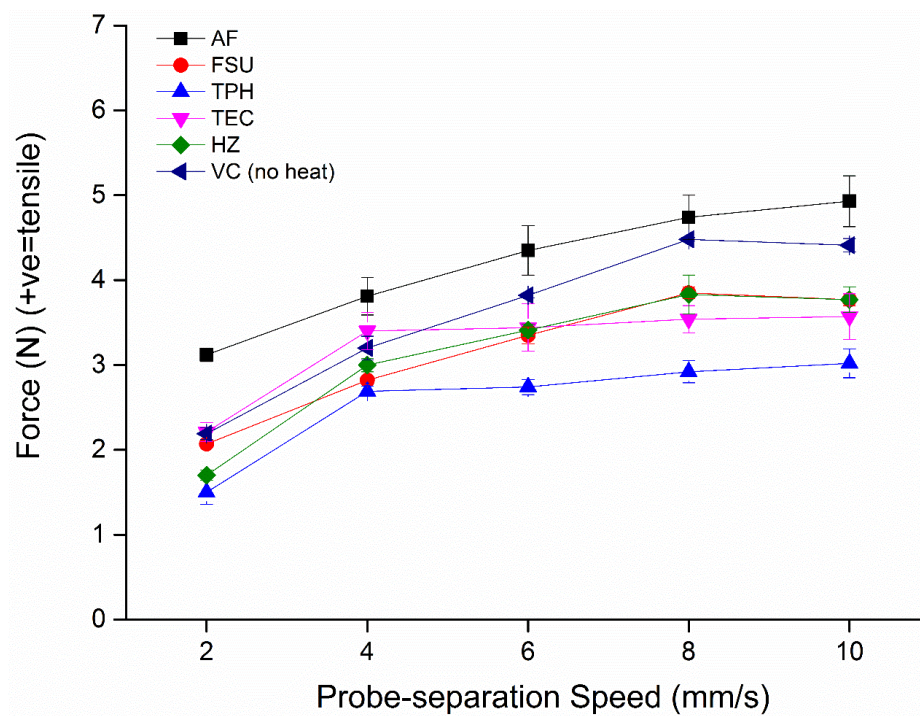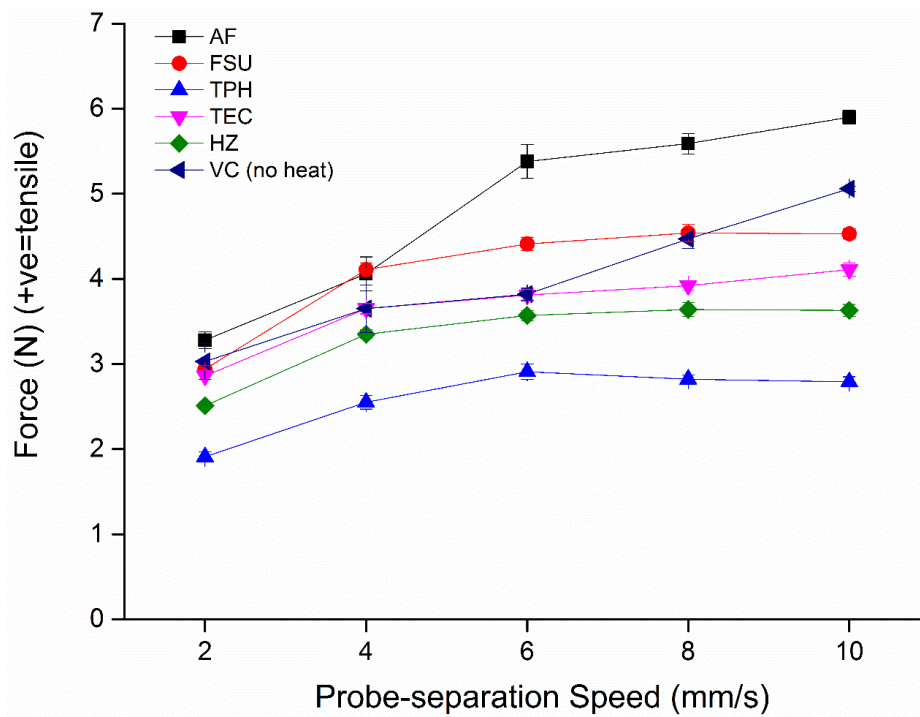
Figure 3.4 Maximum separation force (F_{max}) of different RBCs at different probe withdrawal speeds at 22 °C (top) and 37 °C (bottom).
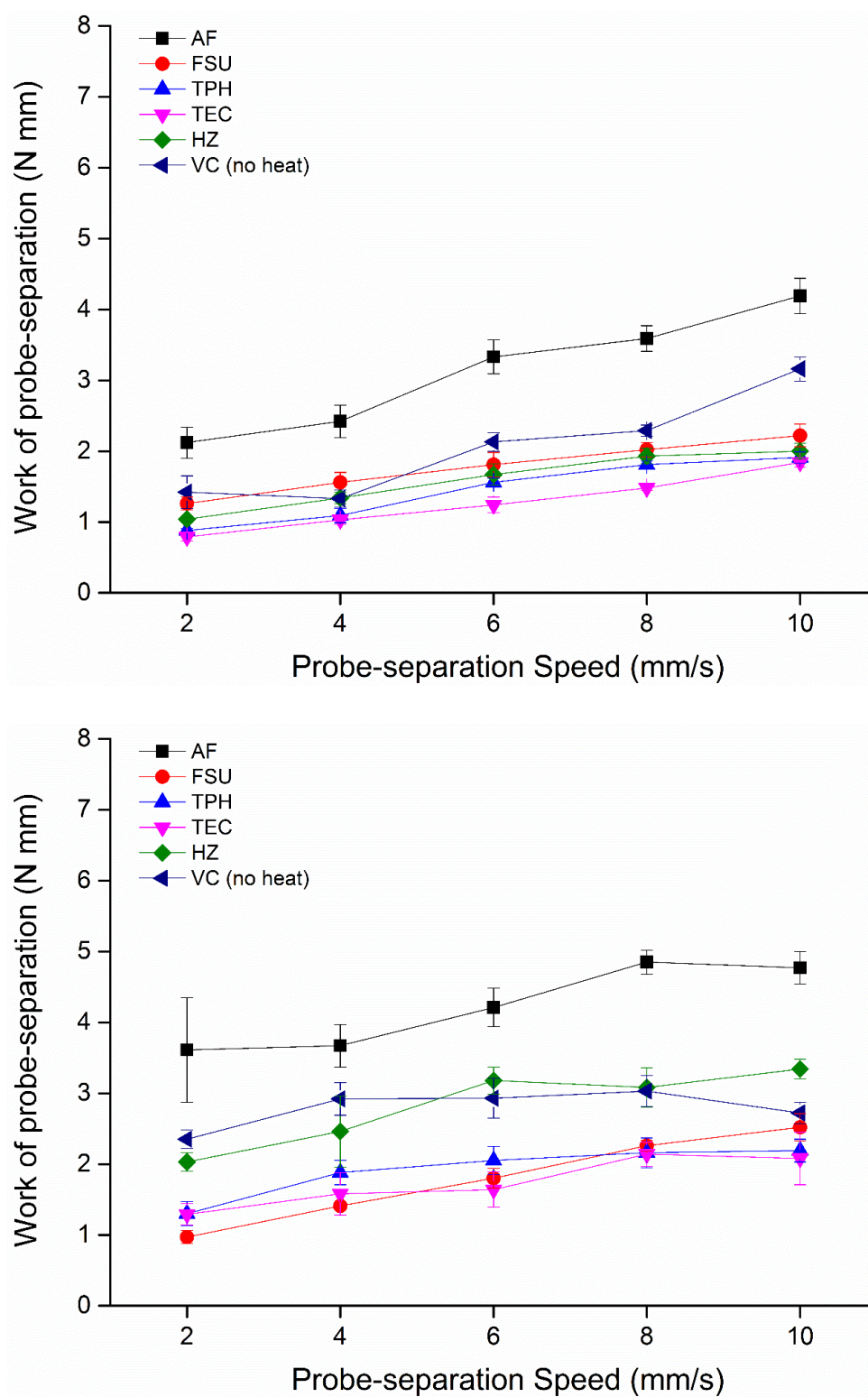
Figure 3.5 Work of probe-separation (W_s) of different RBCs at different probe withdrawal speeds at 22 °C (top) and 37 °C (bottom).
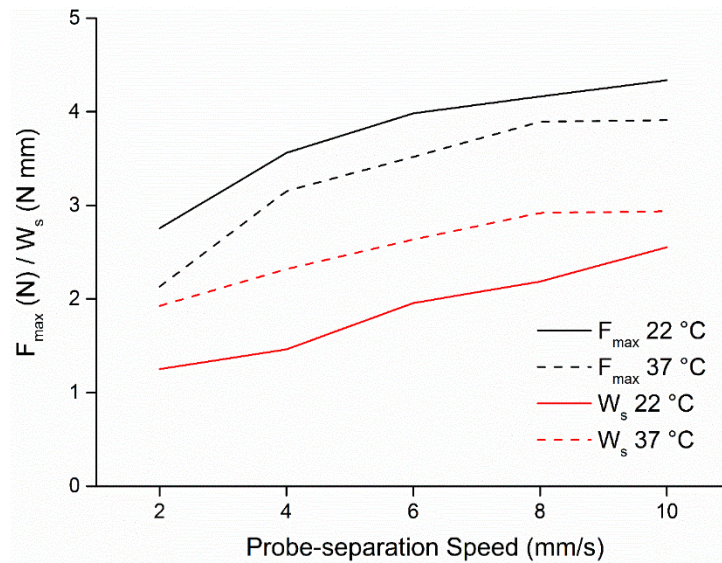
Figure 3.6 Average F_{max} and W_s development trends of investigated RBCs (except pre-heated Viscalor) at different probe withdrawal speeds at 22 and 37 °C.
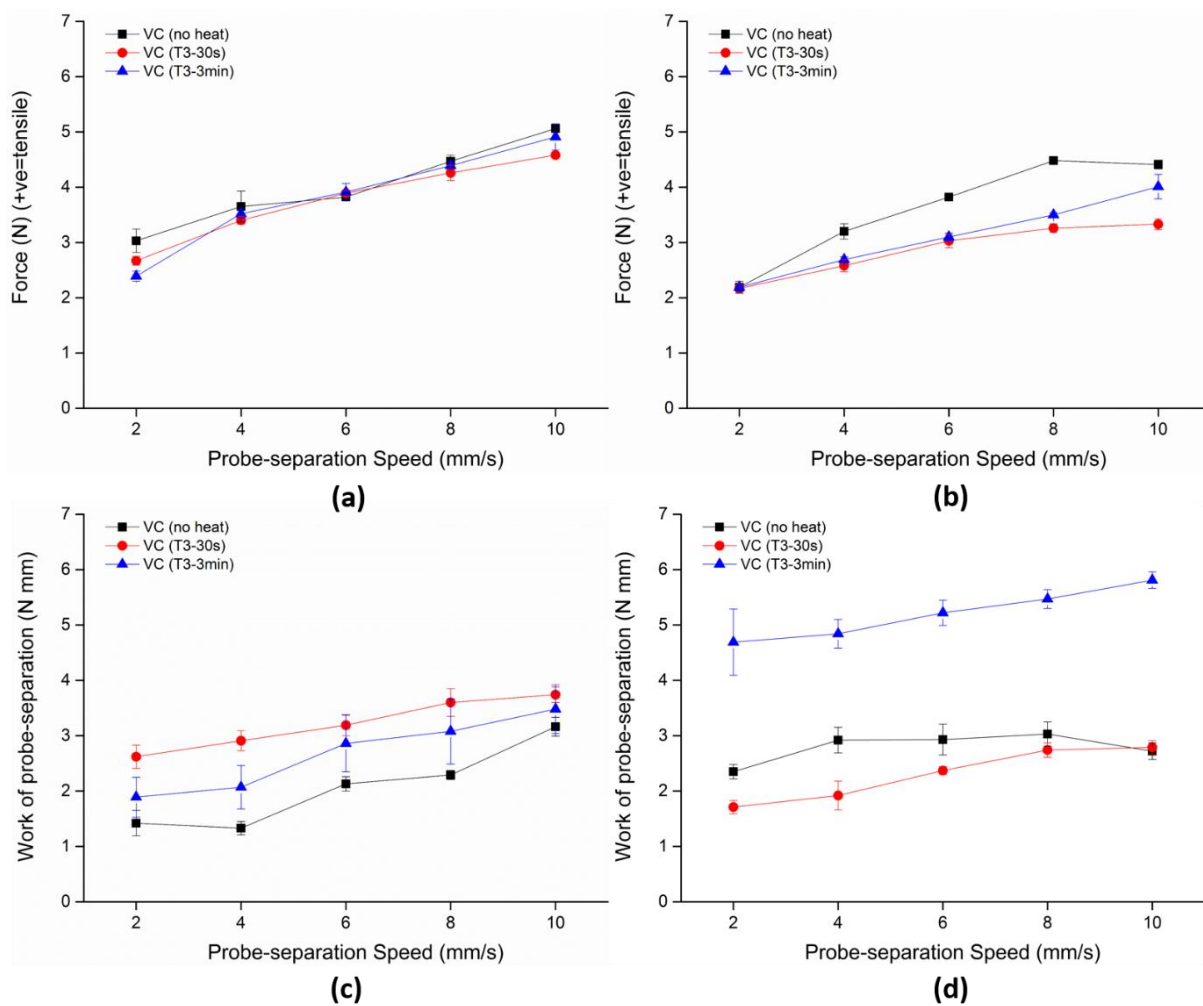
Figure 3.7 (a) & (b): F_{max}; (c) & (d): W_s of Viscalor (no heat, T3-30s and T3-3min) at different probe withdrawal speeds at 22 and 37 °C.

3.4 Discussion

Handling properties, related to the material composition and rheological nature, significantly affect the success of clinical restorations [75, 112]. According to previous studies, many factors influence stickiness parameters (F_{max} and W_s), for example, composite composition, inherent characteristics and the experimental setup [75, 126, 128, 154]. The present study investigated the effects of probe withdrawal speed and temperature on the stickiness parameters (F_{max} and W_s) of different RBCs and determined the effect of pre-heating time on *Viscalor* stickiness. Statistical analysis indicated that all the research hypotheses should be rejected ($p < 0.05$).

In the present study, stickiness parameters (F_{max} and W_s) varied between investigated RBCs. Admira Fusion showed the highest F_{max} and W_s. However, according to conclusions of Lee et al., with the highest filler loading (84 wt.%), Admira Fusion should have had low stickiness [83]. The nanoparticles of Admira Fusion are firmly combined with its ORMOCER-based organic-inorganic hybrid structure [17, 46]. Thus, without compromising viscosity, highly filled Admira Fusion showed the highest stickiness data. *Viscalor* (83 wt.%) and Harmonize (81 wt.%) also showed high F_{max} and W_s values. Harmonize has an Adaptive Response Technology (ART) filler system and TEGDMA, which reduces the viscosity and leads to high stickiness [34]. Given the similar filler loading, there were no significant differences between W_s of Filtek Supreme Ultra (78.5 wt.%), TPH LV (75.5 wt.%) and Tetric EvoCeram (75 wt.%). The small filler particle size (1.35 μm) of TPH LV increased its viscosity by improving matrix/filler interactions and led to the lowest F_{max} among the tested RBCs [112, 113, 227].

Both stickiness parameters, F_{max} and W_s, increased significantly with speed during measurement. This is in line with some previous studies [126, 128]. However, in the study of Ertl et al., F_{max} decreased with speed [156]. During the "bonding" phase, composites gradually deform and wet the probe. Once withdrawing the probe, organic molecular structures within the composites need time to relax and adjust against the

tensile stress [154]. High removal speed limits the relaxation time and thus, causes a high level of resistance - or tensile stress - and thus high F_{max} and W_s values [128]. This is also related to the inherent characteristics of composites, for example, wettability and viscoelasticity [127, 128, 156]. Good wettability ensures sufficient bonding between composites and probe, and higher elastic modulus leads to greater resistance to removal or greater tensile stress [154]. However, in this study, F_{max} and W_s showed no significant changes between the speed of 8 and 10 mm/s, which may be the upper limit for the effect of probe withdrawal speed.

Temperature increase generally reduces composite viscosity and alters their stickiness properties [127]. The present results showed that temperature rise increased W_s, but reduced F_{max}. According to conclusions of Lee et al., temperature rise reduces viscosity and increases stickiness [34, 84]. However, some investigations found that W_s could be lower at high temperatures [127, 128, 156]. With increasing temperature, composites become more extensible, which requires a lower force to separate the probe from the composite paste. However, Kaleem et al. found that F_{max} increased with temperature and attributed this to better interaction and bonding between probe and composites [126]. According to our statistical analysis, temperature rise had no significant influences on F_{max} of TPH LV, Harmonize, *Viscalor* (no heat) and W_s of Filtek Supreme Ultra. TPH LV is designed as a low-viscous composition and it showed a uniformly low F_{max} despite increased temperature. Also, with the use of the ART filler system and thermo-viscous-technology, F_{max} of highly filled Harmonize and *Viscalor* (no heat) showed few changes with temperature. Different results may be due to different measurement methods, which merits further studies.

Stickiness parameters (F_{max} and W_s) of *Viscalor* (T3-30s, T3-3min) were compared with those of *Viscalor* (no heat) to determine the effect of pre-heating time on *Viscalor* stickiness (Figure 3.7). Similar to other tested RBCs, F_{max} and W_s of *Viscalor* (no heat, T3-30s and T3-3min) increased with probe withdrawal speed. Pre-heating for either 30 s or 3 min increased W_s but reduced F_{max}. After a long pre-heating period of 3 min, W_s increased at both temperatures, whereas F_{max} remained.

Once removed from the pre-heating device, composite temperature decreases rapidly and approaches to cavity temperature [132, 134, 138, 139]. Thus, a similar composite temperature may result in similar F_{max}. The increased W_s may occur because of good attachment between composite and the probe after pre-heating [126]. But high W_s also means high stickiness to the instrument, which needs balancing with the stickiness to the cavity. The usage of the probe method to evaluate stickiness parameters (F_{max} and W_s) can provide consistent and reproducible results [127]. However, W_s was more sensitive to pre-heating than F_{max} and maybe more suitable to describe *Viscalor* stickiness.

3.5 Conclusions

The main outcomes of this study were:

1) F_{max} and W_s were useful parameters to describe material stickiness. The tested RBCs varied in stickiness parameters (F_{max} and W_s), which increased with filler content.

2) Probe withdrawal speed strongly affected F_{max} and W_s, whereas extreme high probe withdrawal speeds (8 and 10 mm/s) did not significantly affect F_{max} and W_s.

3) Temperature rise increased W_s, but reduced F_{max}.

4) Pre-heated *Viscalor* showed higher W_s but lower F_{max} than *Viscalor* (no heat). A long pre-heating period of 3 min significantly increased W_s, but did not significantly affect F_{max}.

Chapter Four

Temperature and Experimental Variable Effects on Packability of Resin-based Composites

Abstract

Objectives. To determine the effects of probe penetration distance (2, 2.5 and 3 mm), probe packing speed (0.25, 0.50, 0.75 and 1.00 mm/s) and temperature (22 and 37 °C) on packability parameters: maximum packing force (F_p) and work of packing (W_p) of different resin-based composites (RBCs) and to investigate the effect of pre-heating on packability of *Viscalor*.

Methods. A Texture Analyzer was used to determine the packability parameters (F_p and W_p) of five RBCs and *Viscalor*, pre-heated using a Caps Warmer (VOCO, Germany) in T3 mode (at 68 °C) for 30 s (T3-30s) and 3 min (T3-3min), respectively. Composite pastes were packed into the cylindrical cavity (7 mm × 5 mm) controlled at either 22 or 37 °C. A flat-ended probe was lowered into the pastes at different packing speeds until it reached a pre-set probe penetration distance, then the probe was raised. Maximum packing force (F_p, N) and work of packing (W_p, N mm) were obtained from force/displacement plots. Data were analysed using one-way ANOVA, independent T-test and Tukey post-hoc tests ($p<0.05$).

Results. RBCs varied in F_p ($p<0.001$) and W_p ($p<0.001$), in which Admira Fusion showed the highest F_p and W_p. F_p and W_p increased with penetration distance, whereas F_p of Harmonize did not significantly change at either 22 or 37 °C. High packing speed significantly increased F_p ($p<0.001$) and W_p ($p<0.001$). However, F_p showed no significant change between 0.50, 0.75 and 1.00 mm/s ($p=0.178$), and W_p had no significant differences between 0.75 and 1.00 mm/s ($p=0.838$). Temperature rise significantly reduced F_p ($p<0.001$) and W_p ($p<0.001$). Pre-heating *Viscalor* for either 30 s or 3 min had no significant influences on F_p ($p=0.478$) and W_p ($p=0.151$), relative to non-pre-heated *Viscalor*.

Significance. Composite composition, probe penetration distance, probe packing speed and temperature all had influences on pre-cure packability (F_p and W_p) of RBCs. Pre-heating had no adverse effect on *Viscalor* packability.

Key words: resin-based composite; handling properties; packability; pre-heating

4.1 Introduction

During the clinical manipulation process, dental resin-based composites (RBCs) are carefully packed into the deep tooth cavity to avoid air entrapment and gap formation. Adequate material stickiness to the cavity wall rather than to the instrument may reduce manipulation counts and save operating time [126-128]. This depends upon material pre-cure handling properties, which are related to material composition and rheology.

Viscoelastic RBCs are capable of exhibiting both viscous and elastic properties against the applied force [127, 228]. The viscosity of RBCs describes their resistance to the flow and influences their handling properties and physical/mechanical properties [34, 84, 138]. It has been reported that high-viscous composites have low stickiness [84, 156]. Many intrinsic/extrinsic factors affect RBC viscosity, including monomer composition, filler content and temperature [113, 157]. Due to its rigid chemical structure, high-viscous bis-GMA may inhibit monomer mobility during polymerization and lead to a low degree of conversion [31, 34]. With the addition of diluent monomers, viscosity is modified and enables higher filler loading. However, with the increased filler/matrix interactions, highly packed RBCs are high-viscous [84, 112]. Lightly filled flowable RBCs have lower viscosity but higher polymerization shrinkage [111, 119].

According to the Arrhenius Equation (Equation 1.1), viscosity reduces with the temperature, which makes composite flow more easily to every corner of the tooth cavity and helps to achieve better marginal integrity.

$$\eta = Ae^{E_a/RT} \qquad \text{(Equation 1.1)}$$

Thus, 'pre-heating' may be used before manipulation to reduce material viscosity and ease manipulation [1, 113, 132]. However, possible damage, through elevated composite temperature, to pulp tissue needs further investigation.

The consistency, also called the degree of fluidity, is critical to RBC clinical applications [158]. In 1998, Tyas et al. designed a method to quantify material consistency and concluded that it increases with filler content [151, 158]. Lack of 'feel' or 'packability' may influence material adaptation to the cavity and contact with approximal areas [127, 158]. A gentle packing force helps to eliminate residual stress and avoid damaging the delicate pulp structure during RBC placement. Too much extensive manipulation may damage marginal integrity and form contraction gaps [127]. Reduced manipulation could eliminate complex adhesion effects, but it also depends upon paste aging and pre-polymerization of material [155, 159]. With deeper probe penetration into the material, more material will wet the instrument and result in more adhesion [155]. Kaleem et al. found packing force is material dependent and increases with probe-to-cavity ratio [151, 158]. According to their study, the maximum packing force (F_p, N) obtained from force/displacement plot is useful to describe the stiffness/packability of RBCs.

In clinical conditions, RBCs are packed into the tooth cavity with different dimensions at 37 °C [127]. Moreover, different packing speeds and distances are used during manipulation. Building upon previous stickiness investigation, the objectives of the present study were to investigate packability parameters (F_p and W_p) of different RBCs at different packing speeds with different probe penetration distances at 22 and 37 °C. The effect of pre-heating on *Viscalor* packability was also studied. The null Hypotheses for this investigation were:

(1) there was no difference in packability parameters (F_p and W_p) between different composites,

(2) F_p and W_p did not change with different probe penetration distances, packing speeds or temperatures and

(3) pre-heating did not affect *Viscalor* packability.

4.2 Materials and methods

Five RBCs and *Viscalor*, used with a Caps Warmer (VOCO, Germany), were investigated, as tabulated in the previous chapter (Table. 3.1).

A Texture Analyzer (Figure 3.1) (TA.XT2i, Stable Micro Systems, Godalming, Surrey, UK) was used to measure packability parameters: the maximum packing force (F_p, N) and work of packing (W_p, N mm). Force was applied via a stainless-steel probe ($\phi = 6$ mm). Composite pastes were carefully packed into the cavity ($\phi = 7$ mm, depth = 5 mm) (n=5) controlled at either 22 or 37 °C (Figure 3.2). *Viscalor* was pre-heated using a Caps Warmer (Figure 3.3) in T3 mode (at 68 °C) for 30 s (T3-30s) and 3 min (T3-3min), respectively.

For packability measurement, the probe position was set 10 mm above the cavity. Similar to stickiness measurement, the probe descended into the composite paste at different packing speeds (0.25, 0.50, 0.75 and 1.00 mm/s). When a 'trigger' force of 0.05 N was registered, data acquisition commenced at a rate of 400 p/s until it reached different penetration distances (2, 2.5 and 3 mm), the probe ascended at 2 mm/s.

Data were entered into statistical software (SPSS, SPSS Inc., Illinois, USA) and analysed using one-way ANOVA, independent T-test and Tukey post-hoc tests ($p<0.05$). Homogeneity of variance was calculated using the Kruskal-Wallis Test ($p<0.05$).

4.3 Results

Results showed that RBCs varied in F_p ($p<0.001$) and W_p ($p<0.001$) and Admira Fusion showed the highest F_p and W_p. Subsets for F_p and W_p are shown in Tables 4.1-4.2.

F_p and W_p measured with different probe penetration distances are shown in Tables 4.3-4.4 and Figures 4.1-4.2. F_p and W_p increased with penetration distance and ranged from 10.79 to 43.72 N and from 17.36 to 69.05 N mm, respectively.

Probe packing speed had significant influences on F_p ($p<0.001$) and W_p ($p<0.001$), as shown in Tables 4.5-4.6 and Figures 4.3-4.4. F_p and W_p increased with packing speed. However, F_p had no significant differences between 0.50, 0.75 and 1.00 mm/s ($p=0.178$), and there were no significant changes in W_p ($p=0.838$) between 0.75 and 1.00 mm/s.

Temperature rise significantly reduced F_p ($p<0.001$) and W_p ($p<0.001$), as shown in Figure 4.5.

Overall, pre-heating had no significant influences on F_p ($p=0.478$) and W_p ($p=0.151$) of *Viscalor*. Figures 4.6-4.7 illustrate the effect of penetration distance and packing speed on F_p and W_p of *Viscalor* (no heat, T3-30s and T3-3min) at 22 and 37 °C. F_p and W_p measured at 37 °C were lower than that at 22 °C. Statistical analysis showed that penetration distance had no significant influences on *Viscalor* (no heat, T3-30s and T3-3min) F_p ($p=0.131$) and W_p ($p=0.164$). Packing speed had no significant effect on F_p ($p=0.427$). However, when measured at different packing speeds, pre-heated *Viscalor* showed significantly lower W_p than *Viscalor* (no heat) ($p=0.002$).

Table 4.1 Materials subsets identified by post-hoc Tukey test for F_p.

F_p	1 (p=0.060)	2 (p=0.830)	3 (p=1.000)
	TPH	HZ	AF
	HZ	FSU	
	FSU	TEC	
	TEC	VC (T3-30s)	
		VC (T3-3min)	
		VC (no heat)	

Table 4.2 Materials subsets identified by post-hoc Tukey test for W_p.

W_p	1 (p=0.148)	2 (p=0.335)
	HZ	VC (no heat)
	FSU	AF
	TPH	
	VC (T3-30s)	
	TEC	
	VC (T3-3min)	
	VC (no heat)	

Table 4.3 Maximum packing force (F_p) with different probe penetration distances at 22 and 37 °C.

Materials	22 °C			37 °C		
	2 mm	2.5 mm	3 mm	2 mm	2.5 mm	3 mm
Admira Fusion	41.56[a A] (1.77)	49.50[a B] (1.70)	53.50[a,e C] (2.16)	23.09[a D] (1.00)	30.98[a E] (1.34)	37.68[a F] (1.80)
Filtek Supreme Ultra	27.11[b A] (0.91)	33.33[b,c B] (2.53)	40.31[b C] (1.78)	19.40[b D] (1.66)	22.83[b E] (0.72)	24.05[b A,E] (1.54)
TPH LV	24.10[c A] (0.62)	30.14[b B] (1.45)	35.40[c C] (0.92)	10.79[c D] (1.14)	13.87[c E] (0.43)	16.01[c F] (0.70)
Tetric EvoCeram	32.30[d,e A] (1.24)	39.91[e,f B] (0.50)	45.45[d C] (1.60)	16.64[e D] (0.40)	19.65[d E] (1.01)	23.28[b,d F] (1.40)
Harmonize	35.75[f A] (2.86)	35.46[c,d A] (2.83)	35.44[c A] (2.25)	15.08[d,e B] (1.68)	14.60[c B] (0.59)	16.05[c B] (0.55)
Viscalor (no heat)	31.88[d,e A] (0.66)	41.78[f B] (0.35)	50.35[a C] (1.51)	15.46[d,e D] (1.01)	19.75[d E] (0.33)	24.66[b F] (0.49)
Viscalor (T3-30s)	29.58[b,d A] (1.18)	37.35[d,e B] (0.87)	45.90[d C] (2.41)	14.13[d D] (0.99)	19.37[d E] (0.62)	19.46[c,d E] (3.97)
Viscalor (T3-3min)	34.55[e,f A] (0.17)	49.13[a B] (2.93)	54.72[e C] (1.80)	16.39[d,e D] (0.17)	21.96[b E] (1.39)	29.23[e F] (2.09)

For each probe penetration distance, the same lower case superscript letters indicate homogeneous subsets among the materials. For each material, the same CAPITAL superscript letters indicate homogeneous subsets among different conditions.

Table 4.4 Work of packing (W_p) with different probe penetration distances at 22 and 37 °C.

Materials	22 °C			37 °C		
	2 mm	2.5 mm	3 mm	2 mm	2.5 mm	3 mm
Admira Fusion	33.92[a A] (1.60)	50.07[a,e B] (1.78)	69.05[a C] (3.97)	25.87[a D] (1.18)	38.04[a A] (1.48)	54.11[a B] (2.19)
Filtek Supreme Ultra	24.66[b A] (1.87)	36.31[b B] (3.09)	53.27[b,d C] (1.62)	20.91[b,c A] (3.16)	29.60[b,c D] (1.13)	40.83[b,d E] (1.90)
TPH LV	27.55[b,c A] (1.04)	40.87[b,c B] (2.02)	59.97[b,c C] (2.31)	19.89[b,c,d D] (1.31)	27.35[b A] (1.73)	33.83[c E] (1.18)
Tetric EvoCeram	31.04[a,d A] (1.06)	46.74[a,d B] (1.02)	64.37[a,c C] (2.80)	19.25[c,d D] (0.90)	30.64[c A] (1.82)	42.68[b E] (2.25)
Harmonize	31.40[a,d A] (3.26)	40.55[b,c B] (3.18)	50.67[d C] (3.24)	17.36[d D] (1.70)	23.27[d E] (1.09)	34.05[c A] (0.80)
Viscalor (no heat)	29.29[c,d A] (1.17)	45.16[c,d B] (0.67)	63.89[a,c C] (3.48)	22.56[b D] (1.71)	31.74[c A] (1.02)	44.12[b B] (0.45)
Viscalor (T3-30s)	27.55[b,c A] (1.04)	39.95[b B] (1.64)	57.11[b,c,d C] (3.31)	18.51[c,d D] (0.69)	29.26[b,c A] (1.51)	35.98[c,d B] (5.05)
Viscalor (T3-3min)	30.84[a,c,d A] (0.58)	53.72[e B] (3.79)	69.05[a C] (6.15)	21.06[b,c D] (0.52)	31.33[c A] (1.71)	44.46[b E] (2.52)

For each probe penetration distance, the same lower case superscript letters indicate homogeneous subsets among the materials. For each material, the same CAPITAL superscript letters indicate homogeneous subsets among different conditions.
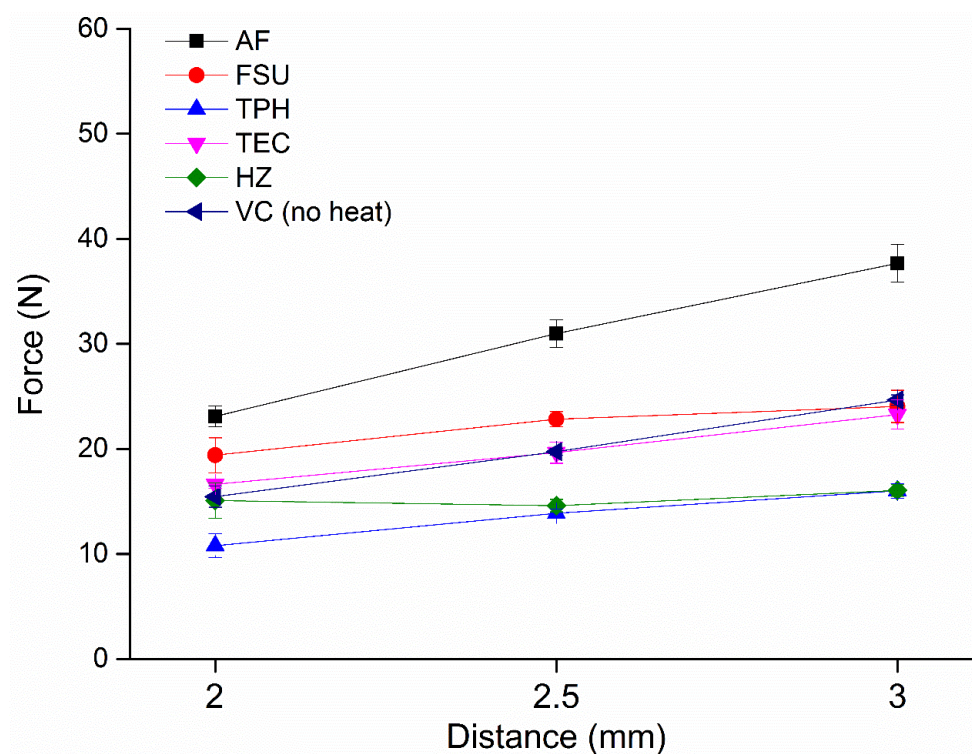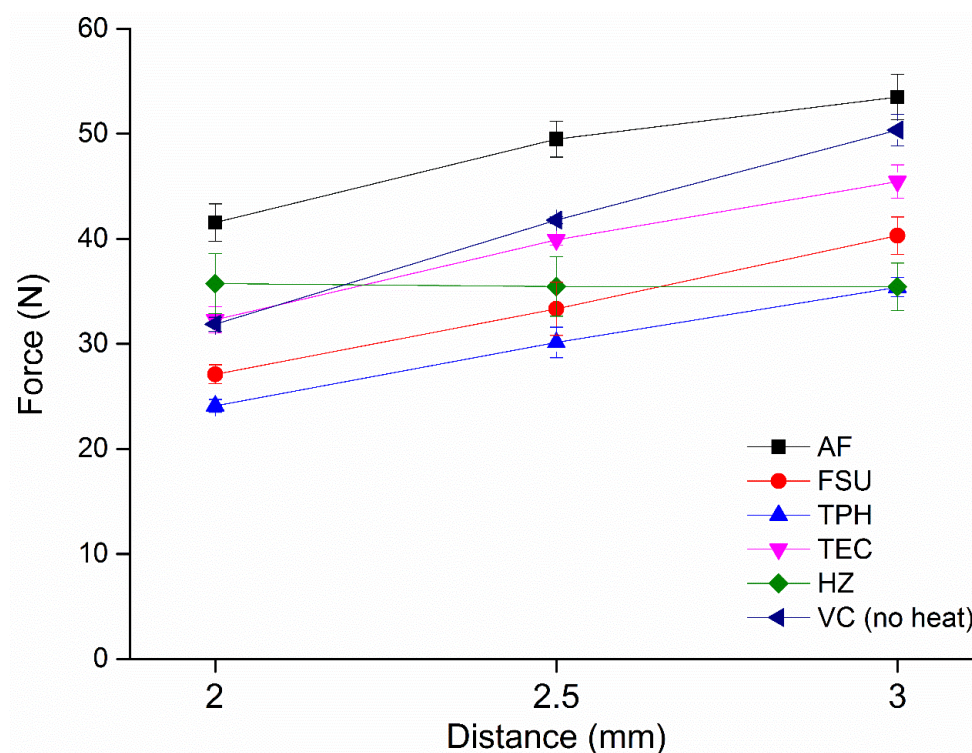
Figure 4.1 Maximum packing force (F_p) of different RBCs with different probe penetration distances at 22 °C (top) and 37 °C (bottom).
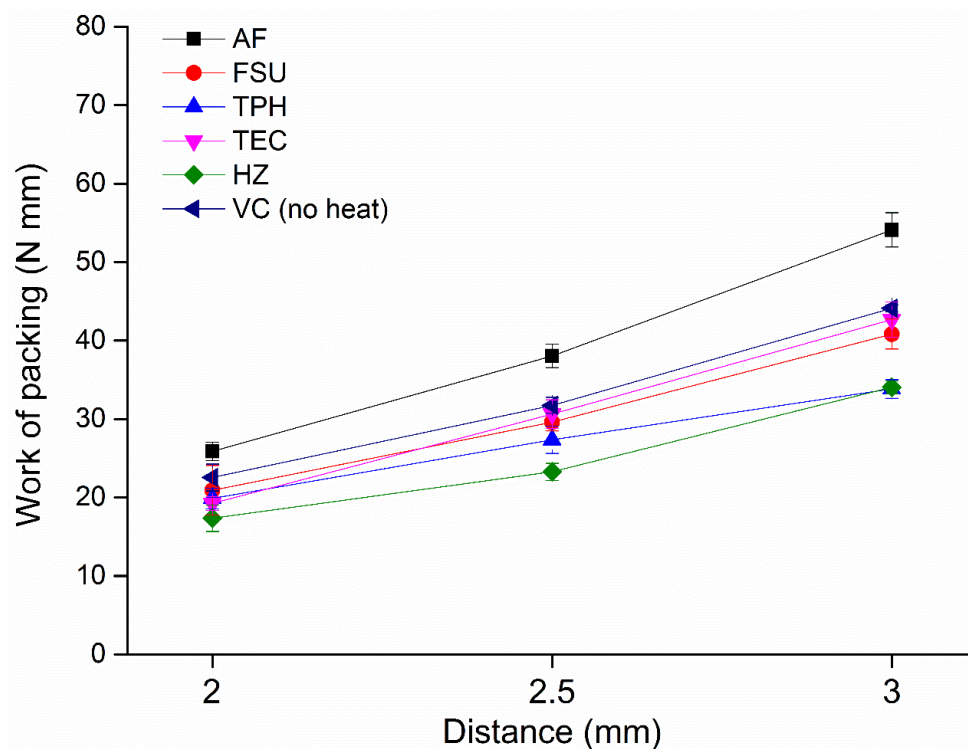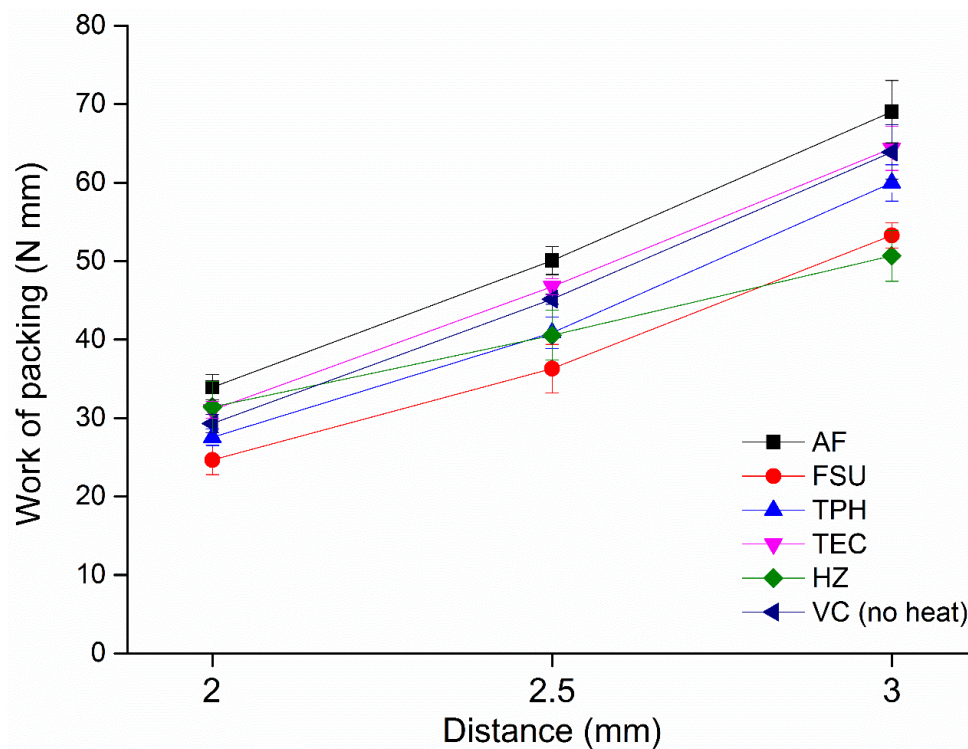
Figure 4.2 Work of packing (W_p) of different RBCs with different probe penetration distances at 22 °C (top) and 37 °C (bottom).

Table 4.5 Maximum packing force (F_p) at different packing speeds at 22 and 37 °C.

Materials	22 °C				37 °C			
	0.25 mm/s	0.50 mm/s	0.75 mm/s	1.00 mm/s	0.25 mm/s	0.50 mm/s	0.75 mm/s	1.00 mm/s
Admira Fusion	28.14$^{a\,A}$ (0.48)	41.56$^{a\,B}$ (1.77)	43.37$^{a,b\,B}$ (0.44)	49.36$^{a\,C}$ (0.88)	19.36$^{a\,D}$ (0.34)	23.09$^{a\,E}$ (1.00)	28.21$^{a\,A}$ (0.97)	34.69$^{a\,F}$ (0.55)
Filtek Supreme Ultra	21.98$^{b,d\,A}$ (0.71)	27.11$^{b\,B}$ (0.91)	40.61$^{b,f\,C}$ (2.13)	38.49$^{b\,C}$ (2.31)	13.10$^{b\,D}$ (0.26)	19.40$^{b\,A}$ (1.66)	21.60$^{b\,A}$ (0.34)	21.46$^{b\,A}$ (0.62)
TPH LV	14.66$^{c\,A}$ (0.42)	24.10$^{c\,B}$ (0.62)	30.07$^{c\,C}$ (2.08)	31.34$^{c\,C}$ (0.39)	8.33$^{c\,D}$ (0.17)	10.79$^{c\,E}$ (1.14)	17.53$^{c\,F}$ (1.38)	18.63$^{c\,F}$ (0.47)
Tetric EvoCeram	22.72$^{b\,A}$ (0.34)	32.30$^{d,e\,B}$ (1.24)	34.58$^{d\,C}$ (0.58)	37.85$^{b\,D}$ (0.47)	12.83$^{b\,E}$ (0.37)	16.64$^{d\,F}$ (0.40)	18.49$^{c,d\,G}$ (0.44)	21.29$^{b\,H}$ (0.25)
Harmonize	22.33$^{b,d\,A}$ (0.29)	35.75$^{f\,B}$ (2.86)	47.54$^{e\,C}$ (1.46)	49.48$^{a\,C}$ (1.53)	8.92$^{c\,D}$ (0.20)	15.08$^{d,e\,E}$ (1.68)	21.53$^{b\,A}$ (0.52)	21.21$^{b\,A}$ (0.45)
Viscalor (no heat)	26.30$^{e\,A}$ (0.66)	31.88$^{d,e\,B}$ (0.66)	45.36$^{a,e\,C}$ (1.72)	49.02$^{a\,D}$ (1.29)	13.42$^{b\,E}$ (0.26)	15.46$^{d,e\,F}$ (1.01)	19.30$^{d\,G}$ (0.60)	22.32$^{b,d\,H}$ (0.78)
Viscalor (T3-30s)	22.29$^{b,d\,A}$ (0.68)	29.58$^{b,d\,B}$ (1.18)	38.32$^{f,g\,C}$ (1.61)	44.09$^{d\,D}$ (0.54)	9.83$^{d\,E}$ (0.45)	14.13$^{e\,F}$ (0.99)	23.63$^{e\,A}$ (0.39)	23.03$^{d\,A}$ (0.42)
Viscalor (T3-3min)	21.20$^{d\,A}$ (1.16)	34.55$^{e,f\,B}$ (0.17)	35.99$^{d,g\,B}$ (0.82)	42.38$^{d\,C}$ (2.02)	8.50$^{c\,D}$ (0.27)	16.39$^{d,e\,E}$ (0.17)	18.14$^{c,d\,E,F}$ (0.20)	19.42$^{c\,A,F}$ (0.73)

For each packing speed, the same lower case superscript letters indicate homogeneous subsets among the materials. For each material, the same CAPITAL superscript letters indicate homogeneous subsets among different conditions.

Table 4.6 Work of packing (W_p) at different packing speeds at 22 and 37 °C.

Materials	22 °C				37 °C			
	0.25 mm/s	**0.50 mm/s**	**0.75 mm/s**	**1.00 mm/s**	**0.25 mm/s**	**0.50 mm/s**	**0.75 mm/s**	**1.00 mm/s**
Admira Fusion	32.58[a A,B,C] (1.75)	33.92[a A,B] (1.60)	41.00[a D] (0.47)	44.44[a E] (1.40)	31.68[a A,C] (1.32)	25.87[a F] (1.18)	30.05[a C] (2.50)	35.26[a B] (1.64)
Filtek Supreme Ultra	24.54[b A] (0.78)	24.66[b A] (1.87)	37.62[a,b,c B] (3.96)	36.80[b,c B] (1.44)	18.06[b,c C] (0.46)	20.91[b,c A,C] (3.16)	24.47[b A] (1.60)	22.49[b A] (1.08)
TPH LV	25.93[b A] (4.16)	27.55[b,c A] (1.04)	33.29[c,d B] (3.41)	32.52[c B] (1.09)	20.20[b C] (1.12)	19.89[b,c,d C] (1.31)	24.76[b A] (1.67)	25.38[c A] (1.31)
Tetric EvoCeram	25.52[b A] (0.41)	31.04[a,d B] (1.06)	34.79[b,c,d C] (0.86)	35.22[b,c C] (0.86)	19.35[b D] (1.03)	19.25[c,d D] (0.90)	19.62[c,e D] (0.90)	22.27[b E] (0.61)
Harmonize	23.66[b A] (0.56)	31.40[a,d B] (3.26)	38.98[a,b C] (1.50)	40.60[d C] (0.63)	16.20[c D] (1.62)	17.36[d D] (1.70)	20.76[c,d A] (0.67)	20.81[b A] (0.69)
Viscalor **(no heat)**	30.91[a A] (1.16)	29.29[c,d A] (1.17)	41.52[a B] (1.17)	43.85[a C] (1.00)	25.95[d D] (0.97)	22.56[b E] (1.71)	23.06[b,d E] (0.71)	25.38[c D] (0.60)
Viscalor **(T3-30s)**	23.48[b A] (0.59)	27.55[b,c B] (1.04)	34.14[c,d C] (0.97)	39.66[d,e D] (2.40)	20.23[b E,F] (1.78)	18.51[c,d E] (0.69)	24.46[b A] (0.56)	21.95[b A,F] (0.51)
Viscalor **(T3-3min)**	22.45[b A] (0.55)	30.84[a,c,d B] (0.58)	32.80[d B,C] (1.90)	35.33[b,c C] (1.70)	17.65[b,c D] (2.22)	21.06[b,c A,E] (0.52)	17.69[e D] (0.57)	18.59[d D,E] (0.82)

For each packing speed, the same lower case superscript letters indicate homogeneous subsets among the materials. For each material, the same CAPITAL superscript letters indicate homogeneous subsets among different conditions.
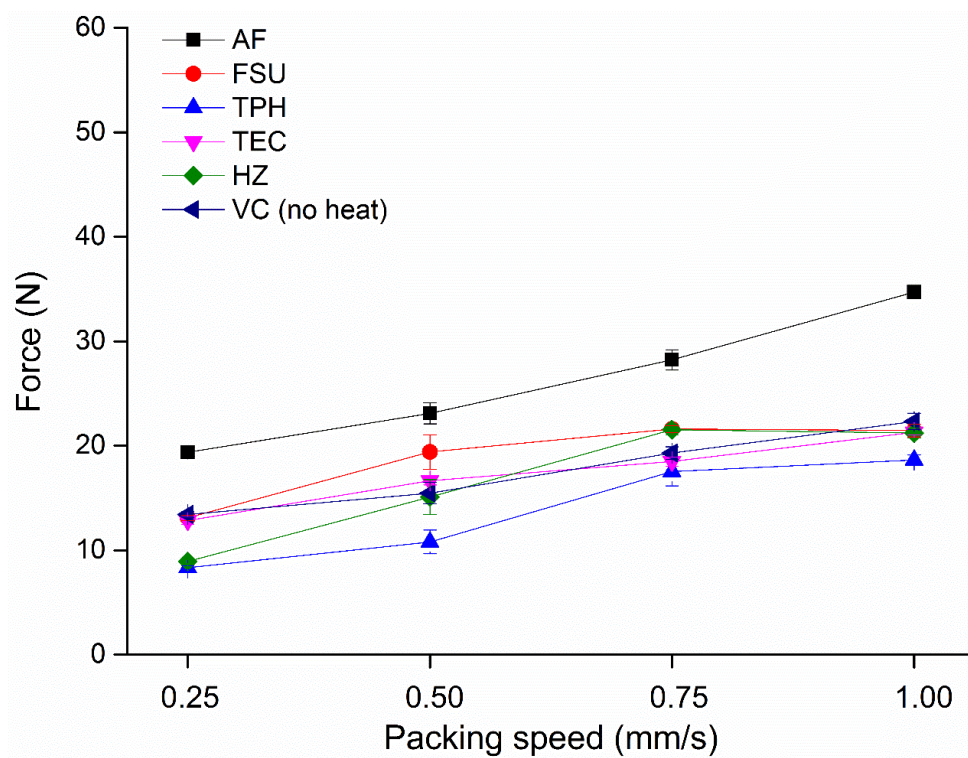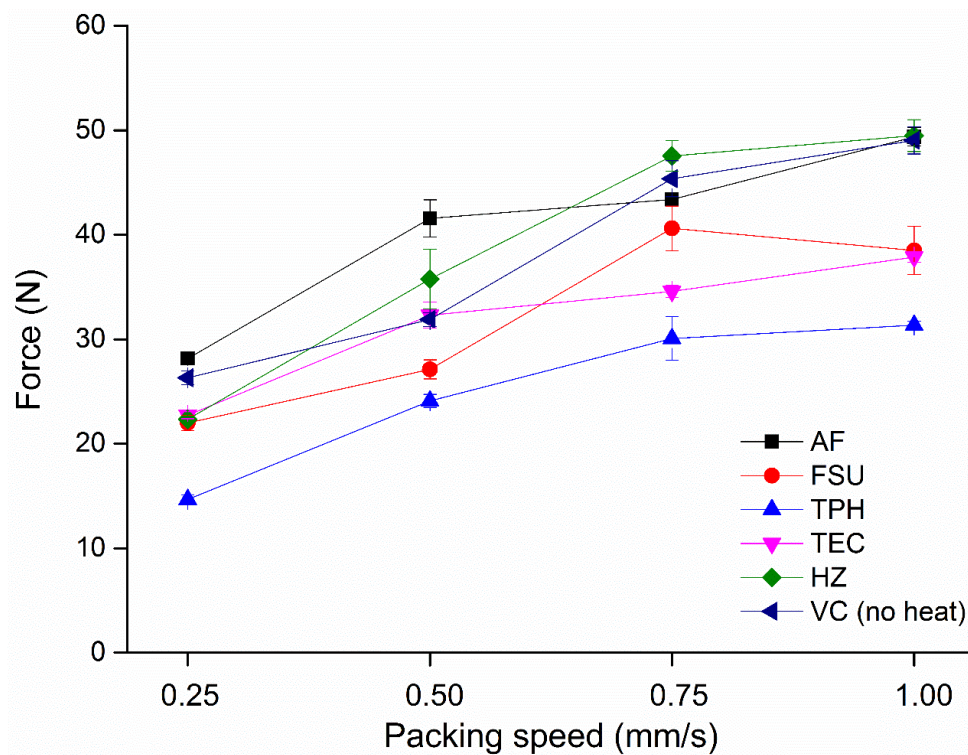
Figure 4.3 Maximum packing force (F_p) of different RBCs at different probe packing speeds at 22 °C (top) and 37 °C (bottom).
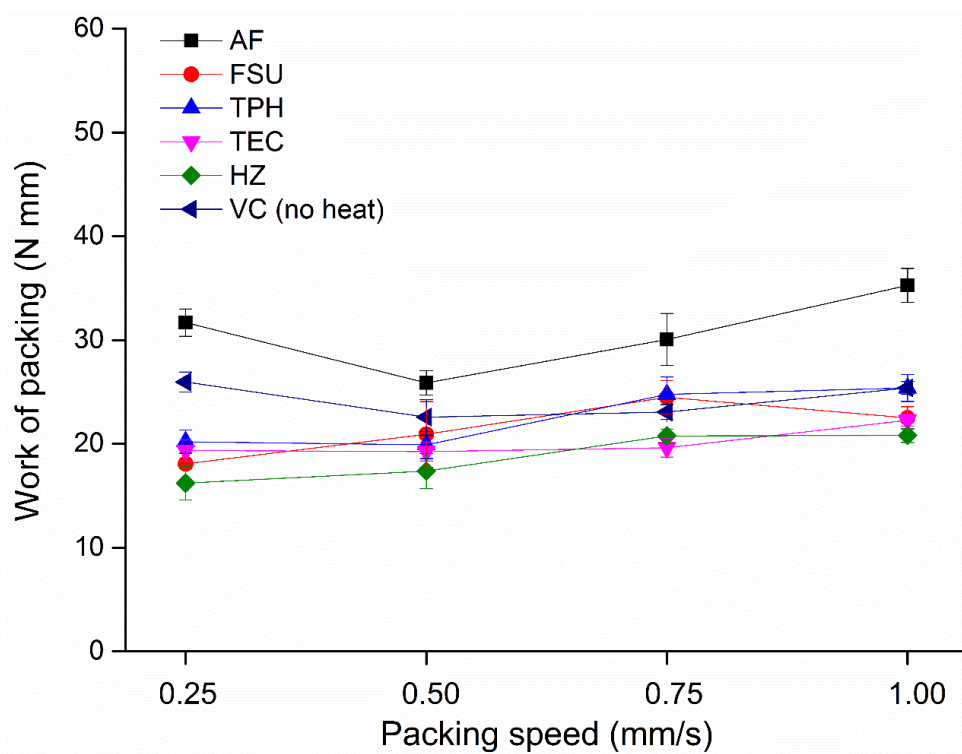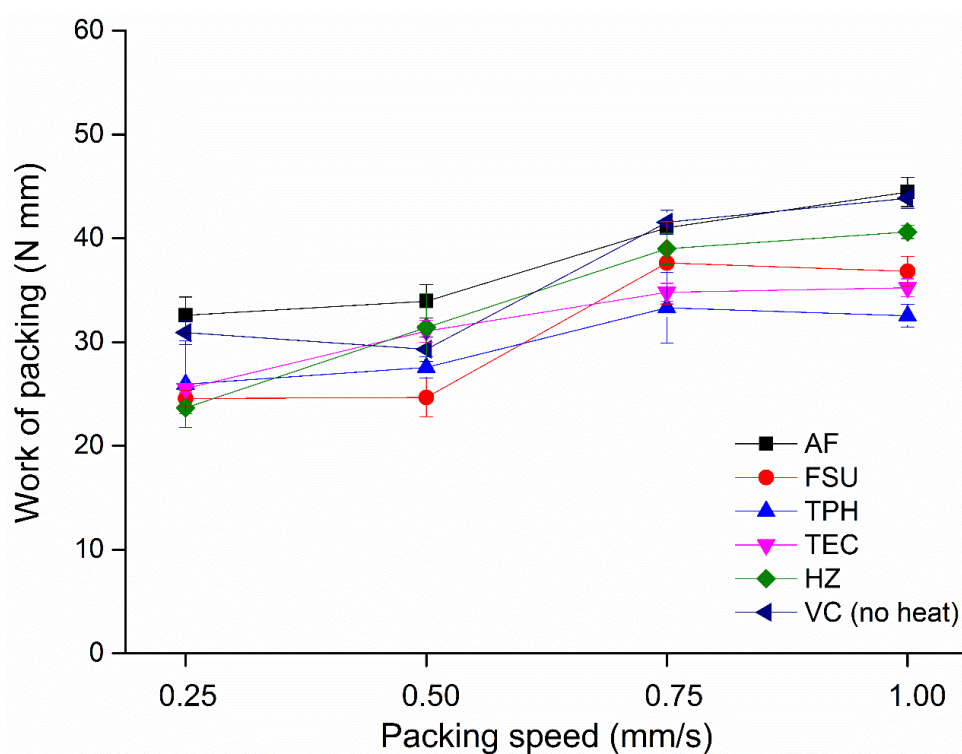
Figure 4.4 Work of packing (W_p) of different RBCs at different probe packing speeds at 22 °C (top) and 37 °C (bottom).
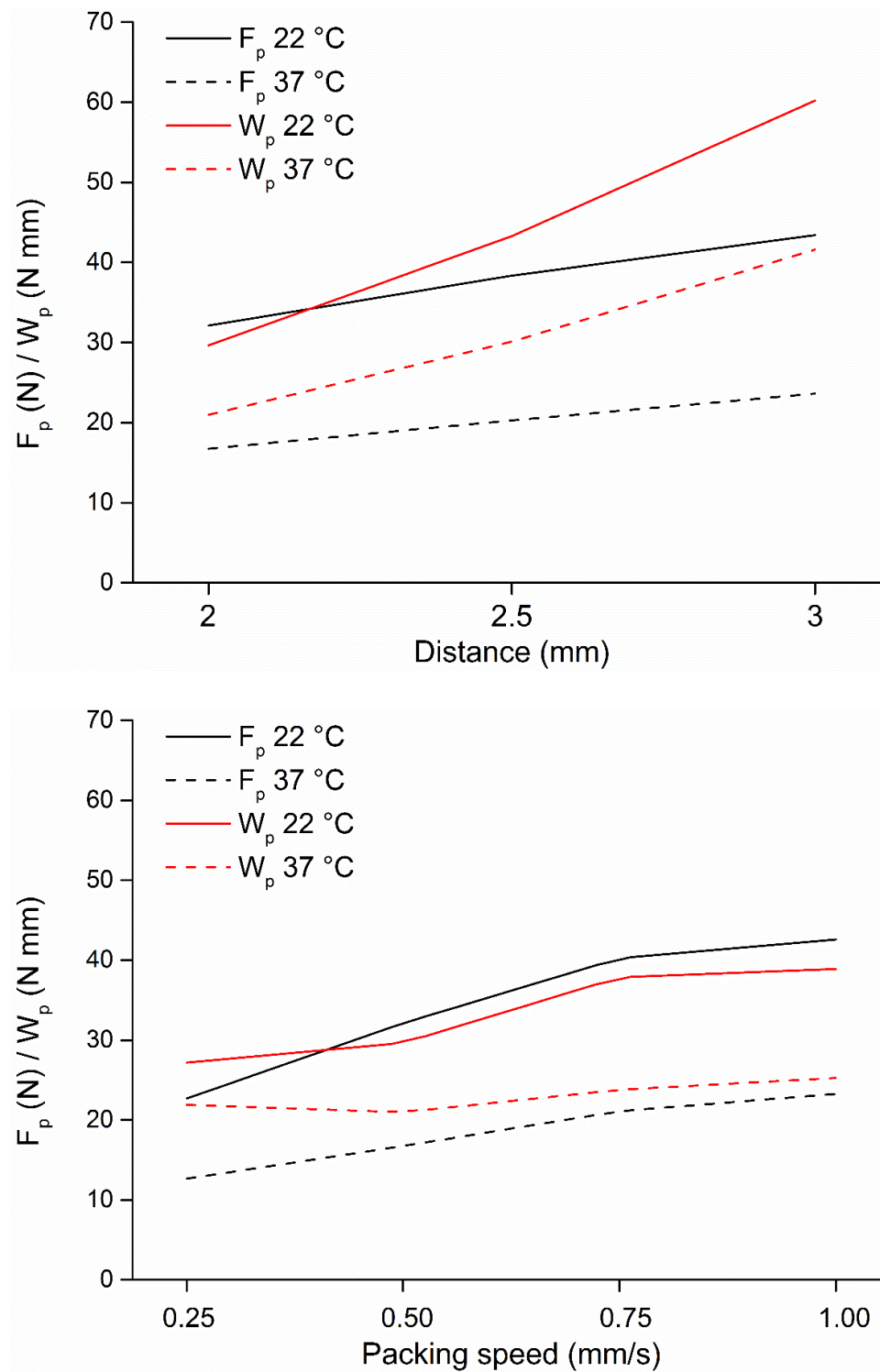
Figure 4.5 Average F_p and W_p development trends of investigated RBCs (except pre-heated Viscalor) with different probe penetration distances (top) and at different probe packing speeds (bottom) at 22 and 37 °C.
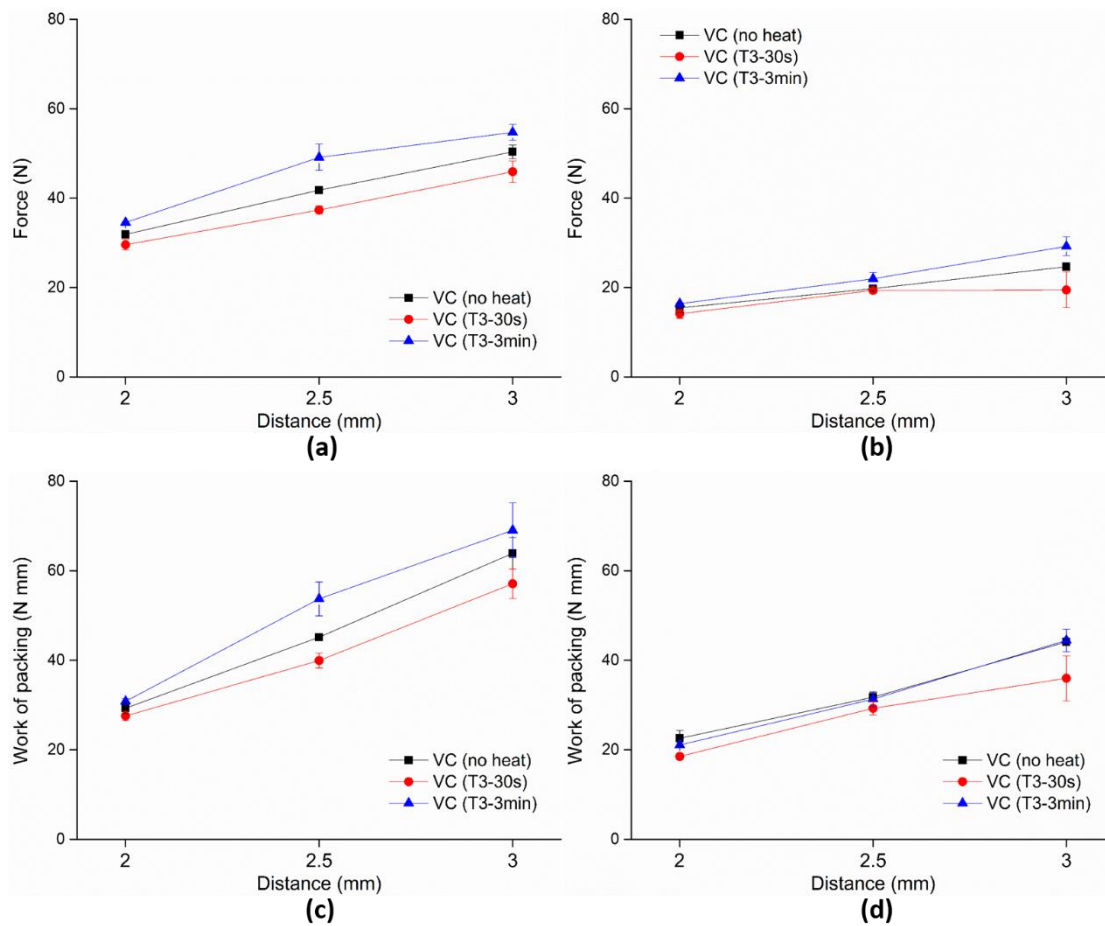
Figure 4.6 (a) & (b): F_p; (c) & (d): W_p of Viscalor (no heat, T3-30s and T3-3min) with different probe penetration distances at 22 and 37 °C.
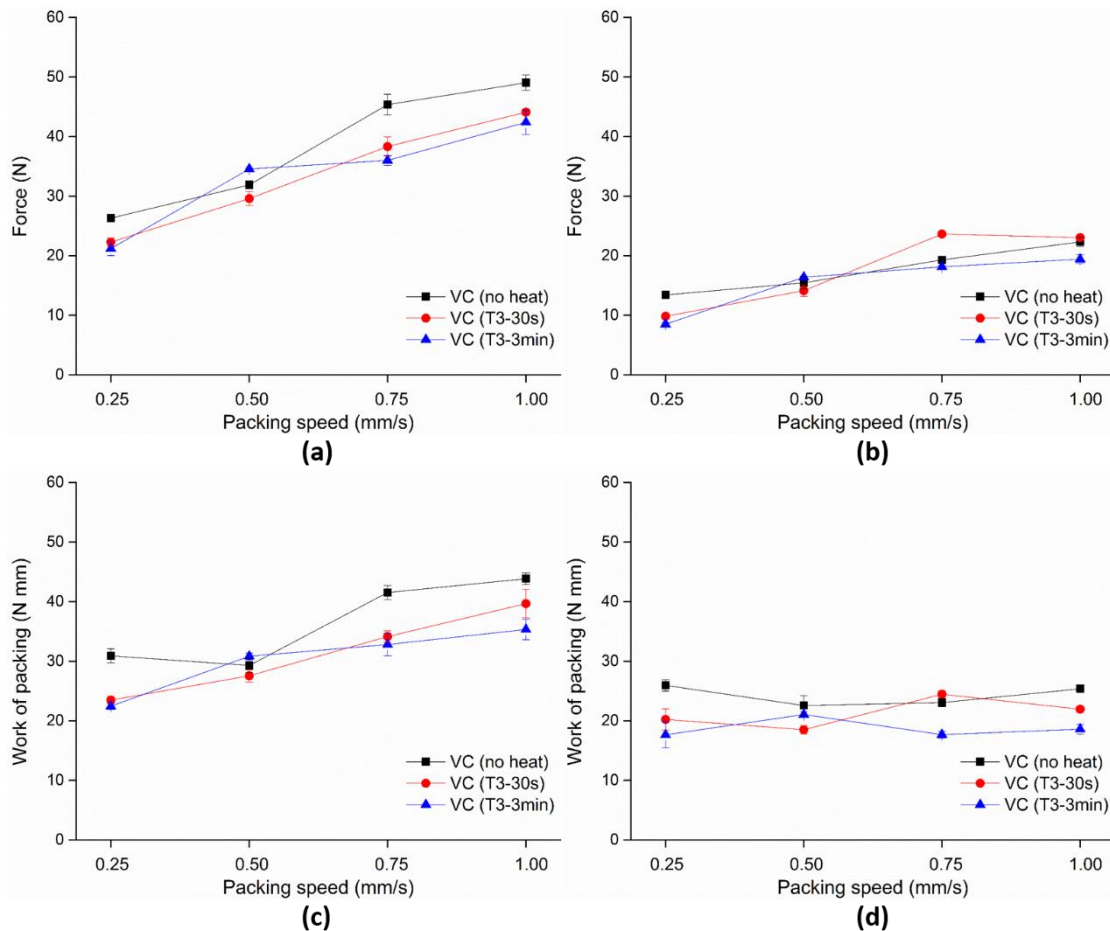
Figure 4.7 (a) & (b): F_p; (c) & (d): W_p of Viscalor (no heat, T3-30s and T3-3min) at different probe packing speeds at 22 and 37 °C.

4.4 Discussion

Dental restorative composites are designed to show good aesthetic and mechanical properties during restoration. However, the maximum properties exhibited and their clinical success depend partly upon the manipulation process, which is related to material handling properties [75]. Packability of RBCs denotes the amount of stress that is needed to pack them and this affects their adaptation to the cavity. However, there are few studies that have investigated packability and the influence of experimental variables. Thus, according to the stickiness investigation in the previous chapter, this study investigated the effects of material composition, probe penetration distance, probe packing speed and temperature on the packability parameters (F_p and W_p) of different RBCs [151]. The effect of pre-heating on *Viscalor* packability was

also studied. The packability measurement setup was similar to that of stickiness measurement in Chapter 3. The null hypotheses 1-4 were rejected, whereas the null hypothesis 5 was partly rejected.

During measurement, compressive force data (N) was plotted against the probe displacement (mm) (Figure 1.7). The compressive force increased with the downward movement of the probe and reduced gradually to zero when probe was withdrawn. The peak height of the plot was F_p (N), the maximum packing force, and the integrated area was W_p (N mm), the work of packing.

The present results showed that packability parameters (F_p and W_p) varied widely between the investigated RBCs, in which Admira Fusion had the highest F_p and W_p. Its high filler content (84 wt.%) results in high viscosity, which may indicate reduced molecular mobility [84, 115]. Thus, a high resistance is generated against the applied force and leads to high F_p and W_p. Harmonize and *Viscalor* (no heat), with similarly high filler loading (81 and 83 wt.%), showed high F_p and W_p as expected. Other RBCs, with lower filler content, exhibited lower F_p and W_p. Hence, in the present study, F_p and W_p increased with filler content. Also, the effect of the resin matrix on packability needs consideration. The presence of TEGDMA in both Filtek Supreme Ultra and TPH LV modified their viscosity and resulted in low F_p and W_p [34, 84]. The monomer bis-EMA reduces the viscosity of Tetric EvoCeram and its F_p and W_p [24, 31]. Hence, packability varied with viscosity.

Different probe penetration distances combined with a constant mould size may create a similar effect to the plunger-cavity ratios investigated previously [151]. Thus, in this study, different probe penetration distances, 2, 2.5 and 3 mm, were considered. The force/displacement plot with different probe penetration distances (Figure 4.8) showed that F_p and W_p significantly increased with penetration distance, from 2 to 3 mm. This may be related to the 'wall effect', which increases the packing force [151]. Increased penetration distance reduces the space between the probe and the cavity, which may limit the flow of RBC paste and increase the force needed for the probe

movement. Restricted flow of RBC paste will also depend on composite paste viscosity. In the present study, Admira Fusion showed the highest F_p and W_p regardless of penetration distance. However, penetration distance had no significant effect on F_p of Harmonize at either 22 or 37 °C. As mentioned before, its ART (Adaptive Response Technology) filler system and TEGDMA within its resin matrix both act as rheological modifiers [34]. Thus, the viscosity of Harmonize is well-controlled and influenced minimally by the 'wall effect' at high packing speed.
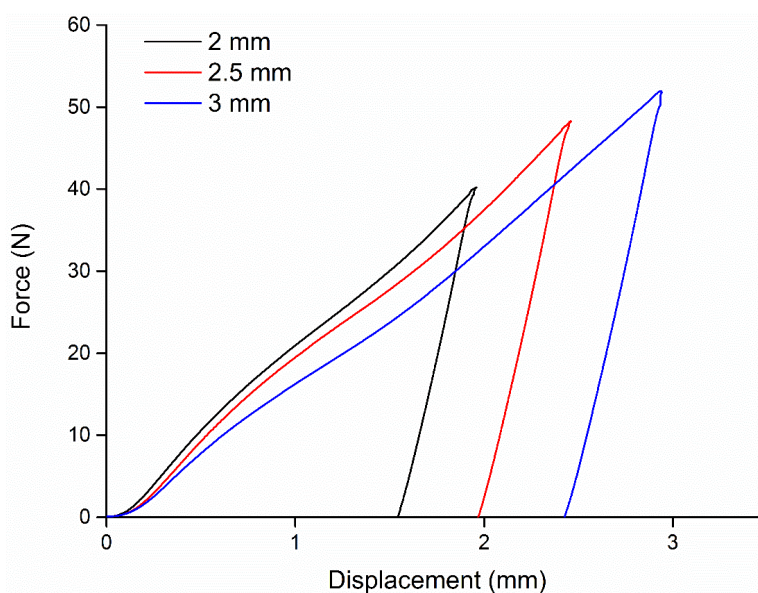
Figure 4.8 Force/displacement plot obtained during packability measurement at 22 °C with different probe penetration distances.

In addition to probe penetration distance, the effect of packing speed was also investigated. F_p and W_p increased with packing speed. Admira Fusion, Harmonize and *Viscalor* (no heat) showed high F_p and W_p at all packing speeds, because of their high filler contents. When the probe starts packing the composite paste, the uncured monomer structure needs time to adjust to the applied force [154]. High packing speed may limit the molecular relaxation time and lead to high F_p and W_p. However, F_p and W_p showed no significant differences between high speeds (0.50, 0.75 and 1.00 mm/s), which may be the upper limit of the effect of packing speed.

Temperature rise significantly reduced F_p and W_p, which is in line with the previous study [151]. According to the Arrhenius Equation (Equation 1.1), low viscosity results

from temperature rise [34]. The sufficient flowability of low-viscous RBC paste ensures more relaxation time against the applied packing force. Thus, low F_p and W_p results are shown.

F_p and W_p results of pre-heated *Viscalor* (T3-30s and T3-3min) were compared with *Viscalor* (no heat), as shown in Figures 4.6-4.7. F_p and W_p of *Viscalor* (no heat, T3-30s and T3-3min) increased with penetration distance and packing speed, but reduced with temperature rise. Pre-heating for either 30 s or 3 min had no significant influences on the *Viscalor* packability. However, when measured at different packing speeds, pre-heated *Viscalor* (T3-30s and T3-3min) showed significantly lower W_p relative to non-pre-heated *Viscalor*. This is in line with the results of the temperature effect. Thus, W_p is more sensitive to pre-heating than F_p and may be more suitable to describe *Viscalor* packability. However, other factors, such as matrix composition and filler/matrix interaction, need consideration when studying the effect of pre-heating on *Viscalor* packability.

4.5 Conclusions

Within the limitations of this study, the conclusions were:

1) RBC paste varied in packability parameters (F_p and W_p), which increased with their filler content.

2) F_p and W_p increased with probe penetration distance. High probe packing speed significantly increased F_p and W_p, but no significant differences exist between the three highest speeds (0.50, 0.75 and 1.00 mm/s) for both F_p and W_p. Temperature rise reduced F_p and W_p.

3) Pre-heating did not significantly influence *Viscalor* packability. However, when measured at different packing speeds, pre-heated *Viscalor* showed significantly lower W_p than *Viscalor* (no heat).

Chapter Five

Pre-heating Effects on Extrusion Force, Stickiness and Packability of Resin-based Composite

Jiawei Yang[1], Nikolaos Silikas[1*], David C. Watts[1,2*]

1. Dentistry, School of Medical Sciences, University of Manchester, Manchester, UK

2. Photon Science Institute, University of Manchester, Manchester, UK

Abstract

Objectives. To measure temperature effects on stickiness and packability of representative resin-based composites and the effect of pre-heating time on pre-cure properties of *Viscalor*, including extrusion force.

Methods. Five resin-based composites (RBC) and an additional RBC, *Viscalor,* used with a Caps Warmer (VOCO, Germany) were studied. The extrusion force (N) and extruded mass (g) were measured from *Viscalor* compules heated in T3 mode for 30 s (T3-30s) and 3 min (T3-3min). For stickiness and packability measurements, RBCs were packed into a brass cylindrical cavity controlled at 22 and 37 °C. A flat-ended probe was lowered into the RBC pastes at constant speed. Stickiness: F_{max} (N) and W_s (N mm) and packability: F_p (N), were measured. *Viscalor* was LED photo-cured at 1200 mW/cm^2 for 40 s. The degrees of conversion at 5 min and 24 h post cure (DC_{5min} and DC_{24h}) of *Viscalor* (no heat, T3-30s and T3-3min) were measured by ATR-FTIR. Data were analysed by one-way ANOVA, independent T-test and Tukey *post-hoc* tests ($p < 0.05$).

Results. The maximum temperature of the Caps Warmer, in T3 mode, reached 68 °C in 20 min. *Viscalor* temperatures of 34.5 °C and 60.6 °C were recorded after 30 s and 3 min pre-heating, respectively. Pre-heating significantly reduced extrusion force and increased extruded mass, especially after 3 min. RBCs varied in F_{max}, W_s and F_p ($p < 0.05$). Temperature also affected F_{max} ($p < 0.001$), W_s ($p = 0.002$) and F_p ($p < 0.001$). Pre-heating *Viscalor* for either 30 s or 3 min did not increase the post-cure DC at either 5 min or 24 h, relative to no pre-heating ($p > 0.05$).

Significance. The composites varied to an extent in stickiness and packability but the overall magnitudes remained within a clinically acceptable range. Pre-heating was beneficial in placement of *Viscalor* and caused no adverse effects through premature polymerization.

5.1 Introduction

Resin-based composites (RBCs) are designed and manipulated with suitable aesthetic and physico-chemical properties to match the tooth structure. They can be fabricated in a range of consistencies and are therefore widely used as direct restorative materials in dentistry [4, 6, 7]. The maximum obtained properties and longevity of composites are dependent on the clinician's skill level and operating conditions [152, 229]. Thus, 'technique sensitivity' should be reduced for good marginal integrity and successful restoration [75]. To avoid the formation of voids and gaps, both insertion technique and adaptation of composites need improvement [152]. The successful clinical handling and placement mainly depends on suitable pre-cure properties of composites that are determined by material composition and viscosity [138].

Pre-cure handling properties, such as flowability, stickiness, ease of placement and adaptation to cavity walls affect product selection for clinical restoration [126, 151]. Stickiness - the adhesion force between two contacted surfaces - has been studied previously [126, 127, 153, 156]. In a related field, the Avery Adhesive Test (AAT) with a spherical probe was used to study pressure-sensitive adhesives (PSA) [154]. In 2003, a method was reported using a flat-ended stainless-steel probe [126, 127]. Clinically, the relationship between stickiness to tooth cavity and stickiness to instruments should be well balanced [126-128]. High stickiness to instruments may result in difficult placement and more porosities/gaps may occur during restoration [126, 127]. RBCs with adequate consistency and packability are important for adapting to the tooth cavity and optimizing approximal contact areas [127, 158]. Tyas et al. designed a method to assess consistency of unset composites [127, 158]. They placed materials in an 8 mm × 8 mm cylindrical mould and pressed with a flat-ended glass rod demonstrating the high consistency of RBCs with increased filler content [151, 158].

RBCs exhibit both viscous and elastic properties against the applied force and the rheological nature of pre-cure RBCs affects their handling properties [126, 127].

Viscosity directly relates to material's handling properties, operating time and quality of restoration [34, 84, 127, 128]. Viscosity decreases with temperature according to the Arrhenius Equation (Equation 1.1) [34]. Viscosity also tends to increase exponentially with filler content [84, 126].

Bis-GMA has higher viscosity than other dimethacrylates, resulting in low degree of conversion (DC) and requiring diluent monomers to facilitate filler particle incorporation [6, 24, 28, 31, 54, 111]. High viscosity of highly filled RBCs may cause insufficient adaptation to the cavity preparation, poor marginal integrity and final restoration failure [1].

There are several possible strategies to achieve good cavity adaptation via reduced viscosity. Ideally, materials should flow into every corner of the cavity but not flow after removing the applied force [126, 127]. High viscous RBC pastes are hard to extrude from the syringe or compule, which may lead to macroscopic voids/porosities during manipulation [1, 34, 126] and this was a major reason for developing flowable composites [2, 83, 116].

The *SonicFill* system (Kerr, USA), contains a highly filled resin matrix including special viscosity modifiers that respond to ultrasonic energy (UE) and reduce the viscosity by 87 %. Once UE is stopped, the viscosity returns to high levels, suitable for carving and contouring [144].

Several studies have evaluated pre-heating RBCs before placement [116, 139, 230]. Pre-heating makes highly packed RBCs more fluid and easier to manipulate, without compromising their superior mechanical properties [113]. But after pre-heating the elevated temperature may cause thermal damage to the pulp [231]. The pulp has a normal temperature of 34-35 °C and with temperature increases ranging from 5.5 to 16 °C, the possibility of pulp necrosis may increase from 15 % to 100 % [134].

Existing pre-heating devices, such as Calset heater (AdDent Inc., Danbury, CT, USA) and ENA heat (Micerium, Avegno, Italy), have operating temperature ranges of 37-68 °C [2, 134, 135, 138, 175].

A new pre-heating RBC, *Viscalor,* has been designed for use with a Caps Warmer device (VOCO, Germany). This has three working modes (T1, T2 and T3) to cover the temperature range 37-68 °C. The objectives of this study were to measure pre-cure properties including stickiness and packability of representative RBCs at different temperatures and determine the effect of pre-heating time on pre-cure properties of *Viscalor*, including extrusion forces. The Null Hypotheses were:
(1) composites did not vary in stickiness and packability at different temperatures and
(2) pre-heating period had no effect on *Viscalor*'s post-cure DC% measured at either 5 min or 24 h.

5.2 Materials and methods

Five commercial RBCs and an additional RBC: *Viscalor* used with a Caps Warmer (VOCO, Germany), were studied. The manufacturers' information is shown in Table 3.1.

A type-K thermocouple was inserted into the Caps Warmer (Figure 3.3) to characterize its temperature profile in T3 mode. When it reached its maximum temperature, *Viscalor* compules were put into the Caps Warmer for 30 s and 3 min pre-heating times. Temperature was measured via a type-K thermocouple inside the compule. After pre-heating, the compule was removed from the Caps Warmer.

The extrusion force (N) of *Viscalor* from both full and half-full compules was measured using a modified compule dispenser and a universal testing machine (Zwick/ Roell Z020, Leominster, UK) (Figure 5.1). *Viscalor* was pre-heated before measurement using the Caps Warmer in T3 mode for 30 s (T3-30s) and 3 min (T3-3min). Compressive force was applied at 1 mm/s until either an upper force limit of 150 N or the maximum extrusion distance of 10 mm was reached (n=3). The mass of extruded composite (g) was also measured.

Figure 5.1 Extrusion measurement setup.

A Texture Analyzer (Figure 3.1) (TA.XT2i, Stable Micro Systems, Godalming, UK) was used to measure stickiness: via maximum separation force (F_{max}, N) and work of probe-separation (W_s, N mm) and packability: maximum packing force (F_p, N). Force was applied to a flat-ended cylindrical stainless-steel probe ($\varphi = 6$ mm). A thermostatically controlled mould at 22 °C and 37 °C with a cylindrical cavity ($\phi = 7$ mm, depth = 5 mm) was fixed to a stand (Figure 3.2). Composite paste was carefully packed into the cavity (n=5).

For stickiness measurement, during the 'bonding' phase, the probe was lowered into the surface of unset composite with a pre-test speed of 0.50 mm/s. When a 'trigger' force of 0.05 N was registered, data acquisition commenced at rate of 400 p/s until a compressive force of 1 N was recorded and held constant for 1 s. In the subsequent 'debonding' phase, the probe was raised vertically at 2 mm/s. Since the unset composite paste adhered to the probe, it elongated and exerted a tensile force as the probe ascended. With further elongation, tensile stress increased until it reached the interfacial strength and the composite paste separated from the probe.

Packability measurement used a similar experimental setup. Before measurement, the probe position was set 10 mm above the cavity. The probe was lowered into the surface of unset composite at 0.50 mm/s. When a 'trigger' force of 0.05 N was registered, data acquisition commenced until the probe penetrated 2 mm. Then the probe ascended vertically at 2 mm/s.

Fourier Transform Infrared (FTIR) Spectroscopy with an attenuated total reflectance (ATR) device (ALPHA II FTIR Spectrometer, Bruker Optik GmbH) was used to measure the DC% of *Viscalor* syringe/compule (no heat, T3-30s and T3-3min) at 5 min and 24 h post-cure. A background reading was collected between 400 to 4000 cm^{-1} using 32 scans at a resolution of 4 cm^{-1}. Composite paste was placed in an acetal mould (4 mm diameter $\times$ 2 mm thickness) directly on top of the ATR crystal. A mylar strip and a glass slide were pressed onto the mould to remove air bubbles and excess paste. The spectrum of uncured *Viscalor* was collected. Photo-cure was

achieved using an Elipar S10 LED unit (3M ESPE, USA) of mean irradiance 1200 mW/cm^2 for 40 s at zero distance from the top surface. Then the spectrophotometer's screw was applied to fix the cured specimen tightly on the reading crystal. The spectrum of the 5 min post-cured composite was collected. Then the spectra were acquired continually in real time for 24 h to obtain DC% at 24 h post-cure.

The spectral region between 1600-1700 cm^{-1} was selected to identify the heights of the aliphatic C=C absorbance peak at 1637 cm^{-1} and the aromatic C=C absorbance peak at 1608 cm^{-1}. The DC% was calculated as:

$$DC\% = 1 - \frac{\left(H_{1637\ cm^{-1}}/H_{1608\ cm^{-1}}\right)_{cured}}{\left(H_{1637\ cm^{-1}}/H_{1608\ cm^{-1}}\right)_{uncured}} \times 100\% \qquad \text{(Equation 5.1)}$$

where $H_{1637\ cm^{-1}}$ is the height of aliphatic C=C peak, $H_{1608\ cm^{-1}}$ is the height of aromatic C=C peak, respectively.

Data were entered into statistical software (SPSS, SPSS Inc., Illinois, USA) and analysed using one-way ANOVA, independent T-test and Tukey post-hoc tests ($p<0.05$). Homogeneity of variance was calculated using the Kruskal-Wallis Test ($p<0.05$).

5.3 Results
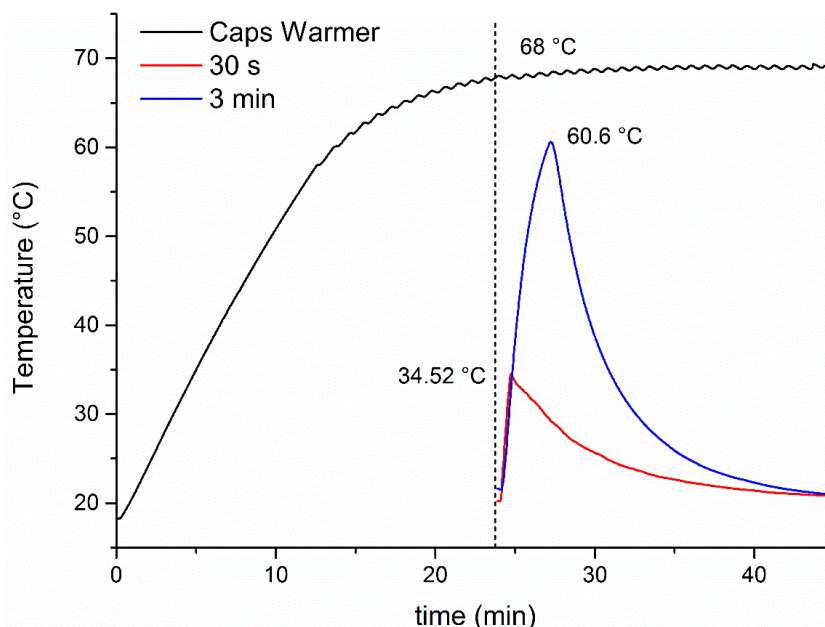
Figure 5.2 Representative temperature/time profiles of Caps Warmer (T3 mode) and Viscalor following pre-heating for different time periods.

Figure 5.2 shows representative temperature/time profiles of the Caps Warmer in T3 mode and the *Viscalor* temperatures following different pre-heating times. The Caps Warmer in T3 mode reached 68 °C after ca. 20 min. Composite temperature increases of 14.3 °C and 39.1 °C were recorded after 30 s and 3 min pre-heating, respectively. After removed from the Caps Warmer, composite temperature gradually returned to ambient temperature.

Table 5.1 Extrusion force (N) and the mass of extruded composite (g) of new/half-used Viscalor compule (no heat, T3-30s and T3-3min).

Materials	Force (N)		Mass (g)	
	New	Half-used	New	Half-used
Viscalor	153.62[a A]	152.40[a A]	0.0055[a B]	0.0134[a C]
(no heat)	(1.56)	(2.38)	(0.00)	(0.00)
Viscalor	145.45[a A]	150.59[a A]	0.1028[b B]	0.2261[b C]
(T3-30s)	(8.15)	(0.36)	(0.04)	(0.01)
Viscalor	66.49[b A]	51.29[b A]	0.1756[b B]	0.2834[c C]
(T3-3min)	(14.16)	(11.93)	(0.04)	(0.02)

For each material, the same lower case superscript letters indicate homogeneous subsets among the materials. For each measurement (F, m), the same CAPITAL superscript letters indicate homogeneous subsets among different conditions (new, half-used).

The extrusion force (N) and extruded mass (g) of full or half-full *Viscalor* compules (for no heat, T3-30s and T3-3min) are shown in Table 5.1 and Figures 5.3-5.4. The extrusion force varied with pre-heating conditions, with 3 min heating giving the lowest extrusion force ($p<0.001$). Partial usage of the compule had no significant influence on the measured extrusion force ($p=0.866$). *Viscalor* compules with no heating yielded the lowest mass of extruded composite ($p<0.001$). Half-used *Viscalor* compules (no heat, T3-30s and T3-3min) showed slightly higher extruded mass, in a fixed period, than full compules ($p<0.05$).
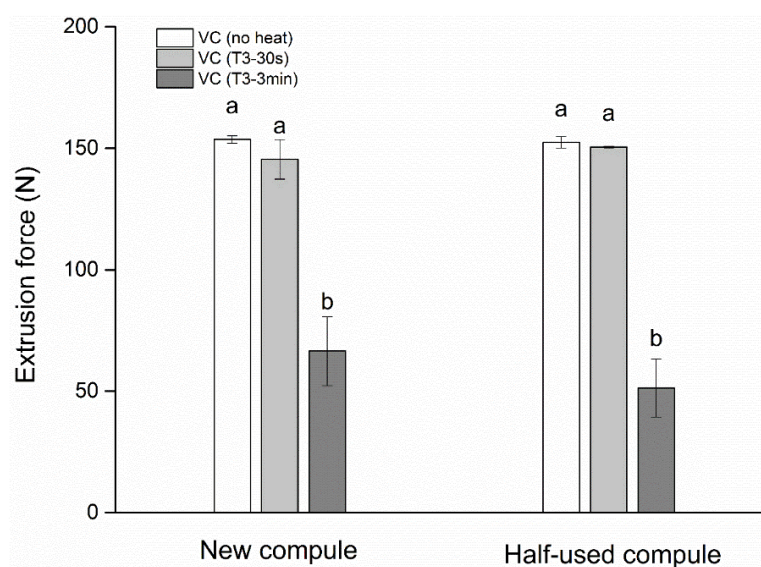
Figure 5.3 Extrusion force (N) of new/half-used Viscalor compule (no heat, T3-30s and T3-3min).
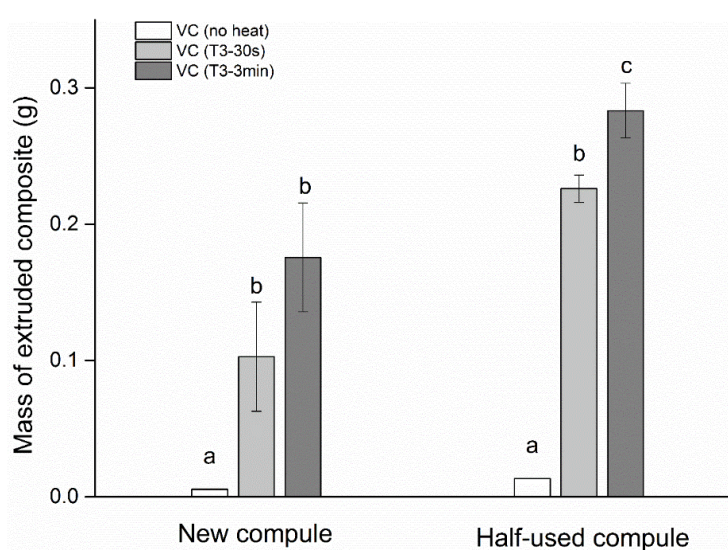
Figure 5.4 Mass of extruded composite (g) of new/half-used Viscalor compule (no heat, T3-30s and T3-3min).

Table 5.2 and Figures 5.5-5.7 show stickiness (F_{max} and W_s) and packability (F_p) data for different composites at 22 and 37 °C. F_{max}, W_s and F_p ranged from 1.50 to 3.28 N, from 0.79 to 4.69 N mm and from 10.79 to 41.56 N, respectively. Different RBCs varied in F_{max} ($p<0.001$), W_s ($p<0.001$) and F_p ($p=0.032$). Temperature also had a significant effect on F_{max} ($p<0.001$), W_s ($p=0.002$) and F_p ($p<0.001$), for which temperature rise reduced F_{max} and F_p, but increased W_s.

Table 5.2 Stickiness parameters: F_{max} (N) and W_s (N mm) and packability, F_p (N) at 22 and 37 °C.

Materials	F_{max} (N)		W_s (N mm)		F_p (N)	
	22 °C	37 °C	22 °C	37 °C	22 °C	37 °C
Admira Fusion	3.28[f A] (0.10)	3.12[d A] (0.08)	2.12[d A] (0.22)	3.61[d A] (0.97)	41.56[f C] (1.77)	23.09[e B] (1.00)
Filtek Supreme Ultra	2.94[e B] (0.04)	2.07[c A,B] (0.02)	1.26[b,c A] (0.09)	0.97[a A] (0.09)	27.11[b D] (0.91)	19.40[d C] (1.66)
TPH LV	1.91[a A] (0.06)	1.50[a A] (0.14)	0.88[a,b A] (0.03)	1.30[a,b A] (0.17)	24.10[a C] (0.62)	10.79[a B] (1.14)
Tetric EvoCeram	2.86[d,e C] (0.04)	2.21[c B,C] (0.11)	0.79[a A] (0.06)	1.29[a,b A,B] (0.15)	32.30[c,d E] (1.24)	16.64[c D] (0.40)
Harmonize	2.51[b,c A] (0.04)	1.70[b A] (0.06)	1.04[a,b,c A] (0.04)	2.03[c A] (0.13)	35.75[e C] (2.86)	15.08[b,c B] (1.68)
Viscalor **(no heat)**	3.03[e B] (0.21)	2.19[c A,B] (0.07)	1.42[c A] (0.23)	2.35[c A,B] (0.13)	31.88[c,d D] (0.66)	15.46[b,c C] (1.01)
Viscalor **(T3-30s)**	2.67[c,d A] (0.08)	2.17[c A] (0.08)	2.62[e A] (0.21)	1.71[b,c A] (0.12)	29.58[b,c C] (1.18)	14.13[b B] (0.99)
Viscalor **(T3-3min)**	2.39[b A] (0.09)	2.19[c A] (0.11)	1.89[d A] (0.36)	4.69[e B] (0.60)	34.55[d,e D] (0.17)	16.39[b,c C] (0.17)

For each temperature, the similar lower case superscript letters indicate homogeneous subsets among the materials. For each material, the similar CAPITAL superscript letters indicate homogeneous subsets among different conditions.
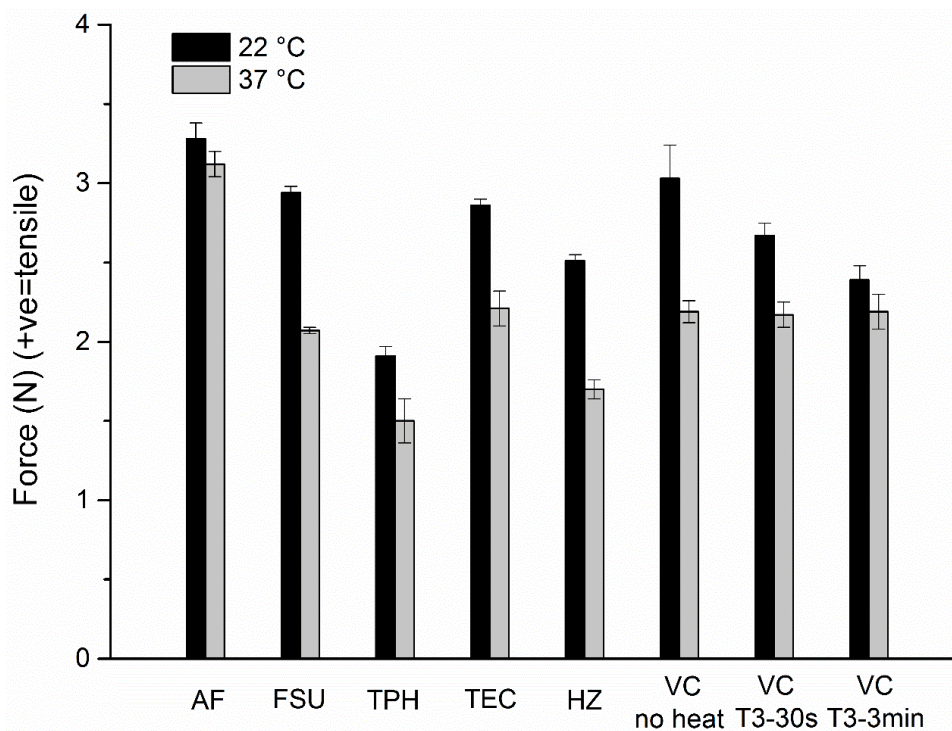
Figure 5.5 Maximum separation force (F_{max}) of investigated composites at 22 and 37 °C.
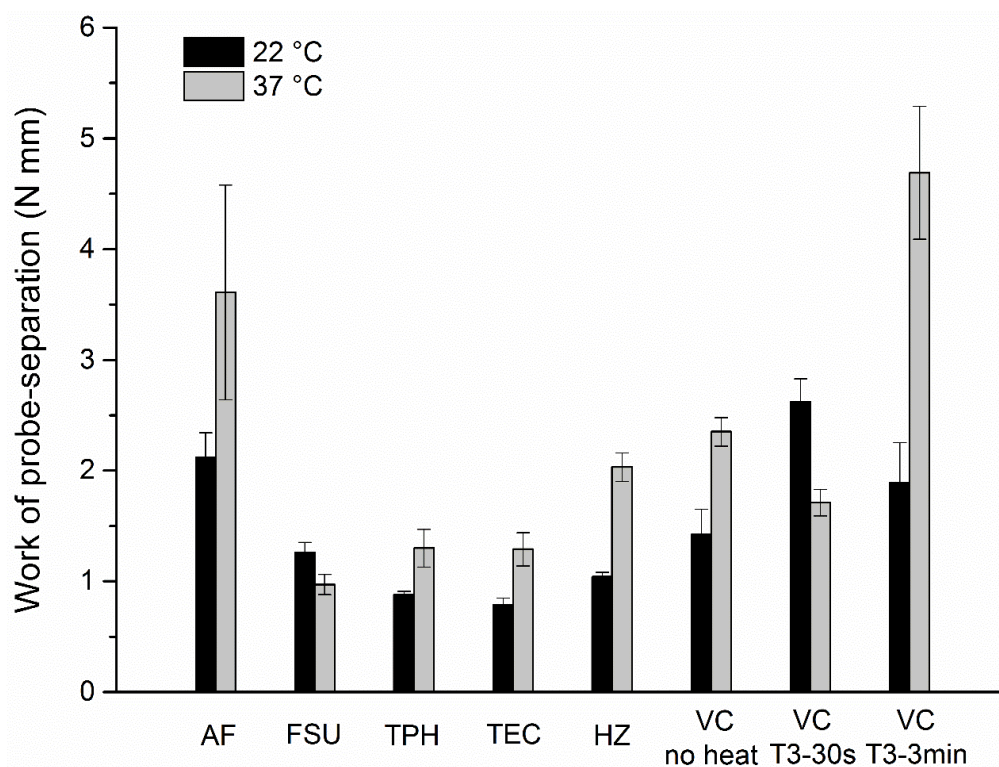
Figure 5.6 Work of probe-separation (W_s) of investigated composites at 22 and 37 °C.
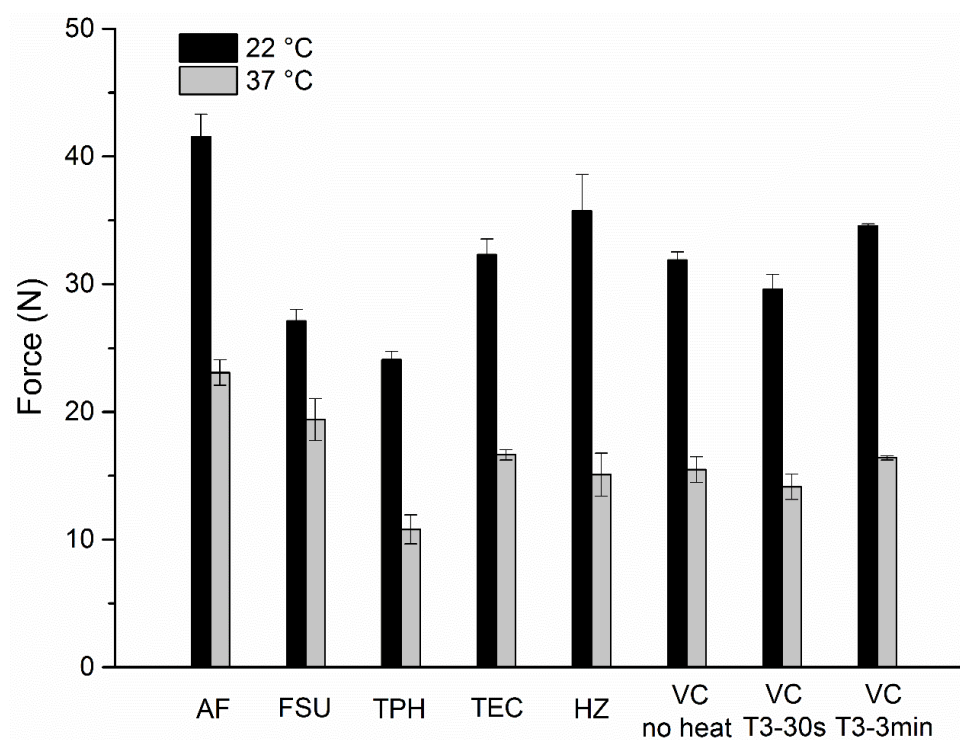
Figure 5.7 Maximum packing force (F_p) of investigated composites at 22 and 37 °C.
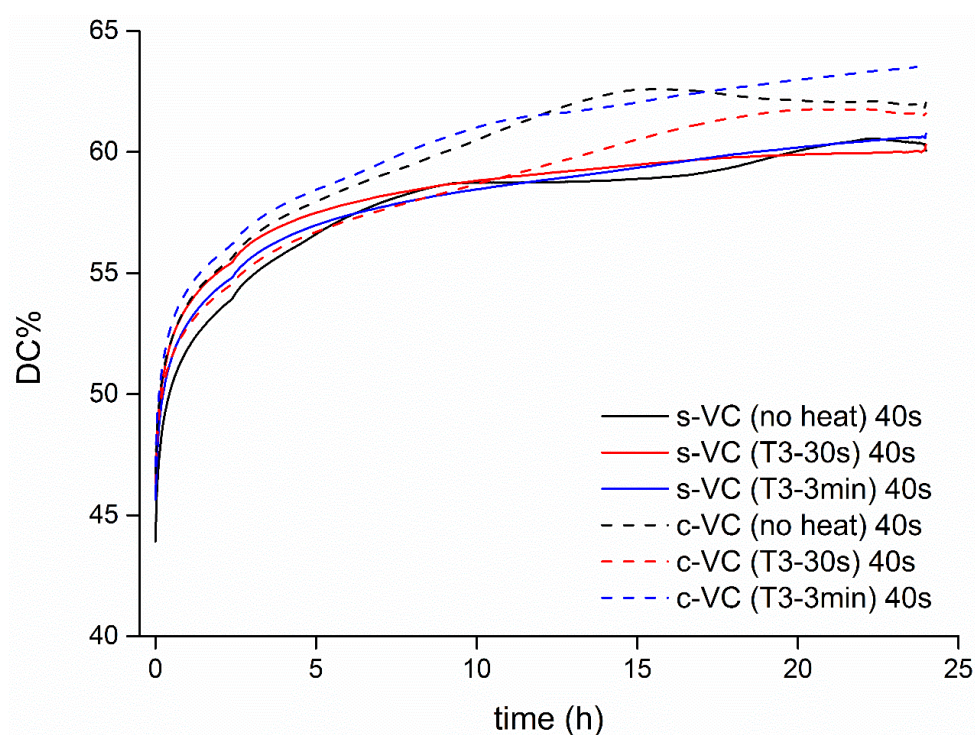
Figure 5.8 Real-time DC% vs. time during 24 h post-polymerization for Viscalor syringe/compule (no heat, T3-30s, T3-3min).

Figure 5.8 represents real-time DC% vs. time during 24 h post-polymerization of *Viscalor* syringe/compule (no heat, T3-30s and T3-3min). Real-time DC% curves of *Viscalor* syringe and compule develop over 24 h with a similar trend. Table 5.3 and Figure 5.9 report the DC% at 5 min and 24 h post-cure (DC$_{5min}$ and DC$_{24h}$) of *Viscalor* syringe/compule (no heat, T3-30s and T3-3min). After 24 h, DC% increased to approximately 60 %. There were no significant differences in DC% results between syringe and compule (p>0.05). Pre-cure heating of *Viscalor* syringe/compule for either 30 s or 3 min in a 68 °C Caps Warmer did not increase the post-cure DC% at either 5 min or 24 h, compared to data for no pre-heating (p>0.05).

Table 5.3 Degree of conversion of Viscalor (no heat, T3-30s and T3-3min) at 5 min and 24 h post cure (DC$_{5min}$ and DC$_{24h}$).

Materials	Syringe		Compule	
	DC$_{5min}$	DC$_{24h}$	DC$_{5min}$	DC$_{24h}$
Viscalor (no heat)	40.78 %[aA] (0.01)	58.04 %[aB] (0.03)	41.99 %[aA] (0.01)	60.17 %[aB] (0.03)
Viscalor (T3-30s)	42.77 %[aA] (0.01)	58.49 %[aB] (0.01)	42.76 %[aA] (0.01)	58.88 %[aB] (0.01)
Viscalor (T3-3min)	40.71 %[aA] (0.01)	58.30 %[aB] (0.01)	41.65 %[aA] (0.00)	60.60 %[aC] (0.01)

For each DC, the same lower case superscript letters indicate homogeneous subsets among the materials. For each material, the same CAPITAL superscript letters indicate homogeneous subsets among different conditions.
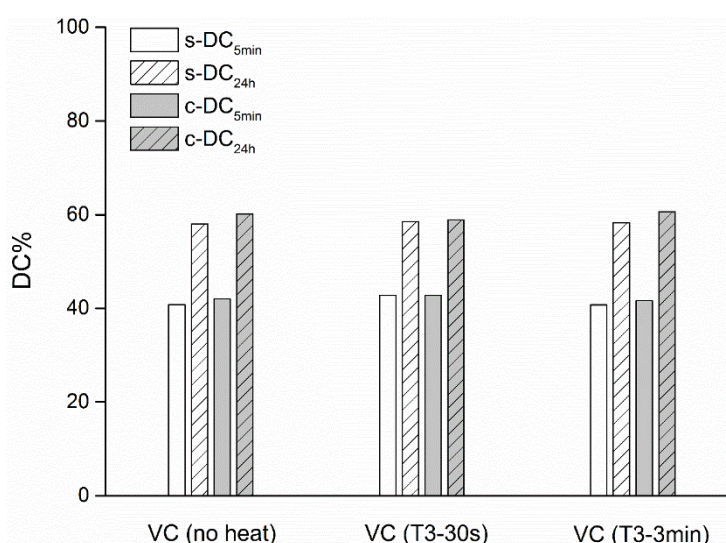
Figure 5.9 DC% results of Viscalor syringe/compule (no heat, T3-30s and T3-3min) at 5 min and 24 h post cure (DC$_{5min}$ and DC$_{24h}$).

5.4 Discussion

Dental RBCs are designed to exhibit good mechanical properties and esthetics after restoration, but their pre-cure properties, including stickiness and packability, mainly affect the clinical handling and placement [132]. These handling properties depend upon the inherent material characteristics and rheological nature of composites [128]. Hence, this study investigated extrusion force, stickiness and packability at different temperatures and evaluated post-cure DC% at 5 min and 24 h for *Viscalor* after different pre-heating times. Thus, the first null hypothesis was rejected and the second null hypothesis was accepted. Regardless of pre-heating time, no significant change in DC% of *Viscalor* was measured (p>0.05).

The thermal properties and heating rates of both Caps Warmer and pre-heated *Viscalor* were previously unreported. Thus, temperature profiles of Caps Warmer in the T3 mode and *Viscalor* following different pre-heating periods were first characterized. Results demonstrated the efficacy of the Caps Warmer since it reached the stated preset temperature of 68 °C after about 20 min. When heating was stopped, a slight temperature rise of 2.09 °C and 0.35 °C was found, respectively. During pre-heating, thermal energy diffused gradually through the container (compule or syringe) into the composite.

With temperature rise the viscosity of *Viscalor* reduced, but its flowability was still somewhat less than certain flowable RBCs at room temperature [132]. After 3 min pre-heating, *Viscalor* had a lower internal temperature than the maximum temperature of the Caps Warmer in T3 mode (68 °C). This corresponds to previous studies where pre-heated composites were cooler than the pre-set temperature of heating devices. Thus reduced pulp temperature changes may ensue [134]. Reduced composite temperature rises also relate to filler properties since inert inorganic particles only absorb small amounts of thermal energy during heating [132, 232]. The high filler content of *Viscalor* implies a low proportion of resin matrix and consequently a low temperature rise [232]. Different filler contents result in different temperature/time

profiles. The temperature of *Viscalor* (T3-3min) decreased to 37 °C within 3 min after removed from the Caps Warmer. To ensure minimal temperature drop and optimal performance, clinicians should work rapidly during manipulation of pre-heated composites.

To quantify the effect of pre-heating on *Viscalor*'s flowability, the extrusion force (N) and extruded mass (g) were measured for both full and half-used *Viscalor* compules. Results showed the beneficial effects of a longer pre-heating period, in which extrusion force reduced and extruded mass increased. This confirmed that 3 min pre-heating did increase the flowability of *Viscalor* leading to easy extrusion and a sufficient mass of extruded composite.

Stickiness measurements were based on previous studies on the effects of temperature and composite composition [126-128, 151]. Generally, there are two types of force/displacement plots (Type I and Type II), in which Type I is more commonly observed (Figure 1.6). A Type I plot has a single peak, whereas a Type II plot has a primary peak followed by a secondary peak [128]. The peak height (F_{max}) is the maximum tensile force during 'debonding'. The work of probe-separation (W_s) is the integrated area under the curve [127].

The force/displacement profiles observed were combined responses of RBC paste viscoelasticity and interfacial behaviour between the probe and paste [126, 154]. F_{max} mainly depends on the wettability of the paste, its resistance against the debonding force and the roughness of both probe and paste [126, 128, 154]. Other factors, such as temperature and visco-elastic properties of the paste also affect F_{max} [128]. W_s depends on the shear characteristics of the pastes, which relates to their molecular entanglements [126, 128, 154]. In the present stickiness results, Admira Fusion exhibited the highest F_{max} and W_s at both 22 and 37 °C. According to previous studies, high filler loading tends to produce low stickiness [84, 126] as it hinders composite flowability and creates high viscosity [115]. Admira Fusion, *Viscalor* and Harmonize have high filler content (84 wt.%, 83 wt.% and 81 wt.%, respectively) and

their F_{max} varied with filler content. However, they did not exhibit particularly low stickiness, as expected. This may be due to their matrix compositions. Admira Fusion is a ceramic-based RBC, in which ORMOCERs function as the matrix system [17, 46, 233]. Nanoparticles and glass ceramic particles are firmly embedded in the ORMOCER matrix [234]. The ART (Adaptive Response Technology) filler system in Harmonize acts as a rheological modifier.

Although containing relatively high filler loading, Filtek Supreme Ultra (78.5 wt.%) showed higher F_{max} and W_s compared to TPH LV (75.5 wt.%) and Tetric EvoCeram (75 wt.%). This may be due to both TEGDMA and bisphenol-A epoxylated dimethacrylate (bis-EMA) within its matrix system [34, 84]. Previous studies have noted that the presence/absence of hydrogen bonding significantly affects viscosity. Bis-EMA, lacks two hydroxyl groups (-OH) in its chemical structure, compared to bis-GMA, which reduces viscosity [235]. But, with a low-viscous matrix system, TPH LV and Tetric EvoCeram still showed low F_{max} and W_s possibly related to their filler characteristics. Many previous studies established that all compositional variables affect RBC rheological and handling properties: resin matrix, filler particle content, shape, size and distribution, silane surface treatment, interlocking between particles and other interfacial interactions between resin matrix and filler [112, 113]. Generally, increasing filler loading and using smaller, irregular-shaped particles increases viscosity [86, 113]. Filler particle sizes of TPH LV (1.35 μm) [227] and Tetric EvoCeram (40 nm - 3 μm) [236] are lower than those in Filtek Supreme Ultra (0.6 -10 μm) [237]. For a similar filler loading, more particles means higher surface area, more matrix/particle interactions and thus higher viscosity [84]. TPH LV and Tetric EvoCeram had low stickiness. Different filler morphologies - following the sequence: round, grains, plates and rods - reduce viscosity of RBCs [84]. Silane surface treatment may slightly lubricate irregular particles and reduce viscosity [84]. However, in this study, the lack of filler morphology information limits the discussion.

For packability measurements, compressive force (N) was plotted against probe displacement (mm) (Figure 1.7). F_p reduced with decreased filler loading. Admira Fusion and TPH LV had the highest and lowest F_p values at both 22 and 37 °C, respectively.

In addition to paste composition, temperature also affected stickiness and packability: reducing F_{max} and F_p, but increasing W_s. Temperature increases the mobility of matrix monomers. Low viscous RBCs are more fluid so temperature further reduces F_p. Composite pastes bond more easily to the probe, increasing F_{max} and W_s [126, 139]. However, some studies found that F_{max} and W_s may be lower at high temperature [84, 128, 151, 156]. Since segmental movement is greater at high temperature, matrix monomers are insufficiently resistant to slippage of internal components. This factor tends to reduce F_{max} and W_s [84, 128, 151, 156].

Viscalor (no heat) showed generally comparable F_{max}, W_s and F_p to the other investigated RBC pastes. Different pre-heating times had significant influence on F_{max}, W_s and F_p at either 22 or 37 °C (p<0.005), except for F_{max} at 37 °C (p=0.884). Composite temperature can reduce rapidly to the ambient physiological level after removed from a pre-heating device [134, 138, 139]. Thus, pre-heated *Viscalor* (T3-30s and T3-3min) inserted into the brass cavity showed similar F_{max} results to *Viscalor* (no heat) at 37 °C due to the similar composite temperature. However, *Viscalor*'s W_s changed significantly with different pre-heating times. So evidently W_s was more sensitive than F_{max} to changes in elongation and arguably more appropriate to describe stickiness [128].

Moderate temperature rise after pre-heating generates greater mobility of monomer free radicals - *as and when they are generated by photo-initiation.* The temperature rise delays auto-deceleration during polymerization and leads to the increased DC% [2, 50, 134, 138, 139, 166]. Higher monomer conversion has been observed after pre-heating composites at 54 °C, however, high polymerization shrinkage also occur with

high DC% [2, 130, 138]. But, after 30 s pre-heating, F_p decreased slightly at either 22 or 37 °C.

To further identify the effect of pre-heating time on pre-cure stickiness and packability of *Viscalor*, DC% was measured. After 24 h at 37 °C, DC% increased [50, 166]. The use of *Viscalor* syringe or compule had no significant influence on DC_{5min} and DC_{24h}. Real-time DC% curves of both *Viscalor* syringe and compule specimens increased similarly. Different pre-heating time had no significant effect on *Viscalor* syringe/compule DC% either measured after 5 min or 24 h. Generally, temperature rise has a positive effect on DC%, since temperature rise aids polymer chain propagation.

Three minutes pre-heating did not affect the DC% of *Viscalor* syringe/compule specimens. This suggests that no premature monomer curing occurred.

5.5 Conclusions

Within the limitations of this study, the following conclusions are drawn:

1) The Caps Warmer exhibited good efficacy as a pre-heating device: pre-heated *Viscalor* showed greatly reduced extrusion force and increased flowability, especially after the longer pre-heating time (3 min).

2) The RBC pastes varied to a statistically significant but limited extent in stickiness and packability. But, their overall magnitudes remained within what may be considered a clinically acceptable range.

3) Pre-heating had no adverse effects on *Viscalor* through any thermal activation causing premature polymerization.

Chapter Six

Pre-heating Time and Exposure Duration: Effects on Post-irradiation Properties of A Thermo-viscous Resin-composite

Jiawei Yang[1], Nikolaos Silikas[1*], David C. Watts[1,2*]

1. Dentistry, School of Medical Sciences, University of Manchester, Manchester, UK

2. Photon Science Institute, University of Manchester, Manchester, UK

Abstract

Objectives. To evaluate the effects of pre-heating time and exposure duration on the degree of conversion (DC), maximum rate of polymerization (RP_{max}), polymerization shrinkage strain (PS) and surface micro-hardness (VHN) of *Viscalor*.

Methods. Viscalor syringes were pre-heated using a Caps Warmer (VOCO, Germany) in T3 mode (at 68 °C) for 30 s (T3-30s) and 3 min (T3-3min) and then the composite paste was extruded into appropriately sized moulds. Light irradiation was applied at zero distance from the upper surface with a LED-LCU of mean irradiance 1200 mW/cm^2 for either 20 s or 40 s. The real-time polymerization kinetics and DC at 5 min and 24 h post-irradiation (DC_{5min} and DC_{24h}) were measured using ATR-FTIR (n=3). PS was obtained with the bonded-disk technique (n=3). Top and bottom Vickers micro-hardness (VHN_{top} and VHN_{bottom}) were measured at 5 min post-irradiation and after 24 h dry storage (n=5). Data were analysed using one-way ANOVA, two-way ANOVA, independent t-test and Tukey post-hoc tests (p<0.05).

Results. Polymerization kinetic curves of *Viscalor* from 0-15 min were similar for different pre-heating times and exposure durations. Pre-heated *Viscalor* (T3-30s and T3-3min) with 40 s exposure had greater VHN_{top} and VHN_{bottom} than for *Viscalor* (no heat) (p<0.05). Exposure duration did not significantly affect DC, RP_{max} and PS (p>0.05). After 24 h storage, DC and VHN increased. Pre-heating did not increase the DC_{24h}, relative to no pre-heating (p>0.05). Two-way ANOVA showed that there was no significant interaction between pre-heating time and exposure duration (p>0.05).

Significance. Increasing irradiation time from 20 to 40 s did not affect DC, RP_{max} or PS, but increased VHN_{top}. Composite pre-heating had no adverse effect through any premature polymerization. For *Viscalor*, 3 min pre-heating and 20 s irradiation were sufficient to provide adequate hardness, without increasing PS or compromising polymerization kinetics.

6.1 Introduction

Chairside pre-heating of dental resin-based composites (RBCs) has been introduced to improve their handling properties [135]. It lowers the viscosity of composites, leading to better flowability and marginal adaptation and reduces microleakage and gap formation [3].

Temperature also has an influence on the efficiency of polymerization, which is important for the post-irradiation properties and clinical performance of polymer-based RBCs. Higher monomer mobility, caused by the increased temperature, facilitates cross-linking among polymer chains and leads to a high degree of conversion (DC) and better mechanical properties [2, 3]. Several studies have investigated the effect of pre-heating on RBCs mechanical properties, finding that micro-hardness and flexural strength increased after pre-heating [1, 2, 135, 211, 213]. However, Uctasli et al. [238] found no significant increases in flexural strength and flexural modulus of pre-heated composites. The diverse outcomes may result from different composite compositions and experimental setups.

Internal molecular densification develops during the irradiation process and leads to macroscopic polymerization shrinkage [239]. It is still a drawback of RBCs and the associated stress may lead to marginal debonding, secondary caries and clinical failure. Different approaches have been taken in attempts to reduce the developed contraction stress, such as adding rigid low-shrinking monomers [38, 240], increasing filler content and using the "soft-start" curing method [48] with various placement techniques [241]. At the post-irradiation stage, the uncured free radicals continue cross-linking slowly, which can produce further shrinkage [212].

Polymerization shrinkage strain (PS) increased with DC. Within certain limits, a linear relationship was demonstrated [18, 64]. Some pre-heated composites also showed higher DC and PS [2, 182]. The increased monomer mobility allows more radical collision, which delays auto-deceleration and improves DC and PS. However,

the increased PS and the related marginal issues could be offset by the enhanced flowability via pre-heating [3].

Recently, a bulk-fill composite designed with thermo-viscous-technology (*Viscalor*) was introduced. Bulk-fill composites have at least 4 mm depth of cure and may exhibit low shrinkage stress [74, 242]. As investigated in Chapter 5, pre-heated *Viscalor* showed similar DC to room-temperature *Viscalor* [243]. However, the previous study included a 40 s irradiation period that is longer than the recommended 10-20 s. The effects of pre-heating time and exposure duration on its PS and surface micro-hardness (VHN) remain unknown. The longer curing time may have masked the effect of pre-heating time on the measured properties.

The objectives of this study were to evaluate the effects of pre-heating time (30 s and 3 min) and exposure duration (20 and 40 s) on the degree of conversion (DC), maximum rate of polymerization (RP_{max}), polymerization shrinkage strain (PS) and surface micro-hardness (VHN) of *Viscalor*. The Null Hypotheses were:
(1) pre-heating time did not influence DC, RP_{max}, PS and VHN of *Viscalor,*
(2) exposure duration did not influence DC, RP_{max}, PS and VHN of *Viscalor* and
(3) there was no interaction between pre-heating time and exposure duration.

6.2 Materials and methods

The manufacturer information of *Viscalor* is presented in Table 6.1. *Viscalor* syringes were pre-heated using a Caps Warmer (VOCO, Germany) in T3 mode (at 68 °C) for 30 s (T3-30s) and 3 min (T3-3min), respectively. According to previous study, the estimated composite temperatures after 30 s and 3 min pre-heating are 34.5 °C and 60.6 °C, respectively [243].

Table 6.1 Manufacturer information of Viscalor.

	Manufacturer	**Resin system**	**Filler wt.%**
Viscalor	VOCO, Germany	Bis-GMA, aliphatic dimethacrylate	83

The degree of conversion at 5 min and 24 h post-irradiation (DC_{5min} and DC_{24h}) and real-time polymerization kinetics were measured using Fourier Transform Infrared (FTIR) Spectroscopy (ALPHA II FTIR Spectrometer, Bruker Optik GmbH) with an attenuated total reflectance (ATR) device. Background readings were collected between 400 to 4000 cm^{-1} using 32 scans at a resolution of 4 cm^{-1}. The uncured composite paste was extruded into a cylindrical Acetal mould (4 mm diameter $\times$ 2 mm thickness) above the diamond ATR crystal. The specimen was pressed from the top with a mylar strip followed by a glass slide to remove air bubbles.

For DC measurements (n=3), the spectrum of uncured *Viscalor* was collected first. Then irradiation was applied at zero distance from the upper surface with an LED-LCU of mean irradiance 1200 mW/cm^2 for either 20 s or 40 s. The spectrophotometer's screw was then applied to ensure good contact between the specimen and the ATR crystal. The DC spectrum was collected after 5 min (DC_{5min}) and after 24 h real-time acquisition (DC_{24h}). The peak heights of the aliphatic C=C absorbance peak at 1637 cm^{-1} and the aromatic C=C absorbance peak at 1608 cm^{-1} were selected to calculate the DC% using Equation 5.1.

For real-time kinetic measurements over 15 min (n=3), the spectral acquisition started immediately before irradiation. Either 20 or 40 s irradiation was applied at 5 s after

the start of the spectral acquisition. Spectra were collected using 10 scans at a resolution of 4 cm^{-1}. The rates of polymerization were obtained by numerical differentiation of real-time DC data with respect to time.

Polymerization shrinkage strain (PS) was measured using the bonded disk method [75, 183], with a 3 mm thick glass base-plate, at 23 °C room temperature (n=3). The specimens were cured for either 20 or 40 s. The axial strain was continuously measured up to 1 h after irradiation.

For hardness measurements, after either 20 or 40 s photo-irradiation from the upper surface, cylindrical specimens were removed from the mould (4 mm diameter × 2 mm thickness). Top and bottom surface Vickers micro-hardness (VHN_{top} and VHN_{bottom}) at 5 min post-irradiation was measured using a micro-hardness instrument (FM-700, Future Tech Corp., Japan) with a Vickers diamond pyramid micro-indenter (n=5). A fixed load of 300 gf was applied for 15 s. Five indentations on both top and bottom surfaces were measured and averaged as the final VHN value. The specimens were then stored in dry conditions at 37°C for 24 h and the 24 h post-irradiation surface hardness was measured.

Data were entered into statistical software (SPSS, SPSS Inc., Illinois, USA) and analysed using one-way ANOVA, two-way ANOVA, independent T-test and Tukey post-hoc tests (p<0.05). Homogeneity of variance was calculated using the Kruskal-Wallis Test (p<0.05).

6.3 Results

Polymerization kinetic curves of *Viscalor* from 0-15 min were similar for different pre-heating times and exposure durations (Figure 6.1). Table 6.2 summarize the DC_{5min} and DC_{24h} of *Viscalor* (no heat, T3-30s and T3-3min) with different exposure durations. DC results ranged from 40.4 to 58.8 %, in which DC_{24h} are significantly higher than DC_{5min} (p<0.05). Pre-heating time and exposure duration did not significantly affect DC results (p>0.05).
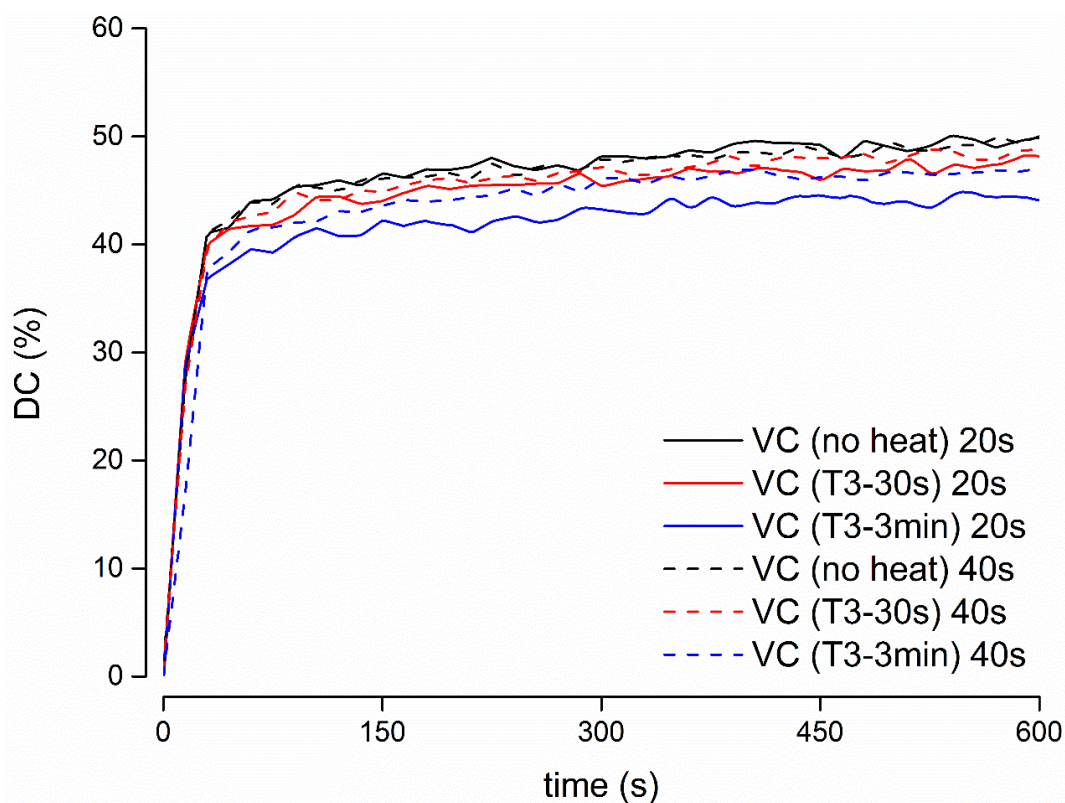
Figure 6.1 Real-time DC% vs. time during 15 min post-polymerization for Viscalor (no heat, T3-30s and T3-3min) with different exposure durations.

Table 6.2 Degree of conversion at 5 min and 24 h post-irradiation (DC_{5min} and DC_{24h}) of Viscalor (no heat, T3-30s and T3-3min) with different exposure durations.

Materials	DC_{5min}		DC_{24h}	
	20 s	**40 s**	**20 s**	**40 s**
Viscalor	41.9 %[a A]	40.8 %[a A]	58.8 %[a B]	58.0 %[a B]
(no heat)	(0.01)	(0.01)	(0.03)	(0.03)
Viscalor	42.3 %[a A]	42.8 %[a A]	58.7 %[a B]	58.5 %[a B]
(T3-30s)	(0.02)	(0.01)	(0.02)	(0.01)
Viscalor	40.4 %[a A]	40.7 %[a A]	58.3 %[a B]	58.3 %[a B]
(T3-3min)	(0.00)	(0.01)	(0.03)	(0.01)

For each exposure duration, the same lower case superscript letters indicate homogeneous subsets among the materials. For each material, the same CAPITAL superscript letters indicate homogeneous subsets among different conditions.

RP_{max} results are shown in Table 6.3 and Figure 6.2. RP_{max} ranged from 1.76 to 1.96 %/s, in which pre-heated *Viscalor* (T3-30s and T3-3min) with 20 s exposure

duration had the highest RP_{max}. Both pre-heating time and exposure duration had no significant influences on RP_{max} (p>0.05).

Table 6.3 Maximum rates of polymerization (RP_{max}, %/s) of Viscalor (no heat, T3-30s and T3-3min) with different exposure durations.

Materials	RP_{max} (%/s)	
	20 s	**40 s**
Viscalor	1.85 [a][A]	1.79[a][A]
(no heat)	(0.42)	(0.32)
Viscalor	1.95[a][A]	1.76[a][A]
(T3-30s)	(0.11)	(0.49)
Viscalor	1.96[a][A]	1.78[a][A]
(T3-3min)	(0.12)	(0.35)

For each exposure duration, the same lower case superscript letters indicate homogeneous subsets among the materials. For each material, the same CAPITAL superscript letters indicate homogeneous subsets among different conditions.

Figure 6.2 Maximum rates of polymerization (RP_{max}, %/s) of Viscalor (no heat, T3-30s and T3-3min) with different exposure durations.

Table 6.4 shows PS results, which ranged from 1.35 to 1.57 %. The real-time polymerization shrinkage strain curves of all measured specimens increased similarly.

Both pre-heating time and exposure duration had no significant influences on PS (p>0.05).

Table 6.4 Polymerization shrinkage strain (PS) of Viscalor (no heat, T3-30s and T3-3min) with different exposure durations at 23 °C.

Materials	PS	
	20 s	**40 s**
Viscalor (no heat)	1.35 % [a A] (0.14)	1.41 % [a A] (0.13)
Viscalor (T3-30s)	1.47 % [a A] (0.07)	1.57 % [a A] (0.16)
Viscalor (T3-3min)	1.43 % [a A] (0.01)	1.45 % [a A] (0.15)

For each exposure duration, the same lower case superscript letters indicate homogeneous subsets among the materials. For each material, the same CAPITAL superscript letters indicate homogeneous subsets among the exposure duration.

Table 6.5 and Figures 6.3-6.4 show VHN_{top} and VHN_{bottom} results of *Viscalor*. At 5 min post-irradiation, *Viscalor* (no heat) with 20 s exposure duration showed the lowest VHN_{top}. At 24 h post-irradiation, *Viscalor* (T3-3min) with 40 s exposure duration showed the highest VHN_{bottom}. Pre-heating significantly increased both VHN_{top} and VHN_{bottom} (p<0.05), whereas exposure duration only significantly improved VHN_{top} in some cases.

Table 6.5 VHN$_{top}$ and VHN$_{bottom}$ of Viscalor (no heat, T3-30s and T3-3min) at 5 min and 24 h post-irradiation with different exposure durations.

Materials	5 min post-irradiation				24 h post-irradiation			
	VHN$_{top}$		VHN$_{bottom}$		VHN$_{top}$		VHN$_{bottom}$	
	20 s	40 s	20 s	40 s	20 s	40 s	20 s	40 s
Viscalor	47.54$^{a\,A}$	49.19$^{a\,A,B}$	49.84$^{a\,B}$	52.08$^{a\,C}$	65.17$^{a\,D}$	66.02$^{a\,D}$	66.76$^{a\,D}$	66.35$^{a\,D}$
(no heat)	(2.75)	(3.68)	(2.58)	(3.02)	(1.15)	(0.81)	(0.75)	(1.76)
Viscalor	52.16$^{b\,A}$	54.58$^{b\,B}$	54.92$^{b\,B}$	55.59$^{b\,B}$	65.74$^{a,b\,C}$	67.40$^{a\,D}$	68.05$^{b\,D,E}$	69.09$^{b\,E}$
(T3-30s)	(1.49)	(1.48)	(1.52)	(0.81)	(0.79)	(2.42)	(0.29)	(0.92)
Viscalor	49.64$^{c\,A}$	53.80$^{b\,B,C}$	51.77$^{c\,B}$	54.30$^{b\,C}$	66.96$^{b\,D}$	69.54$^{b\,E}$	68.46$^{b\,D,E}$	69.03$^{b\,D,E}$
(T3-3min)	(2.85)	(2.87)	(2.73)	(1.51)	(1.54)	(2.85)	(1.68)	(1.22)

For each exposure duration, the same lower case superscript letters indicate homogeneous subsets among the materials. For each material, the same CAPITAL superscript letters indicate homogeneous subsets among different conditions.

Figure 6.3 Top surface micro-hardness (VHN$_{top}$) of Viscalor (no heat, T3-30s and T3-3min) at 5 min and 24 h post-irradiation with different exposure durations. The same lower case letters indicate homogeneous subsets between materials.

Figure 6.4 Bottom surface micro-hardness (VHN$_{bottom}$) of Viscalor (no heat, T3-30s and T3-3min) at 5 min and 24 h post-irradiation with different exposure durations. The same lower case letters indicate homogeneous subsets between materials.

Scatter plots and correlations of DC-PS with different exposure durations at 5 min post-irradiation are shown in Figure 6.5.
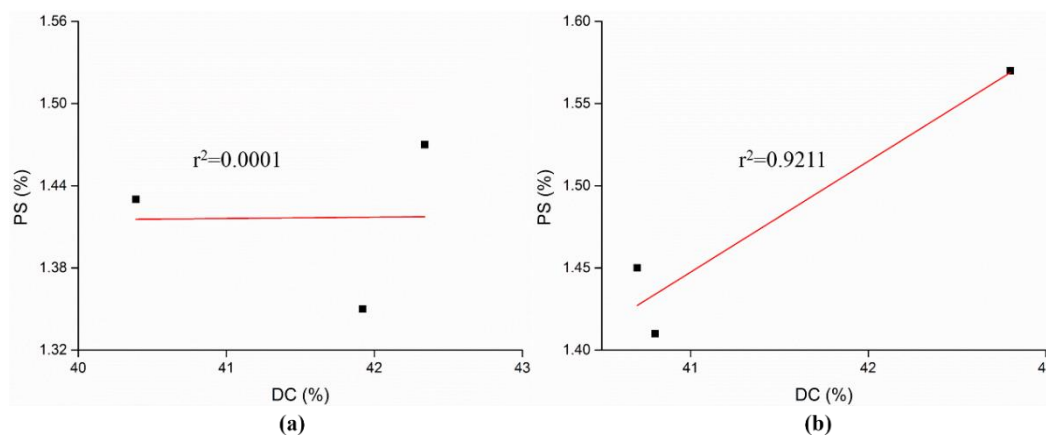
Figure 6.5 Scatter plots showing the correlations and linear regressions of DC-PS with (a) 20 s exposure duration and (b) 40 s exposure duration, both at 5 min post-irradiation at 23 °C.

Two-way ANOVA demonstrated that there was no significant interaction between pre-heating time and exposure duration ($p > 0.05$).

6.4 Discussion

Building upon previous DC results of *Viscalor* in Chapter 5 [243], this study further investigated the effect of pre-heating time and exposure duration on its post-irradiation properties: DC, RP_{max}, PS and VHN. The interaction between the two variables was also studied. Room-temperature and pre-heated *Viscalor* showed similar DC, RP_{max} and PS results, irrespective of exposure duration. After pre-heating and long exposure duration, VHN increased. Thus, the first and second null hypotheses were partly rejected. And the third null hypothesis was accepted since there was no interaction between the two variables ($p > 0.05$).

During clinical applications, RBC paste transforms to a rigid mass through photo-polymerization, which is usually activated by a visible light-curing unit (LCU) [18]. The polymerization rate reaches the maximum value (RP_{max}) during the first few minutes after irradiation [50, 166, 211, 244]. After rapid early-stage polymerization,

the increased monomer conversion limits the mobility of unreacted monomers to reach the reactive sites and reduces the rate of polymerization [50, 166, 244, 245].

Generally, DC is the key parameter describing the effectiveness of monomer conversion and commonly measured using the FTIR technique [138, 166, 246]. Light-curing of dimethacrylate-based monomers results in a highly cross-linking structure. However, due to steric hindrance and limited mobility of free radicals, there are residual unreacted monomers in the final product, which leads to the final DC of 55-75 % [64, 138, 166, 247, 248]. Adequate polymerization leads to a high DC, which is vital to the material's long-term performance and functionality, whereas insufficient polymerization can be deleterious to clinical success [166]. The synergistic effect of *intrinsic* and *extrinsic* factors plays an important role in controlling the efficiency of photo-polymerization [73]. The former includes monomer composition, filler size and content and the type and quantity of photo-initiators [73]. The latter includes the irradiance of LCU, exposure time, curing mode, temperature and the distance between the LCU tip and the restoration surface [73]. Although altering the composition may directly modify the final properties of the composites, it is not changeable by the clinician during the operative placement [73]. However, the extrinsic factors are critically dependent on operator skill, especially during the light-curing process.

It has been reported that pre-heated composites have a greater extent of monomer conversion, polymerization rate and conversion at RP_{max} [50, 130, 141]. In this study, DC and RP_{max} did not vary with pre-heating time. This can be explained by composite temperature decrease after removal from the heating device and during the handling process [132, 139]. As previously mentioned by Daronch et al. [134], pre-heated composites were not as warm as expected. The actual delivery temperature of the pre-heated compule was lower than the pre-set temperature of the heating device [132]. The major temperature rise, however, is related to the exothermic photo-polymerization and the heat produced by the LCU [134, 138].

The heat build-up during photo-polymerization has always been a concern to both researchers and clinicians. By comparing different types of LCU, the significant temperature rises during light-curing can be attributed to the higher irradiance and/or longer exposure duration [48]. In this study, use of a LED-LCU with an average constant irradiance (1200 mW/cm^2), different exposure durations (20 or 40 s) were applied which resulted in a radiant exposure of either 24 or 48 J/cm^2. However, the DC and RP$_{max}$ showed no significant changes between 20 and 40 s. This is in line with a previous study in which, at 2 mm depth, the DC after 20 s exposure duration was equal to that after 40 s [249]. Furthermore, as Daugherty et al. concluded to achieve adequate polymerization of bulk-fill composite, a minimum of 14 J/cm^2 radiant exposure should be delivered by the LED-LCU [73].

Some studies reported that curing pre-heated composites for a short exposure duration produced similar or higher DC, compared to composites cured for longer exposure durations at room temperature [3, 131]. But in this study, both long pre-heating time (3min) and exposure duration (40 s) did not significantly increase DC. The RP$_{max}$ of pre-heated *Viscalor* (T3-30s and T3-3min) with 20 s exposure was maximal. Combined with similar DC magnitudes and similar real-time DC plots, the evidence is that 20 s curing time was sufficient to produce an adequate degree of polymerization for *Viscalor* (no heat, T3-30s and T3-3min). This result may also be related to specimen thickness, light absorption/scattering and composition of the composite, which merits further investigation such as light transmission.

The correlation between DC and PS was far stronger for 40 s than 20 s irradiation (Figure 6.5) but this evidenced that increased DC is associated with high PS [2, 64]. Internal densification occurs during photo-polymerization, in which inter-molecular van der Waals distances convert to covalent (C-C) bond-lengths [37, 250, 251]. Thus, polymerization shrinkage is accompanied by volumetric reduction. A primary design requirement for developing dental restorative composites focuses on increasing DC but reducing PS [252]. A low PS is good for minimizing stress during polymerization, which leads to better marginal sealing and integrity [138]. Many methods have been

used to measure PS, including mercury dilatometer, Archimedes' principles of buoyancy and the bonded-disk technique [74, 75, 138, 182, 183], which has been used in this study. Results showed that exposure duration had no significant influence on PS, which also correlated with the present DC results. The minimal temperature change during different exposure durations may also contribute to similar PS results, which merits further investigation.

Some studies reported that elevated temperatures could increase both DC and PS [2, 64, 138]. However, the present results showed that pre-heating did not significantly increase PS and they ranged lower than the generally accepted shrinkage range of 2-6 % [2, 138, 253]. Pre-heating allows sufficient flow of polymer chains during the early-stage polymerization, which reduces internal stress formation within the cavity [64, 139, 245]. Moreover, enhanced marginal adaptation of pre-heated composite could compensate for the developed shrinkage and stress [3, 64]. Thus, 3 min pre-heating and sufficient exposure duration may lead to a steady rate of polymerization and PS results within clinically acceptable limits.

VHN measurements are an indirect method to determine the effective polymerization of composite [211]. In this study, both VHN_{top} and VHN_{bottom} values were measured and all the bottom/top ratios were over 0.8, which indicated adequate polymerization through the specimen thickness (2 mm) [1, 169, 211]. It is well known that extended post-polymerization times may increase DC and the degree of cross-linking [162]. The increased VHN after 24 h storage indicated the progressive cross-linking reaction post-irradiation [254-256]. Pre-heating enhanced both the VHN_{top} and VHN_{bottom} of *Viscalor*. This suggests that the reduced viscosity improved the cure at the lower surface. Some previous studies showed similar results [1, 211, 213, 257]. At 5 min post-irradiation, *Viscalor* (T3-3min) with 20 s exposure showed lower VHN than that of *Viscalor* (T3-30s). Despite the significant differences, their VHN values are all in an acceptable range and higher than *Viscalor* (no heat). On the contrary, exposure duration only slightly enhanced VHN_{top} values in some cases. Although extended

exposure duration may improve the extent of polymerization, 20 s curing time seems to be sufficient for obtaining adequate VHN results.

6.5 Conclusions

Within the limitations of this study, the following conclusions can be summarized:

1) Use of a longer exposure duration 40 s, compared to 20 s, did not affect DC, RP_{max} or PS, but increased VHN_{top}

2) Pre-heating had no adverse effect through any premature polymerization.

3) For clinical application of *Viscalor*, 3 min pre-heating and 20 s irradiation were sufficient to provide adequate hardness, without increasing PS or compromising polymerization kinetics.

Chapter Seven

Gloss and Surface Roughness of Different Resin-based Composites after Toothbrushing Simulations

Abstract

Objectives. To investigate the effect of toothbrushing simulation on gloss and surface roughness of different resin-based composites (RBCs) and to determine the effect of pre-heating time on surface profiles of *Viscalor*.

Methods. Viscalor was pre-heated using a Caps Warmer (VOCO, Germany) in T3 mode (at 68 °C) for 30 s (T3-30s) and 3 min (T3-3min), respectively. Five cylindrical specimens (13 mm diameter $\times$ 3 mm thickness) of different RBCs were light-cured from both top and bottom sides for 40 s with a LED-LCU of mean irradiance 1200 mW/cm^2. After 24 h storage in a dry condition at 37 °C, specimens were toothbrushed for 10000 cycles. Gloss and surface roughness were measured before and after toothbrushing simulations. Data were analysed using one-way ANOVA, independent t-test and Tukey post-hoc tests (p<0.05).

Results. All materials showed similar gloss and surface roughness before the toothbrushing simulations. After brushing, gloss decreased (p<0.05) and surface roughness increased (p<0.05). RBCs varied in gloss and surface roughness (p<0.05). There were strong polynomial correlations between filler content (%) and gloss (r^2=0.83)/surface roughness (r^2=0.98) and, between filler content (vol.%) and gloss (r^2=0.99)/surface roughness (r^2=0.94). Pre-heating time only significantly affected gloss (after) and surface roughness (before) of *Viscalor* (p<0.05). After toothbrushing simulations, a strong inverse linear correlation between gloss and surface roughness was observed (r^2=0.90).

Significance. Gloss and surface roughness were material dependent. Composites became rougher and lost gloss after toothbrushing simulations. Pre-heating had no adverse effects on gloss and surface roughness of *Viscalor*. There was a negative linear correlation between gloss and surface roughness.

Key words: Gloss; surface roughness; filler content; toothbrushing simulation; pre-heating

7.1 Introduction

With composition improvement, resin-based composites (RBCs) have been widely used as direct dental restorative materials with better aesthetic, wear resistance and mechanical properties [258-260]. A perfectly smooth surface of restoration is desirable for aesthetic appearance and it's better to remain for a long period within the oral cavity [195, 261, 262]. The smooth surface is essential to avoid discoloration and bacteria adhesion [196, 258, 260-262]. A rougher surface may lead to less glossy appearance, plaque maturation and clinical failure of RBCs [263].

Gloss and surface roughness are primary parameters describing the visual appearance and the irregularities of the restoration surface [196, 258, 263, 264]. Gloss represents the extent of surface shine and is related to the surface roughness of the material [195]. 60° angle of illumination is usually used to measure gloss since that is close to the angle of how people observe the tooth surface [195, 196, 264]. There are various techniques to study surface roughness, in which non-contact quantitative methods, such as 2-D and 3-D surface profile measurements, are commonly applied [195]. Within the limitation of different experimental factors, a mean 2-D surface roughness (Ra) of 0.2 μm has been set as the clinical threshold for bacterial retention [265]. The low surface roughness is less detectable by the tip of the tongue, which also adds to the patient's comfort [258, 266].

Clinically, finishing and polishing procedures will be applied to the material after light-curing for the completion of restoration [261, 262]. Finishing refers to contour the restorations and polishing refers to remove the scratches to obtain an ideal surface appearance [199, 261, 262]. Optimal finishing and polishing procedures enhance aesthetic and lifespan of restorations [267, 268]. The effects of finishing and polishing procedures on the appearance of RBCs have been widely studied [197, 261-263, 268, 269]. Different finishing and polishing systems and abrasive sizes result in diverse surface quality. Furthermore, as a consequence of daily toothbrushing, the gloss and surface roughness of restoration will change. The effect of toothbrushing on gloss and

surface roughness of RBCs has been extensively studied using different simulation machines [194, 196, 258, 270, 271].

Many studies concluded that surface quality of finished/polished RBCs mainly related to material inherent characteristics, including resin monomer composition and filler particle properties [105, 198, 261]. Nanohybrid composites have been demonstrated having superior polishability compared to other types of RBCs [105]. Additionally, the composite intrinsic roughness affects the final surface profile after abrasion.

Recently, a bulk-fill composite designed with thermo-viscous-technology (*Viscalor*) was introduced. Bulk-fill composites showed similar polishability and surface performance to nanohybrid composites after abrasion [196, 260, 261]. However, the effect of pre-heating on the surface quality of RBCs is largely unknown.

Hence, the objectives of this study were to investigate the gloss and surface roughness of different RBCs before and after toothbrushing simulations. The effect of pre-heating time on surface profiles of *Viscalor* was also evaluated. The null Hypotheses of this study were:

(1) there were no significant differences in gloss and surface roughness among the tested RBCs before/after toothbrushing simulations,

(2) the gloss and surface roughness remained the same after toothbrushing simulations,

(3) pre-heating time had no significant effects on *Viscalor* gloss and surface roughness before/after toothbrushing simulations and

(4) there was no correlation between the gloss and the surface roughness after toothbrushing simulations.

7.2 Materials and methods

Five commercial RBCs and *Viscalor*, pre-heated using the Caps Warmer in T3 mode (at 68 °C) for different times (30 s and 3 min), were investigated. The manufacturers' information is tabulated in Table 3.1.

Five cylindrical specimens of each material were made using Acetal moulds (diameter 13 mm × thickness 3 mm). The large specimen size was used to cover the light beam during gloss measurement and to ensure sufficient thickness after brushing. After packing composite into the mould, a mylar strip was placed and pressed using a glass slide to remove excess materials. To ensure optimum curing, an Elipar S10 LED LCU (3M ESPE, USA) with a mean irradiance of 1200 mW/cm^2 was used to photo-cure specimens from both top and bottom surfaces for 40 s. After the preparation, the specimens were stored in a dry condition at 37 °C for 24 h without finishing or polishing.
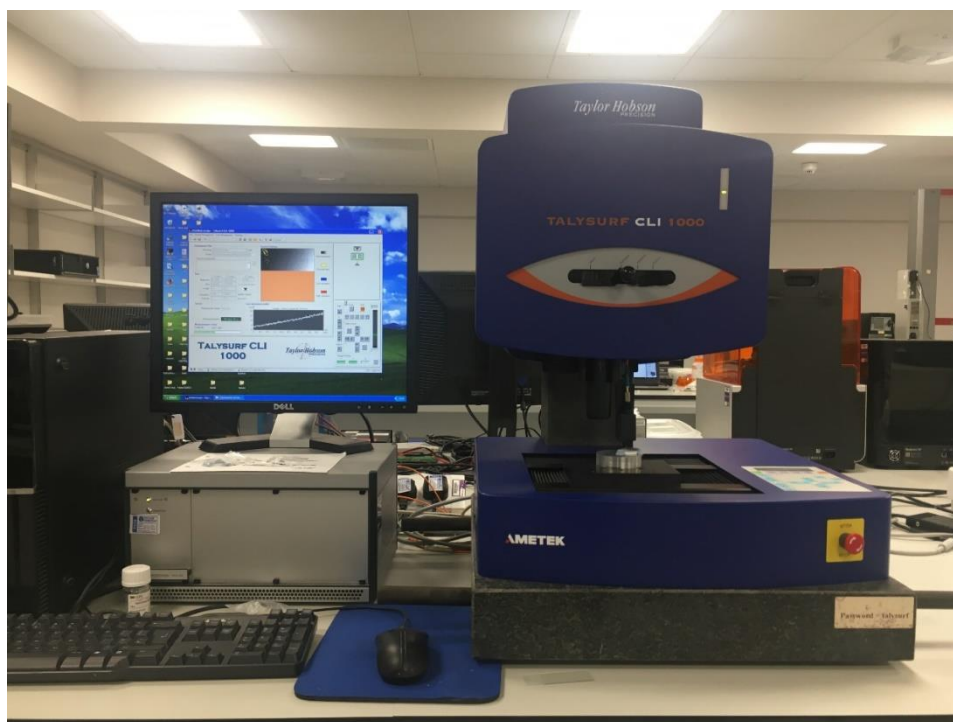
Figure 7.1 Talysuft CLI 1000 profilometer.

The surface roughness before and after toothbrushing simulations were measured using a three-dimensional non-contact profilometer (Talysuft CLI 1000, Taylor Hobson, Leicester, UK) (Figure 7.1). The chromatic length aberration (CLA) gauge at 400 μm

was used to determine the surface roughness of specimens. The same 1 mm × 1 mm area was measured before and after toothbrushing simulation with a spacing of 1 μm at both x-/y-axis directions. The measurement speed was 500 μm/s (average scanning time was 57 min). Ra, the arithmetic mean of the sum of roughness, was recorded during measurement. Three vertical and three horizontal lines were marked on the profiles to get six Ra values and the mean surface roughness was calculated.

The gloss before and after toothbrushing simulations were measured using a Novo-Curve glossmeter (Rhopoint, Bexhill-on-Sea, England). Calibration was operated using a standard black glass sample provided by the manufacturer. The specimen was put on the working stage and covered with a black cap to avoid external light. A light beam struck the top surface of the specimen at a 60° angle and the gloss value was measured. The average of five readings was calculated as the mean gloss.

Toothbrushing was simulated using a custom-made toothbrushing machine with four separate stations and toothbrushes (Figure 7.2). The specimen was placed in the hole inside the station. The toothbrush was fixed in parallel to the specimen and the bristle contacted the top surface of the specimen. Tooth cleaning and the sliding wear of toothbrush were operated at a speed of 78 counts per minute, which equals to 156 cycles per minute.
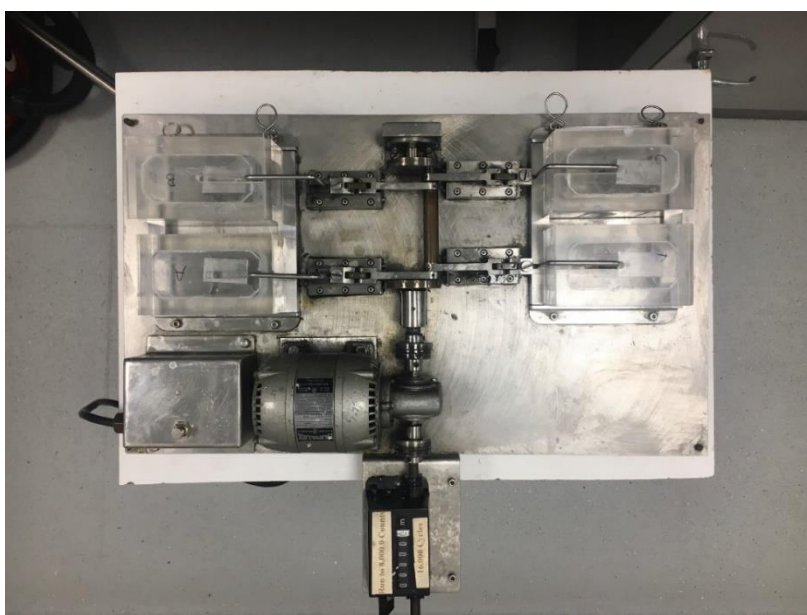
Figure 7.2 Toothbrushing simulation machine.

The toothpaste slurry was made using water and toothpaste (Health Clean, Colgate Total, Manchester, UK) with a ratio of 5:1 to obtain sufficient solubility. After setting the specimen and toothbrush, the slurry was poured into the station to cover the specimen. All specimens were brushed for 10000 cycles (the average time was 64 min). When toothbrushing finished, the specimen was removed from the station, cleaned using an ultrasonic water bath (Elma ultrasonic T 310, Singen, Germany) for 3 mins and gently dried for further tests.

Data were entered into statistical software (SPSS) and analysed using one-way ANOVA, independent T-test and Tukey post-hoc tests ($p<0.05$). Homogeneity of variance was calculated using the Kruskal-Wallis Test ($p<0.05$).

7.3 Results

Table 7.1 and Figures 7.3-7.4 summarize the gloss and surface roughness of all tested composites. Before toothbrushing simulations, all composites had similar gloss and surface roughness results ($p>0.05$). After brushing, gloss and surface roughness varied in composites ($p<0.05$), in which Filtek Supreme Ultra and Harmonize exhibited smoother surfaces compared to other composites, especially compared to Admira Fusion and *Viscalor*. The strong polynomial correlations were plotted between filler content (wt.%) and gloss ($r^2=0.83$)/surface roughness ($r^2=0.98$) and, between filler content (vol.%) and gloss ($r^2=0.99$)/surface roughness ($r^2=0.94$) (Figure 7.5).

Gloss decreased ($p<0.05$) and surface roughness increased ($p<0.05$) after toothbrushing simulations. Pre-heating time only had significant influences on gloss (after) ($p<0.05$) and surface roughness (before) ($p<0.05$). A strong linear correlation between gloss and surface roughness after toothbrushing simulations was found ($r^2=0.90$) (Figure 7.6).

Table 7.1 Gloss and surface roughness (Ra) (µm) of tested RBCs before and after toothbrushing simulations.

Materials	Gloss		Ra (µm)	
	Before	After	Before	After
Admira Fusion	82.4 [a] (1.83)	3.2 [a] (0.39)	0.13 [a] (0.03)	0.45 [d] (0.05)
Filtek Supreme Ultra	77.9 [a] (5.65)	72.9 [c] (9.54)	0.11 [a] (0.02)	0.14 [a] (0.04)
TPH LV	77.6 [a] (9.63)	25.6 [b] (14.71)	0.15 [a] (0.07)	0.32 [b,c] (0.11)
Tetric EvoCeram	67.0 [a] (8.55)	9.9 [a] (2.84)	0.13 [a] (0.03)	0.43 [c,d] (0.08)
Harmonize	70.9 [a] (6.56)	65.8 [c] (4.09)	0.11 [a] (0.02)	0.16 [a] (0.03)
Viscalor **(no heat)**	72.6 [a] (6.60)	2.7 [a] (0.30)	0.12 [a] (0.03)	0.35 [b,c,d] (0.04)
Viscalor **(T3-30s)**	75.1 [a] (3.91)	2.6 [a] (0.19)	0.08 [a] (0.01)	0.36 [b,c,d] (0.02)
Viscalor **(T3-3min)**	78.3 [a] (2.37)	8.6 [a] (2.06)	0.09 [a] (0.02)	0.29 [b] (0.07)

For each measured parameter, the same lower case superscript letters indicate homogeneous subsets among the materials.
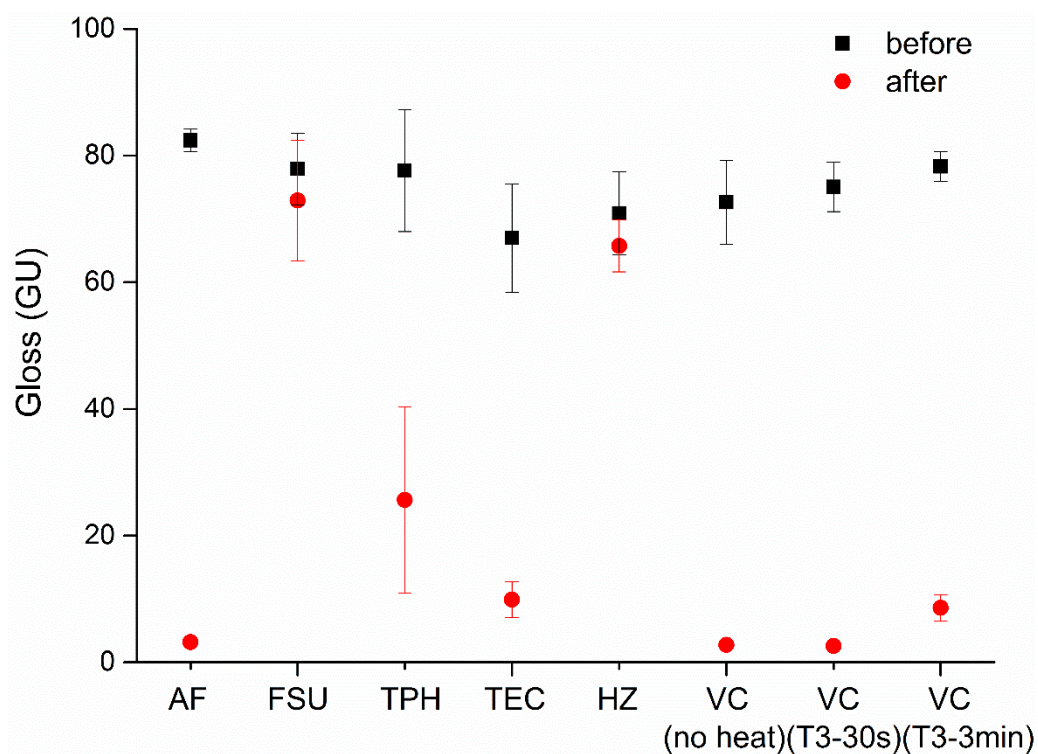
Figure 7.3 Gloss of tested RBCs before and after toothbrushing simulations.
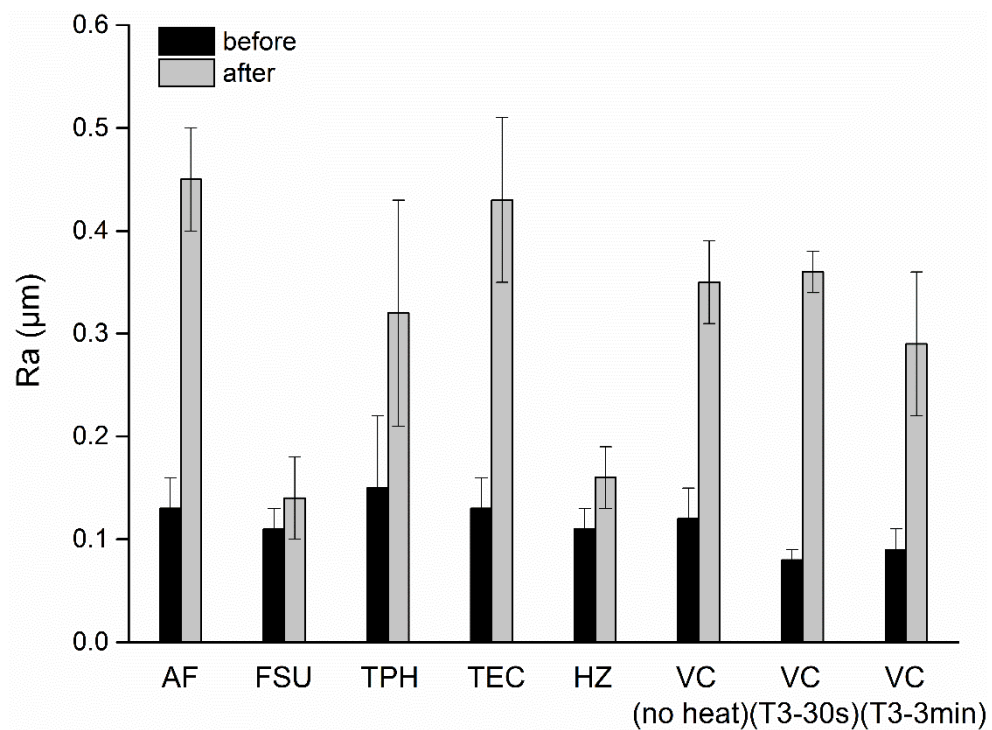
Figure 7.4 Surface roughness (Ra) (μm) of tested RBCs before and after toothbrushing simulations.
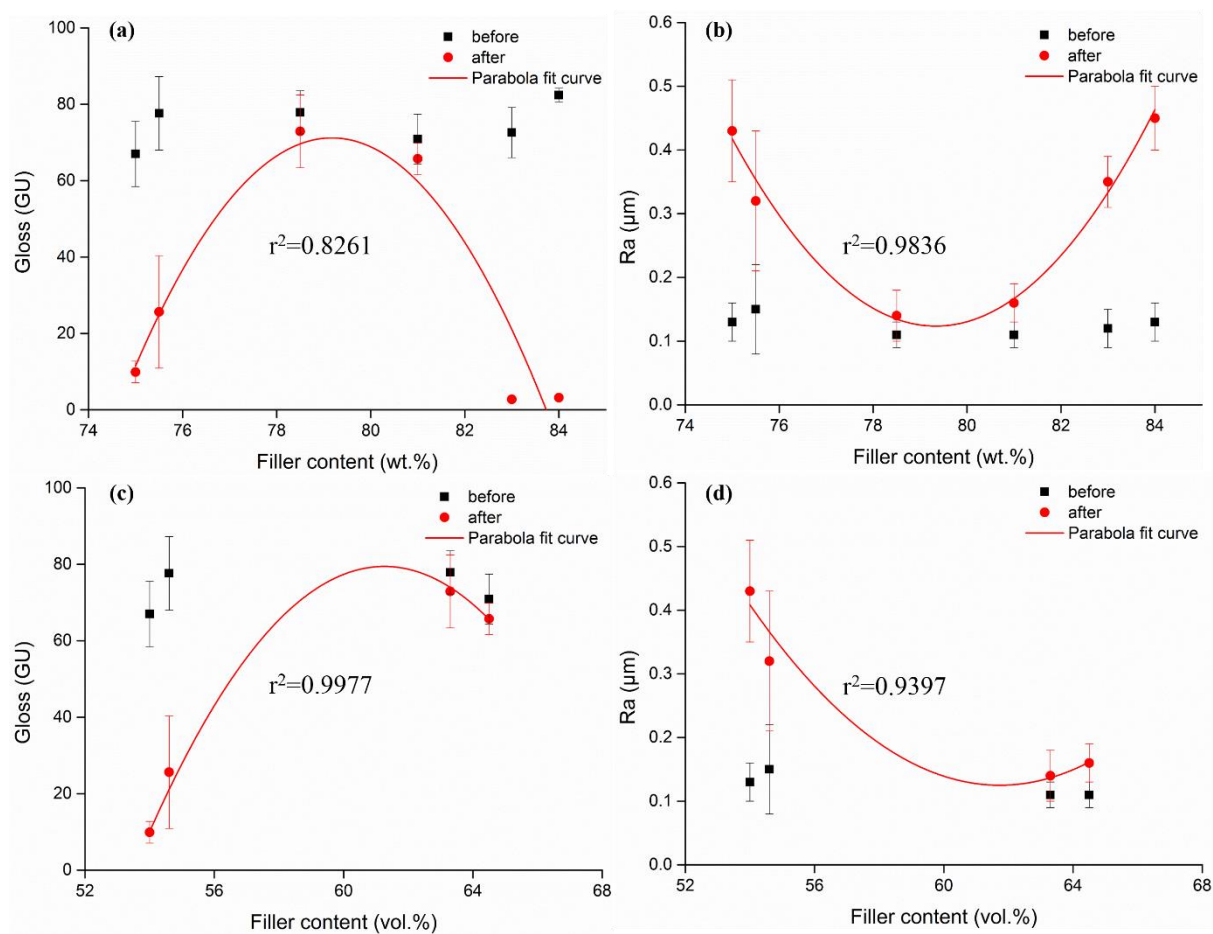
Figure 7.5 Scatter plots showing the polynomial correlations between filler content (wt.%) and (a) gloss/ (b) surface roughness and between filler content (vol.%) and (c) gloss/ (d) surface roughness after toothbrushing simulations.
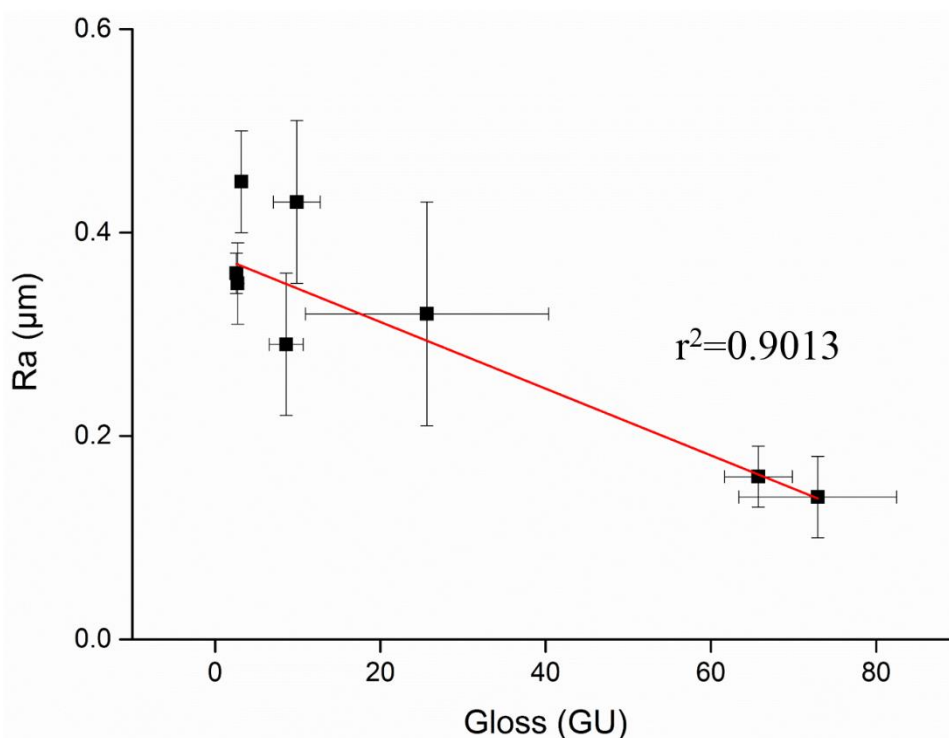
Figure 7.6 Scatter plots showing the correlations and linear regression of gloss-surface roughness after toothbrushing simulations.

7.4 Discussion

Gloss and surface roughness are representative parameters describing the surface properties of RBCs [105, 199]. Generally, after light-curing, composites will experience finishing and polishing to obtain smooth and shine surfaces. However, in this study, RBCs were photo-cured against mylar strips as suggested [262, 263] and directly tooth-brushed without finishing and polishing. The effects of inherent material properties and pre-heating time were mainly investigated. After toothbrushing simulations, gloss and surface roughness significantly varied in RBCs. Due to similar gloss and surface roughness results before brushing, the first null hypothesis was partially accepted. The second and fourth null hypotheses were rejected. The third null hypothesis was partially accepted since different pre-heating time only significantly affected *Viscalor* gloss (after) and surface roughness (before).

There were no significant differences in gloss and surface roughness before toothbrushing simulations among tested RBCs, which illustrated the effectiveness of

using mylar strips during specimen preparation. Regarding surface roughness, three dimensional surface roughness amplitude parameter, Sa, provides complete information on surface topography [193, 269]. However, 2D surface roughness, Ra, was used in this study since Ra results are commonly used in literature and easy for comparison. Before toothbrushing, Ra data ranged from 0.08 to 0.15 μm, which were all lower than 0.2 μm, the clinical threshold of surface roughness [105, 199, 265]. The surface cured against the mylar strip is usually polymer-rich and unstable, but it would be worn out after a few hundred brushings [196]. After 10000 cycles of toothbrushing, RBCs showed significantly different gloss and surface roughness results, in which Filtek Supreme Ultra and Harmonize showed the minimized changes and visibly smooth surfaces.

All tested RBCs are nanohybrid composites, which contain discrete nano-particles/clusters and finely milled glass fillers [105, 259]. However, the wear resistance and surface quality of nanohybrid composites are material dependent [259]. Filtek Supreme Ultra contains nano-sized non-agglomerated fillers and aggregated nanoclusters [237]. The toothbrushing only wore away the filler particles that loosely bounded outside the nanoclusters, rather than directly plucked the filler particles out [199, 268]. As each layer of nanofillers abrading away, a similar nanolayer emerged [196]. When the surrounding resin matrix was removed, nano-sized filler particles were worn out at the same rate and left a uniform abrasion pattern without huge holes [194, 196, 259]. Harmonize has a wide filler size distribution of 5-400 nm. Combined with its relatively high filler loading (81 wt.%), the shortened inter-particle distance leads to enhanced wear resistance [186, 187, 189, 195]. However, the increased mean particle size with a wide size distribution could also lead to inferior surface characteristics [195].

TPH LV showed lower surface roughness and higher gloss than those of Tetric EvoCeram after toothbrushing simulations, although they have similar filler content of 75.5 and 75 wt.%. The latter contains larger filler particles (40 nm-3 μm) [236] than that within the former (1.35 μm) [227]. Some studies concluded that small filler size leads to low surface roughness [194]. After toothbrushing simulations, the larger

particles would be plucked away and leaving a rough surface, which increases surface roughness and reduces gloss. The prepolymer fillers (PPF) in Tetric EvoCeram may also increase surface relief [236]. The limited residual double bonds on the PPF surface may weaken the link between PPF/matrix interfaces and result in debonding at the interface [196]. However, Suzuki et al. found that the PPF could be worn away preferentially and exposing the hard glass fillers against the toothbrushing wear, which reduces surface roughness [194].

Some *in vitro* studies found that high filler loading may enhance the wear resistance of RBCs [259]. However, in this study, highly filled Admira Fusion and *Viscalor* both exhibited less glossy and rougher surfaces after toothbrushing simulations. For Admira Fusion, nano-particles are firmly embedded in its ORMOCER resin matrix. Since the surface abrasion removes the soft matrix part, the exposed large irregular glass particles could be easily abraded away and leaving a rougher surface. This is in line with the study of O'Neill et al., in which fillers were visible in the SEM image after abrading the ORMOCER matrix [196]. Several studies demonstrated that bulk-fill RBCs showed similar surface performance to nanohybrid composites after polishing [196, 260, 261]. However, in this study, *Viscalor*, as a bulk-fill composite, did not show the expected gloss and surface roughness performance. The lack of composition information limits the discussion.

The effect of composite inherent characteristics on wear resistance has been investigated [259, 261-263]. Some studies concluded that there was no correlation between filler content and surface quality [259, 261]. However, the present study demonstrated strong polynomial correlations between filler content (wt.%) and gloss (r^2=0.83)/surface roughness (r^2=0.98). The correlations between filler content (vol.%) and gloss (r^2=0.99)/surface roughness (r^2=0.94) were plotted without Admira Fusion and *Viscalor*, due to the lack of exact filler content (vol.%) information. As shown in Figure 7.5, filler loading with range of 77-82 wt.%/60-64.5 vol.% show superior gloss and surface roughness results, in which the latter was lower than the threshold of 0.2 μm. This may be instructive for design of nanohybrid RBCs with adequate wear

resistance. Furthermore, different compositions and hardness of filler particles may lead to results exhibiting various abrasion patterns and gloss/surface roughnesses.

As a three-body abrasion, toothbrushing machine brushes material surfaces in slurry (dentifrice/water) to simulate tooth cleaning and the sliding wear of a toothbrush [185, 264]. In this study, toothbrushing simulations reduced the gloss and increased surface roughness of RBCs. This is in line with previous studies [196, 258]. The effect of toothbrushing simulation usually depends on the brushing force, cycle and speed. The commonly used brushing force is between 1.4 and 7.2 N and some studies applied an average of 5 N brushing load [105, 194, 272]. The increased load leads to more wear and roughness, even at a low brushing cycle [194]. A large number of brushing cycle may produce more measurable wear depths [196]. 10000 toothbrushing cycle has been reported as equal to 1-year toothbrushing abrasion [194, 258, 273]. Some studies used soft brushes as recommended by dentists. However, the denser tufts on the soft brush may increase retention of toothpaste and contact area with material surface, which leads to more abrasion [194, 258, 274, 275]. The effect of the dentifrice component has also been discussed. Low radioactive relative abrasion (RDA) dentifrices are recommended to achieve cleaning and create mild abrasion [258]. Besides, the abraded filler particles may join the abrasion and result in scratches on the surface [195, 259].

Although handling properties and mechanical properties of pre-heated composites have been studied, the effect of pre-heating time on gloss and surface roughness is unknown. In this study, pre-heating time did significantly influenced gloss after toothbrushing simulations, in which a long period pre-heating of 3 min resulted in better gloss retention. But the corresponding surface roughness results showed no significant differences. Before toothbrushing simulations, *Viscalor* (no heat, T3-30s and T3-3min) showed significant different surface roughness results, whereas they were all lower than 0.2 μm. Additionally, surface roughness of *Viscalor* (no heat, T3-30s and T3-3min) showed no significant differences after toothbrushing simulations. Hence, different pre-heating times had no adverse effects on gloss and surface roughness of *Viscalor*.

The strong linear correlation between gloss and surface roughness evidenced that increased surface roughness is associated with decreased gloss. Some studies presented similar conclusions [195, 196]. The gloss is visually different between rougher and smoother surfaces, in which the former could accumulate more bacteria and causes periodontal problems. In addition to gloss and surface roughness measurements, other techniques can be used to analyse surface profiles after abrasion. Atomic Force Microscopy (AFM) and Scanning Electron Microscopy (SEM) are the commonly used qualitative techniques for surface quality evaluation. The surface topography is detailed presented in the obtained images [194-196, 261, 263]. The examination of volume loss after toothbrushing simulations also merits further investigations.

7.5 Conclusions

In summary, the main outcomes of this study were:

1) Gloss and surface roughness were material dependent and both had strong relationships with filler content (wt.%/vol.%).

2) Gloss decreased and surface roughness increased after toothbrushing simulations.

3) Different pre-heating times had no adverse effects on gloss and surface roughness of *Viscalor*.

4) There was a strong linear correlation between gloss and surface roughness after toothbrushing simulations.

Chapter Eight

Viscoelastic Creep Behaviour of Resin-based Composites and Pre-heated *Viscalor*

Abstract

Objectives. To investigate the effects of material composition and storage condition on compressive creep deformation and recovery of different resin-based composites (RBCs) and to determine the effect of pre-heating time on compressive creep behaviour of *Viscalor*.

Methods. A creep apparatus was used to measure creep deformation and recovery of RBCs. *Viscalor* was pre-heated using a Caps Warmer (VOCO, Germany) in T3 mode (at 68 °C) for 30 s (T3-30s) and 3 min (T3-3min), respectively. The measurement was made under a constant compressive stress of 20 MPa for 2 h and an additional 2 h after removing the load to permit creep recovery. Cylindrical specimens of each material were prepared for measuring at 5 min post-cure (n=3) and after 7 days of storage in tap water at 37 °C (n=3). The maximum creep strain, permanent set and percentage creep recovery were recorded. Data were analysed using one-way ANOVA, two-way ANOVA, independent T-test and Tukey post-hoc tests (p<0.05).

Results. There was a significant interaction between the effects of material type and storage condition (p<0.001). The maximum creep strain, permanent set and percentage recovery of studied RBCs were significantly different under two storage conditions (p<0.001). 7 days of water storage only significantly reduced the maximum creep strain of *Viscalor* (no heat, T3-30s and T3-3min) (p<0.005). The permanent set significantly decreased (p<0.05) after 7 days of water storage, whereas the percentage creep recovery significantly increased (p<0.01). There were strong correlations between filler content (wt.%) and the measured creep parameters after 7 days of water storage. Different pre-heating times had no significant influences on creep behaviours of *Viscalor* (p>0.05).

Significance. The creep behaviour varied with composites. 7 days of water storage beneficially reduced elastic deformation and enhanced the percentage creep recovery

of all tested RBCs. Pre-heating had no adverse influence on the viscoelastic stability of *Viscalor*.

Key words: resin-based composites; viscoelasticity; creep recovery; preheating

8.1 Introduction

During clinical placement, resin-based composites (RBCs) are packed into the cavity and light-cured for 20-40 s. The post-cure behaviours under bite force and occlusal force are vital since dimensional deformation can lead to the formation of microcracks and accumulation of internal stress, which may ultimately cause restoration failure [203]. Viscoelasticity of RBCs enables them to exhibit both solid and fluid characteristics and determines their performance upon the applied stress [4]. One method to study the viscoelasticity of RBCs is to measure creep and stress relaxation. The former is the increased deformation under stress and the latter is the following recovery process of strain [4].

Creep deformation can be divided into a dynamic and static creep, which is obtained under alternating stress and constant stress, respectively [205]. Oden et al. demonstrated that static creep is clinically relevant and can be used to characterize the viscoelastic behaviour of RBCs [200, 201]. Different modes of creep investigation, such as flexural creep deformation [276, 277], nano-indentation creep [278, 279] and compressive creep recovery [280, 281], are available to determine the time-dependent creep under various loading modes: tension, compression and torsion.

The compositional variations of RBCs, such as resin monomers, filler content/shape/size and surface treatment of filler particles, affect the magnitude of viscoelastic deformation [206]. Rigid monomers, such as bis-GMA, may minimize creep strain due to the limited mobility of polymer chains and the resultant stiff network [203, 206]. The presence of diluent monomers usually affects the deformation resistance under stress [205, 206]. High filler loading improves the creep resistance because of its reinforcing effect [204, 206]. Insufficient bonding between the resin matrix and the filler particles may detrimentally affect stress transfer between phases and lead to material rupture [11, 206]. As the resin matrix polymerizes, the crosslinking network is formed in different structures [18]. The complete polymerization with a high crosslinking degree may aid stress distribution

under loading [203]. Some studies found that a high degree of conversion (DC) contributes to low creep deformation [200, 205].

In the oral cavity, durability and clinical performance of RBCs are affected by temperature, humidity, chemicals from food and dynamic/static load [203]. Some studies demonstrated that due to the degradation and hydrolysis raised by the water, the storage solvent has an adverse influence on material creep behaviour [203, 276]. Temperature rise may lead to higher creep deformation by enhancing the thermal polymer-chain segmental motion [206]. The increased temperature affects the degree of polymerization of composites and the further viscoelastic properties. Papadogiannis et al. found that temperature rise from 21 to 37 and 50 °C significantly decreased elastic modulus of composites [282]. El-Safty et al. concluded that creep strain and permanent set increased with temperature, whereas percentage creep recovery reduced [206]. The deterioration of composites relates to their performance under stress [204]. Poor degree of polymerization results in heterogeneous structure, in which voids/cracks will develop at the filler/matrix interface or within the matrix structure. This may lead to more solvent penetration and material fracture [203, 204, 206, 283]. Storage time had different effects on the creep behaviour of RBCs, which also related to storage solvent [282, 284].

Thus, the objectives of this study were to investigate compressive creep behaviours of different RBCs under different storage conditions and determine the effect of pre-heating time on the viscoelastic stability of *Viscalor*. The Null Hypotheses were:
(1) there were no differences in the creep behaviours between investigated RBCs,
(2) storage condition did not influence the creep behaviours of RBCs and
(3) pre-heating time did not influence the viscoelastic performance of *Viscalor*.

8.2 Materials and methods

Five RBCs, with different composite compositions and *Viscalor*, were investigated. The manufacturers' information is tabulated in Table 3.1.

Viscalor was pre-heated using the Caps Warmer (VOCO, Germany) in T3 mode (at 68 °C) for 30 s (T3-30s) and 3 min (T3-3min), respectively. Cylindrical specimens were fabricated using a stainless steel mould (4 mm diameter $\times$ 6 mm thickness). Composite paste was packed into the mould carefully. A mylar strip was pressed against the composite by a glass slide to remove air bubbles and excess materials. Photo-cure was applied using an Elipar S10 LED unit (3M ESPE, USA) of a mean irradiance 1200 mW/cm^2 for 40 s at zero distance from both upper and lower surfaces. Specimens were also cured from radial direction for 40 s with close contact between the curing tip and the specimen, to ensure optimum curing.

After irradiation, specimens were separated from the mould and polished by hand-grinding with 600-grit SiC abrasive paper. The original lengths (L_0) of the specimens were then recorded. Specimens were divided into two groups (n=3 each) for storage and measurement, as follows: Group I: 5 min post-cure at 23 °C; Group II: 7 days in 37 °C tap water.

The compressive creep recovery was measured using a creep apparatus previously described [205, 284]. During measurement, a constant compressive stress of 20 MPa was applied for 2 h followed an additional 2 h of load removal. A linear variable displacement transducer (LVDT) was used to monitor the strain changes in units of voltage. The LVDT signals were amplified and transferred to an A/D converter and recorded via a computer data recorder. The creep strain (%) was calculated as:

Displacement (μm) = LVDT signal (mV) $\times$ 0.1986   (Equation 8.1)

Creep strain (%) $= \frac{Displacement\ (\mu m)}{L_0\ (mm) \times 1000} \times 100\%$ (Equation 8.2)

The maximum creep strain (%), permanent set (%) and percentage creep recovery were obtained from the creep and recovery plots.

Data were entered into statistical software (SPSS) and analysed using one-way ANOVA, two-way ANOVA, independent T-test and Tukey post-hoc tests ($p<0.05$). Homogeneity of variance was calculated using the Kruskal-Wallis Test ($p<0.05$). Linear correlations were performed between filler content (wt.%) and maximum creep strain/permanent set/percentage creep recovery for all tested composites under both storage conditions.

8.3 Results

Figures 8.1-8.3 summarise maximum creep strain, permanent set and percentage creep recovery data of studied composites at 5 min post-cure and after 7 days of water storage. Two-way ANOVA analysis demonstrated significant interactions between the effects of material type and storage condition ($p<0.001$). The comparison between materials under each storage condition was conducted using one-way ANOVA, in which maximum creep strain, permanent set and percentage creep recovery varied significantly with composites ($p<0.001$).

Table 8.1 and Figures 8.4-8.11 show the maximum creep strain, permanent set and percentage creep strain results of different RBCs after 4 h real-time measurements. The maximum creep strain at 5 min post-cure and after 7 days of water storage ranged from 1.25 to 2.89 and from 0.69 to 1.62, respectively. There were no significant differences between maximum creep strain at 5 min post-cure and after 7 days of water storage ($p>0.05$). However, the maximum creep strain of *Viscalor* (no heat, T3-30s and T3-3min) significantly reduced after water storage ($p\leq0.002$). The permanent set at 5 min post-cure ranged from 0.56 to 1.84 and significantly decreased to 0.07-0.68 after 7 days of water storage ($p<0.05$). After 7 days of water storage, the percentage creep recovery significantly increased from 31.74-59.63 to 71.06-90.56

(p<0.01). Different pre-heating times had no significant influences on maximum creep strain, permanent set and percentage creep recovery of *Viscalor* (p>0.05).

For all the tested composites, at 5 min post-cure, the absence of correlations were confirmed between filler loading (wt.%) and maximum creep strain (r^2=0.07)/permanent set (r^2=0.04)/percentage creep recovery (r^2=0.00). However, as shown in Figure 8.12, after 7 days of water storage, strong correlations existed between filler loading (wt.%) and maximum creep strain/permanent set/percentage creep recovery. Correlation coefficients (r^2) were 0.62, 0.84 and 0.85, respectively.
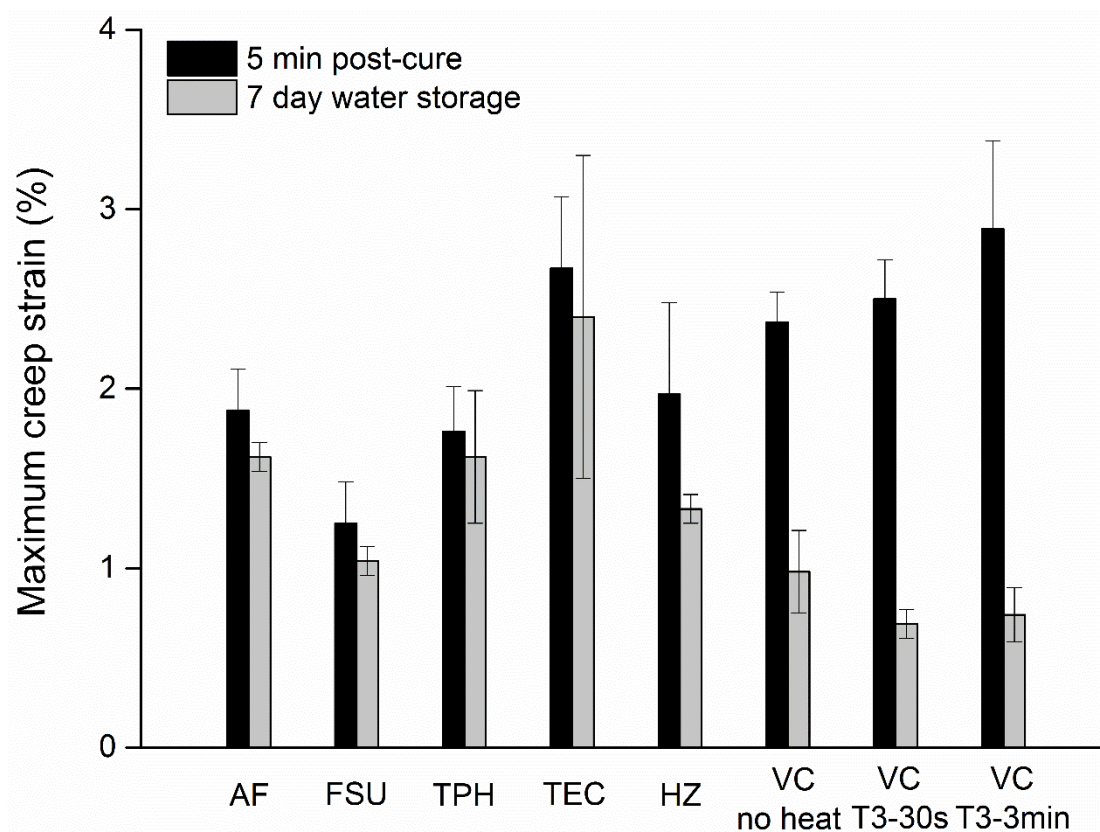
Figure 8.1 Maximum creep strain (%) of investigated composites at 5 min post-cure and after 7 days of water storage.
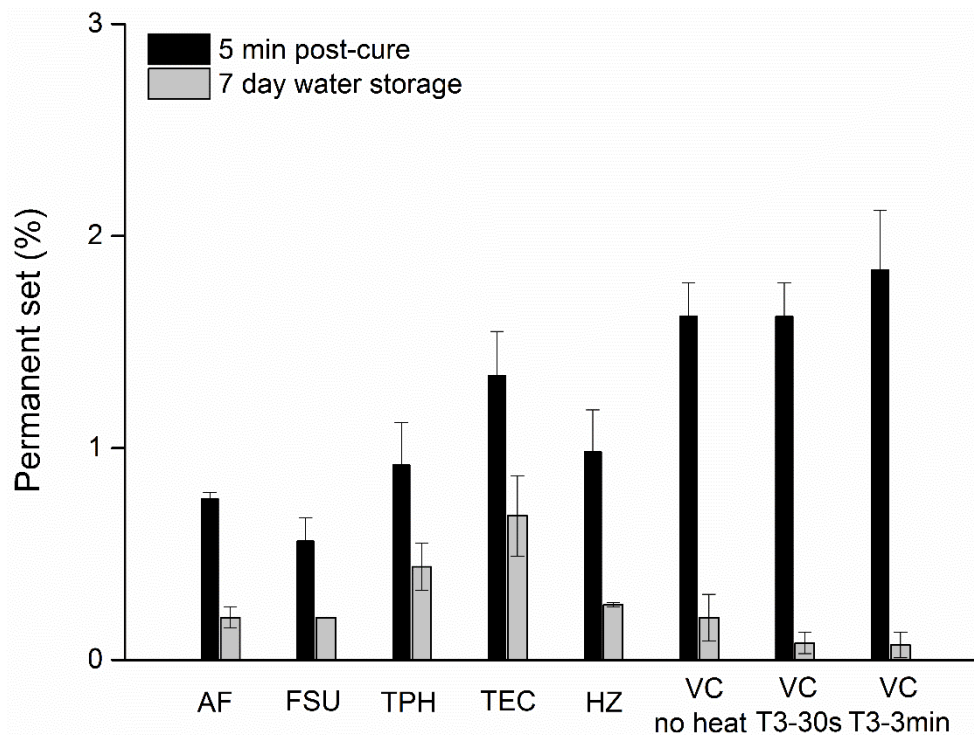
Figure 8.2 Permanent set (%) of investigated composites at 5 min post-cure and after 7 days of water storage.
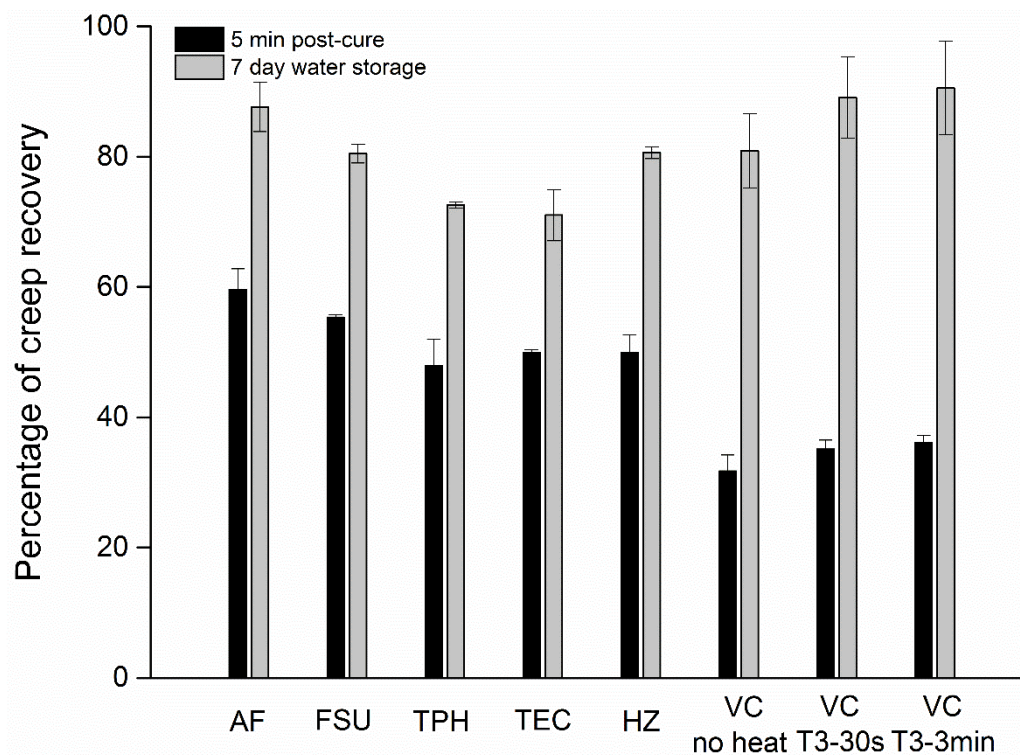
Figure 8.3 Percentage creep recovery of investigated composites at 5 min post-cure and after 7 days of water storage.

Table 8.1 Maximum creep strain (%), permanent set (%) and percentage creep recovery of investigated composites at 5 min post-cure and after 7 days of water storage.

Materials	5 min post-cure			7 days water storage at 37 °C		
	Max. creep strain (%)	Permanent set (%)	Percentage creep recovery	Max. creep strain (%)	Permanent set (%)	Percentage creep recovery
Admira Fusion	1.88[a,b A] (0.23)	0.76[a A] (0.03)	59.63 %[a B] (3.19)	1.62[a,b A] (0.08)	0.20[a,b A] (0.05)	87.66 %[a C] (3.78)
Filtek Supreme Ultra	1.25[a A] (0.23)	0.56[a A] (0.11)	55.36 %[a,b B] (0.38)	1.04[a A] (0.08)	0.20[a,b A] (0.00)	80.49 %[a,b C] (1.44)
TPH LV	1.76[a,b A] (0.25)	0.92[a,b A] (0.20)	47.94 %[c B] (4.11)	1.62[a,b A] (0.37)	0.44[b,c A] (0.11)	72.60 %[b C] (0.43)
Tetric EvoCeram	2.67[b,c A] (0.40)	1.34[b,c A] (0.21)	49.94 %[b,c B] (0.45)	2.40[b A] (0.90)	0.68[c A] (0.19)	71.06 %[b C] (3.94)
Harmonize	1.97[a,b,c A] (0.51)	0.98[a,b A] (0.20)	49.98 %[b,c B] (2.65)	1.33[a A] (0.08)	0.26[a,b A] (0.01)	80.62 %[a,b C] (0.89)
Viscalor **(no heat)**	2.37[b,c A] (0.17)	1.62[c A] (0.16)	31.74 %[d B] (2.48)	0.98[a A] (0.23)	0.20[a,b A] (0.11)	80.91 %[a,b C] (5.73)
Viscalor **(T3-30s)**	2.50[b,c A] (0.22)	1.62[c A] (0.16)	35.10 %[d B] (1.40)	0.69[a A] (0.08)	0.08[a A] (0.05)	89.09 %[a C] (6.23)
Viscalor **(T3-3min)**	2.89[c A] (0.49)	1.84[c A] (0.28)	36.09 %[d B] (1.13)	0.74[a A] (0.15)	0.07[a A] (0.06)	90.56 %[a C] (7.19)

For each measured parameter, the same lower case superscript letters indicate homogeneous subsets among the materials. For each material, the same CAPITAL superscript letters indicate homogeneous subsets among different parameters.
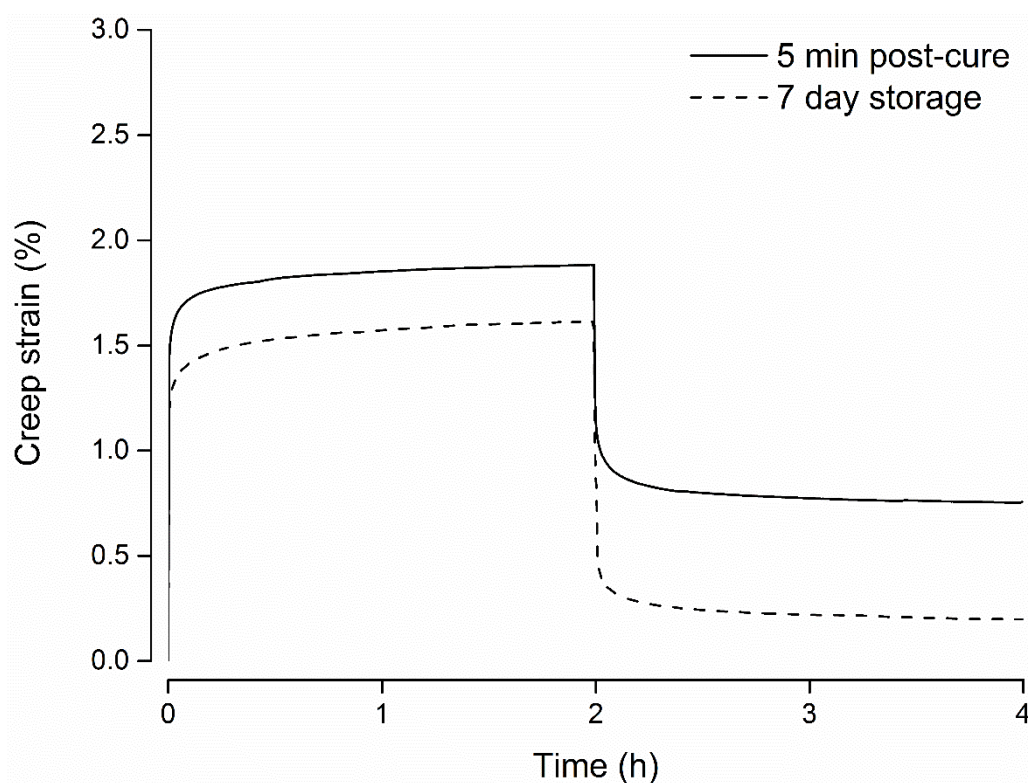
Figure 8.4 Creep and recovery curves of Admira Fusion at 5 min post-cure and after 7 days of water storage.
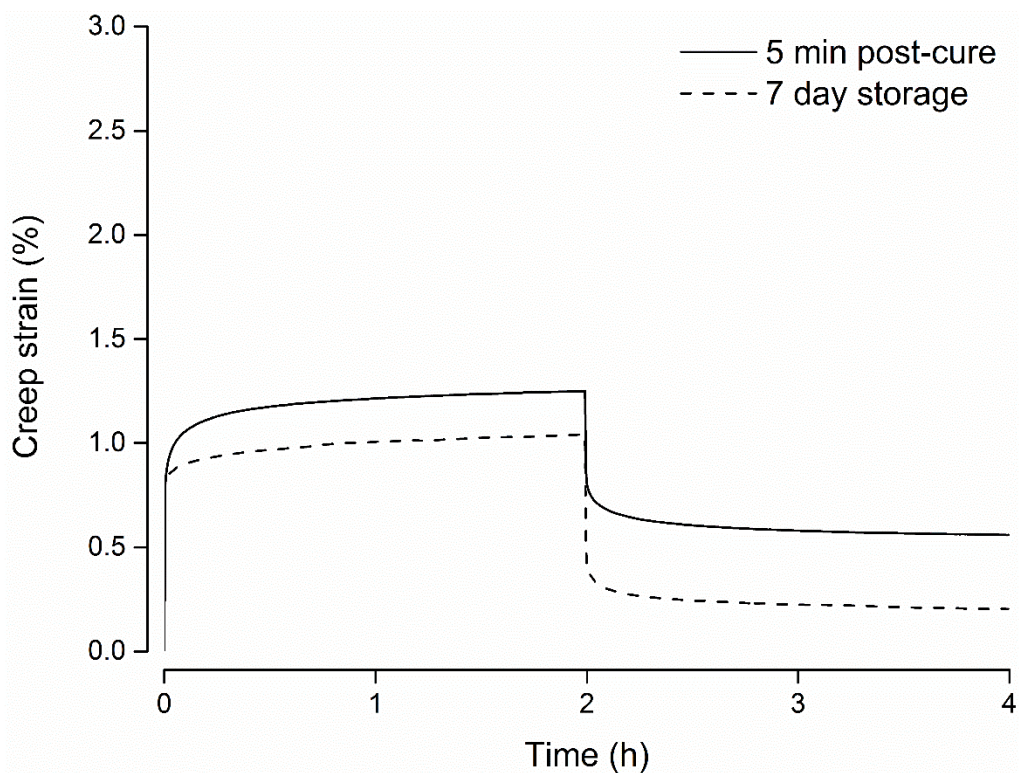
Figure 8.5 Creep and recovery curves of Filtek Supreme Ultra at 5 min post-cure and after 7 days of water storage.
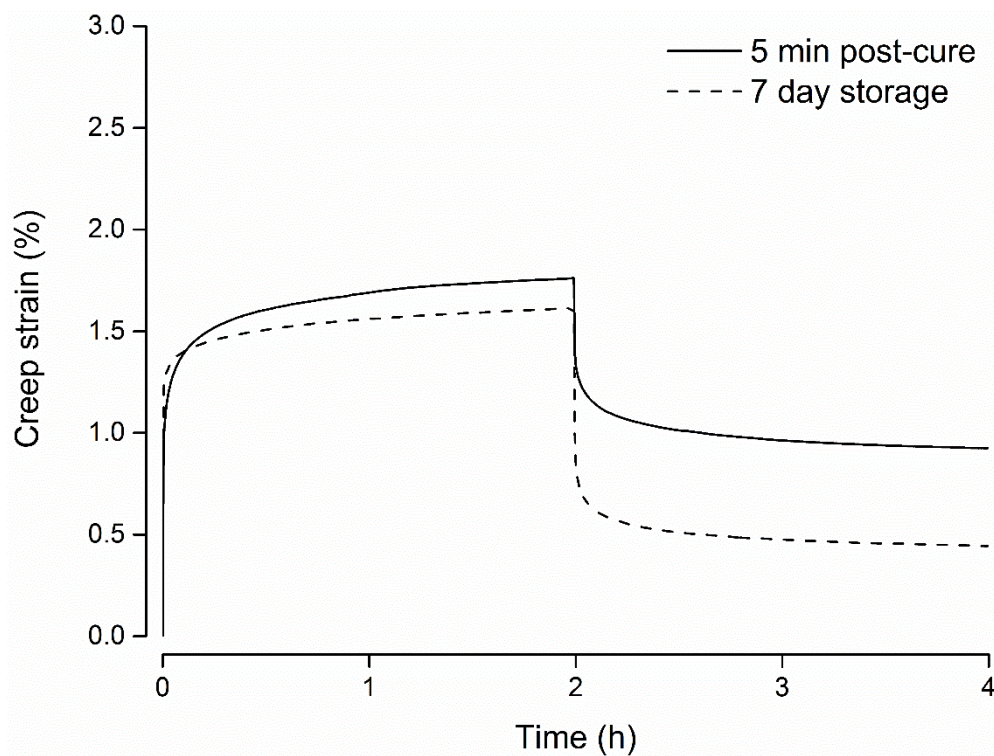
Figure 8.6 Creep and recovery curves of TPH LV at 5 min post-cure and after 7 days of water storage.
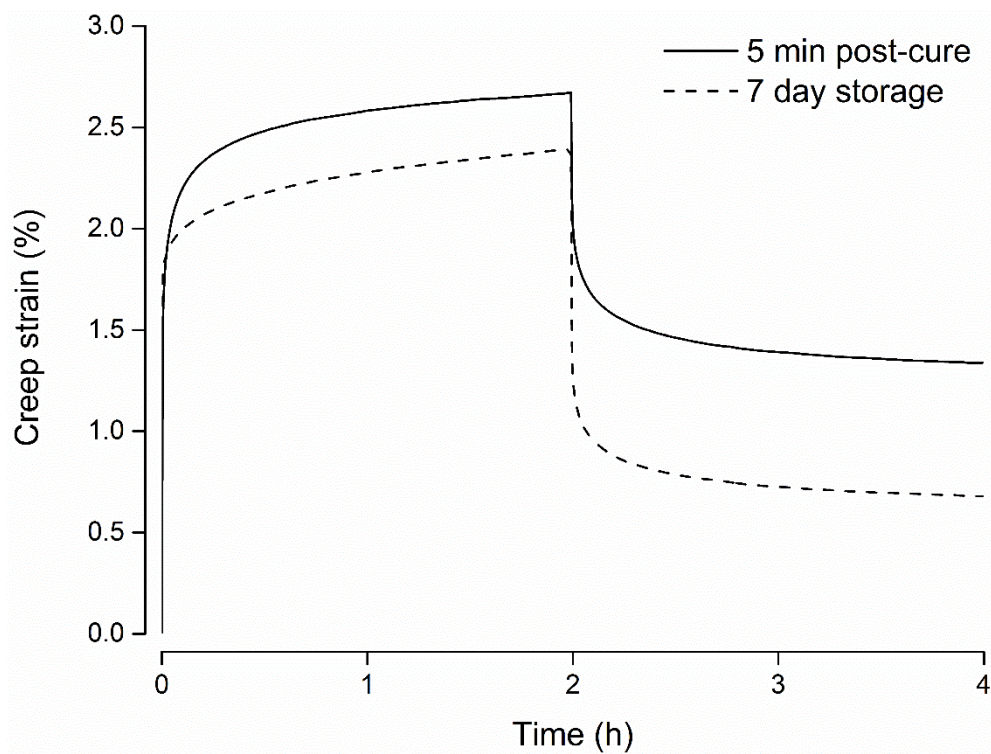
Figure 8.7 Creep and recovery curves of Tetric EvoCeram at 5 min post-cure and after 7 days of water storage.
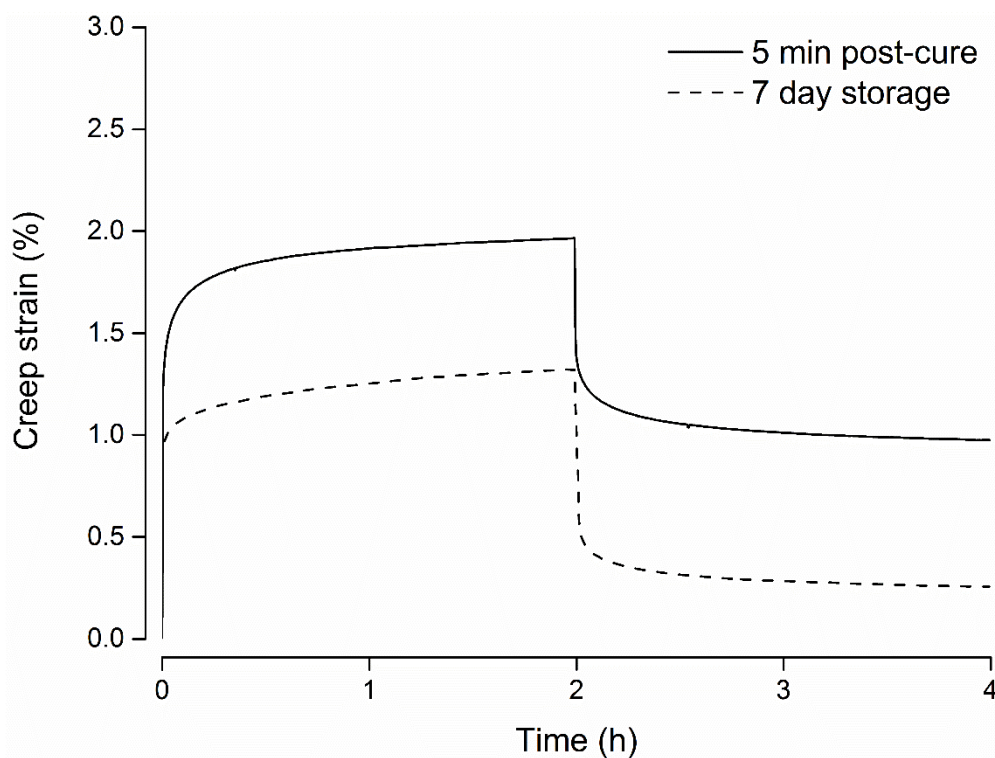
Figure 8.8 Creep and recovery curves of Harmonize at 5 min post-cure and after 7 days of water storage.
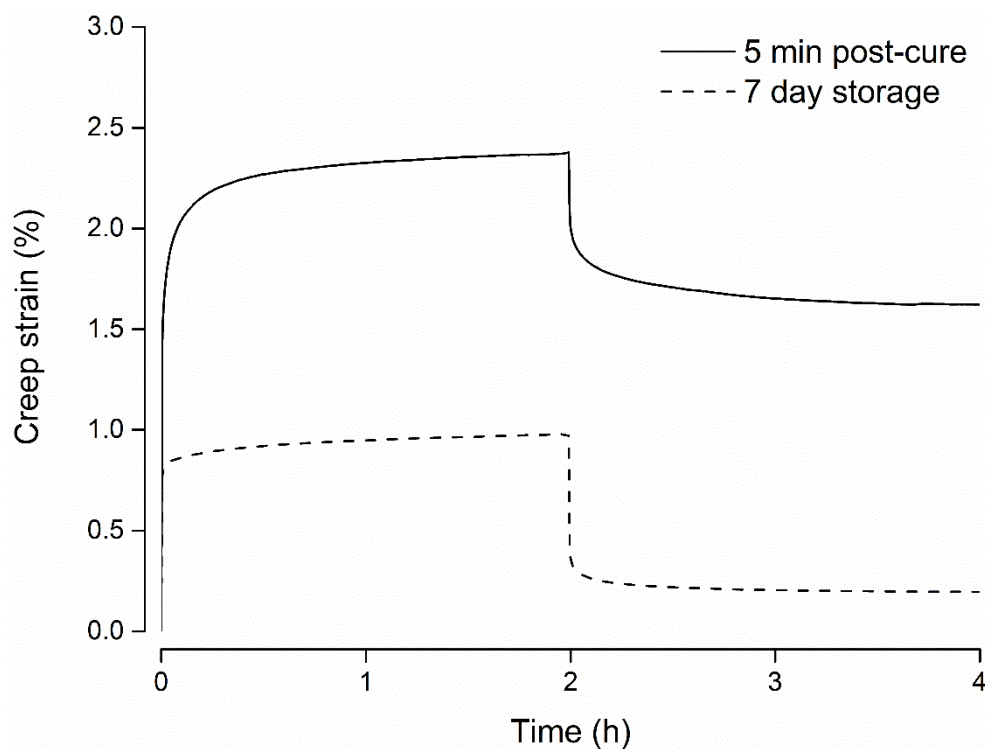
Figure 8.9 Creep and recovery curves of Viscalor (no heat) at 5 min post-cure and after 7 days of water storage.
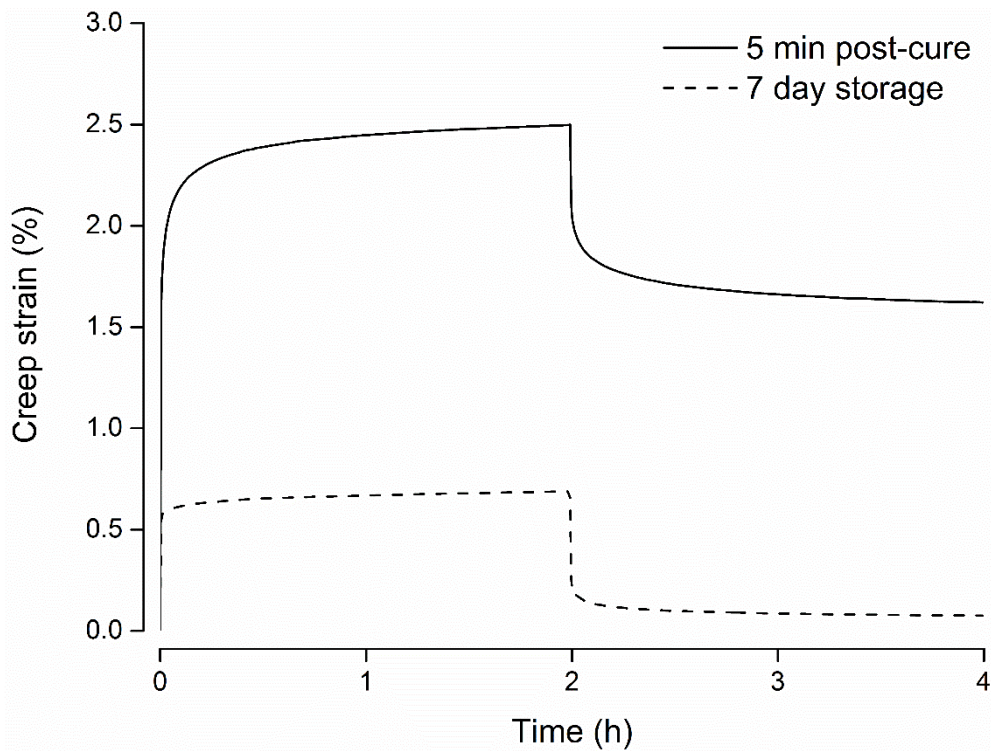
Figure 8.10 Creep and recovery curves of Viscalor (T3-30s) at 5 min post-cure and after 7 days of water storage.
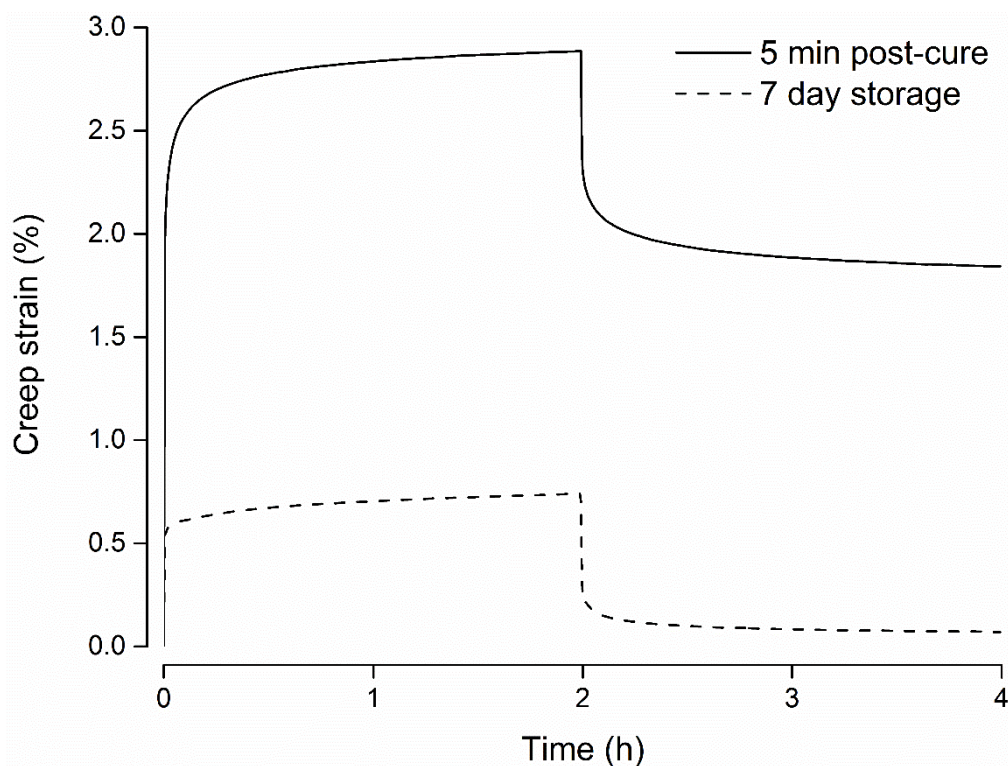
Figure 8.11 Creep and recovery curves of Viscalor (T3-3min) at 5 min post-cure and after 7 days of water storage.
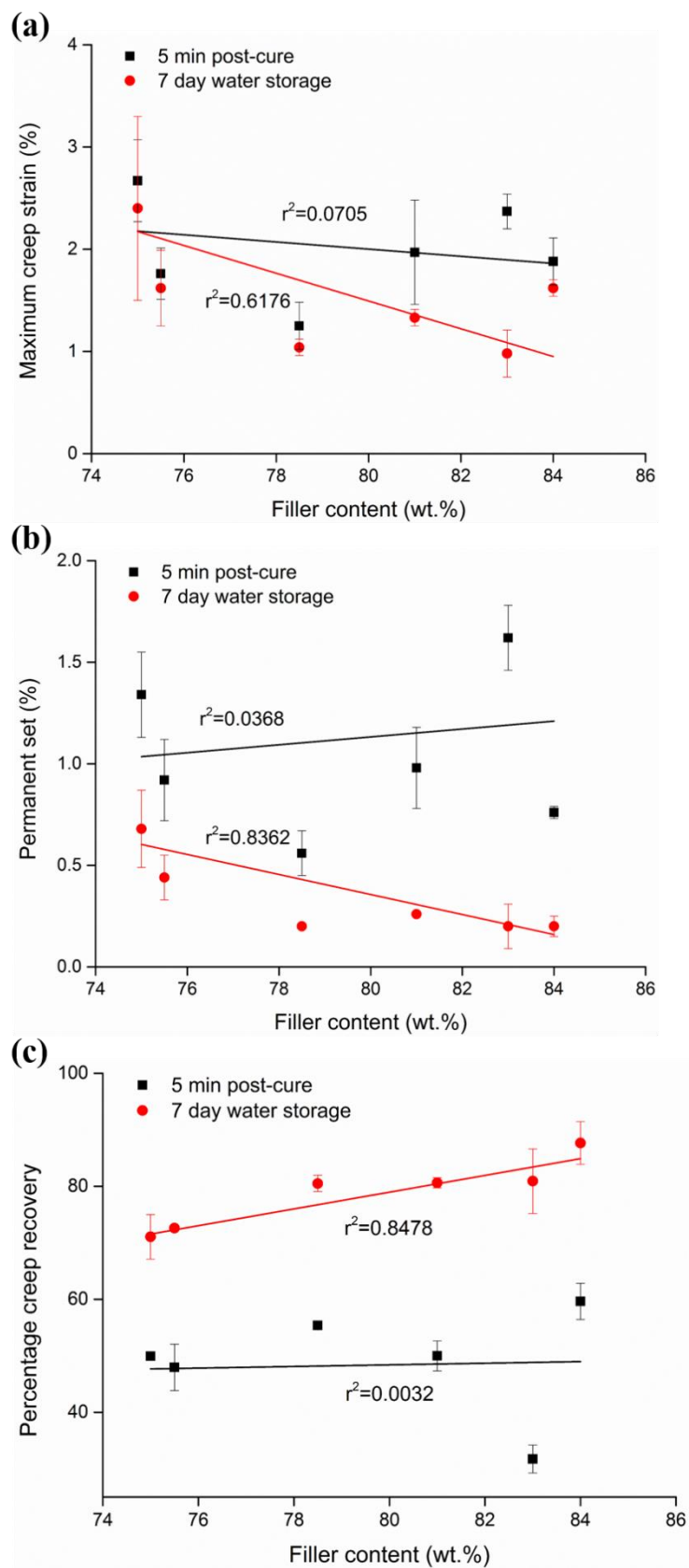
Figure 8.12 Scatter plots showing the correlations and linear regressions between filler content (wt.%) and (a) maximum creep strain, (b) permanent set and (c) percentage creep recovery at 5 min post-cure and after 7 days of water storage.

8.4 Discussion

Viscoelastic behaviours of polymer-based RBCs importantly determine their mechanical properties [228]. Viscoelasticity can be measured in time and frequency, in which the former contains stress relaxation and creep measurement. The strong correlation between the dynamic and static creep deformation validated the clinical relevance of static creep measurement [201]. Hence, this study investigated the creep behaviours of different RBCs using static compressive creep measurements under different storage conditions and evaluated the creep behaviours of *Viscalor* after different pre-heating times. The first and second null hypotheses were rejected, whereas the third null hypothesis was accepted. Regardless of pre-heating time, there was no significant change in viscoelasticity of *Viscalor* (p>0.05).

Viscoelastic creep parameters of composites, including maximum creep strain, permanent set and percentage creep recovery were recorded during measurement. The creep strain curves of different composites developed similarly, regardless of the storage condition. Once the load was applied, elastic deformation occurred immediately, then followed by a time-dependent viscoelastic deformation. The maximum creep strain is the summary of elastic and viscoelastic deformation under constant loading. After loading removal, quick elastic recovery and time-dependent viscoelastic recovery took place. Percentage creep recovery represents the amount of creep deformation returns to the initial state. Due to the inadequate recovery, the remained plastic deformation is the permanent set.

In this study, creep behaviours varied significantly in composites under different storage conditions, in which Tetric EvoCeram showed the highest creep strain and permanent set and Admira Fusion showed the highest percentage creep recovery. The former has 75 wt.% of filler content and the latter has 84 wt.%. Furthermore, with low filler content, Filtek Supreme Ultra (78.5 wt.%), TPH LV (75.5 wt.%) and Tetric EvoCeram (75 wt.%) showed lower percentage creep recovery among both storage conditions. The results were in line with previous studies, that creep behaviour

depends on filler content [206, 276, 284]. Filler particles reinforce the resin matrix part to avoid dimensional changes, mechanical degradation and failure caused by high forces [202]. High filler loading improves the resistance against the applied stress and decreases the maximum creep strain [206].

However, Filtek Supreme Ultra showed lower creep strain and permanent set than those of highly filled composites under different storage conditions. This confirmed the effect of resin matrix composition on creep behaviour. The rigid resin matrix helps to minimize creep stain and permanent deformation [203, 205, 206]. Filtek Supreme Ultra contains structurally rigid monomers, such as bis-GMA and UDMA, which enhances its resistance against the creep strain [205, 276]. ORMOCERs function as the matrix part in Admira Fusion. The stable Si-O-Si networks are considered as strong elastic components to reduce creep deformation [203]. Although Admira Fusion showed higher creep strain, its outstanding percentage creep recovery results proved the good flexibility of ORMOCERs to resist static loading. Some studies reported similar results that low creep resistance of highly packed composites, which was due to the partly silane treatment of filler particles [203, 206]. The weak bonding between the filler particles and the resin matrix may result in chemical degradation, crack initiation and final restoration failure [100, 203, 206].

In this present study, specimens after 7 days of water storage exhibited significantly lower permanent set and higher percentage creep recovery than those measured at 5 min post-cure. The improved creep recovery corresponded to some previous studies [205, 284]. Baroudi et al. found that long-term storage under wet condition reduces creep deformation and enhances percentage creep recovery of composites [205]. The post-cure polymerization occurs during long-time storage, which leads to a more rigid cross-linking structure to resist deformation [205]. Also, the wet condition could promote creep recovery due to the plasticization of water [204, 284]. However, some studies showed high creep strain and low percentage creep recovery after long-time storage in different solvents [201, 202, 276]. The well-known plasticizing effect of water reduces the stiffness of composites and induces swelling stress in the structure

[100, 204, 282, 284]. The absorption of water depends on the polarities of both solvent and monomer. The presence of hydrophilic monomers, for example, TEGDMA, may increase creep strain due to its solvent susceptibility and high water diffusion [35, 36, 203]. Longer storage time could increase resin matrix dissolution and damage the mechanical properties of composites [276]. Water absorption of unreacted residual monomers may also reduce T_g (temperature of glass transition) of the resin matrix and increase creep strain [203]. In this study, 7 days of water storage did not significantly influence the maximum creep strain of studied composites, which illustrates their viscoelastic stability.

Correlations and linear regressions between filler contents (wt.%) and maximum creep strain/permanent set/percentage creep recovery of tested composites under both storage conditions were plotted. The strong correlations were only found after 7 days of water storage, which confirmed that long-term water storage improves material resistance to the static loading. The linear regressions demonstrate that creep behaviours vary with filler content (wt.%). With filler content increasing, the creep strain and permanent set decreased, whereas the percentage creep recovery increased.

After 7 days of water storage, *Viscalor* (no heat, T3-30s and T3-3min) showed comparable creep resistance to other composites. But different pre-heating times had no significant influences on creep behaviours of *Viscalor* (T3-30s and T3-3min), relative to room-temperature *Viscalor* (p>0.05). The results correlated to a previous study, in which pre-heating did not significantly affect composite creep behaviours [278]. On the contrary, Marghalani et al. found that creep deformation and permanent set increased with temperature rise, whereas percentage creep recovery reduced [203]. The ambient temperature is lower than the T_g of composites. The limited mobility of polymer chains reduces the susceptibility of deforming at low temperatures [203]. When the temperature rises from ambient to 37 °C or higher, the temperature-dependent moduli of composites decreases [282]. The higher temperature promotes the thermal mobility of polymer chains and softens the resin matrix. Thus, composites become more susceptible to creep deformation [203]. However, the increased DC

with temperature leads to a more rigid resin matrix with a higher degree of crosslinking to resist static loading [134, 166]. In this study, pre-heating did increase *Viscalor* temperature, whereas once removed from the heating device, composite temperature detrimentally dropped [132, 134]. The similar creep behaviours of *Viscalor* (T3-30s and T3-3min) may be attributed to temperature drop-off, which merits further investigations. According to previously published data, long pre-heating time did not influence DC of *Viscalor*, which further proved that no significant differences between creep behaviours of *Viscalor* (no heat, T3-30s and T3-3min) [243].

The use of the 37 °C water bath during creep measurement simulated the oral environment, which is useful to predict the clinical performance of composites during creep and stress relaxation [282]. The optimized light-curing during specimen preparation ensured the complete polymerization and homogeneous structure of specimens. The applied loading of 20 MPa corresponded to the maximum force level during occlusion [206, 284].

8.5 Conclusions

This study demonstrated the effects of material type and storage condition on compressive creep behaviours of composites. The maximum creep strain and permanent set decreased with filler content (wt.%), but the percentage creep recovery increased. 7 days of water storage beneficially reduced elastic deformation and enhanced the percentage creep recovery of all tested composites. Pre-heating had no adverse effect on the viscoelastic stability of *Viscalor*.

Chapter Nine
Polymerization Shrinkage Strain Kinetics and Fracture Toughness of Bulk-fill Composites

Abstract

Objectives. To determine polymerization shrinkage strain (PS), maximum rate of polymerization shrinkage strain (PS R_{max}) and fracture toughness (K_{IC}) of different types of bulk-fill composites and to investigate the effect of pre-heating time on PS, PS R_{max} and K_{IC} of *Viscalor*.

Methods. SonicFill 3 was applied via the sonic insertion method using a specific handpiece (*SonicFill* Handpiece, Kerr Corporation). *Viscalor* was pre-heated using a Caps Warmer (VOCO, Germany) in T3 mode (at 68 °C) for 30 s (T3-30s) and 3 min (T3-3min), respectively. PS was obtained with the bonded-disk technique (n=3). PS R_{max} was calculated by numerical differentiation of PS data with respect to time (n=3). For three-point bending fracture toughness measurement, single-notched specimens ($32 \times 6 \times 3$ mm) of each bulk-fill composites were prepared and stored in water at 37 °C for 7 days (n=5). Data were analysed using one-way ANOVA, independent T-test and Tukey post-hoc tests ($p<0.05$).

Results. There were no significant differences in PS and PS R_{max} among tested bulk-fill composites ($p>0.05$), whereas *SonicFill* 3 had the highest PS R_{max}. K_{IC} results significantly varied in bulk-fill composites ($p<0.05$), in which Beautifil-Bulk Restorative had the lowest K_{IC}. Different pre-heating times had no significant influences on PS, PS R_{max} and K_{IC} of *Viscalor* ($p>0.05$).

Significance. Different types of bulk-fill composites showed comparable PS and PS R_{max}. All tested bulk-fill composites showed similar K_{IC}, except bulk-fill giomer (Beautifil-Bulk Restorative) showed the lowest K_{IC}. A long pre-heating period (3 min) had no adverse effects on *Viscalor* PS, PS R_{max} and K_{IC}.

Key words: bulk-fill composites; bulk-fill giomer; polymerization shrinkage strain; fracture toughness; preheating

9.1 Introduction

Secondary caries and bulk fractures are considered as major drawbacks of dental RBCs [214, 215]. The former results from gaps forming at the restoration/teeth interface and following bacteria accumulation. The latter relates to material inherent fracture resistance. During polymerization, the reduction of inter-molecular distances leads to volumetric shrinkage [285]. The resulted contraction stress causes adhesion problems, microleakage and clinical failure of restorations. Different measures have been introduced to reduce polymerization shrinkage and avoid relevant clinical issues [48, 212, 241].

The brittle dental RBCs undergo elastic deformation with catastrophic crack growth under applied stress [215, 219, 286]. Fracture resistance of composites is usually characterized using fracture toughness measurement, which describes composite resistance to crack propagation through the pre-crack/flaw [185]. It is hard to predict flaw distribution within the material since it can be created during light-curing or after specimen preparation [185, 219]. The stress intensity factor, K, is independent of the composite composition and fracture happens when K exceeds the critical value, K_c [185, 215, 219]. Different subscript letters refer to how crack grows under loading, in which K_{IC} refers to crack propagating under tensile stress [185, 219, 287].

Various fracture toughness measurements have been developed and due to its simplicity and acceptance, single-edge notch three-point bending (SENB) is commonly used [185]. Theoretically, fracture toughness does not change with the specimen geometry or measurement technique [185]. Filler composition, shape, content and distribution have massive influences on fracture toughness of composites [215, 219, 223]. The internal flaw distribution, air bubbles and inter-particle bonding also affect crack propagation under stress and the resultant K_{IC} [215]. Different storage conditions and test conditions may lead to diverse results [222, 223].

Recently, bulk-fill composites have been introduced with high translucency, which enables cure up to 4-5 mm deep [74, 285, 288]. Compared to incremental filling technique, bulk-fill composites show lower polymerization shrinkage stress [285]. Bulk placement also reduces voids between layers relative to increment placement, which avoids negatively affecting mechanical properties. However, high-viscosity bulk-fill composites may entrap air bubbles during manipulation and lead to internal voids [222]. Sonic vibration is employed to reduce the viscosity of *SonicFill* via the sophisticated handpiece, without compromising its depth of cure and mechanical properties [87, 150]. Heating composites prior to placement, also called "pre-heating", may improve adaptation and monomer conversion, thus enhance the mechanical properties [87].

Bulk-fill composites have been investigated extensively, but very few studies examined the effects of pre-heating and sonication. The aims of this study were to measure the polymerization shrinkage strain kinetics and fracture toughness of sonicated and pre-heated bulk-fill composites and compare them with various commercial bulk-fill composites. Thus, the objectives of this study were to compare polymerization shrinkage strain (PS), maximum rate of polymerization shrinkage strain (PS R_{max}) and fracture toughness (K_{IC}) among different types of bulk-fill composites and investigate the effect of pre-heating time on *Viscalor* PS, PS R_{max} and K_{IC}. The Null Hypotheses were:

(1) there were no differences in PS, PS R_{max} and K_{IC} between investigated bulk-fill composites and

(2) pre-heating time did not influence the PS, PS R_{max} and K_{IC} of *Viscalor*.

9.2 Materials and methods

The manufacturers' information is shown in Table 9.1. *SonicFill* 3 was applied via the sonic insertion method using a specific handpiece (*SonicFill* Handpiece, Kerr Corporation). *Viscalor* was pre-heated using the Caps Warmer (VOCO, Germany) in T3 mode (at 68 °C) for 30 s (T3-30s) and 3 min (T3-3min), respectively.

Table 9.1 Manufacturer information of investigated bulk-fill composites.

Materials	Code	Manufacturer	Resin system	Filler vol.%	Filler wt.%
Beautifil-Bulk Restorative	**BBR**	SHOFU Inc. Kyoto, Japan	bis-GMA, UDMA, bis-MPEPP, TEGDMA	74.5	87
Filtek One Bulk fill	**FBO**	3M ESPE, St. Paul, USA	DDDMA, UDMA, AUDMA, diurethane-DMA	58.4	76.5
SonicFill **3**	**SF3**	Kerr Corporation, USA	bis-EMA, triethylene glycol dimethacrylate	-	81
Viscalor	**VC**	VOCO, Germany	bis-GMA, aliphatic dimethacrylate	-	83

Polymerization shrinkage strain (PS) was measured using the bonded-disk technique as previously introduced [75, 183]. The composites were placed into a brass ring (1 mm thickness), which bonded to a 3 mm thick glass base-plate. The upper surface of the composites was covered by a compliant glass cover-slip. The specimens were cured from the bottom surface with an Elipar S10 LED unit (3M ESPE, USA) of mean irradiance 1200 mW/cm^2 for 40 s at 23 °C room temperature. The axial strain was continuously measured up to 1 h after irradiation (n=3). The maximum rates of polymerization shrinkage strain (PS R_{max}) were obtained by numerical differentiation of PS data with respect to time.

For fracture toughness measurement, the stress intensification factor, K_{IC}, was measured by fracturing the single-edge notched specimens with three-point bending [185]. The geometry of the split PTFE-lined brass mould (34 mm length $\times$ 6 mm height $\times$ 3 mm thickness) conformed to the British Standard 54, 749: 1978 [289]. A

blade was located at mid-length and extended half the height of the specimen to produce the crack during specimen preparation. A pre-crack was made by sharpening the tip of the notch with a razor blade. For each composite (n=5), specimens were photo-cured for a total of 280 s at zero distance from the top surface. By moving half the diameter of the exit window of an Elipar S10 LED unit (3M ESPE, USA), seven centre-overlapping areas were cured along the length of the specimen. After removing from the mould, the specimens were additionally cured along thickness direction with close contact between the curing tip and the specimen, to ensure sufficient curing. The specimens were polished using 1000-grit silicon carbide sandpaper to remove excess material at the edge. The specimen dimensions were measured at three different positions using a caliper with 0.01 mm accuracy. The total crack length for each specimen was determined at 0.7× magnification using a stereomicroscope (EMA-5; Meiji Techno Co. Ltd. Japan) and measured with a calibrated scale bar (0.1 mm accuracy). All specimens were stored in water at 37 °C for 7 days before testing. A Universal Testing Machine (Zwick/Roell-2020, 2.5 kN load cell) was used to measure K_{IC} at room temperature. The load was applied at a crosshead speed of 0.5 mm/min to the centre of the notched beam until reaching the fracture point. The load-deflection curves were recorded. The K_{IC} was calculated as:

$$K_{IC} = \left[\frac{PL}{BW^{1.5}}\right] Y \quad \text{(Equation 9.1)}$$

$$Y = \left\{2.9\left(\frac{a}{w}\right)^{0.5} - 4.6\left(\frac{a}{w}\right)^{1.5} + 21.8\left(\frac{a}{w}\right)^{2.5} - 37.6\left(\frac{a}{w}\right)^{3.5} + 38.7\left(\frac{a}{w}\right)^{4.5}\right\}$$

(Equation 9.2)

where P=fracture load, L= loading span (20 mm), B=thickness of the specimen, W=width of the specimen, a=total notch length, Y=function of (a/W).

Data were entered into statistical software (SPSS) and analysed using one-way ANOVA, independent T-test and Tukey post-hoc tests ($p<0.05$). Homogeneity of variance was calculated using the Kruskal-Wallis Test ($p<0.05$).

9.3 Results

Table 9.2 summarises PS, PS R_{max} and K_{IC} results, in which PS did not vary with materials (p>0.05). Different pre-heating times did not affect *Viscalor* PS (p>0.05).

Figure 9.1 shows the rates of PS of tested bulk-fill composites. Although *SonicFill* 3 had the highest PS R_{max}, there were no significant differences between PS R_{max} of tested composites (p>0.05). Different pre-heating times did not affect *Viscalor* PS R_{max} (p>0.05).

Figure 9.2 and Table 9.2 show the K_{IC} results of investigated composites. There were no significant differences among composites (p<0.05), apart from Beaultifil-Bulk Restorative, which had significantly lower K_{IC}. Different pre-heating times had no significant influence on the K_{IC} of *Viscalor* (p>0.05).

As shown in Figure 9.3, strong correlations existed between filler content (wt.%) and PS/ K_{IC} of tested composites. Correlation coefficients (r^2) were 0.95 and 0.89, respectively.

Table 9.2 Polymerization shrinkage strain (PS) and maximum rate of polymerization shrinkage strain (PS R_{max}) at 23 °C and fracture toughness (K_{IC}) after 7 days of water storage.

Materials	PS (%)	PS R_{max} (%/s)	K_{IC} (M Pa m$^{0.5}$)
Beautifil-Bulk Restorative	1.39 [a] (0.07)	0.14 [a] (0.02)	1.13 [a] (0.04)
Filtek One Bulk fill	1.65 [a] (0.05)	0.15 [a] (0.02)	1.58 [b] (0.20)
SonicFill **3**	1.49 [a] (0.34)	0.24 [a] (0.10)	1.44 [b] (0.04)
Viscalor **(no heat)**	1.41 [a] (0.13)	0.15 [a] (0.04)	1.38 [b] (0.10)
Viscalor **(T3-30s)**	1.57 [a] (0.16)	0.17 [a] (0.05)	1.44 [b] (0.11)
Viscalor **(T3-3min)**	1.45 [a] (0.15)	0.16 [a] (0.04)	1.45 [b] (0.13)

For each property, the same lower case superscript letters indicate homogeneous subsets among the materials.
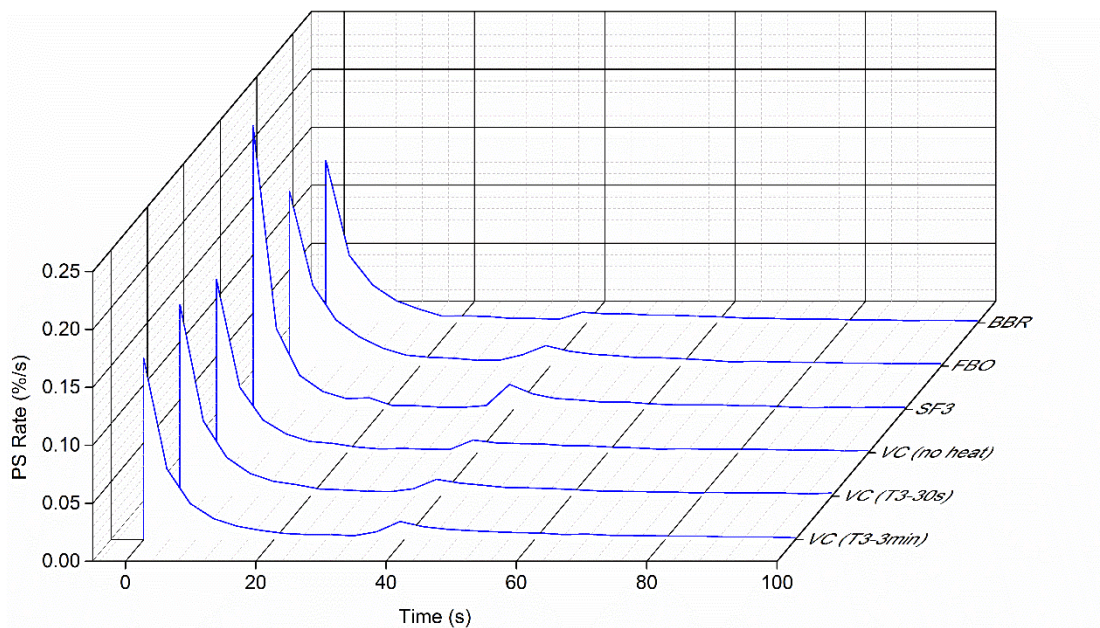
Figure 9.1 Rates of polymerization shrinkage strain of tested composites at 23 °C.
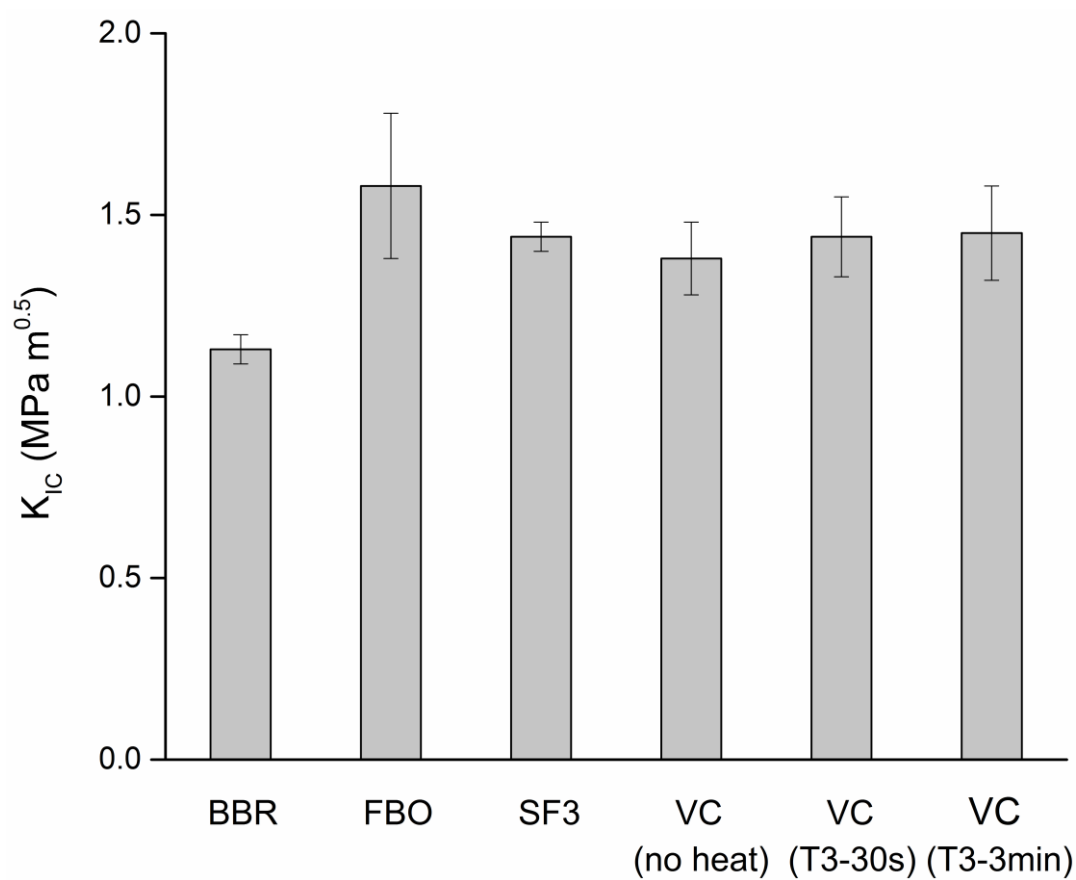
Figure 9.2 Fracture toughness (K_{IC}) after 7 days of water storage.
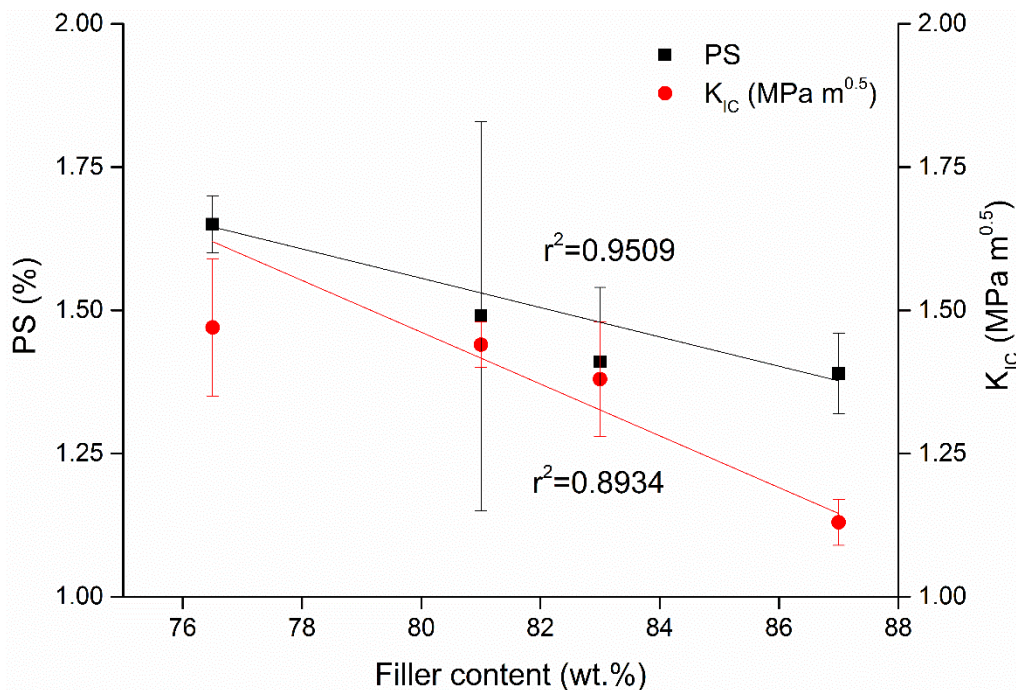
Figure 9.3 Scatter plots showing the correlations and linear regressions between filler content (wt.%) and PS (black)/K_{IC} (red).

9.4 Discussion

Building upon PS results of *Viscalor* in Chapter 6 [290] and K_{IC} result of Filtek One Bulk Fill [221], this study compared PS, PS R_{max} and K_{IC} of different types of bulk-fill composites. PS and PS R_{max} did not vary with tested composites, whereas Beautifil-Bulk Restorative showed significantly low K_{IC}. Pre-heated *Viscalor* showed comparable PS, PS R_{max} and K_{IC} results to room-temperature *Viscalor*. Thus, the first null hypothesis was *partly rejected* and the second null hypothesis was *accepted*.

PS is related to monomer formulation and concentration, filler content and size and photo-initiator systems [291]. A high PS may affect marginal integrity and lead to microleakage and clinical failure. In this study, PS was found to decrease with increasing filler content (Figure 9.3), which is in line with previous studies [23, 74, 119, 123, 212, 292]. Beautifil-Bulk Restorative had the highest filler content (87 wt.%) and showed the lowest PS. The increased filler content reduces the resin matrix portion, where the volumetric shrinkage mainly occurs and results in lower PS results. The high-viscous monomer, such as bis-GMA, could aid in building a rigid structure

to prevent volumetric shrinkage [12, 173, 251, 293]. However, Tsujimoto et al. [291] found that Beautifil Bulk Restorative had higher volumetric shrinkage than other composites, although it contains high filler content. The addition of low-viscous monomers, such as TEGDMA, alters the viscosity and may increase the final degree of conversion (DC) and PS [119, 123, 251, 292, 294]. Different testing methods could also lead to diverse results, which merits further investigations [291].

Due to its low filler content (76.5 wt.%), Filtek One Bulk Fill showed the highest PS among the tested bulk-fill composites. It is designed as Reversible Addition-Fragmentation Transfer (RAFT)-polymerized bulk-fill RBC and its enhanced rate of polymerization may lead to relatively high PS [61, 244, 288]. But the high-molecular-weight monomers, for example, AUDMA and DDDMA, could also increase its resin matrix viscosity and reduce DC and PS [288, 294]. Since the rate of polymerization influences the shrinkage kinetics [244, 250], further investigations about polymerization kinetics of tested composites, such as degree of conversion measurement, are needed.

The rising and falling parts in the PS R_{max} plot (Figure 9.1) represent the auto-acceleration and -deceleration phases of the diffusion-controlled polymerization reaction [23, 251]. During the auto-acceleration stage, the increased viscosity limits the segmental movement of radicals. The radical termination becomes diffusion-controlled and leads to a rapid increase in the propagation rate [18, 251]. With further reacting, the chain propagation rate is impeded by the high-viscous crosslinking network and reaction rates drop off [251]. PS rates of composites are related to monomer functionality and viscosity and filler content [251]. In this study, PS R_{max} was not found to decrease with filler content (wt.%) or vary with tested composites. However, *SonicFill* 3 had the highest PS R_{max}, which may be related to the reduced viscosity after sonication. Its comparable PS result demonstrates that sonication beneficially reduces the viscosity without influencing PS behaviour [150].

Fracture toughness of materials denotes their ability to resist fracture and the amount of stress needed for which to propagate through inherent flaws or pre-cracks. According to Alshabib et al.'s conclusion that K_{IC} of RBCs did not significantly change over storage time [221] and to ensure sufficient post-polymerization, this study directly investigated K_{IC} of bulk-fill composites after 7 days of water storage. The results showed that K_{IC} decreased with filler content (Figure 9.3), in which Beautifil-Bulk Restorative and Filtek One Bulk Fill showed the lowest and highest K_{IC}, respectively. The former is designed as a high-viscosity bulk-fill giomer, combining the advantages of glass ionomers and polymers [222, 291]. Its low K_{IC} may be attributed to the high filler content, which impedes light penetration during light-curing and leads to insufficient polymerization [222, 291]. However, Ilie et al. found that Beautifi-Bulk Restorative has better micro-mechanical properties relative to conventional RBCs due to the increased filler content [295]. Its large filler size reduces the light scattering at the filler/matrix interface and improves the depth of cure [295]. As a RAFT-polymerized composite, Filtek One Bulk Fill contains addition-fragmentation monomers to assist fragmentation and form a well-controlled homogeneous polymer structure [61, 288]. Hence, it showed the highest K_{IC}, albeit the low filler content.

On the contrary, some studies reported that K_{IC} increased with filler content [219, 222]. The crack front needs more energy to propagate through densely-packed reinforcing particles, which limits the crack growth and leads to high K_{IC}. In addition to the crack branching and deflection caused by filler particles, the toughening mechanism of the filler/matrix interaction also plays an important role in enhancing K_{IC} [215]. When filler content exceeds the critical fraction (usually 55-65 vol. %), viscosity increases and more voids/porosities could be involved in the structure [215, 223, 224]. The increased filler loading may also limit the plastic deformation of the resin matrix and finally reduces K_{IC} [296]. Filler size, shape and distribution, air bubbles and inter-particle bonding all have influences on fracture origins and the resultant K_{IC} [215, 223]. Small filler particles increase the filler/matrix interface area

and make composites more susceptible to water penetration and degradation [42, 215]. The weak resin matrix may facilitate crack growth and reduce the K_{IC}.

In this study, PS results of pre-heated and room-temperature *Viscalor* were all lower than the clinically acceptable range of 2-6 % [138] and comparable to that of other tested composites. K_{IC} results of non-heated and pre-heated *Viscalor* are as high as that of Filtek One Bulk Fill. Thus, a long pre-heating period of 3 min did not influence shrinkage behaviour and K_{IC} of *Viscalor*. After removal from the heating device, the composite temperature rapidly dropped and viscosity gradually returned to the initial state [2, 132]. Hence, PS, PS R_{max} and K_{IC} did not significantly vary with temperature change after different pre-heating times. Lloyd found that fracture toughness decreases with temperature rise and the temperature dependence of fracture toughness is not significant in the temperature range of 32-40 °C [297]. Other studies concluded that depending on material microstructure, fracture toughness may remain, increase or, reduce [287]. Temperature mainly affects the resin matrix part rather than filler particles. The thermo-viscous resin matrix within *Viscalor* remains stable after 3 min pre-heating period, which facilitates resisting against the applied load and resultant fracture. But the lack of manufacturer information limits the discussion.

The comparable filler contents of *Viscalor* and *SonicFill* 3 possibly led to similar PS and K_{IC} results. The higher PS R_{max} of *SonicFill* 3 denotes that, compared to pre-heating, sonication results in more stable viscosity reduction. Besides, their effects on polymerization kinetics and post-cure properties need further investigations, for example, measuring the degree of conversion, shrinkage stress and relevant mechanical properties.

9.5 Conclusions

In this study, different bulk-fill composites showed comparable PS and PS R_{max}. All tested bulk-fill composites showed similar K_{IC}, except bulk-fill giomer (Beautifil-

Bulk Restorative) that showed the lowest K_{IC}. A long pre-heating period (3 min) had no adverse effects on *Viscalor* PS, PS R_{max} and K_{IC}.

Chapter Ten

General Discussion, Conclusions and

Future Work Recommendations

10.1 General discussion

Resin-based composites (RBCs) have been widely used as dental restorative materials for decades. The inevitable clinical failure of restorations is primarily related to secondary caries and bulk fractures [15]. Apart from RBC composition, restoration type, cavity size, operator manipulation skills and the type of patient affect the longevity of RBCs [229]. Modified material composition, placement technique and light-curing technology improve RBC longevity.

The clinical performance of RBCs is mainly controlled by their preparation design, dimensional characteristics and mechanical properties [15]. Specific properties are important in the selection and placement of RBCs. Handling properties, also called pre-cure properties, can have an indirect influence on the depth of cure, degree of conversion (DC) and physical/mechanical properties of the material. Handling properties depend on the rheological nature of the material, which depends upon the material composition and external factors. A low viscosity helps material flow into the irregular corner of the cavity. Flowable RBCs, with reduced filler loading, have been introduced with low viscosity but somewhat reduced mechanical properties compared to regular composites. The *SonicFill* system, containing viscosity modifiers, can respond to ultrasonic energy (UE) and reduce its viscosity by 87 %. When the UE is removed, the induced viscosity gradually returns to the initial state, which is suitable for shaping. According to the Arrhenius Equation (Equation 1.1), elevated temperature reduces viscosity and many studies have investigated temperature effects on RBC properties [113, 173, 175, 211].

$$\eta = A e^{Ea/RT} \qquad \text{(Equation 1.1)}$$

Thus, heating materials before light-curing, also known as pre-heating, can be utilised to ease placement, improve monomer conversion and enhance mechanical properties of RBCs. However, the risk of temperature rise needs consideration.

This thesis generally evaluated pre-cure and post-cure properties of a thermo-viscous material, *Viscalor* after different pre-heating times and compared with several commercial RBCs. As a newly designed thermo-viscous RBC, *Viscalor* was pre-heated using a Caps Warmer for different times to achieve different composite temperatures and increased flowability before light-curing. The overall aim was to assess the properties of *Viscalor* during its clinical lifetime and compare with existing commercial products. The properties were divided in sections as pre-cure, post-cure short term and post-cure long term. Chapters 3-5 studied the pre-cure properties, including stickiness, packability and extrusion force, of *Viscalor* and other RBCs. Building upon (published) Chapter 5, Chapter 6 (also published) discussed the effects of exposure duration and pre-heating time on polymerization kinetics, polymerization shrinkage strain and surface micro-hardness of *Viscalor*. Post-cure long term properties of *Viscalor* and other composites, including wear resistance, viscoelastic behaviour and fracture toughness, were studied in Chapters 7-9.

Stickiness (F_{max} and W_s) and packability (F_p and W_p) of RBCs with different resin matrices and filler contents (75-84 wt.%) were investigated with different experimental settings at 22 and 37 °C. Lee et al. concluded that viscosity increases with filler content and leads to low stickiness [84]. However, in this study, stickiness and packability increased with filler content. This may relate to composite matrix compositions, for example, the presence of viscosity modifier (TEGDMA and bis-EMA) and the Adaptive Response Technology (ART) filler system. Filler particle size also affected viscosity such that at a constant filler loading, the smaller particles lead to higher viscosity [84]. Thus, TPH LV and Tetric EvoCeram had lower stickiness than that of Filtek Supreme Ultra. Room-temperature *Viscalor* showed high stickiness and packability, which may relate to its thermo-viscous matrix and nanohybrid particles. But the lack of manufacturer information limits the discussion.

Stickiness and packability of RBCs varied with experimental settings. This is related to RBC viscosity, i.e. the ability to resist flow under the applied stress. Although stickiness and packability increased with probe withdrawal speed and packing speed,

both effects have upper limits. Extremely high withdrawal speed and packing speed had no significant further influences on stickiness and packability. Packability increased with probe penetration distance, which is similar to the wall-effect [151]. However, Harmonize did not significantly change with probe penetration distance. The ART system within Harmonize alters its viscosity and makes it flow easily under the applied force. Investigations regarding experimental settings (probe speed, etc.) may provide guidance on clinical manipulation of composites.

During stickiness and packability measurements, the mould was thermostatically controlled at either 22 or 37 °C. The latter simulated the oral environment temperature. Stickiness and packability of RBCs measured at 37 °C were lower than that measured at 22 °C, except W_s. However, some studies have contrary results [126, 128], which may be due to different experimental settings and investigated composites. Elevated temperature increases monomer mobility and the flowability of RBCs. Thus, less packing force was needed during manipulation.

The effects of pre-heating time on stickiness and packability of *Viscalor* varied with experimental settings and temperatures. Packability of pre-heated *Viscalor* measured with different probe penetration distances did not significantly change, relative to non-pre-heated *Viscalor*. However, at high packing speed, the pre-heated *Viscalor* showed lower W_p than that of room-temperature *Viscalor*. This denotes that, aside from the effect of pre-heating, the influence of the manipulation method needs consideration. Although the effects of pre-heating time on stickiness and packability of *Viscalor* were statistically significant, the results were comparable to that of other RBCs and remained within the clinically acceptable range.

Chapter 5 [243] described further investigations on effects of pre-heating time on the extrusion force and DC of *Viscalor*. As expected, a long pre-heating period reduced extrusion force and increased the extrusion mass of *Viscalor*. This is related to its viscosity reduction after pre-heating. However, different pre-heating times did not significantly change *Viscalor* DC. This demonstrated that pre-heating has no adverse

effects on *Viscalor* DC through any pre-mature polymerization. The rapid temperature decrease after removal from the heating device may also contribute to the similar DC results between pre-heated and non-heated *Viscalor*. Both *Viscalor* syringe and compules showed statistically similar DC results, which may suggest that different containers have no significant differences in thermal conductivity during pre-heating.

Building upon the DC results in Chapter 5, the question of whether the longer curing time (40 s) masked the effect of pre-heating time on DC of *Viscalor* was raised. Many studies have investigated the effect of temperature on material polymerization kinetics and polymerization shrinkage behaviour [138, 173, 182]. Thus, Chapter 6 investigated the effects of exposure duration and pre-heating time on *Viscalor* polymerization kinetics and PS. Surface microhardness was measured to determine the depth of cure and polymerization extent. Results showed that there was no interaction between effects of pre-heating time and exposure duration. The longer exposure duration only increased VHN_{top} of *Viscalor* but did not influence its DC, RP_{max}, or PS. The bottom/top surface micro-hardness ratios were all over 0.8, which indicated an adequate depth of cure and effective polymerization [1, 169]. *Viscalor* pre-heated for 3 min and cured for 20 s showed adequate hardness, without adversely affecting its polymerization kinetics or increasing PS. This is in line with previous studies that pre-heated composites cured for a short time produced similar DC results to that of room-temperature composites cured for a long time [3, 131]. Hence, for the clinical use of *Viscalor*, a 3 min long pre-heating period can be used to reduce irradiation time and obtain similar or better performance.

Different clinically relevant properties were evaluated in Chapters 7-9 to determine further consequences of pre-heating time on *Viscalor* post-cure performance. The degree of polymerization significantly affects the post-cure properties. Thus, all specimens were cured sufficiently by minimizing the distance between the composite surface and LCU tip and employing longer exposure duration. The changes of surface aesthetic and roughness after abrasion reflect the wear resistance of composites. Also, the effect of pre-heating time on RBCs gloss and surface roughness is less discussed.

Thus, in Chapter 7, gloss and surface roughness of *Viscalor* before and after toothbrushing simulations were compared with other composites. Results showed that gloss and surface roughness are material dependent. Composites with a filler content of 77-82 wt.% had superior surface performance after brushing among tested RBCs. This may be instructive for designing nanohybrid RBCs with clinically acceptable wear resistance. Different pre-heating times did not negatively affect gloss and surface roughness of *Viscalor* before or after toothbrushing simulations. Pre-heated *Viscalor* for 3 min led to better gloss retention after brushing, which is a further benefit of the longer pre-heating period.

Viscoelastic stability affects dimensional characteristics of materials in the oral environment and can compromise marginal adaptation and result in the occurrence of secondary caries [15]. In terms of creep behaviour, maximum creep strain, permanent set and percentage creep recovery of composites were measured at 5 min post-cure and after 7 days of water storage. The 37 °C water bath during measurement simulated the oral environment. Different storage conditions were selected according to previous studies [205, 284]. 7 days of water storage allows post-cure polymerization and the plasticizing effect of water [204, 205, 284]. The former leads to a rigid structure and the latter promotes creep recovery. Hence, water storage beneficially reduced the elastic deformation of composites and improved their percentage creep recovery. Results showed that composite creep behaviour varied with filler content, since high filler loading reinforces the soft resin part and reduces dimensional change under stress. Marghalani et al. found that elevated temperature softens the resin matrix and reduces percentage creep recovery [203]. However, different pre-heating times did not significantly influence the creep behaviour of *Viscalor*. Once removed from the heating device, the rapidly reduced composite temperature during manipulation approached the oral cavity temperature. Thus, creep behaviours of pre-heated *Viscalor* showed mostly small changes relative to non-pre-heated *Viscalor*. According to previously published data, the similar DC results of

Viscalor (no heat, T3-30s and T3-3min) further proved that no significant differences between their creep behaviours [243].

Viscalor is designed as a bulk-fill composite, with low PS and superior mechanical properties. Thus, Chapter 9 compared polymerization shrinkage kinetics and fracture toughness (K_{IC}) of pre-heated *Viscalor* to that of different types of commercial bulk-fill composites. All tested composites showed similar PS and PS R_{max}, in which the former varied with filler content. Highly filled Giomer bulk-fill composites had the lowest K_{IC}, whereas others had similar results. A long pre-heating period of 3 min did not reduce either polymerization shrinkage kinetics or K_{IC} of *Viscalor* and results were comparable to that of *SonicFill* 3. Building upon the published papers [243, 290], pre-heating and sonication are useful techniques to enhance composite flowability without either increasing PS or reducing K_{IC}.

This study systematically evaluated the effect of pre-heating time on *Viscalor* pre-cure and post-cure properties and compared them with a wide range of commercial RBCs. The influences of composition, experimental condition, temperature, exposure duration and storage condition were also discussed. These findings provide guidance for the clinical relevance of pre-heated *Viscalor*.

10.2 Conclusions

Within the limitations of this study, the following conclusions were reached:

1) Stickiness (F_{max} and W_s) and packability (F_p and W_p) of RBCs significantly increased with filler content and were affected by resin matrix composition, temperature and experimental conditions.

2) After toothbrushing simulation, gloss reduced and surface roughness increased. Both properties are material dependent and varied with filler content (wt.%/vol.%). 77-82 wt.%/60-64.5 vol.% of filler content led to better wear resistance.

3) Viscoelastic creep behaviour of RBCs was affected by composition and storage condition. Long-term water storage of 7 days enhanced composite percentage creep recovery.

4) The investigated bulk-fill composites showed comparable polymerization shrinkage kinetics. Both PS and K_{IC} decreased with filler content (wt.%). Giomer bulk-fill composite had the lowest K_{IC}.

5) Different pre-heating times beneficially affected the pre-cure properties of *Viscalor* and did not adversely influenced its post-cure properties. Room-temperature and pre-heated *Viscalor* showed comparable pre-cure and post-cure properties to the investigated RBCs. For its clinical application, 3 min pre-heating and 20 s irradiation were sufficient to provide clinically acceptable performance, without compromising polymerization kinetics or increasing PS.

10.3 Future work recommendations

The following aspects are recommended to obtain further understanding:

1) Evaluate rheological properties, such as viscosity, of tested RBCs and compare with the obtained stickiness and packability.

2) Use a thermal imaging camera to monitor the real-time temperature change of *Viscalor* after removing from the heating device until light-cured to explore the effects of different heating settings and longer heating period on *Viscalor* properties.

3) Use micro-CT to determine the effect of pre-heating on the internal porosity/gap formation of *Viscalor*.

4) Investigate PS and DC with instruments heated and measure polymerization kinetics of RBCs apart from *Viscalor*.

5) Evaluate light-transmission and surface micro-hardness of other composites and compare with those of *Viscalor*.

6) Assess the surface change before and after toothbrushing simulation using SEM or AFM.

7) Determine the effect of different food-simulating storage solvents on the creep behaviours of tested RBCs.

8) Investigate the effect of light exposure duration on polymerization shrinkage kinetics of tested RBCs.

9) Investigate the polymerization shrinkage stress and polymerization kinetics of tested bulk-fill composites and compare with those of *Viscalor*.

References

1. Lucey S, Lynch CD, Ray NJ, Burke FM, Hannigan A. Effect of pre-heating on the viscosity and microhardness of a resin composite. J Oral Rehab. 2010;37(4):278-82.
2. Deb S, Di Silvio L, Mackler HE, Millar BJ. Pre-warming of dental composites. Dent Mater. 2011;27(4):e51-e9.
3. Fróes-Salgado NR, Silva LM, Kawano Y, Francci C, Reis A, Loguercio AD. Composite pre-heating: Effects on marginal adaptation, degree of conversion and mechanical properties. Dent Mater. 2010;26(9):908-14.
4. Sakaguchi RL, Powers JM. Craig's Restorative Dental Materials-E-Book: Elsevier Health Sciences; 2012.
5. Kidd EA, Fejerskov O. Essentials of dental caries: Oxford University Press; 2016.
6. Anusavice KJ, Shen C, Rawls HR. Phillips' science of dental materials: Elsevier Health Sciences; 2013.
7. Antoniac IV. Handbook of Bioceramics and Biocomposites: Springer Berlin Heidelberg, New York; 2016.
8. Bowen R. Use of epoxy resins in restorative materials. J Dent Res. 1956;35(3):360-9.
9. Bowen R. Composite and sealant resins: past, present and future. Pediatr Dent. 1982;4(1):10-5.
10. Cook WD, Beech DR, Tyas MJ. Resin-based restorative materials—a review. Aust Dent J. 1984;29(5):291-5.
11. Van Noort R. Introduction to Dental Materials 4th Edition. London: Elsevier Health Sciences; 2013.
12. Ferracane JL. Resin composite--state of the art. Dent Mater. 2011;27(1):29-38.
13. Rezwani-Kaminski T, Kamann W, Gaengler P. Secondary caries susceptibility of teeth with long-term performing composite restorations. J Oral Rehabil. 2002;29(12):1131-8.
14. Pfeifer CS. Dental Composites - Chemistry and Composition.   Dental Biomaterials. World Scientific Series: From Biomaterials Towards Medical Devices. Volume 2: WORLD SCIENTIFIC; 2017. p. 295-333.
15. Ferracane JL. Resin-based composite performance: Are there some things we can't predict? Dent Mater. 2013;29(1):51-8.
16. García AH, Lozano MAM, Vila JC, Escribano AB, Galve PF. Composite resins. A review of the materials and clinical indications. Med Oral Patol Oral Cir Bucal. 2006;11(2):E215-20.
17. Moszner N, Salz U. New developments of polymeric dental composites. Prog Polym Sci. 2001;26(4):535-76.
18. Watts DC. Reaction kinetics and mechanics in photo-polymerised networks. Dent Mater. 2005;21(1):27-35.
19. Pérez-Mondragón AA, Cuevas-Suárez CE, González-López JA, Trejo-Carbajal N, Meléndez-Rodríguez M, Herrera-González AM. Preparation and evaluation of a BisGMA-free dental composite resin based on a novel trimethacrylate monomer.

Dent Mater. 2020;36(4):542-50.

20. Sideridou ID, Vouvoudi EC. Dental composites: Dimethacrylate-based. CRC Press, Boca Raton, FL; 2015.

21. Amirouche-Korichi A, Mouzali M, Watts DC. Effects of monomer ratios and highly radiopaque fillers on degree of conversion and shrinkage-strain of dental resin composites. Dent Mater. 2009;25(11):1411-8.

22. Fugolin AP, de Paula AB, Dobson A, Huynh V, Consani R, Ferracane JL, et al. Alternative monomer for BisGMA-free resin composites formulations. Dent Mater. 2020.

23. Atai M, Watts DC. A new kinetic model for the photopolymerization shrinkage-strain of dental composites and resin-monomers. Dent Mater. 2006;22(8):785-91.

24. Gajewski VE, Pfeifer CS, Fróes-Salgado NR, Boaro LC, Braga RR. Monomers used in resin composites: degree of conversion, mechanical properties and water sorption/solubility. Braz Dent J. 2012;23(5):508-14.

25. Barszczewska-Rybarek I, Jurczyk S. Comparative Study of Structure-Property Relationships in Polymer Networks Based on Bis-GMA, TEGDMA and Various Urethane-Dimethacrylates. Materials. 2015;8(3).

26. Ilie N, Hickel R. Resin composite restorative materials. Aust Dent J. 2011;56 Suppl 1:59-66.

27. Cornelio RB, Wikant A, Mjosund H, Kopperud HM, Haasum J, Gedde UW, et al. The influence of bis-EMA vs bis GMA on the degree of conversion and water susceptibility of experimental composite materials. Acta Odontol Scand. 2014;72(6):440-7.

28. Peutzfeldt A. Resin composites in dentistry: the monomer systems. Eur J Oral Sci. 1997;105(2):97-116.

29. Ravve A. Principles of polymer chemistry: Springer Science & Business Media; 2013.

30. Pfeifer CS, Silva LR, Kawano Y, Braga RR. Bis-GMA co-polymerizations: Influence on conversion, flexural properties, fracture toughness and susceptibility to ethanol degradation of experimental composites. Dent Mater. 2009;25(9):1136-41.

31. Papakonstantinou AE, Eliades T, Cellesi F, Watts DC, Silikas N. Evaluation of UDMA's potential as a substitute for Bis-GMA in orthodontic adhesives. Dent Mater. 2013;29(8):898-905.

32. Gonçalves F, Pfeifer CC, Stansbury JW, Newman SM, Braga RR. Influence of matrix composition on polymerization stress development of experimental composites. Dent Mater. 2010;26(7):697-703.

33. Boaro LC, Goncalves F, Guimaraes TC, Ferracane JL, Versluis A, Braga RR. Polymerization stress, shrinkage and elastic modulus of current low-shrinkage restorative composites. Dent Mater. 2010;26(12):1144-50.

34. Silikas N, Watts DC. Rheology of urethane dimethacrylate and diluent formulations. Dent Mater. 1999;15(4):257-61.

35. Sideridou I, Tserki V, Papanastasiou G. Study of water sorption, solubility and modulus of elasticity of light-cured dimethacrylate-based dental resins. Biomaterials. 2003;24(4):655-65.

36. Sideridou I, Tserki V, Papanastasiou G. Effect of chemical structure on degree of conversion in light-cured dimethacrylate-based dental resins. Biomaterials. 2002;23(8):1819-29.

37. Ferracane JL. Developing a more complete understanding of stresses produced in dental composites during polymerization. Dent Mater. 2005;21(1):36-42.

38. Weinmann W, Thalacker C, Guggenberger R. Siloranes in dental composites. Dent Mater. 2005;21(1):68-74.

39. Hikmet R, Zwerver B, Broer D. Anisotropic polymerization shrinkage behaviour of liquid-crystalline diacrylates. Polymer. 1992;33(1):89-95.

40. Ilie N, Hickel R. Silorane-based dental composite: behavior and abilities. Dent Mater J. 2006;25(3):445-54.

41. Mahmoud SH, Al-Wakeel EES. Marginal adaptation of ormocer-, silorane-, and methacrylate-based composite restorative systems bonded to dentin cavities after water storage. Quintessence Int. 2011;42(10):e131-9.

42. Ilie N, Hickel R. Macro-, micro- and nano-mechanical investigations on silorane and methacrylate-based composites. Dent Mater. 2009;25(6):810-9.

43. Trujillo-Lemon M, Ge J, Lu H, Tanaka J, Stansbury JW. Dimethacrylate derivatives of dimer acid. J Polym Sci Pol Chem. 2006;44(12):3921-9.

44. Ilie N, Jelen E, Clementino-Luedemann T, Hickel R. Low-shrinkage Composite for Dental Application. Dent Mater J. 2007;26(2):149-55.

45. Moszner N, Gianasmidis A, Klapdohr S, Fischer UK, Rheinberger V. Sol–gel materials: 2. Light-curing dental composites based on ormocers of cross-linking alkoxysilane methacrylates and further nano-components. Dent Mater. 2008;24(6):851-6.

46. Cavalcante LM, Schneider LFJ, Silikas N, Watts DC. Surface integrity of solvent-challenged ormocer-matrix composite. Dent Mater. 2011;27(2):173-9.

47. Tagtekin DA, Yanikoglu FC, Bozkurt FO, Kologlu B, Sur H. Selected characteristics of an Ormocer and a conventional hybrid resin composite. Dent Mater. 2004;20(5):487-97.

48. Rueggeberg FA, Giannini M, Arrais CAG, Price RBT. Light curing in dentistry and clinical implications: a literature review. Braz Oral Res. 2017;31.

49. Soh SK, Sundberg DC. Diffusion-controlled vinyl polymerization. I. The gel effect. J Polym Sci Polym Chem Ed. 1982;20(5):1299-313.

50. Daronch M, Rueggeberg FA, De Goes MF, Giudici R. Polymerization Kinetics of Pre-heated Composite. J Dent Res. 2006;85(1):38-43.

51. Gautam R, Singh RD, Sharma VP, Siddhartha R, Chand P, Kumar R. Biocompatibility of polymethylmethacrylate resins used in dentistry. J Biomed Mater Res B Appl Biomater. 2012;100(5):1444-50.

52. May KB, Razzoog ME, Koran III A, Robinson E. Denture base resins: comparison study of color stability. J Prosthet Dent. 1992;68(1):78-82.

53. Blagojevic V, Murphy V. Microwave polymerization of denture base materials. A comparative study. J Oral Rehab. 1999;26(10):804-8.

54. Miletic V. Development of Dental Composites.   Dental Composite Materials for Direct Restorations: Springer; 2018. p. 3-9.

55. Santini A, Gallegos IT, Felix CM. Photoinitiators in dentistry: a review. Prim Dent J. 2013;2(4):30-3.

56. Stansbury JW. Curing dental resins and composites by photopolymerization. J Esthet Restor Dent. 2000;12(6):300-8.

57. Haas M, Radebner J, Eibel A, Gescheidt G, Stueger H. Recent Advances in Germanium-Based Photoinitiator Chemistry. Chem Eur J. 2018;24(33):8258-67.

58. Furuse AY, Mondelli J, Watts DC. Network structures of Bis-GMA/TEGDMA resins differ in DC, shrinkage-strain, hardness and optical properties as a function of reducing agent. Dent Mater. 2011;27(5):497-506.

59. Teshima W, Nomura Y, Tanaka N, Urabe H, Okazaki M, Nahara Y. ESR study of camphorquinone/amine photoinitiator systems using blue light-emitting diodes. Biomaterials. 2003;24(12):2097-103.

60. Neeraj Malhotra M, Kundabala Mala M. Light-curing considerations for Resin-based composite materials: A review Part I. Compendium. 2010;31(7):498-506.

61. Ilie N, Watts DC. Outcomes of ultra-fast (3 s) photo-cure in a RAFT-modified resin-composite. Dent Mater. 2020;36(4):570-9.

62. Rueggeberg FA. State-of-the-art: Dental photocuring—A review. Dent Mater. 2011;27(1):39-52.

63. Kutuk ZB, Gurgan S, Hickel R, Ilie N. Influence of extremely high irradiances on the micromechanical properties of a nano hybrid resin based composite. Am J Dent. 2017;30(1):9-15.

64. Silikas N, Eliades G, Watts DC. Light intensity effects on resin-composite degree of conversion and shrinkage strain. Dent Mater. 2000;16(4):292-6.

65. Baroudi K, Silikas N, Watts DC. In vitro pulp chamber temperature rise from irradiation and exotherm of flowable composites. Int J Paediatr Dent. 2009;19(1):48-54.

66. Kodonas K, Gogos C, Tziafa C. Effect of simulated pulpal microcirculation on intrachamber temperature changes following application of various curing units on tooth surface. J Dent. 2009;37(6):485-90.

67. Yazici AR, Müftü A, Kugel G, Perry RD. Comparison of Temperature Changes in the Pulp Chamber Induced by Various Light Curing Units, In Vitro. Oper Dent. 2006;31(2):261-5.

68. Leprince J, Devaux J, Mullier T, Vreven J, Leloup G. Pulpal-temperature Rise and Polymerization Efficiency of LED Curing Lights. Oper Dent. 2010;35(2):220-30.

69. Neeraj Malhotra M, Kundabala Mala M. Light-curing considerations for resin-based composite materials: a review. Part II. Compendium. 2010;31(8):583-92.

70. Palin WM, Leprince JG, Hadis MA. Shining a light on high volume photocurable materials. Dent Mater. 2018;34(5):695-710.

71. Miller GA, Gou L, Narayanan V, Scranton AB. Modeling of photobleaching for the photoinitiation of thick polymerization systems. J Polym Sci A Polym Chem. 2002;40(6):793-808.

72. Delgado AJ, Castellanos EM, Sinhoreti MAC, Oliveira DC, Abdulhameed N, Geraldeli S, et al. The Use of Different Photoinitiator Systems in Photopolymerizing Resin Cements Through Ceramic Veneers. Oper Dent. 2018;44(4):396-404.

73.   Daugherty MM, Lien W, Mansell MR, Risk DL, Savett DA, Vandewalle KS. Effect of high-intensity curing lights on the polymerization of bulk-fill composites. Dent Mater. 2018;34(10):1531-41.

74.   Zorzin J, Maier E, Harre S, Fey T, Belli R, Lohbauer U, et al. Bulk-fill resin composites: polymerization properties and extended light curing. Dent Mater. 2015;31(3):293-301.

75.   Ferracane JL, Hilton TJ, Stansbury JW, Watts DC, Silikas N, Ilie N, et al. Academy of Dental Materials guidance-Resin composites: Part II-Technique sensitivity (handling, polymerization, dimensional changes). Dent Mater. 2017;33(11):1171-91.

76.   Park J, Chang J, Ferracane J, Lee IB. How should composite be layered to reduce shrinkage stress: Incremental or bulk filling? Dent Mater. 2008;24(11):1501-5.

77.   Price RB, Felix CA, Andreou P. Effects of resin composite composition and irradiation distance on the performance of curing lights. Biomaterials. 2004;25(18):4465-77.

78.   Price RB, Labrie D, Whalen JM, Felix CM. Effect of distance on irradiance and beam homogeneity from 4 light-emitting diode curing units. J Can Dent Assoc. 2011;77:b9.

79.   Leprince JG, Palin WM, Hadis MA, Devaux J, Leloup G. Progress in dimethacrylate-based dental composite technology and curing efficiency. Dent Mater. 2013;29(2):139-56.

80.   Sampaio CS, Atria PJ, Rueggeberg FA, Yamaguchi S, Giannini M, Coelho PG, et al. Effect of blue and violet light on polymerization shrinkage vectors of a CQ/TPO-containing composite. Dent Mater. 2017;33(7):796-804.

81.   Rüttermann S, Wandrey C, Raab WHM, Janda R. Novel nano-particles as fillers for an experimental resin-based restorative material. Acta Biomater. 2008;4(6):1846-53.

82.   Cannon M. Resin-Based Composites. Encyclopedia of Medical Devices and Instrumentation. 2006.

83.   Lee I-B, Son H-H, Um C-M. Rheologic properties of flowable, conventional hybrid, and condensable composite resins. Dent Mater. 2003;19(4):298-307.

84.   Lee J-H, Um C-M, Lee I-b. Rheological properties of resin composites according to variations in monomer and filler composition. Dent Mater. 2006;22(6):515-26.

85.   Ellakwa A, Cho N, Lee IB. The effect of resin matrix composition on the polymerization shrinkage and rheological properties of experimental dental composites. Dent Mater. 2007;23(10):1229-35.

86.   Habib E, Wang R, Zhu XX. Correlation of resin viscosity and monomer conversion to filler particle size in dental composites. Dent Mater. 2018;34(10):1501-8.

87.   Baroudi K, Mahmoud S. Improving Composite Resin Performance Through Decreasing its Viscosity by Different Methods. Open Dent J. 2015;9:235-42.

88.   Kim K-H, Ong JL, Okuno O. The effect of filler loading and morphology on the mechanical properties of contemporary composites. J Prosthet Dent. 2002;87(6):642-9.

89.   Masouras K, Akhtar R, Watts DC, Silikas N. Effect of filler size and shape on local nanoindentation modulus of resin-composites. J Mater Sci Mater Med.

2008;19(12):3561-6.

90. Uo M, Sasaki A, Masuda J, Ino J, Watari F. Application of flake shaped glass (Glass Flake®) filler for dental composite resin. J CERAM SOC JPN. 2010;118(1378):425-7.

91. Abyad A, Zhao Y, Chen X, Watts DC. Novel glassflake resin composites. Dent Mater. 2016;32:e51-e2.

92. Mohseni M, Atai M, Sabet A, Beigi S. Effect of plate-like glass fillers on the mechanical properties of dental nanocomposites. Iran Polym J. 2015;25(2):129-34.

93. Garoushi S, Vallittu PK, Lassila LV. Short glass fiber reinforced restorative composite resin with semi-inter penetrating polymer network matrix. Dent Mater. 2007;23(11):1356-62.

94. Sadr A, Bakhtiari B, Hayashi J, Luong MN, Chen Y-W, Chyz G, et al. Effects of fiber reinforcement on adaptation and bond strength of a bulk-fill composite in deep preparations. Dent Mater. 2020;36(4):527-34.

95. Lassila L, Keulemans F, Säilynoja E, Vallittu PK, Garoushi S. Mechanical properties and fracture behavior of flowable fiber reinforced composite restorations. Dent Mater. 2018;34(4):598-606.

96. Leprince J, Palin WM, Mullier T, Devaux J, Vreven J, Leloup G. Investigating filler morphology and mechanical properties of new low-shrinkage resin composite types. J Oral Rehabil. 2010;37(5):364-76.

97. Wang Z, Lu Z, Mahoney C, Yan J, Ferebee R, Luo D, et al. Transparent and High Refractive Index Thermoplastic Polymer Glasses Using Evaporative Ligand Exchange of Hybrid Particle Fillers. ACS Appl Mater Interfaces. 2017;9(8):7515-22.

98. Cheng L, Weir MD, Xu HH, Kraigsley AM, Lin NJ, Lin-Gibson S, et al. Antibacterial and physical properties of calcium-phosphate and calcium-fluoride nanocomposites with chlorhexidine. Dent Mater. 2012;28(5):573-83.

99. Kim S, Jang J, Kim O. Rheological properties of fumed silica filled Bis-GMA dispersions. Polym Eng Sci. 1998;38(7):1142-8.

100. Nihei T. Dental applications for silane coupling agents. J Oral Sci. 2016;58(2):151-5.

101. Arksornnukit M, Takahashi H, Nishiyama N. Effects of silane coupling agent amount on mechanical properties and hydrolytic durability of composite resin after hot water storage. Dent Mater J. 2004;23(1):31-6.

102. Schulze KA, Zaman AA, Söderholm K-JM. Effect of filler fraction on strength, viscosity and porosity of experimental compomer materials. J Dent. 2003;31(6):373-82.

103. Matinlinna JP, Lung CYK, Tsoi JKH. Silane adhesion mechanism in dental applications and surface treatments: A review. Dent Mater. 2018;34(1):13-28.

104. Fuchigami K, Fujimura H, Teramae M, Nakatsuka T. Precision Synthesis of a Long-Chain Silane Coupling Agent Using Micro Flow Reactors and Its Application in Dentistry. Journal of Encapsulation and Adsorption Sciences. 2016;06(01):35-46.

105. Senawongse P, Pongprueksa P. Surface roughness of nanofill and nanohybrid resin composites after polishing and brushing. J Esthet Restor Dent. 2007;19(5):265-73; discussion 74-5.

106. Lutz F, Phillips RW. A classification and evaluation of composite resin

systems. J Prosthet Dent. 1983;50(4):480-8.

107.   Schneider LF, Cavalcante LM, Silikas N. Shrinkage Stresses Generated during Resin-Composite Applications: A Review. J Dent Biomech. 2010;2010.

108.   Randolph LD, Palin WM, Leloup G, Leprince JG. Filler characteristics of modern dental resin composites and their influence on physico-mechanical properties. Dent Mater. 2016;32(12):1586-99.

109.   Kishen A. Nanotechnology in endodontics: Springer; 2016.

110.   Masouras K, Silikas N, Watts DC. Correlation of filler content and elastic properties of resin-composites. Dent Mater. 2008;24(7):932-9.

111.   Goncalves F, Azevedo CL, Ferracane JL, Braga RR. BisGMA/TEGDMA ratio and filler content effects on shrinkage stress. Dent Mater. 2011;27(6):520-6.

112.   Al-Ahdal K, Silikas N, Watts DC. Rheological properties of resin composites according to variations in composition and temperature. Dent Mater. 2014;30(5):517-24.

113.   Metalwala Z, Khoshroo K, Rasoulianboroujeni M, Tahriri M, Johnson A, Baeten J, et al. Rheological properties of contemporary nanohybrid dental resin composites: The influence of preheating. Polym Test. 2018;72:157-63.

114.   Baroudi K, Rodrigues JC. Flowable Resin Composites: A Systematic Review and Clinical Considerations. J Clin Diagn Res. 2015;9(6):ZE18-ZE24.

115.   Bayne SC, Thompson JY, Swift EJJ, Stamatiades P, Wilkerson M. A characterization of first-generation flowable composites. J Am Dent Assoc. 1998;129(5):567-77.

116.   Blalock JS, Holmes RG, Rueggeberg FA. Effect of temperature on unpolymerized composite resin film thickness. J Pros Dent. 2006;96(6):424-32.

117.   Lokhande NA, Padmai AS, Rathore VPS, Shingane S, Jayashankar DN, Sharma U. Effectiveness of flowable resin composite in reducing microleakage - an in vitro study. J Int Oral Health. 2014;6(3):111-4.

118.   Ergücü Z, Türkün LS, Önem E, Güneri P. Comparative Radiopacity of Six Flowable Resin Composites. Oper Dent. 2010;35(4):436-40.

119.   Baroudi K, Saleh AM, Silikas N, Watts DC. Shrinkage behaviour of flowable resin-composites related to conversion and filler-fraction. J Dent. 2007;35(8):651-5.

120.   Miletic V, Pongprueksa P, De Munck J, Brooks NR, Van Meerbeek B. Curing characteristics of flowable and sculptable bulk-fill composites. Clin Oral Invest. 2017;21(4):1201-12.

121.   Garoushi S, Vallittu P, Shinya A, Lassila L. Influence of increment thickness on light transmission, degree of conversion and micro hardness of bulk fill composites. Odontology. 2016;104(3):291-7.

122.   Leprince JG, Palin WM, Vanacker J, Sabbagh J, Devaux J, Leloup G. Physico-mechanical characteristics of commercially available bulk-fill composites. J Dent. 2014;42(8):993-1000.

123.   Jang JH, Park SH, Hwang IN. Polymerization Shrinkage and Depth of Cure of Bulk-Fill Resin Composites and Highly Filled Flowable Resin. Oper Dent. 2014;40(2):172-80.

124.   Gupta R, Tomer AK, Kumari A, Perle N, Chauhan P, Rana S. Recent advances

in bulkfill flowable composite resins: A review. Int J App Dent Sci. 2017;3(3):79-81.

125.   Ilie N, Rencz A, Hickel R. Investigations towards nano-hybrid resin-based composites. Clin Oral Invest. 2013;17(1):185-93.

126.   Kaleem M, Satterthwaite JD, Watts DC. A method for assessing force/work parameters for stickiness of unset resin-composites. Dent Mater. 2011;27(8):805-10.

127.   Al-Sharaa KA, Watts DC. Stickiness prior to setting of some light cured resin-composites. Dent Mater. 2003;19(3):182-7.

128.   Kaleem M, Satterthwaite JD, Watts DC. Effect of filler particle size and morphology on force/work parameters for stickiness of unset resin-composites. Dent Mater. 2009;25(12):1585-92.

129.   Petrovic LM, Zorica DM, Stojanac IL, Krstonosic VS, Hadnadjev MS, Janev MB, et al. Viscoelastic properties of uncured resin composites: Dynamic oscillatory shear test and fractional derivative model. Dent Mater. 2015;31(8):1003-9.

130.   Trujillo M, Newman SM, Stansbury JW. Use of near-IR to monitor the influence of external heating on dental composite photopolymerization. Dent Mater. 2004;20(8):766-77.

131.   Daronch M, Rueggeberg FA, De Goes MF. Monomer Conversion of Pre-heated Composite. J Dent Res. 2005;84(7):663-7.

132.   Daronch M, Rueggeberg FA, Moss L, De Goes MF. Clinically Relevant Issues Related to Preheating Composites. J Esthet Rest Dent. 2006;18(6):340-50.

133.   Oliveira M, Cesar PF, Giannini M, Rueggeberg FA, Rodrigues J, Arrais CA. Effect of Temperature on the Degree of Conversion and Working Time of Dual-Cured Resin Cements Exposed to Different Curing Conditions. Oper Dent. 2012;37(4):370-9.

134.   Daronch M, Rueggeberg FA, Hall G, De Goes MF. Effect of composite temperature on in vitro intrapulpal temperature rise. Dent Mater. 2007;23(10):1283-8.

135.   Nada K, El-Mowafy O. Effect of Precuring Warming on Mechanical Properties of Restorative Composites. Int J Dent. 2011;2011:5.

136.   D'arcangelo C, De Angelis F, Vadini M, D'Amario M. Clinical evaluation on porcelain laminate veneers bonded with light-cured composite: results up to 7 years. Clin Oral Investig. 2012;16(4):1071-9.

137.   Zach L, Cohen G. Pulp response to externally applied heat. Oral Surgery, Oral Medicine, Oral Pathology. 1965;19(4):515-30.

138.   Lohbauer U, Zinelis S, Rahiotis C, Petschelt A, Eliades G. The effect of resin composite pre-heating on monomer conversion and polymerization shrinkage. Dent Mater. 2009;25(4):514-9.

139.   Lempel E, Őri Z, Szalma J, Lovász BV, Kiss A, Tóth Á, et al. Effect of exposure time and pre-heating on the conversion degree of conventional, bulk-fill, fiber reinforced and polyacid-modified resin composites. Dent Mater. 2019;35(2):217-28.

140.   Rueggeberg FA, Daronch M, Browning WD, De Goes MF. In Vivo Temperature Measurement: Tooth Preparation and Restoration with Preheated Resin Composite. J Esthet Restor Dent. 2010;22(5):314-22.

141.   Karacan AO, Ozyurt P. Effect of preheated bulk-fill composite temperature on intrapulpal temperature increase in vitro. J Esthet Rest Dent. 2019;0(0).

142.   Runnacles P, Arrais CAG, Pochapski MT, dos Santos FA, Coelho U, Gomes JC, et al. In vivo temperature rise in anesthetized human pulp during exposure to a polywave LED light curing unit. Dent Mater. 2015;31(5):505-13.

143.   Watts DC, McAndrew R, Lloyd CH. Thermal Diffusivity of Composite Restorative Materials. J Dent Res. 1987;66(10):1576-8.

144.   SonicFill Portfolio of Scientific Research [cited 2019 Mar 5]. [Available from: ftp://ftp.endoco.com/links/KerrSonicFillResearch.pdf.

145.   Goracci C, Cadenaro M, Fontanive L, Giangrosso G, Juloski J, Vichi A, et al. Polymerization efficiency and flexural strength of low-stress restorative composites. Dent Mater. 2014;30(6):688-94.

146.   Didem A, G?zde Yn, Nurhan z. Comparative Mechanical Properties of Bulk-Fill Resins. Open J Compos Mater. 2014;Vol.04No.02:5.

147.   Alrahlah A, Silikas N, Watts DC. Post-cure depth of cure of bulk fill dental resin-composites. Dent Mater. 2014;30(2):149-54.

148.   Kim RJ-Y, Kim Y-J, Choi N-S, Lee I-B. Polymerization shrinkage, modulus, and shrinkage stress related to tooth-restoration interfacial debonding in bulk-fill composites. J Dent. 2015;43(4):430-9.

149.   Ilie N, Bucuta S, Draenert M. Bulk-fill Resin-based Composites: An In Vitro Assessment of Their Mechanical Performance. Oper Dent. 2013;38(6):618-25.

150.   Hirata R, Pacheco RR, Caceres E, Janal MN, Romero MF, Giannini M, et al. Effect of Sonic Resin Composite Delivery on Void Formation Assessed by Micro-computed Tomography. Oper Dent. 2018;43(2):144-50.

151.   Kaleem M, Watts DC. Stiffness of uncured resin-composites assessed via cavity-packing forces. Dent Mater. 2016;32(9):e199-e203.

152.   Nedeljkovic I, Teughels W, De Munck J, Van Meerbeek B, Van Landuyt KL. Is secondary caries with composites a material-based problem? Dent Mater. 2015;31(11):e247-e77.

153.   Hoseney RC, Smewing JO. Instrumental measurement of stickiness of doughs and other foods. J Texture Studies. 2007;30(2):123-36.

154.   Chuang H, Chiu C, Paniagua R. Avery adhesive test yields more performance data than traditional probe. Adhes Age. 1997;40(10):18-23.

155.   Rosentritt M, Buczovsky S, Behr M, Preis V. Laboratory tests for assessing adaptability and stickiness of dental composites. Dent Mater. 2014;30(9):963-7.

156.   Ertl K, Graf A, Watts DC, Schedle A. Stickiness of dental resin composite materials to steel, dentin and bonded dentin. Dent Mater. 2010;26(1):59-66.

157.   Taylor DF, Kalachandra S, Sankarapandian M, McGrath JE. Relationship between filler and matrix resin characteristics and the properties of uncured composite pastes. Biomaterials. 1998;19(1):197-204.

158.   Tyas MJ, Jones DW, Rizkalla AS. The evaluation of resin composite consistency. Dent Mater. 1998;14(6):424-8.

159.   Hahnel S, Henrich A, Bürgers R, Handel G, Rosentritt M. Investigation of Mechanical Properties of Modern Dental Composites After Artificial Aging for One Year. Oper Dent. 2010;35(4):412-9.

160.   De Santis R, Gloria A, Sano H, Amendola E, Prisco D, Mangani F, et al. Effect

of Light Curing and Dark Reaction Phases on the Thermomechanical Properties of a Bis-GMA Based Dental Restorative Material. J Appl Biomater Biom. 2009;7(2):132-40.

161.   Jerri BA. Evaluate polymer degree of conversion of bulk-fill composite restoration. IOSR J Dent Med Sci. 2015;14(9):5.

162.   Aromaa MK, Vallittu PK. Delayed post-curing stage and oxygen inhibition of free-radical polymerization of dimethacrylate resin. Dent Mater. 2018;34(9):1247-52.

163.   Alshali RZ, Silikas N, Satterthwaite JD. Degree of conversion of bulk-fill compared to conventional resin-composites at two time intervals. Dent Mater. 2013;29(9):e213-7.

164.   Moszner N. State of the art: Photopolymerization in dentistry. Research and Developmental IvoclarVivadent. 2013;19:4-10.

165.   Pavlinec J, Moszner N. Dark reactions of free radicals trapped in densely crosslinked polymer networks after photopolymerization. J Appl Polym Sci. 2003;89(3):579-88.

166.   Al-Ahdal K, Ilie N, Silikas N, Watts DC. Polymerization kinetics and impact of post polymerization on the Degree of Conversion of bulk-fill resin-composite at clinically relevant depth. Dent Mater. 2015;31(10):1207-13.

167.   Cidreira Boaro LC, Pereira Lopes D, de Souza ASC, Lie Nakano E, Ayala Perez MD, Pfeifer CS, et al. Clinical performance and chemical-physical properties of bulk fill composites resin —a systematic review and meta-analysis. Dent Mater. 2019;35(10):e249-e64.

168.   Galvão MR, Caldas SGFR, Bagnato VS, de Souza Rastelli AN, de Andrade MF. Evaluation of degree of conversion and hardness of dental composites photo-activated with different light guide tips. Eur J Dent. 2013;7(1):86.

169.   Farahat F, Daneshkazemi A, Hajiahmadi Z. The Effect of Bulk Depth and Irradiation Time on the Surface Hardness and Degree of Cure of Bulk-Fill Composites. J Dent Biomater. 2016;3(3):284-91.

170.   Gallo M, Abouelleil H, Chenal JM, Adrien J, Lachambre J, Colon P, et al. Polymerization shrinkage of resin-based composites for dental restorations: A digital volume correlation study. Dent Mater. 2019;35(11):1654-64.

171.   Sampaio CS, Fernández Arias J, Atria PJ, Cáceres E, Pardo Díaz C, Freitas AZ, et al. Volumetric polymerization shrinkage and its comparison to internal adaptation in bulk fill and conventional composites: A µCT and OCT in vitro analysis. Dent Mater. 2019;35(11):1568-75.

172.   Tantbirojn D, Pfeifer CS, Braga RR, Versluis A. Do Low-shrink Composites Reduce Polymerization Shrinkage Effects? J Dent Res. 2011;90(5):596-601.

173.   Watts DC, Alnazzawi A. Temperature-dependent polymerization shrinkage stress kinetics of resin-composites. Dent Mater. 2014;30(6):654-60.

174.   Braga RR, Koplin C, Yamamoto T, Tyler K, Ferracane JL, Swain MV. Composite polymerization stress as a function of specimen configuration assessed by crack analysis and finite element analysis. Dent Mater. 2013;29(10):1026-33.

175.   Tauböck TT, Tarle Z, Marovic D, Attin T. Pre-heating of high-viscosity bulk-fill resin composites: Effects on shrinkage force and monomer conversion. J Dent. 2015;43(11):1358-64.

176.   Watts DC, Satterthwaite JD. Axial shrinkage-stress depends upon both C-factor and composite mass. Dent Mater. 2008;24(1):1-8.

177.   Watts DC, Marouf AS, Al-Hindi AM. Photo-polymerization shrinkage-stress kinetics in resin-composites: methods development. Dent Mater. 2003;19(1):1-11.

178.   Han S-H, Sadr A, Tagami J, Park S-H. Internal adaptation of resin composites at two configurations: Influence of polymerization shrinkage and stress. Dent Mater. 2016;32(9):1085-94.

179.   Davidson CL, Feilzer AJ. Polymerization shrinkage and polymerization shrinkage stress in polymer-based restoratives. J Dent. 1997;25(6):435-40.

180.   Fronza BM, Makishi P, Sadr A, Shimada Y, Sumi Y, Tagami J, et al. Evaluation of bulk-fill systems: microtensile bond strength and non-destructive imaging of marginal adaptation. Braz Oral Res. 2018;32.

181.   Sampaio CS, Chiu KJ, Farrokhmanesh E, Janal M, Puppin-Rontani RM, Giannini M, et al. Microcomputed Tomography Evaluation of Polymerization Shrinkage of Class I Flowable Resin Composite Restorations. Oper Dent. 2016;42(1):E16-E23.

182.   Jongsma LA, Kleverlaan CJ. Influence of temperature on volumetric shrinkage and contraction stress of dental composites. Dent Mater. 2015;31(6):721-5.

183.   Watts D, Cash A. Kinetic measurements of photo-polymerization contraction in resins and composites. Meas Sci Technol. 1991;2(8):788.

184.   Wang L, Liu Y, Si W, Feng H, Tao Y, Ma Z. Friction and wear behaviors of dental ceramics against natural tooth enamel. J Eur Ceram Soc. 2012;32(11):2599-606.

185.   Ilie N, Hilton TJ, Heintze SD, Hickel R, Watts DC, Silikas N, et al. Academy of Dental Materials guidance-Resin composites: Part I-Mechanical properties. Dent Mater. 2017;33(8):880-94.

186.   Mair L, Stolarski T, Vowles R, Lloyd C. Wear: mechanisms, manifestations and measurement. Report of a workshop. J Dent. 1996;24(1-2):141-8.

187.   Tsujimoto A, Barkmeier WW, Fischer NG, Nojiri K, Nagura Y, Takamizawa T, et al. Wear of resin composites: Current insights into underlying mechanisms, evaluation methods and influential factors. Jpn Dent Sci Rev. 2018;54(2):76-87.

188.   Kawai K, Iwami Y, Ebisu S. Effect of resin monomer composition on toothbrush wear resistance. J Oral Rehabil. 1998;25(4):264-8.

189.   Turssi CP, Ferracane JL, Vogel K. Filler features and their effects on wear and degree of conversion of particulate dental resin composites. Biomaterials. 2005;26(24):4932-7.

190.   Shimokawa CAK, Giannini M, André CB, Sahadi BO, Faraoni JJ, Palma-Dibb RG, et al. In Vitro Evaluation of Surface Properties and Wear Resistance of Conventional and Bulk-fill Resin-based Composites After Brushing With a Dentifrice. Oper Dent. 2019;44(6):637-47.

191.   Pieniak D, Walczak A, Walczak M, Przystupa K, Niewczas AM. Hardness and wear resistance of dental biomedical nanomaterials in a humid environment with non-stationary temperatures. Materials. 2020;13(5):1255.

192.   DeLong R. Intra-oral restorative materials wear: rethinking the current

approaches: how to measure wear. Dent Mater. 2006;22(8):702-11.

193.   Ho TK, Satterthwaite JD, Silikas N. The effect of chewing simulation on surface roughness of resin composite when opposed by zirconia ceramic and lithium disilicate ceramic. Dent Mater. 2018;34(2):e15-e24.

194.   Suzuki T, Kyoizumi H, Araki Y, Finger WJ, Kanehira M. Toothbrush abrasion of resin composites with different filler concepts. World J Dent. 2012;3(2):184-93.

195.   Kakaboura A, Fragouli M, Rahiotis C, Silikas N. Evaluation of surface characteristics of dental composites using profilometry, scanning electron, atomic force microscopy and gloss-meter. J Mater Sci: Mater Med. 2007;18(1):155-63.

196.   O'Neill C, Kreplak L, Rueggeberg FA, Labrie D, Shimokawa CAK, Price RB. Effect of tooth brushing on gloss retention and surface roughness of five bulk-fill resin composites. J Esthet Restor Dent. 2018;30(1):59-69.

197.   Reis AF, Giannini M, Lovadino JR, Ambrosano GM. Effects of various finishing systems on the surface roughness and staining susceptibility of packable composite resins. Dent Mater. 2003;19(1):12-8.

198.   Lemos CAA, Mauro SJ, Briso ALF, de Lima Navarro MF, Fagundes TC. Surface roughness, gloss and color change of different composites after exposure to ultimate challenges. Braz J Oral Sci. 2017:e17077-e.

199.   Rodrigues-Junior SA, Chemin P, Piaia PP, Ferracane JL. Surface Roughness and Gloss of Actual Composites as Polished With Different Polishing Systems. Oper Dent. 2015;40(4):418-29.

200.   El Hejazi AA, Watts DC. Creep and visco-elastic recovery of cured and secondary-cured composites and resin-modified glass-ionomers. Dent Mater. 1999;15(2):138-43.

201.   Odén A, Ruyter IE, Øysɪd H. Creep and recovery of composites for use in posterior teeth during static and dynamic compression. Dent Mater. 1988;4(3):147-50.

202.   El-Safty S, Silikas N, Watts DC. Creep deformation of restorative resin-composites intended for bulk-fill placement. Dent Mater. 2012;28(8):928-35.

203.   Marghalani HY, Watts DC. Viscoelastic stability of resin-composites aged in food-simulating solvents. Dent Mater. 2013;29(9):963-70.

204.   Hirano S, Hirasawa T. Compressive creep and recovery of composite resins with various filler contents in water. Dent Mater J. 1992;11(2):165-76,218.

205.   Baroudi K, Silikas N, Watts DC. Time-dependent visco-elastic creep and recovery of flowable composites. Eur J Oral Sci. 2007;115(6):517-21.

206.   El-Safty S, Silikas N, Watts DC. Temperature-dependence of creep behaviour of dental resin-composites. J Dent. 2013;41(4):287-96.

207.   Abouelleil H, Pradelle N, Villat C, Attik N, Colon P, Grosgogeat B. Comparison of mechanical properties of a new fiber reinforced composite and bulk filling composites. Restor Dent Endod. 2015;40(4):262-70.

208.   El-Safty S, Akhtar R, Silikas N, Watts DC. Nanomechanical properties of dental resin-composites. Dent Mater. 2012;28(12):1292-300.

209.   Badawy R, Aboalazm E. Microhardness of two bulk-fill resin composites. Egypt   Dent J. 2015;61(5573):5582.

210. Moore BK, Platt JA, Borges G, Chu TMG, Katsilieri I. Depth of Cure of Dental Resin Composites: ISO 4049 Depth and Microhardness of Types of Materials and Shades. Oper Dent. 2008;33(4):408-12.

211. Dionysopoulos D, Tolidis K, Gerasimou P. The Effect of Composition, Temperature and Post-Irradiation Curing of Bulk Fill Resin Composites on Polymerization Efficiency. Mater Res. 2016;19:466-73.

212. Germscheid W, de Gorre LG, Sullivan B, O'Neill C, Price RB, Labrie D. Post-curing in dental resin-based composites. Dent Mater. 2018;34(9):1367-77.

213. AlShaafi M. Effects of Different Temperatures and Storage Time on the Degree of Conversion and Microhardness of Resin-based Composites. J Contemp Dent Pract. 2016;17(3):217-23.

214. Sarrett DC. Clinical challenges and the relevance of materials testing for posterior composite restorations. Dent Mater. 2005;21(1):9-20.

215. Ilie N, Hickel R, Valceanu AS, Huth KC. Fracture toughness of dental restorative materials. Clin Oral Invest. 2012;16(2):489-98.

216. Belli R, Wendler M, Zorzin JI, Lohbauer U. Practical and theoretical considerations on the fracture toughness testing of dental restorative materials. Dent Mater. 2018;34(1):97-119.

217. Griffith AA, Taylor GI. VI. The phenomena of rupture and flow in solids. Philos Trans R Soc London. 1921;221(582-593):163-98.

218. Irwin GR. Analysis of stresses and strains near the end of a crack transversing a plate. Trans ASME, Ser E, J Appl Mech. 1957;24:361-4.

219. Yap A, Chung S, Chow W, Tsai K, Lim C. Fracture resistance of compomer and composite restoratives. Oper Dent. 2004;29(1):29-34.

220. Heintze SD, Ilie N, Hickel R, Reis A, Loguercio A, Rousson V. Laboratory mechanical parameters of composite resins and their relation to fractures and wear in clinical trials—A systematic review. Dent Mater. 2017;33(3):e101-e14.

221. Alshabib A, Silikas N, Watts DC. Hardness and fracture toughness of resin-composite materials with and without fibers. Dent Mater. 2019;35(8):1194-203.

222. Hegde V, Sali AV. Fracture resistance of posterior teeth restored with high-viscosity bulk-fill resin composites in comparison to the incremental placement technique. J Conserv Dent. 2017;20(5):360-4.

223. Lloyd CH, Iannetta RV. The fracture toughness of dental composites I. The development of strength and fracture toughness. J Oral Rehabil. 1982;9(1):55-66.

224. Kim K-H, Park J-H, Imai Y, Kishi T. Fracture toughness and acoustic emission behavior of dental composite resins. Eng Fract Mech. 1991;40(4):811-9.

225. Curtis AR, Shortall AC, Marquis PM, Palin WM. Water uptake and strength characteristics of a nanofilled resin-based composite. J Dent. 2008;36(3):186-93.

226. Fujishima A, Ferracane JL. Comparison of four modes of fracture toughness testing for dental composites. Dent Mater. 1996;12(1):38-43.

227. TPH Spectra Universal Composite Restorative Science EN [cited 2019 Aug 3]. [Available from: https://www.dentsplysirona.com/content/dam/dentsply/pim/manufacturer/Restora

tive/Direct_Restoration/Composites__Flowables/Universal_Composites/TPH_Spectr
a_Universal_Composite_Restorative/TPH-Spectra-xnzlfpn-en-us-1402.

228.	Watts DC. Elastic moduli and visco-elastic relaxation. J Dent. 1994;22(3):154-8.

229.	Demarco FF, Corrêa MB, Cenci MS, Moraes RR, Opdam NJM. Longevity of posterior composite restorations: Not only a matter of materials. Dent Mater. 2012;28(1):87-101.

230.	Wagner W, Aksu M, Neme A, Linger J, Pink F, Walker S. Effect of pre-heating resin composite on restoration microleakage. Oper Dent. 2008;33(1):72-8.

231.	Da Costa JB, Hilton TJ, Swift JEJ. Preheating Composites. J Esthet Rest Dent. 2011;23(4):269-75.

232.	Al-Qudah AA, Mitchell CA, Biagioni PA, Hussey DL. Thermographic investigation of contemporary resin-containing dental materials. J Dent. 2005;33(7):593-602.

233.	Judeinstein P, Sanchez C. Hybrid organic–inorganic materials: a land of multidisciplinarity. J Mater Chem. 1996;6(4):511-25.

234.	Scientific Compendium: Admira Fusion [cited 2019 Aug 13]. [Available from: http://212.227.148.121/e-paper/scientific_compendium/admira-fusion_en/.

235.	Kalachandra S, Sankarapandian M, Shobha HK, Taylor DF, McGrath JE. Influence of hydrogen bonding on properties of BIS-GMA analogues. J Mats Sci: Mater in Med. 1997;8(5):283-6.

236.	Tetric EvoCeram Instructions for Use [cited 2019 Aug 13]. [Available from: http://downloads.ivoclarvivadent.com/zoolu-website/media/document/827/Tetric+EvoCeram.

237.	Filtek Supreme Ultra Technical Product Profile [cited 2019 Aug 13]. [Available from: http://multimedia.3m.com/mws/media/629066O/filtektm-supreme-ultra-universal-restorative.pdf.

238.	Uctasli MB, Arisu HD, Lasilla LV, Valittu PK. Effect of preheating on the mechanical properties of resin composites. Eur J Dent. 2008;2(4):263-8.

239.	Watts DC, Schneider LFJ, Marghalani HY. Bond-Disruptive Stresses Generated by Resin Composite Polymerization in Dental Cavities. J Adhes Sci Tech. 2009;23(7-8):1023-42.

240.	Chen M-H, Chen C-R, Hsu S-H, Sun S-P, Su W-F. Low shrinkage light curable nanocomposite for dental restorative material. Dent Mater. 2006;22(2):138-45.

241.	Loguercio AD, Reis A, Ballester RY. Polymerization shrinkage: effects of constraint and filling technique in composite restorations. Dent Mater. 2004;20(3):236-43.

242.	Chesterman J, Jowett A, Gallacher A, Nixon P. Bulk-fill resin-based composite restorative materials: a review. Br Dent J. 2017;222(5):337-44.

243.	Yang J, Silikas N, Watts DC. Pre-heating effects on extrusion force, stickiness and packability of resin-based composite. Dent Mater. 2019;35(11):1594-602.

244.	Wang R, Liu H, Wang Y. Different depth-related polymerization kinetics of dual-cure, bulk-fill composites. Dent Mater. 2019;35(8):1095-103.

245.	Sirovica S, Guo Y, Guan R, Skoda MWA, Palin WM, Morrell AP, et al. Photo-

polymerisation variables influence the structure and subsequent thermal response of dental resin matrices. Dent Mater. 2020;36(3):343-52.

246.   Guo X, Wang Y, Spencer P, Ye Q, Yao X. Effects of water content and initiator composition on photopolymerization of a model BisGMA/HEMA resin. Dent Mater. 2008;24(6):824-31.

247.   Palin WM, Fleming GJP, Trevor Burke FJ, Marquis PM, Randall RC. Monomer conversion versus flexure strength of a novel dental composite. J Dent. 2003;31(5):341-51.

248.   Eliades GC, Vougiouklakis GJ, Caputo AA. Degree of double bond conversion in light-cured composites. Dent Mater. 1987;3(1):19-25.

249.   Frauscher KE, Ilie N. Degree of conversion of nano-hybrid resin-based composites with novel and conventional matrix formulation. Clin Oral Invest. 2013;17(2):635-42.

250.   Atai M, Ahmadi M, Babanzadeh S, Watts DC. Synthesis, characterization, shrinkage and curing kinetics of a new low-shrinkage urethane dimethacrylate monomer for dental applications. Dent Mater. 2007;23(8):1030-41.

251.   Atai M, Watts DC, Atai Z. Shrinkage strain-rates of dental resin-monomer and composite systems. Biomaterials. 2005;26(24):5015-20.

252.   Dewaele M, Truffier-Boutry D, Devaux J, Leloup G. Volume contraction in photocured dental resins: The shrinkage-conversion relationship revisited. Dent Mater. 2006;22(4):359-65.

253.   Labella R, Lambrechts P, Van Meerbeek B, Vanherle G. Polymerization shrinkage and elasticity of flowable composites and filled adhesives. Dent Mater. 1999;15(2):128-37.

254.   Watts DC, Amer OM, Combe EC. Surface hardness development in light-cured composites. Dent Mater. 1987;3(5):265-9.

255.   Marghalani HY. Post-irradiation vickers microhardness development of novel resin composites. Mater Res. 2010;13:81-7.

256.   Alshali RZ, Salim NA, Satterthwaite JD, Silikas N. Post-irradiation hardness development, chemical softening, and thermal stability of bulk-fill and conventional resin-composites. J Dent. 2015;43(2):209-18.

257.   Munoz CA, Bond PR, Sy-Munoz J, Tan D, Peterson J. Effect of pre-heating on depth of cure and surface hardness of light-polymerized resin composites. Am J Dent. 2008;21(4):215-22.

258.   da Costa J, Adams-Belusko A, Riley K, Ferracane JL. The effect of various dentifrices on surface roughness and gloss of resin composites. J Dent. 2010;38:e123-e8.

259.   Han J-m, Zhang H, Choe H-S, Lin H, Zheng G, Hong G. Abrasive wear and surface roughness of contemporary dental composite resin. Dent Mater J. 2014;33(6):725-32.

260.   Pişkin Mehmet B, Atalı Pınar Y, Figen Aysel K. Thermal, spectral, and surface properties of LED light-polymerized bulk fill resin composites. Biomed Eng-Biomed Tech. 2015;60(1):65.

261.   Magdy NM, Kola MZ, Alqahtani HH, Alqahtani MD, Alghmlas AS. Evaluation

of Surface Roughness of Different Direct Resin-based Composites. J Int Soc Prev Community Dent. 2017;7(3):104-9.

262.   Rigo LC, Bordin D, Fardin VP, Coelho PG, Bromage TG, Reis A, et al. Influence of Polishing System on the Surface Roughness of Flowable and Regular-Viscosity Bulk Fill Composites. Int J Periodontics Restorative Dent. 2018;38(4):e79-e86.

263.   Costa JD, Ferracane J, Paravina RD, Mazur RF, Roeder L. The Effect of Different Polishing Systems on Surface Roughness and Gloss of Various Resin Composites. J Esthet Restor Dent. 2007;19(4):214-24.

264.   Takahashi R, Jin J, Nikaido T, Tagami J, Hickel R, Kunzelmann K-H. Surface characterization of current composites after toothbrush abrasion. Dent Mater J. 2013;32(1):75-82.

265.   Bollenl CML, Lambrechts P, Quirynen M. Comparison of surface roughness of oral hard materials to the threshold surface roughness for bacterial plaque retention: A review of the literature. Dent Mater. 1997;13(4):258-69.

266.   Jones CS, Billington RW, Pearson GJ. The in vivo perception of roughness of restorations. Br Dent J. 2004;196(1):42-5.

267.   Jefferies SR. Abrasive finishing and polishing in restorative dentistry: a state-of-the-art review. Dent Clin North Am. 2007;51(2):379-97, ix.

268.   Kaminedi RR, Penumatsa NV, Priya T, Baroudi K. The influence of finishing/polishing time and cooling system on surface roughness and microhardness of two different types of composite resin restorations. J Int Soc Prev Community Dent. 2014;4(Suppl 2):S99.

269.   Endo T, Finger WJ, Kanehira M, Utterodt A, Komatsu M. Surface texture and roughness of polished nanofill and nanohybrid resin composites. Dent Mater J. 2010;29(2):213-23.

270.   Suzuki T, Kyoizumi H, Finger WJ, Kanehira M, Endo T, Utterodt A, et al. Resistance of nanofill and nanohybrid resin composites to toothbrush abrasion with calcium carbonate slurry. Dent Mater J. 2009;28(6):708-16.

271.   Heintze SD, Forjanic M, Rousson V. Surface roughness and gloss of dental materials as a function of force and polishing time in vitro. Dent Mater. 2006;22(2):146-65.

272.   Kon M, Kakuta K, Ogura H. Effects of Occlusal and Brushing Forces on Wear of Composite Resins. Dent Mater J. 2006;25(1):183-94.

273.   Wang L, Garcia FCP, De AraÚJo PA, Franco EB, Mondelli RFL. Wear Resistance of Packable Resin Composites after Simulated Toothbrushing Test. J Esthet Restor Dent. 2004;16(5):303-14.

274.   Wiegand A, Kuhn M, Sener B, Roos M, Attin T. Abrasion of eroded dentin caused by toothpaste slurries of different abrasivity and toothbrushes of different filament diameter. J Dent. 2009;37(6):480-4.

275.   Tellefsen G, Liljeborg A, Johannsen A, Johannsen G. The role of the toothbrush in the abrasion process. Int J Dent Hyg. 2011;9(4):284-90.

276.   Alrahlah A, Khan R, Alotaibi K, Almutawa Z, Fouad H, Elsharawy M, et al. Simultaneous Evaluation of Creep Deformation and Recovery of Bulk-Fill Dental Composites Immersed in Food-Simulating Liquids. Materials. 2018;11(7).

277.   Vaidyanathan J, Vaidyanathan TK. Flexural creep deformation and recovery in dental composites. J Dent. 2001;29(8):545-51.

278.   Didron PP, Ellakwa A, Swain MV. Effect of preheat temperatures on mechanical properties and polymerization contraction stress of dental composites. Materials Sciences and Applications. 2013;4(06):374.

279.   El-Safty S, Silikas N, Akhtar R, Watts DC. Nanoindentation creep versus bulk compressive creep of dental resin-composites. Dent Mater. 2012;28(11):1171-82.

280.   Marghalani HY, Al-jabab AS. Compressive creep and recovery of light-cured packable composite resins. Dent Mater. 2004;20(6):600-10.

281.   Cock DJ, Watts DC. Time-dependent Deformation of Composite Restorative Materials in Compression. J Dent Res. 1985;64(2):147-50.

282.   Papadogiannis DY, Lakes RS, Papadogiannis Y, Palaghias G, Helvatjoglu-Antoniades M. The effect of temperature on the viscoelastic properties of nano-hybrid composites. Dent Mater. 2008;24(2):257-66.

283.   Ruyter IE, Øysæd H. Compressive creep of light cured resin based restorative materials. Acta Odontol Scand. 1982;40(5):319-24.

284.   Alamoush RA, Satterthwaite JD, Silikas N, Watts DC. Viscoelastic stability of pre-cured resin-composite CAD/CAM structures. Dent Mater. 2019;35(8):1166-72.

285.   Rosatto CMP, Bicalho AA, Veríssimo C, Bragança GF, Rodrigues MP, Tantbirojn D, et al. Mechanical properties, shrinkage stress, cuspal strain and fracture resistance of molars restored with bulk-fill composites and incremental filling technique. J Dent. 2015;43(12):1519-28.

286.   Skalskyi V, Makeev V, Stankevych O, Dubytskyi O. Acoustic properties of fracture of dental restorative materials and endocrown restorations under quasi-static loading. Dent Mater. 2020;36(5):617-25.

287.   Al-Shayea NA, Khan K, Abduljauwad SN. Effects of confining pressure and temperature on mixed-mode (I–II) fracture toughness of a limestone rock. Int J Rock Mech Min Sci. 2000;37(4):629-43.

288.   Ilie N. Sufficiency of curing in high-viscosity bulk-fill resin composites with enhanced opacity. Clin Oral Invest. 2019;23(2):747-55.

289.   Astm E. 399-90: Standard test method for plane-strain fracture toughness of metallic materials. Annu Book ASTM Stand. 1997;3(01):506-36.

290.   Yang J, Silikas N, Watts DC. Pre-heating time and exposure duration: Effects on post-irradiation properties of a thermo-viscous resin-composite. Dent Mater. 2020;36(6):787-93.

291.   Tsujimoto A, Barkmeier WW, Takamizawa T, Latta MA, Miyazaki M. Depth of cure, flexural properties and volumetric shrinkage of low and high viscosity bulk-fill giomers and resin composites. Dent Mater J. 2017;advpub.

292.   Kleverlaan CJ, Feilzer AJ. Polymerization shrinkage and contraction stress of dental resin composites. Dent Mater. 2005;21(12):1150-7.

293.   Stansbury JW. Dimethacrylate network formation and polymer property evolution as determined by the selection of monomers and curing conditions. Dent Mater. 2012;28(1):13-22.

294.   Wang R, Wang Y. Depth-dependence of Degree of Conversion and

Microhardness for Dual-cure and Light-cure Composites. Oper Dent. 2019.

295.   Ilie N, Fleming GJP. In vitro comparison of polymerisation kinetics and the micro-mechanical properties of low and high viscosity giomers and RBC materials. J Dent. 2015;43(7):814-22.

296.   Johnson WW, Dhuru VB, Brantley WA. Composite microfiller content and its effect on fracture toughness and diametral tensile strength. Dent Mater. 1993;9(2):95-8.

297.   Lloyd CH. The fracture toughness of dental composites II. The environmental and temperature dependence of the stress intensification factor (K_{IC}). J Oral Rehabil. 1982;9(2):133-8.

Appendices

Appendix 1: Publication 1 (Dental Materials 2019;35(11):1594-602)

Available online at www.sciencedirect.com

ScienceDirect

ELSEVIER

journal homepage: www.intl.elsevierhealth.com/journals/dema

Pre-heating effects on extrusion force, stickiness and packability of resin-based composite

Jiawei Yang[a], *Nikolaos Silikas*[a,*], *David C. Watts*[a,b,*]

[a] *Dentistry, School of Medical Sciences, University of Manchester, Manchester, UK*
[b] *Photon Science Institute, University of Manchester, Manchester, UK*

ARTICLE INFO

ABSTRACT

Objectives. To measure temperature effects on stickiness and packability of representative resin-based composites and the effect of pre-heating time on pre-cure properties of *Viscalor*, including extrusion force.

Methods. Five resin-based composites (RBC) and an additional RBC, *Viscalor*, used with a Caps Warmer (VOCO, Germany) were studied. The extrusion force (N) and extruded mass (g) were measured from *Viscalor* compules heated in T3 mode for 30 s (T3-30 s) and 3 min (T3-3 min). For stickiness and packability measurements, RBCs were packed into a brass cylindrical cavity controlled at 22 and 37 °C. A flat-ended probe was lowered into the RBC pastes at constant speed. Stickiness: F_{max} (N) and W_s (N mm), and packability: F_P (N), were measured. *Viscalor* was LED photo-cured at 1200 mW/cm^2 for 40 s. The degrees of conversion at 5 min and 24 h post cure (DC_{5min} and DC_{24h}) of *Viscalor* (no heat, T3-30 s and T3-3 min) were measured by ATR-FTIR. Data were analysed by one-way ANOVA, independent t-test and Tukey post-hoc tests ($p < 0.05$).

Results. The maximum temperature of the Caps Warmer, in T3 mode, reached 68 °C in 20 min. *Viscalor* temperatures of 34.5 °C and 60.6 °C were recorded after 30 s and 3 min pre-heating, respectively. Pre-heating significantly reduced extrusion force and increased extruded mass, especially after 3 min. RBCs varied in F_{max}, W_s and F_P ($p < 0.05$). Temperature also affected F_{max} ($p = 0.000$), W_s ($p = 0.002$) and F_P ($p = 0.000$). Pre-heating *Viscalor* for either 30 s or 3 min did not increase the post-cure DC at either 5 min or 24 h, relative to no pre-heating ($p > 0.05$).

Significance. The composites varied to an extent in stickiness and packability but the overall magnitudes remained within a clinically acceptable range. Pre-heating was beneficial in placement of *Viscalor* and caused no adverse effects through premature polymerization.

© 2019 The Academy of Dental Materials. Published by Elsevier Inc. All rights reserved.

1. Introduction

Resin-based composites (RBCs) are designed and manipulated with suitable esthetic and physico-chemical properties to match the tooth structure. They can be fabricated in a range of consistencies and are therefore widely used as direct restorative materials in dentistry [1–3]. The maximum obtained properties and longevity of composites are dependent on the clinician's skill level and operating conditions [4,5]. Thus, 'technique sensitivity' should be reduced for good marginal integrity and successful restoration [6]. To avoid the formation

Table 1 – Manufacturer information of investigated composites.

	Code	Manufacturer	Resin system	Filler vol.%	Filler wt.%
Admira Fusion	AF	VOCO, Cuxhaven Germany	ORMOCER®	–	84
Filtek Supreme Ultra	FSU	3M ESPE, St. Paul, USA	bis-GMA, UDMA, TEGDMA, bis-EMA	63.3	78.5
TPH LV	TPH	Dentsply, Germany	Urethane modified bis-GMA, TEGDMA, polymerizable dimethacrylate	54.6	75.5
Tetric EvoCeram	TEC	Ivoclar Vivadent, USA	bis-GMA, urethane dimethacrylate, bis-EMA	54	75
Harmonize	HZ	Kerr, USA	bis-GMA, bis-EMA, TEGDMA	64.5	81
Viscalor	VC	VOCO, Cuxhaven Germany	bis-GMA, aliphatic dimethacrylate	–	83

of voids and gaps, both insertion technique and adaptation of composites need improvement [4]. The successful clinical handling and placement mainly depends on suitable pre-cure properties of composites that are determined by material composition and viscosity [7].

Pre-cure handling properties, such as flowability, stickiness, ease of placement and adaptation to cavity walls affect product selection for clinical restoration [8,9]. Stickiness - the adhesion force between two contacted surfaces - has been studied previously [8,10–12]. In a related field, the Avery Adhesive Test (AAT) with a spherical probe was used to study pressure-sensitive adhesives (PSA) [13]. In 2003, a method was reported using a flat-ended stainless-steel probe [8,10]. Clinically, the relationship between stickiness to tooth cavity and stickiness to instruments should be well balanced [8,10,14]. High stickiness to instruments may result in difficult placement and more porosities/gaps may occur during restoration [8,10]. RBCs with adequate consistency and packability are important for adapting to the tooth cavity and optimizing approximal contact areas [10,15]. Tyas et al. designed a method to assess consistency of unset composites [10,15]. They placed materials in an 8 mm × 8 mm cylindrical mould and pressed with a flat-ended glass rod demonstrating the high consistency of RBCs with increased filler content [9,15].

RBCs exhibit both viscous and elastic properties against the applied force and the rheological nature of pre-cure RBCs affects their handling properties [8,10]. Viscosity directly relates to material's handling properties, operating time and quality of restoration [10,14,16,17]. Viscosity decreases with temperature according to the Arrhenius Equation:

$$\eta = Ae^{E_a/RT}$$

where η, A, E_a, R and T represent viscosity, pre-exponential factor, activation energy for flow, universal gas constant and absolute temperature, respectively [16]. Viscosity also tends to increase exponentially with filler content [8,17].

Bis-GMA has higher viscosity than other dimethacrylates, resulting in low degree of conversion (DC) and requiring diluent monomers to facilitate filler particle incorporation [2,18–22]. High viscosity of highly-filled RBCs may cause insufficient adaptation to the cavity preparation, poor marginal integrity, and final restoration failure [23].

There are several possible strategies to achieve good cavity adaptation via reduced viscosity. Ideally, materials should flow into every corner of the cavity but not flow after removing the applied force [8,10]. High viscous RBC pastes are hard to extrude from the syringe or compule, which may lead to

macroscopic voids/porosities during manipulation [8,16,23] and this was a major reason for developing flowable composites [24–26].

The SonicFill system (Kerr, USA), contains a highly-filled resin matrix including special viscosity modifiers that respond to ultrasonic energy (UE) and reduce the viscosity by 87%. Once UE is stopped, the viscosity returns to high levels, suitable for carving and contouring [27].

Several studies have evaluated pre-heating RBCs before placement [25,28,29]. Pre-heating makes highly-packed RBCs more fluid and easier to manipulate, without compromising their superior mechanical properties [30]. But after pre-heating the elevated temperature may cause thermal damage to the pulp [31]. The pulp has a normal temperature of 34–35 °C, and with temperature increases ranging from 5.5 to 16 °C, the possibility of pulp necrosis may increase from 15% to 100% [32].

Existing pre-heating devices, such as Calset heater (AdDent Inc., Danbury, CT, USA) and ENA heat (Micerium, Avegno, Italy), have operating temperature ranges of 37–68 °C [7,26,32–34].

A new pre-heating RBC, *Viscalor*, has been designed for use with a *Caps Warmer* device (VOCO, Germany). This has three working modes (T1, T2 and T3) to cover the temperature range 37–68 °C. The objectives of this study were to measure pre-cure properties including stickiness and packability of representative RBCs at different temperatures, and determine the effect of pre-heating time on pre-cure properties of *Viscalor*, including extrusion forces. The Null Hypotheses were: (1) composites did not vary in stickiness and packability at different temperatures, and (2) pre-heating period had no effect on *Viscalor*'s post-cure DC% measured at either 5 min or 24 h.

2. Materials and methods

Five commercial RBCs and an additional RBC: *Viscalor* used with a Caps Warmer (VOCO, Germany), were studied. The manufacturers' information is shown in Table 1.

A type-K thermocouple was inserted into the Caps Warmer (Fig. S1) to characterize its temperature profile in T3 mode. When it reached its maximum temperature, *Viscalor* compules were put into the Caps Warmer for 30 s and 3 min pre-heating times. Temperature was measured via a type-K thermocouple inside the compule. After pre-heating, the compule was removed from the Caps Warmer.

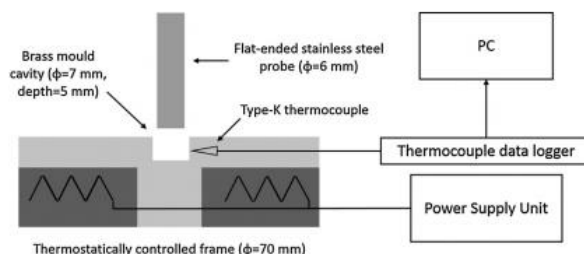The extrusion force (N) of *Viscalor* from both full and half-full compules was measured using a modified com-

Fig. 1 – Mold setup with temperature regulation.

pule dispenser and a universal testing machine (Zwick/ Roell Z020, Leominster, UK) (Fig. S2). Viscalor was pre-heated before measurement using the Caps Warmer in T3 mode for 30 s (T3-30 s) and 3 min (T3-3 min). Compressive force was applied at 1 mm/s until either an upper force limit of 150 N or the maximum extrusion distance of 10 mm was reached (n = 3). The mass of extruded composite (g) was also measured.

A Texture Analyzer (Fig. S3) (TA.XT2i, Stable Micro Systems, Godalming, UK) was used to measure stickiness: via maximum separation force (F_{max}, N) and work of probe-separation (W_s, N mm), and packability: maximum packing force (F_p, N). Force was applied to a flat-ended cylindrical stainless-steel probe ($\varphi = 6$ mm). A thermostatically controlled mold at 22 °C and 37 °C with a cylindrical cavity ($\phi = 7$ mm, depth = 5 mm) was fixed to a stand (Fig. 1). Composite paste was carefully packed into the cavity (n = 5).

For stickiness measurement, during the 'bonding' phase, the probe was lowered into the surface of unset composite with a pre-test speed of 0.50 mm/s. When a 'trigger' force of 0.05 N was registered, data acquisition commenced at rate of 400 p/s until a compressive force of 1 N was recorded, and held constant for 1 s. In the subsequent 'debonding' phase, the probe was raised vertically at 2 mm/s. Since the unset composite paste adhered to the probe, it elongated and exerted a tensile force as the probe ascended. With further elongation, tensile stress increased until it reached the interfacial strength and the composite paste separated from the probe.

Packability measurement used a similar experimental setup. Before measurement, the probe position was set 10 mm above the cavity. The probe was lowered into the surface of unset composite at 0.50 mm/s. When a 'trigger' force of 0.05 N was registered, data acquisition commenced until the probe penetrated 2 mm. Then the probe ascended vertically at 2 mm/s.

Fourier Transform Infrared (FTIR) Spectroscopy with an attenuated total reflectance (ATR) device (ALPHA II FTIR Spectrometer, Bruker Optik GmbH) was used to measure the DC% of Viscalor syringe/compule (no heat, T3-30 s and T3-3 min) at 5 min and 24 h post-cure. A background reading was collected between 400 to 4000 cm^{-1} using 32 scans at a resolution of 4 cm^{-1}. Composite paste was placed in an acetal mold (4 mm diameter x 2 mm thickness) directly on top of the ATR crystal. A Mylar strip and a glass slide were pressed onto the mold to remove air bubbles and excess paste. The spectrum
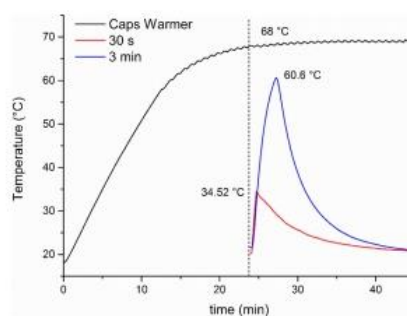

Fig. 2 – Representative temperature/time profiles of Caps Warmer (T3 mode) and Viscalor following pre-heating for different time periods.

of uncured Viscalor was collected. Photo-cure was achieved using an Elipar S10 LED unit (3 M ESPE, USA) of mean irradiance 1200 mW/cm^2 for 40 s at zero distance from the top surface. Then the spectrophotometer's screw was applied to fix the cured specimen tightly on the reading crystal. The spectrum of the 5 min post-cured composite was collected. Then the spectra were acquired continually in real time for 24 h to obtain DC% at 24 h post-cure.

The spectral region between 1600–1700 cm^{-1} was selected to identify the heights of the aliphatic C = C absorbance peak at 1637 cm^{-1} and the aromatic C = C absorbance peak at 1608 cm^{-1}. The DC% was calculated as:

$$DC\% = 1 - \frac{(H_{1637\,cm^{-1}}/H_{1608\,cm^{-1}})_{cured}}{(H_{1637\,cm^{-1}}/H_{1608\,cm^{-1}})_{uncured}} \times 100\%$$

where $H_{1637\,cm^{-1}}$ is the height of aliphatic C = C peak, $H_{1608\,cm^{-1}}$ is the height of aromatic C = C peak, respectively.

Data were entered into statistical software (SPSS, SPSS Inc., Illinois, USA) and analysed using one-way ANOVA test, independent t-test and Tukey post-hoc tests (p < 0.05). Homogeneity of variables was calculated using the Kruskal-Wallis Test (p < 0.05).

Table 2 – Extrusion force (N) and the mass of extruded composite (g) of new/half-used *Viscalor* compule (no heat, T3-30 s and T3-3 min).

Materials	Force (N)		Mass (g)	
	New	Half-used	New	Half-used
Viscalor (no heat)	153.62[a A] (1.56)	152.40[a A] (2.38)	0.0055[a B] (0.00)	0.0134[a C] (0.00)
Viscalor (T3-30 s)	145.45[a A] (8.15)	150.59[a A] (0.36)	0.1028[b B] (0.04)	0.2261[b C] (0.01)
Viscalor (T3-3 min)	66.49[b A] (14.16)	51.29[b A] (11.93)	0.1756[b B] (0.04)	0.2834[c C] (0.02)

For each material, same lower case superscript letters indicate homogeneous subsets among the materials. For each measurement (F, m), same capital superscript letters indicate homogeneous subsets among different conditions (new, half-used).
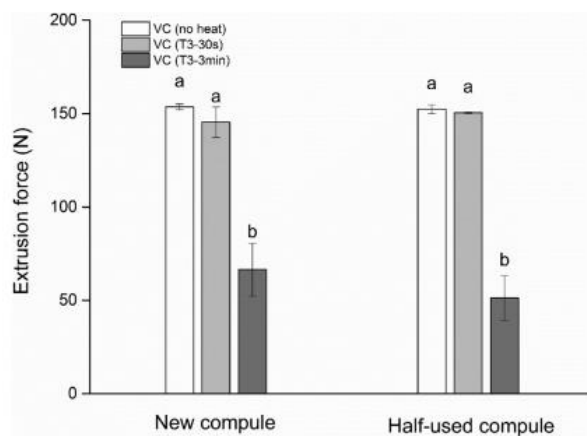
Fig. 3 – Extrusion force (N) of new/half-used *Viscalor* compule (no heat, T3-30 s and T3-3 min).
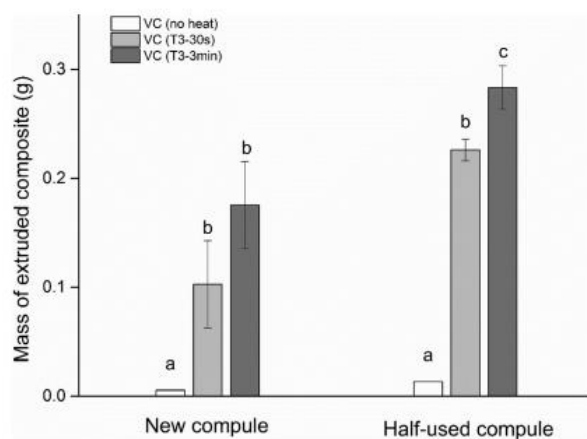
Fig. 4 – Mass of extruded composite (g) of new/half-used *Viscalor* compule (no heat, T3-30 s and T3-3 min).

Fig. 5 – Maximum separation force (F_{max}) of investigated composites at 22 and 37 °C.

Fig. 6 – Work of probe-separation (W_s) of investigated composites at 22 and 37 °C.

3. Results

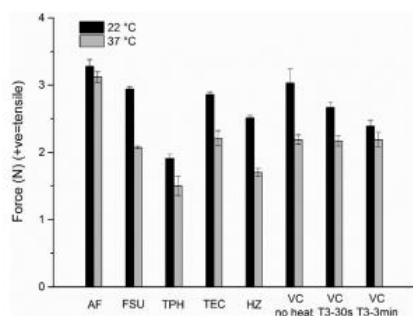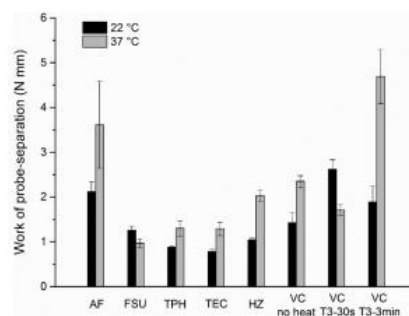Fig. 2 shows representative temperature/time profiles of the Caps Warmer in T3 mode and the Viscalor temperatures following different pre-heating times. The Caps Warmer in T3 mode reached 68 °C after ca. 20 min. Composite temperature increases of 14.3 °C and 39.1 °C were recorded after 30 s and 3 min pre-heating, respectively. After removed from the Caps Warmer, composite temperature gradually returned to ambient temperature.

The extrusion force (N) and extruded mass (g) of full or half-full Viscalor compules (for no heat, T3-30s and T3-3 min) are shown in Table 2 and Figs. 3 and 4. The extrusion force varied with pre-heating conditions, with 3 min heating giving the lowest extrusion force (p = 0.000). Partial usage of the compule had no significant influence on the measured extrusion force (p = 0.866). Viscalor compules with no heating yielded the lowest mass of extruded composite (p = 0.000). Half-used Viscalor compules (no heat, T3-30s and T3-3 min) showed slightly higher extruded mass, in a fixed period, than full compules (p < 0.05).

Table. 3 and Figs. 5–7 show stickiness (F_{max} and W_s) and packability (F_P) data for different composites at 22 and 37 °C. F_{max}, W_s and F_P ranged from 1.50 to 3.28 N, from 0.79 to 4.69 N mm and from 10.79 to 41.56 N, respectively. Different RBCs varied in F_{max} (p = 0.000), W_s (p = 0.000) and F_P (p = 0.032). Temperature also had a significant effect on F_{max} (p = 0.000), W_s (p = 0.002) and F_P (p = 0.000), for which temperature rise reduced F_{max} and F_P, but increased W_s.

Fig. 8 represents real-time DC% vs. time during 24 h post-polymerization of Viscalor syringe/compule (no heat, T3-30s and T3-3 min). Real-time DC% curves of Viscalor syringe and compule develop over 24 h with a similar trend. Table 4 and Fig. 9 report the DC% at 5 min and 24 h post-cure (DC_{5min} and DC_{24h}) of Viscalor syringe/compule (no heat, T3-30s and T3-3 min). After 24 h, DC% increased to approximately 60%. There were no significant differences in DC% results between syringe and compule (p > 0.05). Pre-cure heating of Viscalor syringe/compule for either 30 s or 3 min in a 68 °C Caps
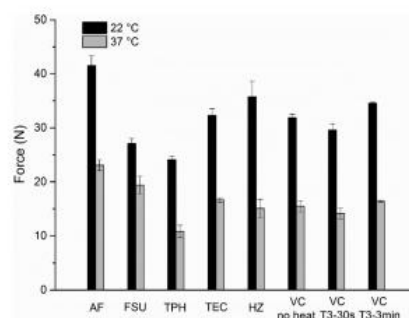

Fig. 7 – Maximum packing force (F_p) of investigated composites at 22 and 37 °C.
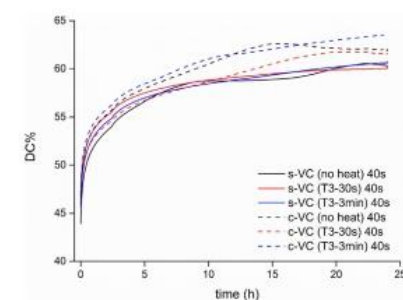

Fig. 8 – Real-time DC% vs. time during 24 h post-polymerization for Viscalor syringe/compule (no heat, T3-30 s, T3-3 min).

Table 3 – Stickiness parameters: F_{max} (N) and W_s (N mm), and packability, F_p (N) at 22 and 37 °C.

Materials	F_{max} (N)		W_s (N mm)		F_p (N)	
	22 °C	37 °C	22 °C	37 °C	22 °C	37 °C
Admira Fusion	3.28$^{f\,A}$ (0.10)	3.12$^{d\,A}$ (0.08)	2.12$^{d\,A}$ (0.22)	3.61$^{d\,A}$ (0.97)	41.56$^{f\,C}$ (1.77)	23.09$^{e\,B}$ (1.00)
Filtek Supreme Ultra	2.94$^{e\,B}$ (0.04)	2.07$^{c\,A,B}$ (0.02)	1.26$^{b,c\,A}$ (0.09)	0.97$^{a\,A}$ (0.09)	27.11$^{b\,D}$ (0.91)	19.40$^{d\,C}$ (1.66)
TPH LV	1.91$^{a\,A}$ (0.06)	1.50$^{a\,A}$ (0.14)	0.88$^{a,b\,A}$ (0.03)	1.30$^{a,b\,A}$ (0.17)	24.10$^{a\,C}$ (0.62)	10.79$^{a\,B}$ (1.14)
Tetric EvoCeram	2.86$^{d,e\,C}$ (0.04)	2.21$^{c\,B,C}$ (0.11)	0.79$^{a\,A}$ (0.06)	1.29$^{a,b\,A,B}$ (0.15)	32.30$^{c,d\,E}$ (1.24)	16.64$^{c\,D}$ (0.40)
Harmonize	2.51$^{b,c\,A}$ (0.04)	1.70$^{b\,A}$ (0.06)	1.04$^{a,b,c\,A}$ (0.04)	2.03$^{c\,A}$ (0.13)	35.75$^{e\,C}$ (2.86)	15.08$^{b,c\,B}$ (1.68)
Viscalor (no heat)	3.03$^{e\,B}$ (0.21)	2.19$^{c\,A,B}$ (0.07)	1.42$^{c\,A}$ (0.23)	2.35$^{c\,A,B}$ (0.13)	31.88$^{c,d\,D}$ (0.66)	15.46$^{b,c\,C}$ (1.01)
Viscalor (T3-30 s)	2.67$^{c,d\,A}$ (0.08)	2.17$^{c\,A}$ (0.08)	2.62$^{e\,A}$ (0.21)	1.71$^{b,c\,A}$ (0.12)	29.58$^{b,c\,C}$ (1.18)	14.13$^{b\,B}$ (0.99)
Viscalor (T3-3 min)	2.39$^{b\,A}$ (0.09)	2.19$^{c\,A}$ (0.11)	1.89$^{d\,A}$ (0.36)	4.69$^{e\,B}$ (0.60)	34.55$^{d,e\,D}$ (0.17)	16.39$^{b,c\,C}$ (0.17)

For each temperature, same lower case superscript letters indicate homogeneous subsets among the materials. For each material, same capital superscript letters indicate homogeneous subsets among different conditions.

Table 4 – Degree of conversion of *Viscalor* (no heat, T3-30 s and T3-3 min) at 5 min and 24 h post cure (DC_{5min} and DC_{24h}).

Materials	Syringe		Compule	
	DC_{5min}	DC_{24h}	DC_{5min}	DC_{24h}
Viscalor (no heat)	40.78 %$^{a\,A}$ (0.01)	58.04 %$^{a\,B}$ (0.03)	41.99 %$^{a\,A}$ (0.01)	60.17 %$^{a\,B}$ (0.03)
Viscalor (T3-30 s)	42.77 %$^{a\,A}$ (0.01)	58.49 %$^{a\,B}$ (0.01)	42.76 %$^{a\,A}$ (0.01)	58.88 %$^{a\,B}$ (0.01)
Viscalor (T3-3 min)	40.71 %$^{a\,A}$ (0.01)	58.30 %$^{a\,B}$ (0.01)	41.65 %$^{a\,A}$ (0.00)	60.60 %$^{a\,C}$ (0.01)

For each DC, same lower case superscript letters indicate homogeneous subsets among the materials. For each material, same capital superscript letters indicate homogeneous subsets among different conditions.
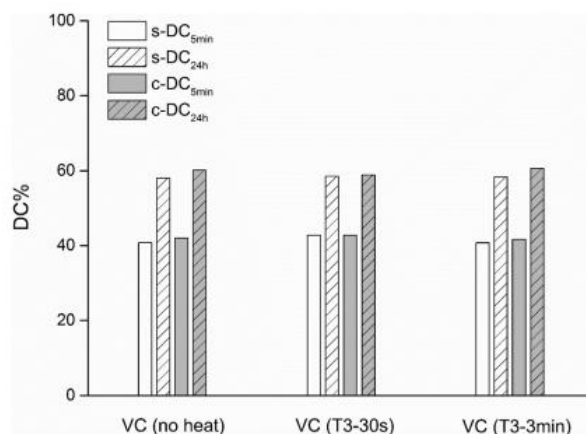
Fig. 9 – DC% results of *Viscalor* syringe/compule (no heat, T3-30 s and T3-3 min) at 5 min and 24 h post cure (DC_{5min} and DC_{24h}).

Warmer did not increase the post-cure DC% at either 5 min or 24 h, compared to data for no pre-heating ($p > 0.05$).

4. Discussion

Dental RBCs are designed to exhibit good mechanical properties and esthetics after restoration, but their pre-cure properties, including stickiness and packability, mainly affect the clinical handling and placement [35]. These handling properties depend upon the inherent material characteristics and rheological nature of composites [14]. Hence, this study investigated extrusion force, stickiness and packability at different temperatures and evaluated post-cure DC% at 5 min and 24 h for *Viscalor* after different pre-heating times. Thus, the first null hypothesis was rejected and the second null hypothesis was accepted. Regardless of pre-heating time, no significant change in DC% of *Viscalor* was measured ($p > 0.05$).

The thermal properties and heating rates of both Caps Warmer and pre-heated *Viscalor* were previously unreported.

Thus, temperature profiles of Caps Warmer in the T3 mode and *Viscalor* following different pre-heating periods were first characterized. Results demonstrated the efficacy of the Caps Warmer since it reached the stated preset temperature of 68 °C after about 20 min. When heating was stopped, a slight temperature rise of 2.09 °C and 0.35 °C was found, respectively. During pre-heating, thermal energy diffused gradually through the container (compule or syringe) into the composite.

With temperature rise the viscosity of *Viscalor* reduced, but its flowability was still somewhat less than certain flowable RBCs at room temperature [35]. After 3 min pre-heating, *Viscalor* had a lower internal temperature than the maximum temperature of the Caps Warmer in T3 mode (68 °C). This corresponds to previous studies where pre-heated composites were cooler than the pre-set temperature of heating devices. Thus reduced pulp temperature changes may ensue [32]. Reduced composite temperature rises also relate to filler properties since inert inorganic particles only absorb small amounts of thermal energy during heating [35,36]. The high filler content of *Viscalor* implies a low proportion of resin matrix and consequently a low temperature rise [36]. Different filler contents result in different temperature/time profiles. The temperature of *Viscalor* (T3-3 min) decreased to 37 °C within 3 min after removed from the Caps Warmer. To ensure minimal temperature drop and optimal performance, clinicians should work rapidly during manipulation of pre-heated composites.

To quantify the effect of pre-heating on *Viscalor*'s flowability, the extrusion force (N) and extruded mass (g) were measured for both full and half-used *Viscalor* compules. Results showed the beneficial effects of a longer pre-heating period, in which extrusion force reduced and extruded mass increased. This confirmed that 3 min pre-heating did increase the flowability of *Viscalor* leading to easy extrusion and a sufficient mass of extruded composite.

Stickiness measurements were based on previous studies on the effects of temperature and composite composition [8–10,14]. Generally, there are two types of force/displacement plots (Type I and Type II), in which Type I is more commonly observed (Fig. S4). A Type I plot has a single peak, whereas a Type II plot has a primary peak followed by a secondary peak [14]. The peak height (F_{max}) is the maximum tensile force during 'debonding'. The work of probe-separation (W_s) is the integrated area under the curve [10].

The force/displacement profiles observed were combined responses of RBC paste viscoelasticity and interfacial behaviour between the probe and paste [8,13]. F_{max} mainly depends on the wettability of the paste, its resistance against the debonding force, and the roughness of both probe and paste [8,13,14]. Other factors, such as temperature and viscoelastic properties of the paste also affect F_{max} [14]. W_s depended on the shear characteristics of the pastes, which relates to their molecular entanglements [8,13,14]. In the present stickiness results, Admira Fusion exhibited the highest F_{max} and W_s at both 22 and 37 °C. According to previous studies, high filler loading tends to produce low stickiness [8,17] as it hinders composite flowability and creates high viscosity [37]. Admira Fusion, *Viscalor* and Harmonize have high filler content (84 wt.%, 83 wt.% and 81 wt.%, respectively) and

their F_{max} varied with filler content. However, they did not exhibit particularly low stickiness, as expected. This may be due to their matrix compositions. Admira Fusion is a ceramic-based RBC, in which ORMOCERs function as the matrix system [38–40]. Nanoparticles and glass ceramic particles are firmly embedded in the ORMOCER matrix [41]. The ART (Adaptive Response Technology) filler system in Harmonize acts as a rheological modifier.

Although containing relatively high filler loading, Filtek Supreme Ultra (78.5 wt.%) showed higher F_{max} and W_s compared to TPH LV (75.5 wt.%) and Tetric EvoCeram (75 wt.%). This may be due to both TEGDMA and bisphenol-A epoxylated dimethacrylate (bis-EMA) within its matrix system [16,17]. Previous studies have noted that the presence/absence of hydrogen bonding significantly affects viscosity. Bis-EMA, lacks two hydroxyl groups (−OH) in its chemical structure, compared to bis-GMA, which reduces viscosity [42]. But, with a low-viscous matrix system, TPH LV and Tetric EvoCeram still showed low F_{max} and W_s possibly related to their filler characteristics. Many previous studies established that all compositional variables affect RBC rheological and handling properties: resin matrix, filler particle content, shape, size and distribution, silane surface treatment, interlocking between particles and other interfacial interactions between resin matrix and filler [30,43]. Generally, increasing filler loading and using smaller, irregular-shaped particles increases viscosity [30,44]. Filler particle sizes of TPH LV (1.35 μm) [45] and Tetric EvoCeram (40 nm–3 μm) [46] are lower than those in Filtek Supreme Ultra (0.6–10 μm) [47]. For a similar filler loading, more particles means higher surface area, more matrix/particle interactions and thus higher viscosity [17]. TPH LV and Tetric EvoCeram had low stickiness. Different filler morphologies - following the sequence: round, grains, plates and rods - reduce viscosity of RBCs [17]. Silane surface treatment may slightly lubricate irregular particles and reduce viscosity [17]. However, in this study, the lack of filler morphology information limits the discussion.

For packability measurements, compressive force (N) was plotted against probe displacement (mm) (Fig. S5). F_p reduced with decreased filler loading. Admira Fusion and TPH LV had the highest and lowest F_p values at both 22 and 37 °C, respectively.

In addition to paste composition, temperature also affected stickiness and packability: reducing F_{max} and F_p, but increasing W_s. Temperature increases the mobility of matrix monomers. Low viscous RBCs are more fluid so temperature further reduces F_p. Composite pastes bond more easily to the probe, increasing F_{max} and W_s [8,29]. However, some studies found that F_{max} and W_s may be lower at high temperature [9,11,14,17]. Since segmental movement is greater at high temperature, matrix monomers are insufficiently resistant to slippage of internal components. This factor tends to reduce F_{max} and W_s [9,11,14,17].

Viscalor (no heat) showed generally comparable F_{max}, W_s and F_p to the other investigated RBC pastes. Different pre-heating times had significant influence on F_{max}, W_s and F_p at either 22 or 37 °C (p < 0.005), except for F_{max} at 37 °C (p = 0.884). Composite temperature can reduce rapidly to the ambient physiological level after removed from a pre-heating device [7,29,32]. Thus, pre-heated *Viscalor* (T3-30 s and T3-

3 min) inserted into the brass cavity showed similar F_{max} results to *Viscalor* (no heat) at 37 °C due to the similar composite temperature. However, *Viscalor*'s W_s changed significantly with different pre-heating times. So evidently W_s was more sensitive than F_{max} to changes in elongation and arguably more appropriate to describe stickiness [14].

Moderate temperature rise after pre-heating generates greater mobility of monomer free radicals - *as and when they are generated by photo-initiation*. The temperature rise delays auto-deceleration during polymerization and leads to the increased DC% [7,26,29,32,48,49]. Higher monomer conversion has been observed after pre-heating composites at 54 °C, however, high polymerization shrinkage also occur with high DC% [7,26,50]. But, after 30 s pre-heating, F_p decreased slightly at either 22 or 37 °C.

To further identify the effect of pre-heating time on pre-cure stickiness and packability of *Viscalor*, DC% was measured. After 24 h at 37 °C, DC% increased [48,49]. The use of *Viscalor* syringe or compule had no significant influence on DC_{Smin} and DC_{24h}. Real-time DC% curves of both *Viscalor* syringe and compule specimens increased similarly. Different pre-heating time had no significant effect on *Viscalor* syringe/compule DC% either measured after 5 min or 24 h. Generally, temperature rise has a positive effect on DC%, since temperature rise aids polymer chain propagation.

Three minutes pre-heating did not affect the DC% of *Viscalor* syringe/compule specimens. This suggests that no premature monomer curing occurred.

5. Conclusions

Within the limitations of this study, the following conclusions are drawn:

1) The Caps Warmer exhibited good efficacy as a pre-heating device: pre-heated *Viscalor* showed greatly reduced extrusion force and increased flowability, especially after the longer pre-heating time (3 min).
2) The RBC pastes varied to a statistically significant but limited extent in stickiness and packability. But, their overall magnitudes remained within what may be considered a clinically acceptable range.
3) Pre-heating had no adverse effects on *Viscalor* through any thermal activation causing premature polymerization.

Appendix A. Supplementary data

Supplementary material related to this article can be found, in the online version, at doi:https://doi.org/10.1016/j.dental.2019.08.101.

REFERENCES

[1] Sakaguchi RL, Powers JM. Craig's restorative dental Materials-E-Book. Elsevier Health Sciences; 2012.
[2] Anusavice KJ, Shen C, Rawls HR. Phillips' science of dental materials. Elsevier Health Sciences; 2013.
[3] Antoniac IV. Handbook of bioceramics and biocomposites. Berlin Heidelberg, New York: Springer; 2016.
[4] Nedeljkovic I, Teughels W, De Munck J, Van Meerbeek B, et al. Is secondary caries with composites a material-based problem? Dent Mater 2015;31(11):e247–77.
[5] Demarco FF, Corrêa MB, Cenci MS, Moraes RR, Opdam NJM. Longevity of posterior composite restorations: not only a matter of materials. Dent Mater 2012;28(1):87–101.
[6] Ferracane J, Hilton T, Stansbury J, Watts D, Silikas N, Ilie N, et al. Academy of Dental Materials guidance—resin composites: part II—technique sensitivity (handling, polymerization, dimensional changes). Dent Mater 2017;33(11):1171–91.
[7] Lohbauer U, Zinelis S, Rahiotis C, Petschelt A, Eliades G. The effect of resin composite pre-heating on monomer conversion and polymerization shrinkage. Dent Mater 2009;25(4):514–9.
[8] Kaleem M, Satterthwaite JD, Watts DC. A method for assessing force/work parameters for stickiness of unset resin-composites. Dent Mater 2011;27(8):805–10.
[9] Kaleem M, Watts DC. Stiffness of uncured resin-composites assessed via cavity-packing forces. Dent Mater 2016;32(9):e199–203.
[10] Al-Sharaa KA, Watts DC. Stickiness prior to setting of some light cured resin-composites. Dent Mater 2003;19(3):182–7.
[11] Ertl K, Graf A, Watts D, Schedle A. Stickiness of dental resin composite materials to steel, dentin and bonded dentin. Dent Mater 2010;26(1):59–66.
[12] Hoseney RC, Smewing JO. Instrumental measurement of stickiness of doughs and other foods. J Texture Stud 2007;30(2):123–36.
[13] Chuang H, Chiu C, Paniagua R. Avery adhesive test yields more performance data than traditional probe. Adhes Age 1997;40(10):18–23.
[14] Kaleem M, Satterthwaite JD, Watts DC. Effect of filler particle size and morphology on force/work parameters for stickiness of unset resin-composites. Dent Mater 2009;25(12):1585–92.
[15] Tyas MJ, Jones DW, Rizkalla AS. The evaluation of resin composite consistency. Dent Mater 1998;14(6):424–8.
[16] Silikas N, Watts D. Rheology of urethane dimethacrylate and diluent formulations. Dent Mater 1999;15(4):257–61.
[17] Lee J-H, Um C-M, Lee I-b. Rheological properties of resin composites according to variations in monomer and filler composition. Dent Mater 2006;22(6):515–26.
[18] Papakonstantinou AE, Eliades T, Cellesi F, Watts DC, Silikas N. Evaluation of UDMA's potential as a substitute for Bis-GMA in orthodontic adhesives. Dent Mater 2013;29(8):898–905.
[19] Gajewski VE, Pfeifer CS, Fróes-Salgado NR, Boaro LC, Braga RR. Monomers used in resin composites: degree of conversion, mechanical properties and water sorption/solubility. Braz Dent J 2012;23(5):508–14.
[20] Miletic V. Development of dental composites. In: Dental composite materials for direct restorations. Springer; 2018. p. 3–9.
[21] Peutzfeldt A. Resin composites in dentistry: the monomer systems. Eur J Oral Sci 1997;105(2):97–116.
[22] Gonçalves F, Azevedo CL, Ferracane JL, Braga RR. BisGMA/TEGDMA ratio and filler content effects on shrinkage stress. Dent Mater 2011;27(6):520–6.
[23] Lucey S, Lynch CD, Ray NJ, Burke FM, Hannigan A. Effect of pre-heating on the viscosity and microhardness of a resin composite. J Oral Rehabil 2010;37(4):278–82.
[24] Lee I-B, Son H-H, Um C-M. Rheologic properties of flowable, conventional hybrid, and condensable composite resins. Dent Mater 2003;19(4):298–307.

[25] Blalock JS, Holmes RG, Rueggeberg FA. Effect of temperature on unpolymerized composite resin film thickness. J Prosthet Dent 2006;96(6):424–32.

[26] Deb S, Di Silvio L, Mackler HE, Millar BJ. Pre-warming of dental composites. Dent Mater 2011;27(4):e51–9.

[27] SonicFill Portfolio of Scientific Research. Available from: ftp://ftp.endoco.com/links/KerrSonicFillResearch.pdf.

[28] Wagner W, Aksu M, Neme A, Linger J, Pink F, Walker S. Effect of pre-heating resin composite on restoration microleakage. Oper Dent 2008;33(1):72–8.

[29] Lempel E, Öri Z, Szalma J, Lovász BV, Kiss A, Tóth Á, et al. Effect of exposure time and pre-heating on the conversion degree of conventional, bulk-fill, fiber reinforced and polyacid-modified resin composites. Dent Mater 2019;35(2):217–28.

[30] Metalwala Z, Khoshroo K, Rasoulianboroujeni M, Tahriri M, Johnson A, Baeten J, et al. Rheological properties of contemporary nanohybrid dental resin composites: The influence of preheating. Polym Test 2018;72:157–63.

[31] Da Costa JB, Hilton TJ, Swift JEJ. Preheating composites. J Esthet Restor Dent 2011;23(4):269–75.

[32] Daronch M, Rueggeberg FA, Hall G, De Goes MF. Effect of composite temperature on in vitro intrapulpal temperature rise. Dent Mater 2007;23(10):1283–8.

[33] Tauböck TT, Tarle Z, Marovic D, Attin T. Pre-heating of high-viscosity bulk-fill resin composites: effects on shrinkage force and monomer conversion. J Dent 2015;43(11):1358–64.

[34] Nada K, El-Mowafy O. Effect of precuring warming on mechanical properties of restorative composites. Int J Dent 2011;2011:5.

[35] Daronch M, Rueggeberg FA, Moss L, De Goes MF. Clinically relevant issues related to preheating composites. J Esthet Restor Dent 2006;18(6):340–50.

[36] Al-Qudah AA, Mitchell CA, Biagioni PA, Hussey DL. Thermographic investigation of contemporary resin-containing dental materials. J Dent 2005;33(7):593–602.

[37] Bayne SC, Thompson JY, Swift EJJ, Stamatiades P, Wilkerson M. A characterization of first-generation flowable composites. J Am Dent Assoc 1998;129(5):567–77.

[38] Judeinstein P, Sanchez C. Hybrid organic–inorganic materials: a land of multidisciplinarity. J Mater Chem 1996;6(4):511–25.

[39] Moszner N, Salz U. New developments of polymeric dental composites. Prog Polym Sci 2001;26(4):535–76.

[40] Cavalcante LM, Schneider LFJ, Silikas N, Watts DC. Surface integrity of solvent-challenged ormocer-matrix composite. Dent Mater 2011;27(2):173–9.

[41] Scientific Compendium: Admira Fusion. Available from: http://212.227.148.121/e-paper/scientific_compendium/admira-fusion_en/.

[42] Kalachandra S, Sankarapandian M, Shobha HK, Taylor DF, McGrath JE. Influence of hydrogen bonding on properties of BIS-GMA analogues. J Mater Sci Mater Med 1997;8(5):283–6.

[43] Al-Ahdal K, Silikas N, Watts DC. Rheological properties of resin composites according to variations in composition and temperature. Dent Mater 2014;30(5):517–24.

[44] Habib E, Wang R, Zhu XX. Correlation of resin viscosity and monomer conversion to filler particle size in dental composites. Dent Mater 2018;34(10):1501–8.

[45] TPH Spectra Universal Composite Restorative Science EN. Available from: https://www.dentsplysirona.com/content/dam/dentsply/pim/manufacturer/Restorative/Direct_Restoration/Composites_Flowables/Universal_Composites/TPH_Spectra_Universal_Composite_Restorative/TPH-Spectra-xnzlfpn-en-us-1402.

[46] Tetric EvoCeram Instructions for Use. Available from: http://downloads.ivoclarvivadent.com/zoolu-website/media/document/827/Tetric+EvoCeram.

[47] Filtek Supreme Ultra Technical Product Profile. Available from: http://multimedia.3m.com/mws/media/629066O/filtektm-supreme-ultra-universal-restorative.pdf.

[48] Al-Ahdal K, Ilie N, Silikas N, Watts DC. Polymerization kinetics and impact of post polymerization on the degree of conversion of bulk-fill resin-composite at clinically relevant depth. Dent Mater 2015;31(10):1207–13.

[49] Daronch M, Rueggeberg FA, De Goes MF, Giudici R. Polymerization kinetics of pre-heated composite. J Dent Res 2006;85(1):38–43.

[50] Trujillo M, Newman SM, Stansbury JW. Use of near-IR to monitor the influence of external heating on dental composite photopolymerization. Dent Mater 2004;20(8):766–77.

Appendix 2: Publication 2 (Dental Materials 2020;36(6):787-93)

Pre-heating time and exposure duration: Effects on post-irradiation properties of a thermo-viscous resin-composite

Jiawei Yang [a], *Nikolaos Silikas* [a,*], *David C. Watts* [a,b,*]

[a] *Dentistry, School of Medical Sciences, University of Manchester, Manchester, UK*
[b] *Photon Science Institute, University of Manchester, Manchester, UK*

ARTICLE INFO

ABSTRACT

Objective. To evaluate the effects of pre-heating time and exposure duration on the degree of conversion (DC), maximum rate of polymerization (RP_{max}), polymerization shrinkage strain (PS) and surface micro-hardness (VHN) of *Viscalor*.

Methods. *Viscalor* syringes were pre-heated using a Caps Warmer (VOCO, Germany) in T3 mode (at 68 °C) for 30 s (T3-30s) and 3 min (T3-3min) and then the composite paste was extruded into appropriately sized molds. Light irradiation was applied at zero distance from the upper surface with a LED-LCU of mean irradiance 1200 mW/cm^2 for either 20 or 40 s. The real-time polymerization kinetics and DC at 5 min and 24 h post-irradiation (DC_{5min} and DC_{24h}) were measured using ATR-FTIR ($n=3$). PS was obtained with the bonded-disk technique ($n=3$). Top and bottom Vickers micro-hardness (VHN_{top} and VHN_{bottom}) were measured at 5 min post-irradiation and after 24 h dry storage ($n=5$). Data were analysed using one-way ANOVA, two-way ANOVA, independent *t*-test and Tukey post hoc tests ($p < 0.05$).

Results. Polymerization kinetic curves of *Viscalor* from 0 to 15 min were similar for different pre-heating times and exposure durations. Pre-heated *Viscalor* (T3-30s and T3-3min) with 40 s exposure had greater VHN_{top} and VHN_{bottom} than for *Viscalor* (no heat) ($p < 0.05$). Exposure duration did not significantly affect DC, RP_{max} and PS ($p > 0.05$). After 24 h storage, DC and VHN increased. Pre-heating did not increase the DC_{24h}, relative to no pre-heating ($p > 0.05$). Two-way ANOVA showed that there was no significant interaction between pre-heating time and exposure duration ($p > 0.05$).

Significance. Increasing irradiation time from 20 to 40 s did not affect DC, RP_{max} or PS, but increased VHN_{top}. Composite pre-heating had no adverse effect through any premature polymerization. For *Viscalor*, 3 min pre-heating and 20 s irradiation were sufficient to provide adequate hardness, without increasing PS or compromising polymerization kinetics.

© 2020 The Academy of Dental Materials. Published by Elsevier Inc. All rights reserved.

1. Introduction

Chairside pre-heating of dental resin-based composites (RBCs) has been introduced to improve their handling properties [1]. It lowers the viscosity of composites, leading to better flowability and marginal adaptation and reduces microleakage and gap formation [2].

Temperature also has an influence on the efficiency of polymerization, which is important for the post-irradiation properties and clinical performance of polymer-based RBCs. Higher monomer mobility, caused by the increased temperature, facilitates cross-linking among polymer chains and leads to a high degree of conversion (DC) and better mechanical properties [2,3]. Several studies have investigated the effect of pre-heating on RBCs mechanical properties, finding that micro-hardness and flexural strength increased after pre-heating [1,3–6]. However, Uctasli et al. [7] found no significant increases in flexural strength and flexural modulus of pre-heated composites. The diverse outcomes may result from different composite compositions and experimental setups.

Internal molecular densification develops during the irradiation process and leads to macroscopic polymerization shrinkage [8]. It is still a drawback of RBCs and the associated stress may lead to marginal debonding, secondary caries and clinical failure. Different approaches have been taken in attempts to reduce the developed contraction stress, such as adding rigid low-shrinking monomers [9,10], increasing filler content, and using the "soft-start" curing method [11] with various placement techniques [12]. At the post-irradiation stage, the uncured free radicals continue cross-linking slowly, which can produce further shrinkage [13].

Polymerization shrinkage strain (PS) increased with DC. Within certain limits, a linear relationship was demonstrated [14,15]. Some pre-heated composites also showed higher DC and PS [3,16]. The increased monomer mobility allows more radical collision, which delays auto-deceleration and improves DC and PS. However, the increased PS and the related marginal issues could be offset by the enhanced flowability via pre-heating [2].

Recently, a bulk-fill composite designed with thermo-viscous-technology (Viscalor) was introduced. Bulk-fill composites have at least 4 mm depth of cure and may exhibit low shrinkage stress [17,18]. Pre-heated Viscalor showed similar DC to room-temperature Viscalor [19]. However, the previous study included a 40 s irradiation period that is longer than the recommended 10–20 s. The effects of pre-heating time and exposure duration on its PS and surface micro-hardness (VHN) remain unknown. The longer curing time may have masked the effect of pre-heating time on the measured properties.

The objectives of this study were to evaluate the effects of pre-heating time (30 s and 3 min) and exposure duration (20 and 40 s) on the degree of conversion (DC), maximum rate of polymerization (RP_{max}), polymerization shrinkage strain (PS) and surface micro-hardness (VHN) of Viscalor. The Null Hypotheses were: (1) pre-heating time did not influence DC, RP_{max}, PS and VHN of Viscalor, (2) exposure duration did not influence DC, RP_{max}, PS and VHN of Viscalor, and (3) there was no interaction between pre-heating time and exposure duration.

Table 1 – Manufacturer information of Viscalor.			
	Manufacturer	Resin system	Filler wt.%
Viscalor	VOCO, Cuxhaven Germany	Bis-GMA, aliphatic dimethacrylate	83

2. Materials and methods

The manufacturer information of Viscalor is presented in Table 1. Viscalor syringes were pre-heated using a Caps Warmer (VOCO, Germany) in T3 mode (at 68 °C) for 30 s (T3-30s) and 3 min (T3-3min), respectively. According to the previous study, the estimated composite temperatures after 30 s and 3 min pre-heating are 34.5 and 60.6 °C, respectively [19].

The degree of conversion at 5 min and 24 h post-irradiation (DC_{5min} and DC_{24h}) and real-time polymerization kinetics were measured using Fourier transform infrared (FTIR) spectroscopy (ALPHA II FTIR Spectrometer, Bruker Optik GmbH) with an attenuated total reflectance (ATR) device. Background readings were collected between 400 and 4000 cm^{-1} using 32 scans at a resolution of 4 cm^{-1}. The uncured composite paste was extruded into a cylindrical Acetal mold (4 mm diameter × 2 mm thickness) above the diamond ATR crystal. The specimen was pressed from the top with a Mylar strip followed by a glass slide to remove air bubbles.

For DC measurements ($n = 3$), the spectrum of uncured Viscalor was collected first. Then irradiation was applied at zero distance from the upper surface with an LED-LCU of mean irradiance 1200 mW/cm^2 for either 20 or 40 s. The spectrophotometer's screw was then applied to ensure good contact between the specimen and the ATR crystal. The DC spectrum was collected after 5 min (DC_{5min}) and after 24 h real-time acquisition (DC_{24h}). The peak heights of the aliphatic C=C absorbance peak at 1637 cm^{-1} and the aromatic C=C absorbance peak at 1608 cm^{-1} were selected to calculate the DC%:

$$DC\% = 1 - \frac{(H_{1637\,cm^{-1}}/H_{1608\,cm^{-1}})_{cured}}{(H_{1637\,cm^{-1}}/H_{1608\,cm^{-1}})_{uncured}} \times 100\%$$

where $H_{1637\,cm^{-1}}$ is the height of aliphatic CC peak, $=H_{1608cm^{-1}}$ is the height of aromatic C=C peak, respectively.

For real-time kinetic measurements over 15 min ($n = 3$), the spectral acquisition started immediately before irradiation. Either 20 or 40 s irradiation was applied at 5 s after the start of the spectral acquisition. Spectra were collected using 10 scans at a resolution of 4 cm^{-1}. The rates of polymerization were obtained by numerical differentiation of real-time DC data with respect to time.

Polymerization shrinkage strain (PS) was measured using the bonded disk method [20,21], with a 3 mm thick glass baseplate, at 23 °C room temperature ($n = 3$). The specimens were cured for either 20 or 40 s. The axial strain was continuously measured up to 1 h after irradiation.

For hardness measurements, after either 20 or 40 s photo-irradiation from the upper surface, cylindrical specimens were removed from the mold (4 mm diameter × 2 mm thickness). Top and bottom surface Vickers micro-hardness (VHN$_{top}$ and VHN$_{bottom}$) at 5 min post-irradiation was measured using a
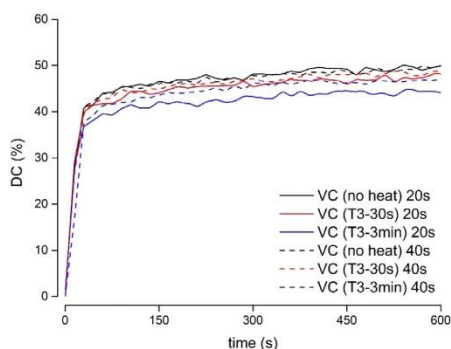
Fig. 1 – Real-time DC% vs. time during 10 min post-polymerization for Viscalor (no heat, T3-30s and T3-3min) with different exposure durations.

micro-hardness instrument (FM-700, Future Tech Corp., Japan) with a Vickers diamond pyramid micro-indenter ($n = 5$). A fixed load of 300 gf was applied for 15 s. Five indentations on both top and bottom surfaces were measured and averaged as the final VHN value. The specimens were then stored in dry conditions at 37 °C for 24 h, and the 24 h post-irradiation surface hardness was measured.

Data were entered into statistical software (SPSS, SPSS Inc., Illinois, USA) and analysed using one-way ANOVA test, two-way ANOVA test, independent T-test and Tukey post hoc tests ($p < 0.05$). Homogeneity of variables was calculated using the Kruskal–Wallis Test ($p < 0.05$).

3. Results

Polymerization kinetic curves of *Viscalor* from 0 to 10 min were similar for different pre-heating times and exposure durations (Fig. 1). Table 2 summarize the DC_{5min} and DC_{24h} of *Viscalor* (no heat, T3-30s and T3-3min) with different exposure durations. DC results ranged from 40.4% to 58.8%, in which DC_{24h} are significantly higher than DC_{5min} ($p < 0.05$). Pre-heating time and exposure duration did not significantly affect DC results ($p > 0.05$).

RP_{max} results are shown in Table 3 and Fig. 2. RP_{max} ranged from 1.76% to 1.96%/s, in which pre-heated *Viscalor* (T3-30s

Table 3 – Maximum rates of polymerization (RP_{max}, %/s) of Viscalor (no heat, T3-30s and T3-3min) with different exposure durations.

Materials	RP_{max}	
	20 s	40 s
Viscalor (no heat)	1.85 [a][A] (0.42)	1.79[a][A] (0.32)
Viscalor (T3-30s)	1.95[a] (0.11)	1.76[a][A] (0.49)
Viscalor (T3-3min)	1.96[a][A] (0.12)	1.78[a][A] (0.35)

For each exposure duration, the same lower case superscript letters indicate homogeneous subsets among the materials. For each material, the same CAPITAL superscript letters indicate homogeneous subsets among different conditions.

Fig. 2 – Maximum rates of polymerization (RP_{max}, %/s) of Viscalor (no heat, T3-30s and T3-3min) with different exposure durations.

and T3-3min) with 20 s exposure duration had the highest RP_{max}. Both pre-heating time and exposure duration had no significant influences on RP_{max} ($p > 0.05$).

Table 4 shows PS results, which ranged from 1.35% to 1.57%. The real-time polymerization shrinkage strain curves of all measured specimens increased similarly. Both pre-heating time and exposure duration had no significant influences on PS ($p > 0.05$).

Table 5 and Figs. 3 and 4 show VHN_{top} and VHN_{bottom} results of *Viscalor*. At 5 min post-irradiation, *Viscalor* (no heat) with

Table 2 – Degree of conversion at 5 min and 24 h post-irradiation (DC_{5min} and DC_{24h}) of Viscalor (no heat, T3-30s and T3-3min) with different exposure durations.

Materials	DC_{5min}		DC_{24h}	
	20 s	40 s	20 s	40 s
Viscalor (no heat)	41.9%[a][A] (0.01)	40.8%[a][A] (0.01)	58.8%[a][B] (0.03)	58.0%[a][B] (0.03)
Viscalor (T3-30s)	42.3%[a][A] (0.02)	42.8%[a][A] (0.01)	58.7%[a][B] (0.02)	58.5%[a][B] (0.01)
Viscalor (T3-3min)	40.4%[a][A] (0.00)	40.7%[a][A] (0.01)	58.3%[a][B] (0.03)	58.3%[a][B] (0.01)

For each exposure duration, the same lower case superscript letters indicate homogeneous subsets among the materials. For each material, the same CAPITAL superscript letters indicate homogeneous subsets among different conditions.
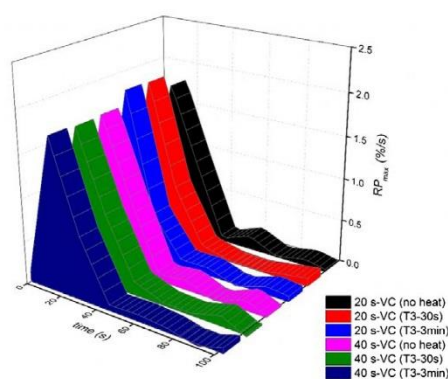
Table 4 – Polymerization shrinkage strain (PS) of Viscalor (no heat, T3-30s and T3-3min) with different exposure durations at 23 °C.

Materials	PS	
	20 s	40 s
Viscalor (no heat)	1.35%[aA] (0.14)	1.41%[aA] (0.13)
Viscalor (T3-30s)	1.47%[aA] (0.07)	1.57%[aA] (0.16)
Viscalor (T3-3min)	1.43%[aA] (0.01)	1.45%[aA] (0.15)

For each exposure duration, the same lower case superscript letters indicate homogeneous subsets among the materials. For each material, the same CAPITAL superscript letters indicate homogeneous subsets among the exposure duration.
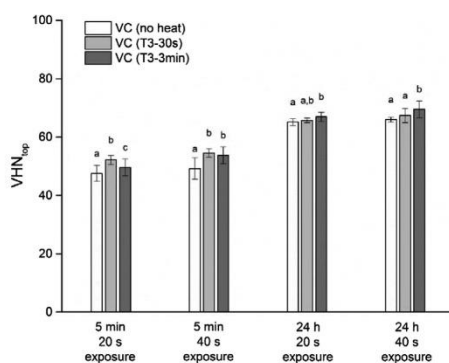

Fig. 3 – Top surface micro-hardness (VHN_{top}) of Viscalor (no heat, T3-30s and T3-3min) at 5 min and 24 h post-irradiation with different exposure durations. The same lower case letters indicate homogeneous subsets between materials.

20 s exposure duration showed the lowest VHN_{top}. At 24 h post-irradiation, Viscalor (T3-3min) with 40 s exposure duration showed the highest VHN_{bottom}. Pre-heating significantly increased both VHN_{top} and VHN_{bottom} ($p < 0.05$), whereas exposure duration only significantly improved VHN_{top} in some cases.

Fig. 4 – Bottom surface micro-hardness (VHN_{bottom}) of Viscalor (no heat, T3-30s and T3-3min) at 5 min and 24 h post-irradiation with different exposure durations. The same lower case letters indicate homogeneous subsets between materials.

Scatter plots and correlations of DC-PS with different exposure durations at 5 min post-irradiation are shown in Fig. 5.

Two-way ANOVA demonstrated that there was no significant interaction between pre-heating time and exposure duration ($p > 0.05$).

4.   Discussion

Building upon previous DC results of Viscalor [19], this study further investigated the effect of pre-heating time and exposure duration on its post-irradiation properties: DC, RP_{max}, PS, and VHN. The interaction between the two variables was also studied. Room-temperature and pre-heated Viscalor showed similar DC, RP_{max} and PS results, irrespective of exposure duration. After pre-heating and long exposure duration, VHN increased. Thus, the first and second null hypotheses were partly rejected. And the third null hypothesis was accepted since there was no interaction between the two variables ($p > 0.05$).

During clinical applications, RBC paste transforms to a rigid mass through photo-polymerization, which is usually

Table 5 – VHNtop and VHNbottom of Viscalor (no heat, T3-30s and T3-3min) at 5 min and 24 h post-irradiation with different exposure durations.

Materials	5 min post-irradiation				24 h post-irradiation			
	VHN_{top}		VHN_{bottom}		VHN_{top}		VHN_{bottom}	
	20 s	40 s	20 s	40 s	20 s	40 s	20 s	40 s
Viscalor (no heat)	47.54[aA] (2.75)	49.19[aA,B] (3.68)	49.84[aB] (2.58)	52.08[aC] (3.02)	65.17[aD] (1.15)	66.02[aD] (0.81)	66.76[aD] (0.75)	66.35[aD] (1.76)
Viscalor (T3-30s)	52.16[bA] (1.49)	54.58[bB] (1.48)	54.92[bB] (1.52)	55.59[bB] (0.81)	65.74[a,bC] (0.79)	67.40[aD] (2.42)	68.05[bD,E] (0.29)	69.09[bE] (0.92)
Viscalor (T3-3min)	49.64[cA] (2.85)	53.80[bB,C] (2.87)	51.77[cB] (2.73)	54.30[bC] (1.51)	66.96[bD] (1.54)	69.54[bE] (2.85)	68.46[bD,E] (1.68)	69.03[bD,E] (1.22)

For each exposure duration, the same lower case superscript letters indicate homogeneous subsets among the materials. For each material, the same CAPITAL superscript letters indicate homogeneous subsets among different conditions.
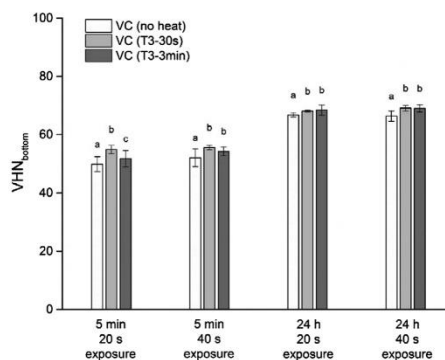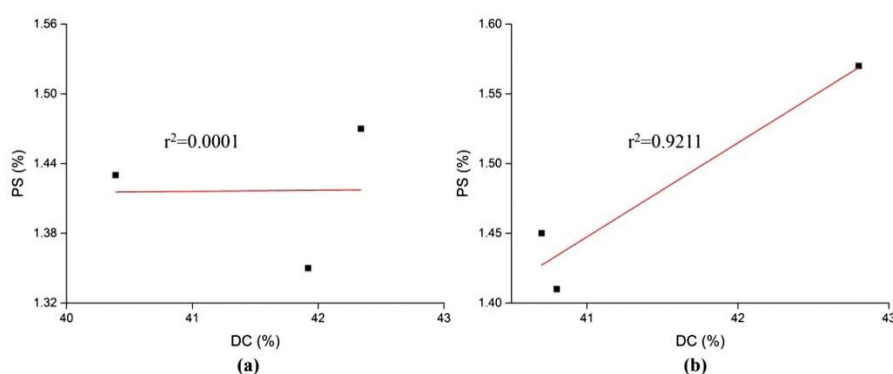
Fig. 5 – Scatter plots showing the correlations and linear regressions of DC-PS with (a) 20 s exposure duration, and (b) 40 s exposure duration, both at 5 min post-irradiation at 23 °C.

activated by a visible light-curing unit (LCU) [15]. The polymerization rate reaches the maximum value (RP_{max}) during the first few minutes after irradiation [6,22–24]. After rapid early-stage polymerization, the increased monomer conversion limits the mobility of unreacted monomers to reach the reactive sites and reduces the rate of polymerization [22–25].

Generally, DC is the key parameter describing the effectiveness of monomer conversion and commonly measured using the FTIR technique [23,26,27]. Light-curing of dimethacrylate-based monomers results in a highly cross-linking structure. However, due to steric hindrance and limited mobility of free radicals, there are residual unreacted monomers in the final product, which leads to the final DC of 55–75% [14,23,27–29]. Adequate polymerization leads to a high DC, which is vital to the material's long-term performance and functionality, whereas insufficient polymerization can be deleterious to clinical success [23]. The synergistic effect of *intrinsic* and *extrinsic* factors plays an important role in controlling the efficiency of photo-polymerization [30]. The former includes monomer composition, filler size and content, and the type and quantity of photo-initiators [30]. The latter includes the irradiance of LCU, exposure time, curing mode, temperature, and the distance between the LCU tip and the restoration surface [30]. Although altering the composition may directly modify the final properties of the composites, it is not changeable by the clinician during the operative placement [30]. However, the extrinsic factors are critically dependent on operator skill, especially during the light-curing process.

It has been reported that pre-heated composites have a greater extent of monomer conversion, polymerization rate, and conversion at RP_{max} [22,31,32]. In this study, DC and RP_{max} did not vary with pre-heating time. This can be explained by composite temperature decrease after removal from the heating device and during the handling process [33,34]. As previously mentioned by Daronch et al. [35], pre-heated composites were not as warm as expected. The actual delivery temperature of the pre-heated compule was lower than the

pre-set temperature of the heating device [33]. The major temperature rise, however, is related to the exothermic photo-polymerization and the heat produced by the LCU [27,35].

The heat build-up during photo-polymerization has always been a concern to both researchers and clinicians. By comparing different types of LCU, the significant temperature rises during light-curing can be attributed to the higher irradiance and/or longer exposure duration [11]. In this study, use of a LED-LCU with an average constant irradiance (1200 mW/cm²), different exposure durations (20 or 40 s) were applied which resulted in a radiant exposure of either 24 or 48 J/cm². However, the DC and RP_{max} showed no significant changes between 20 and 40 s. This is in line with a previous study in which, at 2 mm depth, the DC after 20 s exposure duration was equal to that after 40 s [36]. Furthermore, as Daugherty et al. concluded to achieve adequate polymerization of bulk-fill composite, a minimum of 14 J/cm² radiant exposure should be delivered by the LED-LCU [30].

Some studies reported that curing pre-heated composites for a short exposure duration produced similar or higher DC, compared to composites cured for longer exposure durations at room temperature [2,37]. But in this study, both long pre-heating time (3 min) and exposure duration (40 s) did not significantly increase DC. The RP_{max} of pre-heated *Viscalor* (T3-30s and T3-3min) with 20 s exposure was maximal. Combined with similar DC magnitudes and similar real-time DC plots, the evidence is that 20 s curing time was sufficient to produce an adequate degree of polymerization for *Viscalor* (no heat, T3-30s and T3-3min). This result may also be related to specimen thickness, light absorption/scattering and composition of the composite, which merits further investigation.

The correlation between DC and PS was far stronger for 40 than 20 s irradiation (Fig. 5) but this evidenced that increased DC is associated with high PS [3,14]. Internal densification occurs during photo-polymerization, in which inter-molecular van der Waals distances convert to covalent (C—C) bond-lengths [38–40]. Thus, polymerization shrinkage

is accompanied by volumetric reduction. A primary design requirement for developing dental restorative composites focuses on increasing DC but reducing PS [41]. A low PS is good for minimizing stress during polymerization, which leads to better marginal sealing and integrity [27]. Many methods have been used to measure PS, including mercury dilatometer, Archimedes' principles of buoyancy, and the bonded-disk technique [16,17,20,21,27], which has been used in this study. Results showed that exposure duration had no significant influence on PS, which also correlated with the present DC results. The minimal temperature change during different exposure durations may also contribute to similar PS results, which merits further investigation.

Some studies reported that elevated temperatures could increase both DC and PS [3,14,27]. However, the present results showed that pre-heating did not significantly increase PS and they ranged lower than the generally accepted shrinkage range of 2–6% [3,27,42]. Pre-heating allows sufficient flow of polymer chains during the early-stage polymerization, which reduces internal stress formation within the cavity [14,25,34]. Moreover, enhanced marginal adaptation of pre-heated composite could compensate for the developed shrinkage and stress [2,14]. Thus, 3 min pre-heating and sufficient exposure duration may lead to a steady rate of polymerization and PS results within clinically acceptable limits.

VHN measurements are an indirect method to determine the effective polymerization of composite [6]. In this study, both VHN_{top} and VHN_{bottom} values were measured, and all the bottom/top ratios were over 0.8, which indicated adequate polymerization through the specimen thickness (2 mm) [4,6,43]. It is well known that extended post-polymerization times may increase DC and the degree of cross-linking [44]. The increased VHN after 24 h storage indicated the progressive cross-linking reaction post-irradiation [45–47]. Pre-heating enhanced both the VHN_{top} and VHN_{bottom} of *Viscalor*. This suggests that the reduced viscosity improved the cure at the lower surface. Some previous studies showed similar results [4–6,48]. At 5 min post-irradiation, *Viscalor* (T3-3min) with 20 s exposure showed lower VHN than that of *Viscalor* (T3-30s). Despite the significant differences, their VHN values are all in an acceptable range and higher than *Viscalor* (no heat). On the contrary, exposure duration only slightly enhanced VHN_{top} values in some cases. Although extended exposure duration may improve the extent of polymerization, 20 s curing time seems to be sufficient for obtaining adequate VHN results.

5. Conclusions

Within the limitations of this study, the following conclusions can be summarized:

(1) Use of a longer exposure duration 40 s, compared to 20 s, did not affect DC, RP_{max} or PS, but increased VHN_{top}.
(2) Pre-heating had no adverse effect through any premature polymerization.
(3) For clinical application of *Viscalor*, 3 min pre-heating and 20 s irradiation were sufficient to provide adequate hardness, without increasing PS or compromising polymerization kinetics.

REFERENCES

[1] Nada K, El-Mowafy O. Effect of precuring warming on mechanical properties of restorative composites. Int J Dent 2011;2011:5.

[2] Fróes-Salgado NR, Silva LM, Kawano Y, Francci C, Reis A, Loguercio AD. Composite pre-heating: effects on marginal adaptation, degree of conversion and mechanical properties. Dent Mater 2010;26(9):908–14.

[3] Deb S, Di Silvio L, Mackler HE, Millar BJ. Pre-warming of dental composites. Dent Mater 2011;27(4):e51–9.

[4] Lucey S, Lynch CD, Ray NJ, Burke FM, Hannigan A. Effect of pre-heating on the viscosity and microhardness of a resin composite. J Oral Rehabil 2010;37(4):278–82.

[5] AlShaafi M. Effects of different temperatures and storage time on the degree of conversion and microhardness of resin-based composites. J Contemp Dent Pract 2016;17(3):217–23.

[6] Dionysopoulos D, Tolidis K, Gerasimou P. The effect of composition, temperature and post-irradiation curing of bulk fill resin composites on polymerization efficiency. Mater Res 2016;19:466–73.

[7] Uctasli MB, Arisu HD, Lasilla LV, Valittu PK. Effect of preheating on the mechanical properties of resin composites. Eur J Dent 2008;2(4):263–8.

[8] Watts DC, Schneider LFJ, Marghalani HY. Bond-disruptive stresses generated by resin composite polymerization in dental cavities. J Adhes Sci Technol 2009;23(7–8):1023–42.

[9] Weinmann W, Thalacker C, Guggenberger R. Siloranes in dental composites. Dent Mater 2005;21(1):68–74.

[10] Chen M-H, Chen C-R, Hsu S-H, Sun S-P, Su W-F. Low shrinkage light curable nanocomposite for dental restorative material. Dent Mater 2006;22(2):138–45.

[11] Rueggeberg FA, Giannini M, Arrais CAG, Price RBT. Light curing in dentistry and clinical implications: a literature review. Braz Oral Res 2017;31.

[12] Loguercio AD, Reis A, Ballester RY. Polymerization shrinkage: effects of constraint and filling technique in composite restorations. Dent Mater 2004;20(3):236–43.

[13] Germscheid W, de Gorre LG, Sullivan B, O'Neill C, Price RB, Labrie D. Post-curing in dental resin-based composites. Dent Mater 2018;34(9):1367–77.

[14] Silikas N, Eliades G, Watts DC. Light intensity effects on resin-composite degree of conversion and shrinkage strain. Dent Mater 2000;16(4):292–6.

[15] Watts DC. Reaction kinetics and mechanics in photo-polymerised networks. Dent Mater 2005;21(1):27–35.

[16] Jongsma LA, Kleverlaan CJ. Influence of temperature on volumetric shrinkage and contraction stress of dental composites. Dent Mater 2015;31(6):721–5.

[17] Zorzin J, Maier E, Harre S, Fey T, Belli R, Lohbauer U, et al. Bulk-fill resin composites: polymerization properties and extended light curing. Dent Mater 2015;31(3):293–301.

[18] Chesterman J, Jowett A, Gallacher A, Nixon P. Bulk-fill resin-based composite restorative materials: a review. Br Dent J 2017;222(5):337–44.

[19] Yang J, Silikas N, Watts DC. Pre-heating effects on extrusion force, stickiness and packability of resin-based composite. Dent Mater 2019;35(11):1594–602.

[20] Watts D, Cash A. Kinetic measurements of photo-polymerization contraction in resins and composites. Meas Sci Technol 1991;2(8):788.

[21] Ferracane JL, Hilton TJ, Stansbury JW, Watts DC, Silikas N, Ilie N, et al. Academy of Dental Materials guidance – resin composites. Part II. Technique sensitivity (handling, polymerization, dimensional changes). Dent Mater 2017;33(11):1171–91.

[22] Daronch M, Rueggeberg FA, De Goes MF, Giudici R. Polymerization kinetics of pre-heated composite. J Dent Res 2006;85(1):38–43.

[23] Al-Ahdal K, Ilie N, Silikas N, Watts DC. Polymerization kinetics and impact of post polymerization on the degree of conversion of bulk-fill resin-composite at clinically relevant depth. Dent Mater 2015;31(10): 1207–13.

[24] Wang R, Liu H, Wang Y. Different depth-related polymerization kinetics of dual-cure, bulk-fill composites. Dent Mater 2019;35(8):1095–103.

[25] Sirovica S, Guo Y, Guan R, Skoda MWA, Palin WM, Morrell AP, et al. Photo-polymerisation variables influence the structure and subsequent thermal response of dental resin matrices. Dent Mater 2020;36(3):343–52.

[26] Guo X, Wang Y, Spencer P, Ye Q, Yao X. Effects of water content and initiator composition on photopolymerization of a model BisGMA/HEMA resin. Dent Mater 2008;24(6):824–31.

[27] Lohbauer U, Zinelis S, Rahiotis C, Petschelt A, Eliades G. The effect of resin composite pre-heating on monomer conversion and polymerization shrinkage. Dent Mater 2009;25(4):514–9.

[28] Palin WM, Fleming GJP, Trevor Burke FJ, Marquis PM, Randall RC. Monomer conversion versus flexure strength of a novel dental composite. J Dent 2003;31(5):341–51.

[29] Eliades GC, Vougiouklakis GJ, Caputo AA. Degree of double bond conversion in light-cured composites. Dent Mater 1987;3(1):19–25.

[30] Daugherty MM, Lien W, Mansell MR, Risk DL, Savett DA, Vandewalle KS. Effect of high-intensity curing lights on the polymerization of bulk-fill composites. Dent Mater 2018;34(10):1531–41.

[31] Karacan AO, Ozyurt P. Effect of preheated bulk-fill composite temperature on intrapulpal temperature increase in vitro. J Esthet Rest Dent 2019.

[32] Trujillo M, Newman SM, Stansbury JW. Use of near-IR to monitor the influence of external heating on dental composite photopolymerization. Dent Mater 2004;20(8):766–77.

[33] Daronch M, Rueggeberg FA, Moss L, De Goes MF. Clinically relevant issues related to preheating composites. J Esthet Rest Dent 2006;18(6):340–50.

[34] Lempel E, Őri Z, Szalma J, Lovász BV, Kiss A, Tóth Á, et al. Effect of exposure time and pre-heating on the conversion degree of conventional, bulk-fill, fiber reinforced and polyacid-modified resin composites. Dent Mater 2019;35(2):217–28.

[35] Daronch M, Rueggeberg FA, Hall G, De Goes MF. Effect of composite temperature on in vitro intrapulpal temperature rise. Dent Mater 2007;23(10):1283–8.

[36] Frauscher KE, Ilie N. Degree of conversion of nano-hybrid resin-based composites with novel and conventional matrix formulation. Clin Oral Invest 2013;17(2):635–42.

[37] Daronch M, Rueggeberg FA, De Goes MF. Monomer conversion of pre-heated composite. J Dent Res 2005;84(7):663–7.

[38] Atai M, Ahmadi M, Babanzadeh S, Watts DC. Synthesis, characterization, shrinkage and curing kinetics of a new low-shrinkage urethane dimethacrylate monomer for dental applications. Dent Mater 2007;23(8):1030–41.

[39] Atai M, Watts DC, Atai Z. Shrinkage strain-rates of dental resin-monomer and composite systems. Biomaterials 2005;26(24):5015–20.

[40] Ferracane JL. Developing a more complete understanding of stresses produced in dental composites during polymerization. Dent Mater 2005;21(1):36–42.

[41] Dewaele M, Truffier-Boutry D, Devaux J, Leloup G. Volume contraction in photocured dental resins: the shrinkage-conversion relationship revisited. Dent Mater 2006;22(4):359–65.

[42] Labella R, Lambrechts P, Van Meerbeek B, Vanherle G. Polymerization shrinkage and elasticity of flowable composites and filled adhesives. Dent Mater 1999;15(2):128–37.

[43] Farahat F, Daneshkazemi A, Hajiahmadi Z. The effect of bulk depth and irradiation time on the surface hardness and degree of cure of bulk-fill composites. J Dent Biomater 2016;3(3):284.

[44] Aromaa MK, Vallittu PK. Delayed post-curing stage and oxygen inhibition of free-radical polymerization of dimethacrylate resin. Dent Mater 2018;34(9):1247–52.

[45] Watts DC, Amer OM, Combe EC. Surface hardness development in light-cured composites. Dent Mater 1987;3(5):265–9.

[46] Marghalani HY. Post-irradiation Vickers microhardness development of novel resin composites. Mater Res 2010;13:81–7.

[47] Alshali RZ, Salim NA, Satterthwaite JD, Silikas N. Post-irradiation hardness development, chemical softening, and thermal stability of bulk-fill and conventional resin-composites. J Dent 2015;43(2):209–18.

[48] Munoz CA, Bond PR, Sy-Munoz J, Tan D, Peterson J. Effect of pre-heating on depth of cure and surface hardness of light-polymerized resin composites. Am J Dent 2008;21(4):215–22.